THE STUDY OF THE BEHAVIOUR OF DROPS AND COALESCENCE PHENOMENA IN DISPERSION BANDS

by

ALI MOHAMMED ALI ALLAK

A thesis submitted to the University of Aston in Birmingham for the degree of Doctor of Philosophy

Department of Chemical Engineering
The University of Aston in Birmingham

AUGUST 1973

TO MY WIFE EILEEN

MY LATE FATHER AND TO MY MOTHER

ACKNOWLEDGEMENTS.

The author wishes to express his sincere thanks and gratitude to the Head of the Chemical Engineering Department, Professor G.V.Jeffreys, for providing the facilities for this research and for his helpful guidance and personal interest in the supervision of this project, the members of the technical staff of the workshop and the photographic section of this department, and to Dr.G.L.Rogers of the Physics Department for his useful suggestions on matters appertaining to the optical aspects of this project.

SUMMARY.

A refractive index matching technique has been developed to study the behaviour and coalescence phenomena of drops in dispersion bands. The above technique resulted in extending the type of information that can be obtained e.g. the probability of coalescence, flow pattern and packing arrangement of the drops. Five systems were studied and a correlation was developed, using dimensional analysis to evaluate the parameters affecting dispersion bands. The least square fit method was used to evolve an equation for estimating the coalescence probability at any particular plane in the bed. Finally a mathematical model has been developed, based on the drainage of the continuous phase. The model predicted holdup, the critical film thickness in the dispersion band and explained the relationship between drop size and bed height.

Good agreement was obtained between the predicted and the experimental results.

LIST OF CONTENTS

LIST OF CONTENTS (contd)

LIST OF CONTENTS (contd)

INTRODUCTION.

In recent years the coalescence of drops in liquid systems has attracted increasing attention. The study of the behaviour of drops and coalescence phenomena in liquid-liquid extraction equipment is important since the tendency or failure of a dispersed phase to coalesce markedly influences the capacity of the extraction equipment. In all types of extraction columns the drops produced at the distributor plate and/or at the agitator finally form a closely packed dispersion band at the coalescing interface at which they must coalesce rapidly with the phase boundary. Failure to do so will result in a longer residence time of the drops in the band and flooding of the column ensues. It is evident, therefore, that the ultimate phase separation occurs at such a band. Thus the behaviour of the drops, coalescence phenomena and the continuous phase film drainage in dispersion bands must influence the rate of phase separation.

Previous studies on dispersion bands have been based on overall balances and macroflow of the phases. The resulting correlations were therefore based on observations made on the overall picture of the bed and in some instances assumptions were made of the coalescence process.

In this study an attempt has been made to investigate the coalescence mechanism via the developments of new techniques facilitating the observation of the coalescence process in dispersion bands, in order to predict phase separation more accurately. This will ultimately result in a more accurate design of the liquid-liquid extraction equipment.

C H A P T E R 1.

DROP FORMATION.

1) Drop Formation.

The importance of drop size and interfacial area in liquid-liquid operations has necessitated the development of reliable correlations for predicting drop sizes.

It is of particular importance in this study to find such a correlation which can be applied over a wide range of flow rates and physical properties due to the refractive index matching technique developed[15]. This technique will be discussed in Chapter 3.

1.1) Drop formation below Jetting Velocities.

Many factors affect the formation of drops at orifices. Guye and Perrot[1] were the first to report that the rate of formation might have an influence on the drop volume, and since that time many authors have made qualitative remarks on the influence of formation rate on drop volume[2-6], though no reliable correlations have been produced. The first reliable quantitative studies of the factors affecting drop size on formation at nozzles were those by Hayworth and Treybal [7] and Null and Johnson[8]. Hayworth and Treybal [7] were the first authors to give a theoretical prediction for drop volume. They proposed the correlation

$$V + 4.11\times10^{-4}\, V^{\frac{2}{3}}\left(\frac{\rho_d\, U_N^2}{\Delta\rho}\right) = 21\times10^{-4}\left(\frac{\gamma\, D_N}{\Delta\rho}\right) + 1.069\times10^{-2}\left(\frac{D_N^{0.747} U_N^{0.365} \mu_c^{0.186}}{\Delta\rho}\right)^{3/2} \qquad (1.1)$$

where the symbols are defined in the nomenclature. Equation (1.1) was presented in the form of a chart from which the drop diameter could be estimated directly without resorting to a trial and error procedure. A major objection

1.1) contd.

to their investigation was the use of surfactants to evaluate the affects of interfacial tension. Its effect cannot be characterized solely by the resultant equilibrium interfacial tension lowering. Scheele and Meister[14] explained the error that can be caused by the use of surfactants. They stated that for a given surfactant concentration the interfacial tension increases with increasing velocity through the nozzle, as a result of slow diffusion of surfactant to the interface. This causes a much greater increase in drop volume with increasing nozzle velocity than is observed for pure liquids.

Null and Johnson[8] presented an experimental correlation based on the observed geometry of the drops. Their results were presented in the form of a correlation which included the Froncle, Laplace and Weber numbers. Both Hayworth and Treybal[7] and Null and Johnson[8] based their analysis on photographs which illustrated the drop formation process.

Harkins and Brown[9] derived an expression for calculating the drop volume at low injection velocities by equating buoyant and interfacial forces. They introduced a correction coefficient (F) to allow for the fraction of the pendant drop remaining at the nozzle when the drop detaches. This was

$$V_o = \frac{\pi D_N \gamma}{\Delta\rho g} F \qquad (1.2)$$

These authors also showed that F is a function of the ratio $\phi/2a$ where a is the Laplace constant

$$a = \left(\frac{2\gamma}{\Delta\rho g}\right)^{\frac{1}{2}} \qquad (1.3)$$

Ryan[10] presented a semi-empirical correlation based on a wide range of experiments and found that

1.1) contd.

$$V = V_o\left[1 + 1.38\,\frac{g\Delta\rho D_F}{\gamma F}\,\frac{D_N U_N}{2U_T} - 2.3\,\frac{\rho_D D_N U_N^2}{2\gamma F}\right] \qquad (1.4)$$

where U_T is the drop terminal velocity which can be estimated from the Hu-Kintner Correlation[20]. The constants in equation (1.4) have been obtained by a statistical treatment of his experimental results.

Rao et al.[11] have recently developed a correlation based on a two stage drop formation process. In the static stage the drop is assumed to expand until the buoyant forces balance the interfacial tension forces. The drop volume at the end of the static stage is given by the equation

$$V_s = \frac{2\pi D_N \gamma F(D_N/V^{\frac{1}{3}})}{(\rho_c-\rho_d)g} \qquad (1.5)$$

where $F(R/V^{\frac{1}{3}})$ is the Harkins and Brown correction factor. During the second stage when the drop is detaching from the nozzle it continues to grow. The authors proposed two models for the second stage. The first model is applicable to low viscosity liquids

$$V = \frac{C}{A} + B\left(\frac{t}{A} - \frac{1}{A^2}\right) + \left(\frac{B}{A^2} - \frac{C}{A}\right)C\,\exp(-At) \qquad (1.6)$$

where

$$A = \frac{6\pi r\mu}{m}\,,\quad B = \frac{Q(\rho_c-\rho_d)g}{m} \text{ and } C = \frac{Q\,v_{c,}\rho_d}{m}$$

The second applies for very viscous liquids

$$A.\ D_s = \frac{B\,t^2}{2} \qquad (1.7)$$

$$\text{where } t = \left(\frac{2AD_s}{B}\right)$$

Like Hayworth and Treybal these authors predicted the effect of interfacial tension from the results of the experiments using surface active agents.

1.1) contd.

A recent analysis by Heertjes, de Nie and de Vries[12] was also based on two stage drop formation. The drop volume released was given by

$$V_F = V_{eg} + V_{re} \tag{1.8}$$

where $V_{eg} = FV$.

The value of V can be obtained from a balance of forces. F is the Harkinsand Brown correction factor.

$$\text{also } V_{re} = 2\, T_9\, t_{re} \tag{1.9}$$

in which the time of release t_{re} follows from

$$T_2\, t_{re}^2 + (T_8 - T_9)\, t_{re} - T_7 = 0 \tag{1.10}$$

where the terms T_2, T_7, T_8 and T_9 are mathematical expressions listed in the paper. There are several expressions to evaluate the T terms depending on the flowrate.

Izard[13], in a recent paper, described a method based on the calculation of the shape of the drop forming at the nozzle tip by means of a pressure balance over the drop interface. The equation considers the vertical forces acting on the drop during formation at a horizontal section increment i

$$F_{NET} = V_i\, g(\rho_c - \rho_d) + \frac{4}{3}\left(1 + \frac{2\rho_d}{2\rho_d - \rho_c}\right)\left(\frac{M^2}{\rho_d\, \pi\, R_n^2}\right)$$

$$- 2\pi\, \gamma\, x_i \sin\phi_i - \frac{2M\,\mu_c}{\rho_d\, x_{max}}\left(\frac{\mu_c + 1.5\mu_d}{\mu_c + \mu_d}\right) \tag{1.11}$$

Equation (1.11) is then integrated over the profile of the drop to predict the final volume of the drop.

A more sophisticated model for drop formation based on the forces acting on the drop has been published by Scheele and Meister[14]. Their analysis was based on a two-stage process of drop formation. They also presented a plot

1.1) contd.

of the Harkinsand Brown correction factor F rs $D_N\left(F/VF\right)^{\frac{1}{3}}$ -

for the use in their correlation

$$V_F = F\left[\frac{\pi\,\gamma\,D_N}{g\Delta\rho} + \frac{20\mu_c Q\,D_N}{D_F^2 g\Delta\rho} - \frac{4\,\rho_d\,Q\,U_N}{3g\Delta\rho} + 4.5\left(\frac{Q^2\,D_N^2\,\rho_d\gamma}{(g\Delta\rho)^2}\right)^{\frac{1}{3}}\right] \qquad (1.12)$$

On review the most suitable correlation giving best agreement with the experimental determination was that of Scheele and Meister. It was found to be easier to apply when the continuous phase viscosity is less than 10 centipoises because the drag term is negligible and an iterative method is not necessary. Moreover they have published comprehensive results of their studies to predict jetting velocity[16], stability of jets[17], jet length[18] and drop formation from cylindrical jets[19]. The significance of the Scheele/Meister procedure will be discussed in paragraph (1.3).

The Null and Johnson and Hayworth and Treybal correlation are empirical so that they cannot be safely extrapolated beyond the range of conditions for which they are established. Further Null and Johnson did not study systems with highly viscous continuous phase and so did not include in their analysis the effect of viscous drag in increasing the drop volume. Hayworth and Treybal used a synthetic wetting agent to lower the interfacial tension in their studies. This must give rise to inaccuracies in predicting the drop volume for reasons stated previously at the beginning of this paragraph.

Rao et al. used the volume formed at infinitely slow formation rate as a basis for their model. This gave rise

1.1) contd.

to some objections to their model since the rate of formation affects the drop volume; they also used a surfactant to lower the interfacial tension of their systems and this also introduces further inaccuracies. Moreover the introduction of two different models for growth during the second period has no connection with the experimental observations made by other workers in this field.

Ryan presented a semi-empirical correlation and he calculated the constants in the correlation using statistical methods which must limit his correlation to the experimental results he employed.

The application of Heertjes, de Nie and de Vries correlation was found to be impractical for repetitive calculation because of the continuing change in the "T" terms when applied to different situations.

Izard's model, while not containing the Harkins and Brown factor, suffers from the fact that the profile of the drop has to be known before the drop volume can be calculated. This has proved to be impractical in this study since numerous drops were formed at the distributor plate containing several orifices.

1.2) Predicting Jetting Velocity.

Above certain dispersed phase velocities through the nozzle the mechanism of drop formation changes. A jet of liquid is formed at the nozzle which breaks into drops. The size of the drops formed from the jets varies considerably from the drops formed at subjetting velocities.

Several correlations can be found in the

1.2) contd.

literature to evaluate the jetting velocity U_J. Hayworth and Treybal[7] have proposed 10 cm/sec as a rough indication for the critical velocity. Ryan[10] obtained

$$\frac{\rho_d}{\Delta\rho}\left(\frac{2\,U_J^2}{D_N\,g}\right)^{\frac{1}{2}} = 1.64\left(\frac{\gamma}{\Delta\rho\,g D_N^2}\right)^{0.95} \qquad (1.13)$$

which can be approximated to ($0.95 \approx 1$)

$$U_J \approx 1.16\left(\frac{\gamma}{\rho_d\,D_N}\right)\frac{1}{\sqrt{g\,D_N}} \qquad (1.14)$$

Scheele and Meister[14] theoretically studied two kinds of jet formation and presented the following correlation for predicting jetting velocity

$$V_J = 2.0\left[\frac{\gamma}{\rho_d\,D_N}\left(1 - \frac{D_N}{D_F}\right)\right]^{\frac{1}{2}} \qquad (1.15)$$

Heertjes, de Nie and de Vries[21] stated that the conditions for jet formation are reached when the necking of a drop begins before the proceeding drop has been released. This criterion is equivalent to the condition that the volume predicted for the rest drop V_{rd} would exceed the equilibrium volume V_{eg} i.e. $V_{rd} = V_{eg}$ (1.16)

They emphasise that the experimental justification of equation (1.16) is difficult, because experimental observation of the transition from normal drop formation to jetting is not sharp. However they used some of the results from the experiment performed to test the validity of their equation and concluded that their criteria for jetting as predicted seem to be valid.

1.3) Drop formation from jets.

Perrut and Loutaty[22] using a photographic technique, proposed the following correlation for predicting the mean size of drops resulting from break up of jets

$$\frac{D_F}{D_N} = 2.07(1 - 0.193\ E_o) \tag{1.16}$$

where E_o is the Eotros number $E_o = \frac{g\Delta\rho\ \Delta_N^2}{\gamma}$.

Christiansen and Hixson[108] had previously proposed a graphical correlation that can be written

$$\frac{D_F}{D_N} = \frac{2.07}{0.485\ E_o + 1} \quad \text{for } E_o < 0.615 \tag{1.17}$$

$$\frac{D_F}{D_N} = \frac{2.07}{1.15\ E_o + 0.12} \quad \text{for } E_o > 0.615 \tag{1.18}$$

As mentioned above in Section (1.1) Meister and Scheele[19] also published the correlation for predicting the volume of drops formed from cylindrical jets

$$V_F = F\left[\frac{2\pi\gamma a}{g\Delta\rho} - \frac{4\ \rho_d\ Q\ U_N}{3\left(\frac{a}{a_N}\right)^2 g\Delta\rho} + \frac{40\mu\ Qa}{D_F^2\, g\Delta\rho} + 7.15\left(\frac{Q^2 a^2 \rho_d \gamma}{(g\Delta\rho)^2}\right)^{\frac{1}{3}}\right] \tag{1.19}$$

where a is the jet radius on drop diameter from the end of the jet which can be predicted from Shifflers jet Contraction Construction[18]

$$\bar{a}^4\left(g\Delta\rho\ D_N\ \bar{z} + \rho_d\ U_N^2 + \frac{8\gamma}{D_N}\right) - \bar{a}^3\left(\frac{8\gamma}{D_N}\right) = \rho_d\ U_N^2 \tag{1.20}$$

which also includes the prediction of jet length L in immiscible liquid systems

1.2) contd.

$$L = \frac{1}{2\alpha}\left[\left(\frac{a^2 U_I}{a_N^2}\right)_{z=5} + \left(\frac{a^2 U_I}{a_N^2}\right)_{z=L}\right] \ell n\left(\frac{a_n}{\xi_o}\right) \qquad (1.21)$$

From the above, it appears that the Scheele and Meister method for predicting drop volume at drop formation is preferable to the others for the following reasons

a) It is based on sound rate of momentum balance

b) It covers the whole range of conditions of drop formation from infinitely slow drop formation to drop forming by the break up of jets, and the predicted volumes agree with experimental volumes obtained.

Most of the systems encountered in solvent extraction problems have continuous phase viscosity less than 10 cp and therefore equation (1.12) can be solved analytically to give values closely agreeing with the experimental values.

CHAPTER 2.

COALESCENCE.

2) Coalescence.

The study of coalescence of drops in dispersions is important in the design of liquid-liquid extraction equipment and other liquid phase separation processes such as jet engine combustions and effluent treatment,

The study of coalescence can be considered in three major sections

a) Coalescence of a single drop at an interface

b) Coalescence of a pair of drops (drop-drop coalescence)

c) The coalescence of drops in closely packed dispersions.

The first has been extensively studied being the simplest practical situation and is relatively easy to reproduce. Drop-Drop coalescence is by far the most difficult to simulate as it occurs in liquid-liquid dispersions. Category (c) is the situation commonly found in dispersion bands of extraction equipment and in effluent treatment tanks. Relatively little research has been undertaken in this field. This is due to the complexity of the process and the lack of techniques which permit observation of the behaviour of drops inside the dispersion.

While this project is primarily concerned with the coalescence of drops in dispersion bands, a review of the work on single drops and pairs of drops will be included. The relevance of the research on the coalescence of single and pairs of drops and their behaviour in a dispersion band will be discussed later.

Firstly the mechanism of coalescence will be discussed briefly. When a drop approaches an interface a film of the continuous phase is trapped between the drop and the interface. This film is squeezed out due to the buoyancy forces between the dispersed and the continuous phase. At a certain

2) contd.

critical thickness the film ruptures allowing the contents of the drop to pass into the dispersed phase homophase. A similar process occurs when two drops approach each other. However the situation becomes more complicated in a closely packed dispersion. The continuous phase is trapped in between many drops and it must drain from in between adjacent drops for the pair of drops to coalesce. This drainage however is restricted by the presence of other drops surrounding the coalescing pair.

To summarize, therefore, it is evident that before coalescence can take place the continuous phase film must drain from between the drop and interface or from between the two coalescing drops.

2.1) Coalescence of single drops at an interface.

Extensive studies on the coalescence of single drops at a plane interface have revealed many of the complex stages involved. The earliest reported work was by Reynolds[23] in 1861 when he observed the behaviour of a rain drop resting momentarily on the surface of the pond. However it was not until the second half of this century that a significant study of coalescence of single drops at an interface was undertaken. All investigators studying coalescence problems have found that the time interval between the arrival of a droplet at an interface and its final disappearance into its parent phase is not constant; there is rather a distribution of times - the distribution being approximately Gaussian. Most investigators found it necessary to make numerous determinations

2,1) contd.

of the coalescence times in order to estimate the mean time from the distribution in the experimental results. Gillespie and Rideal[24] studied 100-200 samples whilst Jeffreys and Hawkesley[25] studied 70-100 drops in a greatly improved apparatus. Cockbain and McRoberts[29] working with drops stabilized by surfactant, were able to obtain reproduceable results from the study of 30 drops.

The coalescence time has been expressed as a mean rest time t_m or the half-life rest time $t_{\frac{1}{2}}$. Generally $t_{\frac{1}{2}}$ has been more reproduceable than t_m and the ratio $(t_m/t_{\frac{1}{2}})$ is always in the range 1.01-1.27. Another phenomenon which has been observed by investigators is the formation of a secondary or sattelite drop. When a drop resides at an interface it may coalesce completely or it may coalesce partially, producing a second smaller drop which will behave in a similar manner to produce yet another even smaller drop. It was first reported by Wark and Cox[26] and later by Mahagan[27] during experiments at air-liquid interface. More recently Lawson[28] photographed the formation of the sattelite drop using high speed photography.

2.1.1) Correlation of rest times and coalescence times.

Several correlations have been reported in the literature for the prediction of rest and coalescence time. Cockbain and McRoberts[29] were among the first to report quantitative measurement of single drop rest times. They reported that the coalescence time data obtained with 30 consecutive drops gave a distribution which agrees with the correlation

$$\ell n\ N = -\ kt + \text{constant} \qquad (2.1)$$

2.1.1) contd.

where N = number of drops not coalesced after time t sec.

Watanabe and Kusui[30], who also worked with a stabilized system, agreed with the type of correlation made by Cockbain and McRoberts. Gillespie and Rideal extended the work to pure systems and found that the relation given as equation (2.1) was in fact exponential.

They also observed that a certain time had to elapse before coalescence was possible and proposed the following equation to correlate coalescence time

$$\log \frac{N}{N_o} = - K(t-t_o)^{1.5} \qquad (2.2)$$

where $K = f\ C_o A_o \left(\frac{6\sigma}{d\mu}\right)^{0.5}$

where C_o A_o characterized the disturbance.

Elton and Picknett[32] studied coalescence in the presence of an electrolyte and suggested the correlation of the form

$$\log \frac{N}{N_o} = ct^n \qquad (2.3)$$

where n was 2 for concentrated electrolyte solution and 3 for other systems.

Differing opinions exist as to which of the above equations (2.2) or (2.3) is applicable; Neilsen, Wall and Adams[31] correlated some of their results with equation (2.2) whereas Konnecke[34] correlated his results for two component systems with equation (2.4). However he plotted his results in the form of log(log) in order to obtain a straight line so that it is possible that such a plot could conceal a curvature. Charles and Mason[45] and Jeffreys and Hawkesley[33] both found that their results were best correlated by equation (2.2) Although Jeffreys and Hawkesley found that the exponent of

2.1.1) contd.

$(t-t_o)$ varied between 1 and 5 for different systems. Sawistowski and James[35] also reported the existence of a minimum time interval (t_o) while Lang[36] showed theoretically that there was a critical thickness below which the film was likely to rupture if subjected to different types of disturbance. Jeffreys and Davies[37] and Hittit[38] review the subject in greater detail.

The most recent study on residence time of a single drop at an interface was by Hittit[38]. He used pilot plant size extraction equipment. Using 6" and 9" Spray Columns he observed that there was no significant difference between mean and half-life coalescence times. Moreover, changing the distance of fall and the bulk dispersed phase static head above the interface had no significant effect on rest times. He concluded that it was difficult to obtain reproducible results in large equipment and questioned the applicability of laboratory single drop measurement in specially constructed cells to the behaviour of drops in swarms in pilot plant or industrial settlers.

2.1.2) <u>Correlation of coalescence times with physical properties.</u>

Relatively few attempts have been made to correlate coalescence time with the physical properties of the system. Perhaps the first attempt published was by Jeffreys and Hawkesley[33]. They proposed the correlation

$$t_{\frac{1}{2}} = 4.53 \times 10^5 \left[\left(\frac{\mu_c^{\frac{1}{2}} \Delta \rho^{1.2}}{\gamma^3} \right) \left(\frac{T}{25} \right)^{-0.7\mu^{\frac{1}{2}}} d^{0.02} \left(\frac{\gamma^2}{\mu_c^{\frac{1}{2}}} \right)^{0.55} L^{0.001} \left(\frac{\gamma^2}{\mu_c^{\frac{1}{2}}} \right) \right]^{0.91} \qquad (2.4)$$

where the significance of the symbols are present in the

2.1.2) contd.

nomenclature.

Jeffreys and Lawson[39] simplified the analysis by stating thatthe temperature only affects the physical properties of the system, and, as such, need not be considered as a variable. The resulting correlation became

$$\frac{\gamma t}{\mu_c d} = 1.32 \times 10^5 \left(\frac{L}{d}\right)^{0.18} \left(\frac{d^2 \Delta\rho g}{\gamma}\right)^{0.32} \qquad (2.5)$$

The above correlation was further supported by Smith and Davies[40]. They showed that

$$\left(\frac{\gamma t}{\mu_c d}\right) \propto \left(\frac{d^2 \Delta\rho g}{\gamma}\right)^{0.25} \qquad (2.6)$$

On comparing the experimental results with their correlation they found that 90% of the experimental results are within $\pm$ 20% of the predicted curve which they argued to be acceptable in view of the nature of rest time phenomenon.

2.2) Factors affecting Coalescence.

Several authors have discussed the factors that affect the rate of coalescence of drops[28,37,40,41,42]. Most of the factors that have been considered were based on the study of single drops residing at a plane interface. It was assumed that similar factors controlled the coalescence of a pair of drops, and the coalescence of drops in dispersion bands. The coalescence of single drops at an interface is accomplished through the draining and rupture of the film of the continuous phase. Therefore the factors that most affect the drainage and rupture process of the film, control the coalescence process. These factors will be discussed below.

2.2.1) System properties.

The rate of film drainage has been established to be of prime importance to the coalescence process and is effected by the system properties.

The correlations to predict coalescence times in terms of the physical properties of the system and various other parameters are listed in paragraph 2.12.

An empirical expression relating to the film drainage area **A** to the drop volume V_d and physical properties has been given by Hartland[43]

$$A = k(v_d)^{\frac{2(n+1)}{3}} \left(\frac{g\Delta\rho}{\gamma}\right)^n \qquad (2.7)$$

where k = 0.5, n = 0.6 for a deformable interface k = 0.25, n = 0.75 for a rigid plane interface. This demonstrates the opposing effects of density differences, and interfacial tension on the drainage rate. Examination of the correlation in Section 2.1.2 shows that the influence of density difference $\Delta\rho$ on the rest time varies with its power in equations (2.4, 2.5, 2.6) which are 1,2, 0.32 and 0.25 respectively. The effect of intefacial tension appears to be less significant in the three equations. However, a high value of interfacial tension results in a very small deformation of the drop at the interface, and this should bring about rapid coalescence. Lang and Wilke[44], on the other hand, have shown that an increase in the interfacial tension also increases the strength of the film with a consequential resistance to film rupture. Large differences in density result in deformation of the drop which increases the area of the drainage film, whereas the hydrostatic forces causing

2.2.1) contd.

drainage do not increase proportionately. Again, this physical property produces opposing effects. Many confirm, however, that the rest time increases with an increase in the density difference between the phases. Finally an increase in the viscosity of the continuous phase relative to the drop phase increases the rest time as would be expected because the resistance to drainage of the film is increased. Robinson and Hartland[47] working with high viscosity liquids (Golden Syrup and Liquid Paraffin) illustrated this effect.

2.2.2) Drop Size.

Numerous investigators have studied the effect of drop size on coalescence time. Using a variety of systems and conditions the majority concluded that the following relation held between the half life of the drop $t_{\frac{1}{2}}$ and the drop diameter d

$$t_{\frac{1}{2}} \propto d^{n}$$ where n varied with the conditions.

Cockbain and McRoberts[29] studied stabilized benzene-water system and found an approximately constant coalescence time for drop sizes in the range of 0.2 to 0.92 cm diameter. Jeffreys and Hawkesley[33] concluded that coalescence time for pure binary systems depended on the drop size by the following relationship $t_{\frac{1}{2}} \propto d^{1.02}$ whilst Lawson[28] found the value of n to be 1.54. An empirical correlation of coalescence time was made by Charles and Mason who gave the value of n = 3.15. The first investigators to give a negative value for n = n-1.28 were Davies, Jeffreys and Smith They stated that the coalescence time was inversely proportional to drop size. Lang[44], in his

2.2.2) contd.

recent work, illustrated no consistent variation with the drop size, rather it varied from system to system. He found that for certain systems there was an increase in coalescence time and with others a decrease as the drop size was increased.

In conclusion the reports on the effect of drop size are far from consistent. This is argued by Hittit[38] to be due to the inevitable contamination in the systems which supersedes the effect of drop size.

2.2.3) Distance of fall of the drop to the interface.

Many investigators working on coalescence time have found that it is generally affected by the settling distance of the drop to the interface. Neilsen[31] reported that coalescence time was dependent on the settling distance of the drop; Lang[36] on the other hand suggested that increase in distance of fall could either increase or decrease the stability of the drop depending on the thermal or mechanical disturbances produced. Lawson[28], Hawkesley[42] and Jeffreys and Hawkesley[33] have shown however that the stability of the drop increases with increase in the distance of fall. Lawson[28] and Jeffreys and Davies[37] suggested that the most logical explanation offered for the discrepancy in the reported results was due to the dimensions of the apparatus and particularly the dimension of the cup that receives the drop. Lawson[28] however showed that the difference between the first step coalescence time and the pre-drainage time was independent of distance of fall. This confirms that the variation of coalescence time with distance of fall is related to disturbances in the interface between the two liquids.

2.2.4) Temperature.

Temperature affects all the physical properties which affect the coalescence time, so that the effects of change in temperature can be predicted from its effect on density, viscosity and interfacial tension. Charles and Mason[45] found the effect of temperature on film thickness to be variable with carbon tetrachloride-water, water-carbon tetrachloride and benzene-water systems respectively. Jeffreys and Hawkesley[33] correlated rest time with temperature of the medium and found $t_{\frac{1}{2}} \propto \left(\frac{T}{25}\right)^{-0.7} \mu_d^{0.5}$. Thus generally an increase in temperature tends to reduce coalescence time unless there is a change brought about in the coalescence process.

In practical situations however there exists a temperature gradient. This tends to have a different effect from the previous situation where steady state exists. Gillespie and Rideal[24], on substituting their water jacket temperature control for an air-bath, found that the coalescence time varied by about 300%. Further both Lawson[28] and Jeffreys and Hawkesley[33] demonstrated that the coalescence mechanism changes in the presence of temperature gradient. Under such conditions they observed the formation of twin secondary drops.

2.2.5) Vibrational effects.

There are conflicting reports on the effects of vibrations on coalescence times of single drops at an interface. Cockbain and McRoberts[29] and Lawson[28] observed the coalescence of groups of drops at an interface and reported that relatively large disturbances propagated

2.2.5) contd.

by the coalescence of one of the drops tended to stabilize the surviving drops. The same conclusion was arrived at by Gillespie and Rideal[24]. They suggested that vibration tended to stabilize the drainage of the film thereby impeding coalescence. Neilsen et al.[31] observed that room vibration and mild agitation had only a slight effect on the rate of coalescence, whilst Brown and Hanson[48] using high energy A.C. field of varying frequencies concluded that coalescence time was virtually independent of the frequency of vibration. On the other hand Lang[36] proposed that vibration introduced random variations in the coalescence times reported by different workers, thereby explaining the distribution in in residence times found in all experimental results. Lang and Wilke[44] recently studied extensively the effect of sonic frequency disturbances and concluded that there was a decrease in drop rest times when these disturbances were applied to tributylphosphate-water system. In conclusion, the general view that vibration tends to stabilize the drops at the interface resulting in longer rest times because of the constant renewal of the continuous phase film, seems to be more acceptable. It must be emphasized at this stage that the above mentioned argument applies only to single or general drops at an interface because the effect of vibration on the coalescence of a pair of drops or of drops in closely packed dispersion is different. Smith[49] has shown that drops travelling freely in a spray column tend to coalesce when vibration is applied to the column, further the coalescence of drops is also enhanced in the bed of drops.

2.2.6) Mass transfer.

Mass transfer may either increase or decrease the rate of coalescence depending upon the direction of solute transfer[37]. If solute is transferred from the drop to the continuous phase coalescence is promoted, but is inhibited when transfer is in the reverse direction. As early as 1946 Johnson and Bliss[50] found that drop sizes in industrial spray extraction towers were considerably larger when solute was diffusing from the drop phase to the continuous phase than for the reverse case, a phenomenon which could be attributed to increasedinterdrop coalescence. This was assumed to be undesirable since it reduced the interfacial area and thus the efficiency of the column.

Since little is known about mass transfer during coalescence of drop the above assumption needs to be confirmed.

Groothius and Zuiderweg[51] demonstrated the effect of mass transfer on coalescence of a pair of drops by pushing two drops together while they were still attached to nozzles. They reported that in every case coalescence was promoted if the transfer of solute was from the drops. Coalescence was also promoted if the solute was transferred from one drop only. More recently Al-Hemiri[52] developed a technique to observe the coalescence of two freely moving drops associated with mass transfer from the drops. His observation was similar to that of Groothius and Zuiderweg.

Jeffreys and Lawson[39] studied a ternary system of benzene-water-acetone. They concluded that their results were in accordance with the theory of Groothius and Zuiderweg. Similar conclusions were arrived at by Sawistowski[53] when working with water-diethylcarbonate

2.2.6) contd.

system with propionic acid as the solute.

McKay and Mason [54] using interferometric methodswere able to confirm that mass transfer changed the rate of film thinning but not the film thickness at rupture. Using isobutanol-water as a binary system and water-benzene-acetone as a ternary system Heertjes and de Nie[55] concluded from their results that the dependence of the rate of coalescence of drop on mass transfer in binary systems cannot be explained entirely by interfacial phenomena. The effect of mass transfer on coalescence was explained by Jeffreys and Davies[37] which was based on the work by Davies[56] on interfacial phenomena. They suggest that the addition of a third component to a pair of immiscible liquids results in the lowering of the interfacial tension. Thus when mass transfer takes place from the drop the concentration of solute in the contact zone between the two approaching drops rapidly reaches equilibrium with the drop. This results in a decrease in the interfacial tension locally and causes the interface in the contact zone to dilate drawing with it part of the intervening film which promotes coalescence. When solute is transferred into the drop the situation is reversed and material from the bulk continuous phase is drawn towards the contact area which retards film drainage and hence stabilizes the drop. They further suggest that other factors doubtless contribute to the change in film stability during mass transfer such as the effect of interfacial turbulence and the variation of the other physical properties in the contact zone.

In conclusion, the effect of mass transfer on coalescence has not yet been fully explained and further

2.2.6) contd.

work on this subject is required to fully understand and explain the above phenomena.

2.2.7) Surfactant.

Whilst the effect of surface active material on coalescence is well established and most investigators agree that it retards the coalescence process, no consistent or a satisfactory explanation has been established. A quantitative approach has been attempted by Neilsen[31]. He proposed the following correlation

$$t_m \propto C^n$$

where t_m = mean coalescence time

C = surfactant concentration

n = a constant which ranges between 0.45 and 0.3.

Gillespie and Rideal[24] postulated that the interfacial tension varies with the surface concentration of the stabilizing agent. Distortion of the film is therefore curtailed by the fact that as the area changes the interfacial tension increases and takes up the tangential stress of the interfacial tension. Cockbain and McRoberts[29] explained this stabilization in terms of the changed wetting properties of the segments. However, Hartland[43] stipulated that the surface active molecules collect on the bulk interface but not on the drop interface, hence the film has one immobile and one mobile boundary causing the drop to sink into the bulk interface more than with pure binary systems, thereby retarding the drainage process. Davies[58] explained the effect of surface active material in the internal circulation of the drop. He stated that the mechanism by which the surface film inhibits

2.2.7) contd.

internal circulation is that the fluid flow will drive the absorbed material towards the rear of the drop, consequently the surface concentration and surface pressure will be higher here and the monolayer will tend to resist further local compression as shown below

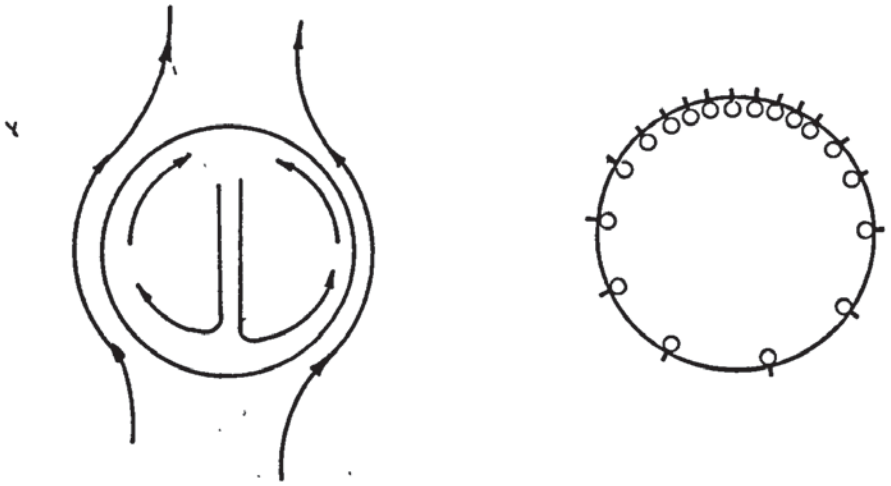

This resistance in the surface damps down circulation inside the drop by reducing the movement of the interface and hence reduces the transfer of momentum. The above theory can be used to explain the resistance of surface active substance in the drop to the movement and subsequent drainage of the continuous film resulting in a stable drop.

2.2.8) Electrical effects.

The effects of electrical field on the rate of coalescence have been carried out by Allen, Charles and Mason[59] and by Allen and Mason[60]. They applied a d.c. field to the drop in such a manner that the force promoting coalescence was several hundred times the gravity. They found that the coalescence rate was greatly increased, although the drop had flattened which gave rise to an increase

2.2.8) contd.

in the area of the draining film. Further they found that stepwise coalescence occurred and the satellite drop produced was considerably smaller. Coalescence was instantaneous at a potential of 900 v.d.c. in most systems studied. Allen and Mason [60] extended this work to study the effect of induced electrostatic fields and showed that the potential difference across the aqueous phase was negligible compared with that across the organic phase. By replacing the water phase with a solution of potassium chloride in water, they could not detect any difference between the rate of coalescence of the water drops and the drops containing Potassium Chloride solution. Brown and Hanson [61] repeated the work of Mason et al. using high energy a.c. field with varying frequencies between 50 c/s and 10 K c/s. They found that there exist critical values for the field strength to bring about instantaneous coalescence. Further the critical value is independent of frequency. The results for the water-Kerosene system agreed with that published by Allen and Mason [60]. Brown and Hanson proposed that the a.c. field induced a very large attractive force between the charged interface and the oppositely charged lower surface of the drops so that drainage and rupture became instantaneous.

2.3) Theoretical Models for the film drainage process.

Many mathematical models have been developed to predict coalescence time in terms of the relevant physical properties by considering the parameters that affect the rate of drainage of the film. These models can be conveniently divided into two categories, those assuming the film profile is of uniform thickness (uniform film models) and those assuming

2.3) contd.

a non-uniform film profile (non-uniform film models). A selection of these models is presented in Tables 2.1a and 2.1b.

All of these models have been discussed in greater detail by many authors[28,49,41,38,37]. The models were based on the drainage of a viscous fluid from in between surfaces of known shapes. A special mention will be made of the parallel plate model (Model I Table 2.1a) since it was found, in the course of this study, that the drops in a closely packed dispersion deform from their spherical shape to a flat sided one (Dodecahedron); this will be discussed in greater detail in paragraph (6.2). Thus the drainage of the continuous phase film can best be described by the parallel plate model.

Model III Table 2.1a (deformable drop-deformable interface) will also be discussed below since it can be used to describe the final coalescence of the drops with the phase boundary.

2.3.1) Parallel plate model (Model I Table 2.1a).

Charles and Mason[45] showed that for a single drop resting at a plane interface and deformed by its own weight

$$c = \frac{d^2}{4}\left[\frac{2\Delta\rho g}{3\gamma}\right]^{\frac{1}{2}} \qquad (2.8)$$

where c is the radius of circle of contact.

Further at equilibrium, the force acting on the drop F is given by

2.3.1) contd.

$$F = \frac{4\pi\gamma}{d} C^2 \qquad (2.9)$$

when the approaching surface is a flat disc of radius C, the film thickness h is uniform and the rate of drainage is

$$\frac{dh}{dt} = - \frac{2F}{3\pi \mu_c C^4} h^3 \qquad (2.10)$$

It follows from integration of equation (2.10) that the time required for the disc to approach the plane surface from a distance h_1 to h_2 is

$$t = \frac{3\pi \mu_c C^4}{4F} \left[\frac{1}{h_2^2} - \frac{1}{h_1^2} \right] \qquad (2.11)$$

Substituting for the area of contact $A = \pi C^2$ in equation (2.11)

$$t = \frac{3\mu_c A^2}{4\pi F} \left[\frac{1}{h_2^2} - \frac{1}{h_1^2} \right] \qquad (2.12)$$

substituting for C and F in equation (2.11) gives

$$t = \frac{\mu_c \Delta\rho \, g \, d^5}{128 \, \gamma^2} \left[\frac{1}{h_2^2} - \frac{1}{h_1^2} \right] \qquad (2.13)$$

When $h_1 >> h_2$

equation (2.12) can be approximated to

$$t = \frac{\mu_c \, \Delta\rho \, g \, d^5}{128 \, \gamma^2} \left[\frac{1}{h_2^2} \right] \qquad (2.14)$$

The forces acting on a drop in a dispersion band are different from those acting on a single drop at an interface, therefore equation (2.9) cannot be used to evaluate F and a new expression for F must be used. Moreover the value of A is fixed and equals the area of one face of the dodecahedra. Equation 2.12 will therefore be used with modification to the values of F and A.

2.3.2) Model III Deformable drop-deformable interface.

Elton and Pickett[32] by neglecting the weight of the drop below the interface and assuming an arbitrary value for the radius R at the surface of contact R = d, obtained an expression of the form

$$t = \frac{\mu_c \Delta\rho\ g\ d^5}{32\ \gamma^2}\left[\frac{1}{h_2}^2\right] \qquad (2.15)$$

This was based on the general drainage equation (2.10)

$$\frac{dh}{dt} = -\frac{2\pi F}{3\mu_c A^2}\ h^3 \qquad (2.16)$$

Models I and II are the limiting cases for this model when $T = \infty$ and $R = \frac{d}{2}$ respectively. Later Chappelear[62] justified the selection of R = 2b by considering the pressure differences in the film and the adjacent phases and by neglecting the thickness of the film i.e. $h \ll R$

$$\rho_1 - \rho_2 = \frac{2\gamma}{R} = \rho_2 - \rho_3 \qquad (2.17)$$

where ρ_1, ρ_2 and ρ_3 are the pressures inside the drop, in the middle of the film and in the dispersed phase homophase respectively. For small drops the internal pressure is large compared with the hydrostatic head and since the pressure drop across the interface is zero

$$\rho_1 - \rho_3 = \rho_1 - \rho_4 \qquad (2.18)$$

$$\therefore\ 2\left(\frac{2\gamma}{R}\right) = \frac{4\gamma}{d} \quad \text{i.e. } R = d.$$

Princen[63] extended this model to include the case of a large drop. He stated that in the limit of an infinitely large drop where the drop is a hemisphere with radius $R = \frac{d}{2}\sqrt[3]{2}$, A and F are given by $A = 2\pi R^2$ and $F = 2\pi R\gamma$ respectively. Substituting for A and F in equation (2.16) leads to

2.3.2) contd.

$$-\frac{dh}{dt} = \frac{\gamma}{3\,\mu_c\,R^3}\,h^3 = \frac{4\gamma}{3\mu_c\,d^3}\,h^3 \qquad (2.19)$$

Integrating equation (2.19)

$$\therefore\ t = \frac{3\mu_c d^3}{8\gamma} \cdot \frac{1}{h^2} \qquad (2.20)$$

Once again, Model III cannot be used without modification to the values of F and A in equation (2.16) to fit the situation of drop coalescence at a phase boundary in a closely packed dispersion.

The studies of single drops must have originated from the desire to simplify the problems associated with multiple drop systems by considering the elementary unit of a dispersion. Whilst useful information has emerged from these studies, such as the above drainage models, the situation described is far removed from the behaviour of drops in dispersion bands. Further it is believed that the behaviour of a drop at an interface does not represent the elementary unit of dispersion. Consequently any data obtained cannot be directly used to describe the behaviour of drops in dispersions. Several techniques have been developed in the course of this work which facilitated the study of the elementary unit in a dispersion. These will be discussed in greater detail in Chapters 3 and 5.

TABLE 2.1a.

UNIFORM FILM MODELS

I Deformable Drop
Rigid interface (45,24)
Uniform film

$$t = \frac{\mu_c \Delta\rho g d^5}{128\,\gamma^2}\left[\frac{1}{h_2^2} - \frac{1}{h_1^2}\right]$$

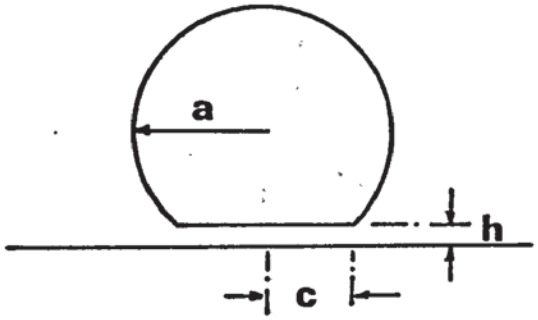

II Rigid drop
Deformable Interface (36,62)
Uniform film

$$t = \frac{9\mu a^3(a-s)^2}{(2a^3-3a^2s-s^3)(\Delta\rho g)}\left[\frac{1}{h_2^2}\right]$$

For small drops

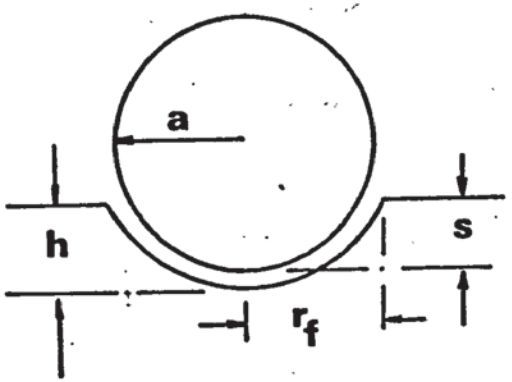

III Deformable drop
Deformable Interface (32,63)
Uniform film

$$t = \frac{\mu_c\ \Delta\rho g d^5}{32\gamma^2}\left[\frac{1}{h_2^2}\right]$$

where R = 2d

For large drops

$$t = \frac{3\mu_c d^3}{8\gamma}\left[\frac{1}{h_2^2}\right]$$

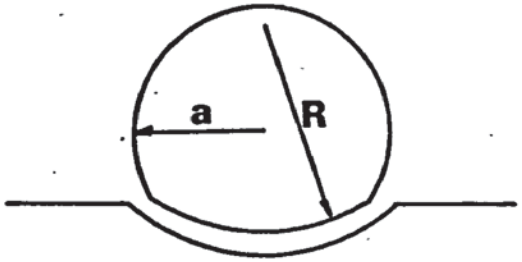

a is the radius of the drop = $\frac{d}{2}$

TABLE 2.1b

NON-UNIFORM FILM MODELS.

IV Rigid drop, Rigid Interface [45], Non-Uniform film

$$t = \frac{a\,\mu_c}{2a\Delta\rho\,g} \cdot \ell n(n_1/n_2)$$

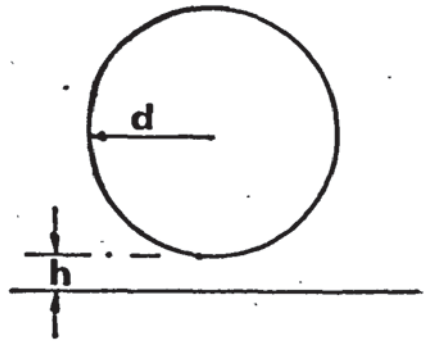

V Deformable drop, Deformable Interface [64], Non-uniform film

$$h = \left[\frac{0.0096n^2\mu_c r_f^{\,6}}{t\,a\,\gamma}\right]$$

where n = number of surfaces that resists heat

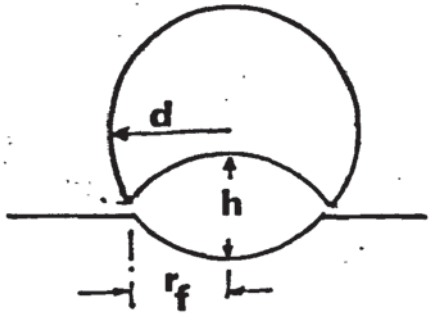

VI Rigid drop, deformable Interface [33], Non-Uniform film

for $\lambda = R/d > 1$

$$t = \frac{6\,\pi\mu}{4\phi^2 F}\left[\ell n\,\frac{h_2}{h_1} + \ell n\left(\frac{h_1+\theta}{h_2+\theta}\right) + \frac{\theta}{h_2+\theta} - \frac{\theta}{h_1+\theta}\right]$$

for $\lambda = R/d < 1$

$$t = \frac{6\,\pi\mu}{4\phi^2 F}\left[\ell n\,\frac{h_2'-\theta}{h_1'-\theta} + \ell n\,\frac{h_1'}{h_2'} + \frac{\theta}{h_2'} - \frac{\theta_1}{h_1'}\right]$$

where $\phi = \frac{1}{d}\left(1 - \frac{1}{\lambda}\right)$, $\theta = (\lambda-1)\left(\frac{d}{2} - s\right)$

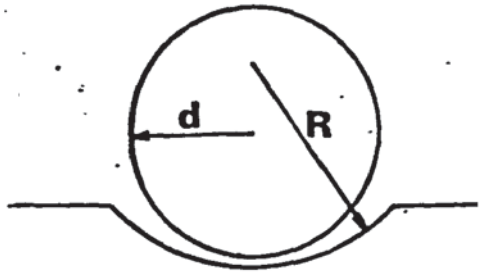

h' is the minimum film thickness at the periphery of the film

a is the radius of the drop $= \frac{d}{2}$

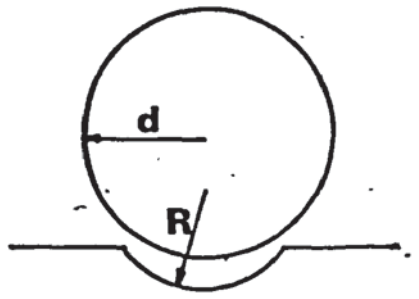

2.4) Drop-Drop Coalescence.

The coalescence between drops within a dispersion must be considered before kinetics of phase separation can be predicted quantitatively. In contrast to the experimental work carried out on drop-interface coalescence, relatively little work has been undertaken on drop-drop coalescence. As stated above, this is undoubtedly due to the difficulties in performing such experiments in a system which is inherently unstable. In spite of these difficulties a few techniques have been developed to study drop-drop coalescence[66,67,68,73,69]. It is worth noting that the area of drop-drop coalescence in liquid-liquid dispersions is closely related to the coalescence of drops in a gaseous phase and therefore certain investigations of the latter may prove useful[70,71,72].

2.4.1) Experimental investigations.

Kintner[69] was one of the first to report on drop-drop coalescence. Using two drops of n-butyl benzoate in water which was placed in a watch glass, he observed the same succession of events as for a drop coalescing at a flat interface. By dyeing one drop he further observed that no mixing occurred initially but some mixing by slow connection currents did occur after coalescence was complete. McKay and Mason[73] formed a water drop in an immiscible organic phase and allowed it to settle into a flat non-wettable surface of lucite. A second drop with 1% of acetone was allowed to fall gently on to this. The acetone promoted instantaneous coalescence and prevented the second drop from rolling off. They showed from this work that partial coalescence took place when the ratio of drop diameter was greater than 3.50; below this value no secondary drop was formed. When this ratio was greater than

2.4.1) contd.

12 the surface of the larger drop was undisturbed by the coalescence and the mechanism was identical to that observed for partial coalescence at an interface. Robinson and Hartland[67] studied the approach of two or more drops towards an interface and towards each other using liquids with high viscosity in a two dimensional bed. They measured the arc lengths of the profile. Observation was also made of one drop resting at an interface and of two or more drops resting on this one in a vertical column.

Scheele and Leng[66] described an experimental technique and apparatus using anisole droplets formed in water from two horizontal nozzles which were adjustable through 30°. Collision velocities were in the range of 1.9 to 11.2 $cm.sec^{-1}$ and a high speed photo-kinetic camera was used to record the phenomenon. They reported that the drops were oscillating and the oscillation frequency (w) was predicted from the equation given by Schroeder and Kintner[74]

$$w = \frac{1}{2\pi}\left[\frac{24\,\gamma\,q}{\left(\frac{d}{2}\right)^3(3\,\rho_d - 2\,\rho_c)}\right]^{\frac{1}{2}} \qquad (2.21)$$

where q is an amplitude dependent coefficient given by

$$q = 1 - \left[\frac{d_{max} - d_{min}}{2\,d_{ave}}\right]$$

Their conclusion based on the results they obtained can be summarized as follows:-

2.4.1) contd.

a) There were no obvious relations between coalescence probability and impact velocity.

b) Coalescence phenomena appeared to be very sensitive to the phase of oscillation at point of contact.

c) The classical parallel disc immobile interface model, describing film thinning, fails by several orders of magnitude to predict fast enough rates of thinning to enable rputure to occur within the apparent time of contact.

d) The dependence of the rate of expansion of the radius of apparent contact on the oscillation phase at moment of contact,can explain the sensitivity of coalescence phenomena to drop oscillation behaviour.

In a recent study to measure the coalescence time between liquid drops by Sivokova and Eichler[88] one drop was situated vertically above another and they measured the time between the drops touching and resting in a special section.

In conclusion, some of the techniques required mechanical support to carry out the coalescence of a pair of drops, others used mass transfer to enhance coalescence. This could affect the mechanism of coalescence. This is not the case with the technique developed by Scheele and Leng, however it is limited to liquids with low density differences.

It is clear, therefore, that these experimental techniques require improvement to cover the case of "overtaking collisions" as distinct from "head on" collisions.

2.4.2) Theoretical Studies.

The mechanism of coalescence of two drops is very

2.4.2) contd.

similar in principle to that of the coalescence of a single drop with an interface. The two drops approach each other, squeezing out the continuous phase film separating them, and when the film is thin enough, disturbances of a random nature rupture it and coalescence follows.

Most of the models published are based on the above criteria, McAvoy and Kintner[65] analysed the approach of equal size spheres. They derived an equation for the rate of film thinning by assuming that the initial and final film thicknesses h_1 and h_2 were negligible compared to the drops diameter d

$$t = \frac{3\pi \mu_c}{F}\left[\frac{d^2}{4}\, \ell n\left(\frac{h_1}{h_2}\right)\right] \qquad (2.21)$$

They pointed out that the only difference between equation (2.21) and the equation derived by Charles and Mason[45] for the rate of approach of a spherical drop to a flat interface

$$t = \frac{6\pi \mu_c}{F}\left[\frac{d^2}{4}\, \ell n\, \frac{h_1}{h_2}\right] \qquad (2.22)$$

is a numerical constant. Jeffreys and Davies[37] stated that the McAvoy and Kintner model was analogous with the solution proposed by MacKay and Mason[73] for a rigid drop approaching a rigid plane interface, and can be readily extended to the case of two spheres of diameters d_1 and d_2. For this case, the rate of approach of the spheres becomes

$$\frac{dh}{dt} = -\frac{F\, h}{6\pi\mu}\left[\frac{2}{d_1} + \frac{2}{d_2}\right]^2 \qquad (2.23)$$

They further argued that none of the above models were applicable to large drops since some deformation must take place. By assuming the deformation to result in parallel

2.4.2) contd.

surfaces analogous to the conditions assumed by Gillespie and Rideal[24] they stipulated that the rate of approach for equal sized drops of diameter (d) is

$$\frac{dh}{dt} = - \frac{32\pi\gamma^2}{3\mu_c d^2 F} h^3 \qquad (2.24)$$

Princen[63] considered the formation of a dimple in the drop surface resulting in a non-uniform film between the drops. His study resulted in a modification of equation (2.24)

$$\frac{dh}{dt}\,\text{min} = \frac{2.78\pi\gamma^2}{\frac{d^2}{4}\mu_c F} h^3_{min} \qquad (2.25)$$

and

$$\frac{dh}{dt}\,\text{max} = \frac{13.0\pi^3\gamma^4}{\mu\frac{d^2}{4}F^3} h^5_{max} \qquad (2.26)$$

In all of the above models the interface was assumed to be immobile. Murdoch and Leng[75] considered the case of a mobile film. They obtained the following model for the rate of drainage of film between equal size drops

$$h = \frac{h_o}{1 + K h_o \bar{\mathcal{J}}_o} \qquad (2.27)$$

where $$\bar{\mathcal{J}}_o = \int_o^t \frac{F}{R^4}\, dt \qquad (2.28)$$

and $$K = \frac{8 R_d}{\pi \mu_d} \qquad (2.29)$$

where R = radius of the disc at the rim

R_d = effective distance in the drop

which was verified with the data obtained by Scheele and Leng[66]. However their model was based on the assumptions that the collision was symmetrical and the thinning fluid

2.4.2) contd.

was bounded by two flat disc-like expanding interfaces. This must limit the application of their model. A further limitation is the fact that values of $\mathcal{J}_o$ should be calculated from information recorded photographically. They concluded that the thinning rate was greatly dependent on the mobility of the interface.

The connection between the drop interface and drop-drop coalescence has been established in terms of film drainage from the previous paragraphs. However further work is required both experimentally and theoretically in the field of drop-drop coalescence so that the drop-drop coalescence phenomena can be fully understood.

2.5) Coalescence in dispersions.

Mass transfer between two liquids may be enhanced by increasing the interfacial area and interfacial turbulence. This is usually brought about by dispersing one phase in another in the form of drops. When the mass transfer is complete the drops must lie recombined to form the bulk phase. The drops are allowed to collect in a closely packed dispersion in which they may coalesce with each other (this will be referred to as "interdrop coalescence" as distinct from drop-drop coalescence referred to in paragraph (2.4)), but finally coalescence at the phase boundary must occur. (This will be referred to as Drop-Interface Coalescence).

In some cases drops appear to coalesce with the vessel wall when they are in fact coalescing with the phase boundary residing at the vessel wall. (This will be referred to as "drop wall coalescence".)

As the dispered phase flowrate increases so does

2.5) contd.

the thickness of the close packed dispersion[81]. At steady state the rate of drop coalescence at the phase boundary must equal the flowrate. As stated in Section 2, the rate of inter-drop, drop interface and drop wall coalescence depends on the rate of drainage of the film of the continuous phase trapped between either the drops or the drop and the coalescing interface.

If however the dispersed phase flowrate is reduced such that the rate of drop interface coalescence is greater than the rate of drops arriving at the interface, an incomplete or a monolayer of drops is formed at the phase boundary. This seems to be the logical extension in the study of single drop and drop-drop coalescence, to the study of the behaviour of drops in dispersion bands.

2.5.1) Monolayers.

Monolayers are produced and maintained via a dynamic process i.e. the continuous arrival and removal of drops at an interface. Various kinds of disturbances can result from such a process which were found to change the rest times of the drops in monolayer from that of a single drop. The arrival of a drop can affect the drops in the monolayer in the following manner

a) Direct collision of the arriving drop with the coalescence drop in the monolayer.

b) Impact of the arriving drop with the interface inducing wave propagation and causing oscillation of the coalescence drop as well as the interface.

Another cause of disturbance is the coalescence of a drop with the interface or with an adjacent drop. All

2.5.1) contd.

of the above disturbances result in vibrations of the interface. The effect of vibration on coalescence time was discussed in paragraph (2.2.5). In general the effect of vibration at an interface tends to bring about an increase in coalescence time due to the repeated renewal of the continuous film. Lawson[28], by observing the impingement of one drop with another at the interface, concluded that the coalescence times of both drops generally increased. Furthermore Jeffreys and Hawkesley[33] observed that a small tilt of the mid-axis of a single drop with an interface affected the coalescence time. Robinson and Hartland[67] investigated the effect of neighbouring droplets in a two dimensional array. They calculated the arc lengths from drop profiles which were obtained from photographs. On comparing these lengths they reported that the arc length was least for the drop in the middle and reached a minimum when there were about four drops present. The reduction in the arc length was about 30% less than that for a single drop for liquid paraffin - golden syrup and liquid paraffin-glycerol systems and 12% for aqueous glycerol-silicone system. They also observed that for small drops, the one in the middle which had the shortest arc length coalesced first with the interface, but for larger drops interdrop coalescence occurred first.

The decrease in arc length was explained by the increase of the horizontal forces exerted by the neighbouring drops. They concluded that the shape of liquid drops approaching a deformable interface was affected by the presence of adjacent drops.

2.5.1) contd.

Davies, Jeffreys and Smith[46] correlated the drop interface and interdrop coalescence times in monolayers. The equation obtained from drop interface was

$$\frac{t\,\gamma}{\mu_c d} = 31 \times 10^3 \left(\frac{d^2 g \Delta\rho}{\gamma}\right)^{-1.24} \left(\frac{\mu_d}{\mu_c}\right)^{1\,03} \qquad (2.30-$$

and for interdrop coalescence the equation was

$$\frac{t\,\gamma}{\mu_c d} = 413 \times 10^3 \left(\frac{d^2 g \Delta\rho}{\gamma}\right)^{-0.3} (t'N)^{-0.5} \left(\frac{\mu_d}{\mu_c}\right) \qquad (2.31)$$

Their results were obtained on a spray column of 2" diameter and measurement of coalescence times were made from cine films. It was reported that the coalescence time t was inversely proportional to the drop size. This is evident in equation (2,,30) and (2.31) where $t \propto d^{-2.48}$ and $t \propto d^{-0.6}$ respectively. Also if the rate of drop arrival at an interface was increased, the mean drop interface coalescence time decreased slowly. However they found that the incidence of interdrop coalescence increased rapidly as the inlet drop size decreased and to a lesser extent as the drop arrival rate decreased.

Topliss[78] studied the behaviour of drops in monolayers using a specially designed apparatus. The test section was a 6" diameter glass column. A glass heat-exchanger was used to control the temperature of the dispersed phase and the whole equipment was enclosed in an air bath. The dispersed phase was not recycled but a freshly dispersed phase which had been saturated prior to the experiment was used. Finally high speed cine films were taken to record the behaviour and to evaluate drop sizes, interdrop and drop inter-

2.5.1) contd.

face coalescence times. He found that the coalescence times for drops in monolayer to be higher than for single drops, the variation being dependent on the proximity of adjacent drops. No satisfactory distribution was obtained for drop-drop coalescence. Such coalescences were found to be low for the continuous production of drops but high for the batchwise production of drops. In the latter the high rate of interdrop coalescence results in a final few drops which coalesce with the interface.

Using toluene-water system in a 6" diameter column Hittit[38] studied the residence time of drops in monolayers. Measurements were made using a stop watch on dyed drops produced from a syringe assembly in a swarm of undyed drops. From a plot of the residence times of single drops and of drops in monolayers versus drop diameter, he concluded that for single drops at a plane interface coalescence times show an increase with drop diameter over the range 0.09 cm. to 0.3 cm, but then apparently attain an almost constant level. For monolayer, however, no drop size effect is apparent and the data obtained was approximately constant at about 2 seconds. The wider distribution of monolayer data he argues to be indicative of the more complicated environment. This was attributed to the difficulty of obtaining a true monolayer, due to the tendency of assembling of the drops on 2-3 layers at the column wall, and due to higher turbulence in the midsection.

Komasawa and Otake[77], using benzene water system in glass-brass apparatus, studied the behaviour of stabilized and non-stabilized drops at an interface. Their readings were

2.5.1) contd.

obtained from photographs taken every 0.25 sec or every 2 sec. They stated that no large differences were seen between the stabilities of a single drop and of multi-drop in a layer in the absence of a stabilizing agent.

Finally little has been reported on the formation of secondary drops (partial coalescence). Davies, Jeffreys and Smith[46] showed a photograph of anisole drops in water giving evidence of stepwise coalescence, resulting in secondary drop formation. However no explanation was forwarded as to whether the formation of secondary drops resulted from interdrop or drop-interface coalescence.

2.5.2) Multi-layers or dispersion bands.

As stated previously, when the rate of arrival of drops to the coalescence boundary is greater than the rate of removal of drops at that boundary, an accumulation of drops takes place. This results in the formation of multilayers of closely packed drops i.e. a dispersion band, sometimes referred to as a bed of drops. In this case the behaviour of drops becomes more complicated than for a monolayer and to fully explain and express this in mathematical terms presented some difficulties. Despite these difficulties several attempts have been made and the resulting mathematical models will be discussed.

The models can be conveniently divided into unsteady and steady state. The formerinclude the models by

2.5.2) contd.

a) Lee and Lewis[79]

b) Komasawa and Otake[77]

the latter include the models proposed by

c) Jeffreys et al.(Ideal model[80])

d) Jeffreys et al. (differential models[81])

e) Smith[49]

f) Hittit[38]

The above mentioned models can however be divided in a different way based on continuous phase hold up. When the model assumes high hold ups this implies little or no deformation in the shapes of the drops and limited fluidization of the drops takes place. In this situation the bed behaves as "liquid-liquid froths". Models (a,b,f,c) can be included in the above category. On the other hand, when the model assumes low continuous phase hold up with a consequential deformation to the shape of the drops and no fluidization of the drops, the dispersion band then behaves as "liquid-liquid foams". This category includes model (e).

2.5.3) Mathematical Models for dispersion bands.

a)Lee and Lewis Model[79].

They produced their dispersion band in a 7" diameter cylindrical stainless steel tank fitted with baffles and two vertical glass windows. A varied-disc turbine type impeller was used to disperse the organic phase in water. The dispersion was then allowed to settle to form the bed of drops. They observed that the interdrop mode of phase separation occurred when the phases were clean. This resulted in large drops which finally coalesced with the interface. In the

2.5.3) contd.

presence of sodium benzoate however, interdrop coalescence was reduced and the drops mainly coalesced with the interface. They stated that the latter mode of phase separation was similar to the sedimentation or fluidization of a dispersion of solids. This was the basis of their model since they also stated that mathematical analysis of the interdrop mode of phase separation appears to be difficult at present.

By assuming uniformly sized drops of diameter d coalesce with the interface, they derived an expression for the total number of drops per unit volume N of emulsion layer

$$N = \frac{(1 - \varepsilon)}{\pi d^3/6} \qquad (2.32)$$

They further assume that for fluidization to be maintained, two conditions must be satisfied simultaneously.

a) The drops at the interface must coalesce and thus release continuous phase which has a superficial downward velocity U relative to the drops.

b) The downward velocity U must be sufficient to fluidize the drops beneath the interface and the voidage ε of the emulsion layer will adjust itself to accommodate the flow.

c) The number of drops adjacent to the interface at any time is $N^{\frac{2}{3}}$ providing that the voidage does not change in the vicinity of the interface.

The number of drops released per unit time per unit area of interface is

2.5.3) contd.

$$M = N^{\frac{2}{3}}/\tau \qquad (2.33)$$

where τ is the rest time of a drop at an interface. The volume of dispersed phase released per unit time per unit area is

$$V = U(1-\varepsilon)/\varepsilon \qquad (2.34)$$

Relating this to the number of drops and the volume of each drop

$$\frac{\pi\, d^3 N^{\frac{2}{3}}}{6\tau} = \frac{U(1-\varepsilon)}{\varepsilon} \qquad (2.35)$$

Substituting in equation (2.33) and rearranging

$$U = \left(\frac{\pi}{6}\right)^{\frac{1}{3}} \frac{\varepsilon}{(1-\varepsilon)^{\frac{1}{3}}} \frac{d}{\tau} = V \frac{\varepsilon}{(1-\varepsilon)} \qquad (2.36)$$

for fluidized emulsion layer U and ε may be related by the equation of Richardson and Zaki[107]

$$U = U_t\, \varepsilon^n \qquad (2.37)$$

where U_t is the terminal velocity of the drop. Thus

$$\frac{\tau}{d}\left(\frac{6}{\pi}\right)^{\frac{1}{3}} U_t = \frac{1}{(1-\varepsilon)^{\frac{1}{3}}\ \varepsilon^{n-1}} \qquad (2.38)$$

The final equation was proposed to evaluate ε hence V and the total time required for phase separation.

Two objections can be made against this model.

1) The assumption that only drop interface coalescence occurs is not valid even for stabilized systems, since, in a close packed dispersion, drainage is not restricted to the film between the drops and the interface alone, but drainage of the film between the drops also takes place. Further, the two drainage mechanisms are interrelated and occur simultaneously. It is therefore

2.5.3) contd.

1) contd.

conceivable that the film between the drops could also reach its critical thickness for rupture. This would inevitably lead to interdrop coalescence.

2) The assumption that the downward flow of the continuous phase is sufficient to fluidize the drops beneath the interface implies that close packing does not take place. It was found by many researchers in this field that close packing of the drops does take place[49,41,38,15,67]. Moreover, distortion to the shape of the drops may also occur, which would result in an even smaller hold up of the continuous phase scarcely enough to cause fluidization.

b) Komasawa and Otake Model[77].

The dispersion band was formed in a brass column of rectangular cross section. Drops of benzene were dispersed in water from several nozzles. The height of the bed was adjusted by varying the flowrate of the dispersed phase. When steady state was reached at the desired bed height the supply of the dispersed phase was shut off. The collapse of the bed was then observed photographically.

They defined the measure of stability of a drop-layer L as the average time (life time) that drops can remain in that layer, as follows

$$L = \frac{1}{V_o}\int_0^{V_o} t\, dV = \int_0^{T} \left(\frac{Z}{Z_o}\right) dt \qquad (2.39)$$

where V and Z refer to the volume and the height of a drop layer at time t respectively, the original values being V_o and Z_o.

2.5.3) contd.

b) contd.

Observations were made of the variation of height $\left(\frac{Z}{Z_o}\right)$ with time t. From their observations they concluded that when an exponential relation holds between $\left(\frac{Z}{Z_o}\right)$ and t, integration can be readily performed mathematically as follows

$$\frac{Z}{Z_o} = \exp(-kt) \qquad (2.40)$$

$$\therefore \quad L = \int_o^\infty \exp(-kt)dt = {}^1/k \qquad (2.41)$$

where k is a constant, particular to each drop layer.

The above model examines the overall picture of a collapsing bed and does not investigate the internal mechanism of the bed such as film drainage and interdrop coalescence. This tends to result in over-simplification of the problem. The term life time L is not fully explained since the life of a drop can end via interdrop or drop wall coalescence as well as drop interface coalescence.

Finally, Ali[41] showed that under certain circumstances a bed can split in the middle rather than the gradual layer by layer disappearance.

c) Jeffreys et al. (Ideal model)[80].

Jeffreys et al. was one of the first workers in this field to examine the behaviour of drops in dispersion bands under steady state conditions. The observation was made in a laboratory mixer settler. The mixing chamber was a cylindrical glass tank and a four bladed

2.5.3) contd.

c) contd.

brass paddle impeller was used to disperse the phases. The dispersion was then allowed to flow into the settler which was a rectangular tank constructed from perspex. After separation the phases were recycled to the mixer.

The dispersion formed a horizontal wedge shape which extended over about 70% of length of the settler. The model assumed the following

1) The drops packing arrangement in the wedge is a face-centred cubic configuration.
2) There is no distribution of coalescence times irrespective of whether coalescence is interdrop or drop-interface, then the idealised wedge will assume the shape shown in Figure (2.1).
3) In this idealised situation one row of drops adjacent to the interface passes into the bulk of the dispersed phase while the remainder coalesce to half their original number. The coalescence processes occur within one step called a "coalescence stage".
4) Drops are rigid and spherical.
5) Inlet drop sizes are all equal.

By conducting a number balance over the wedge they obtained the following equation

$$x_n = A\, 2^{-2n/3} - 1.73 \qquad (1)$$

where A is an arbitrary constant and x_n is number of droplets in vertical column of stage n. By further considering the feed rate V and the number of drops entering the settler per unit time an expression for the number of the drops in a vertical column at the entry to the wedge

2.5.3) contd.

c) contd.

x_o was produced

$$x_o = \frac{8.46\ aV}{\pi d_o(w-0.29d_o)(1.41v-0.41d_o)} \qquad (2)$$

Equation (1) was solved for the value of n = 0 to give

$$\frac{x_o + 1.73}{x_n + 1.73} = 1.59^n \qquad (3)$$

They concluded that at the tip of the coalescence wedge x_n is equal to 1.0 and therefore x_o was estimated from equation (2), the number of coalescence stage n was evaluated from equation (3). Finally, the length of the coalescence section was estimated from

$$L = n\ v\ \tau$$

where τ is the idealized coalescence time.

On comparing their model with the experimental data obtained using Kerosene dispersed in water, they found that the predicted ratio of d_n/d_o was greater than the one determined experimentally. They attributed these discrepancies to the assumption that the velocity of the dispersed phase in the wedge was constant. Further the theoretical holdup of the dispersed phase of 74% based on the rigid spheres is not valid and photographs showed a much higher holdup value. The values of τ used were that of a single drop at an interface. This could be a further source of error since coalescence times in dispersions are different from those of a single drop.

Finally the model predicts not the overall length of the wedge but only the length of the coalescence section and the latter could be 5 to 25% of the total wedge length.

FIG. 2·1

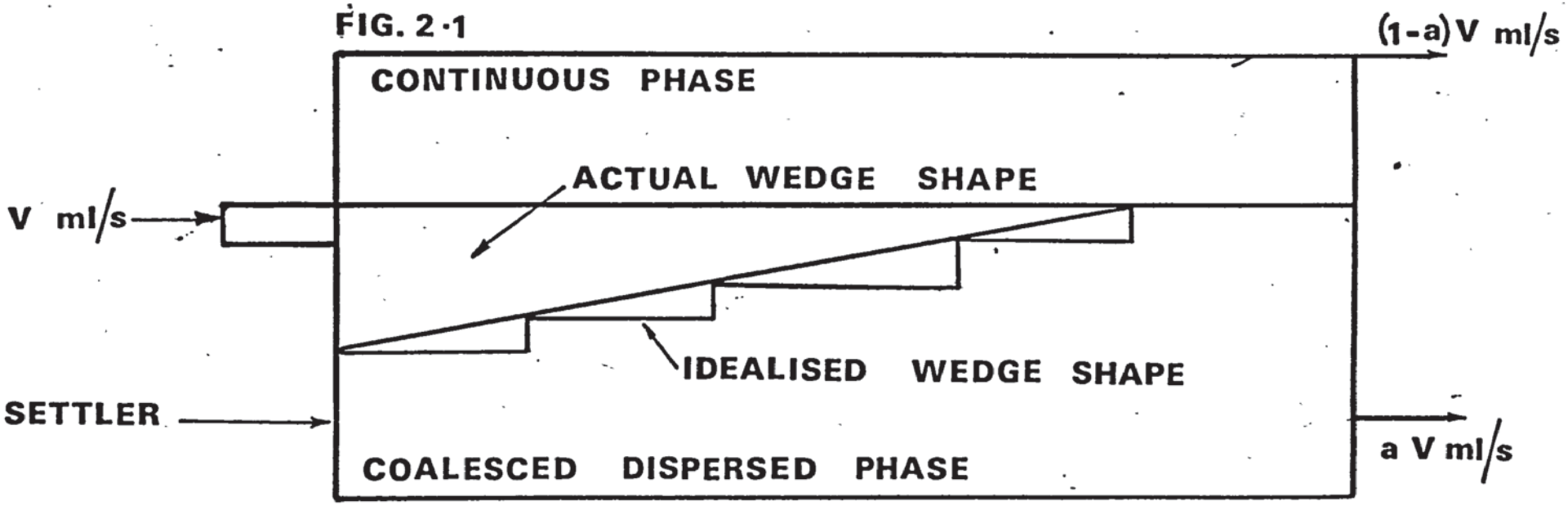

SHAPE OF ACTUAL AND IDEALISED COALESCENCE WEDGES

2.5.3) contd.

d) Jeffreys et al.[81] (differential model).

Based on the results obtained from the equipment described for model (d) Jeffreys et al. derived a more realistic and sophisticated model to describe the behaviour of drops in a horizontal dispersion wedge. By considering a small increment $\delta\ell$ in the wedge at a distance ℓ from the inlet (Figure 2.2) they derived an equation for the material balance over the increment

$$\frac{n\pi d^3}{6} = \left(n - \frac{dn}{d\ell}\,\delta\ell\right)\frac{\pi}{6}\left(d + \frac{dd}{d\ell}\,\delta\ell\right)^3 + \frac{\pi\phi^3}{6}\left(\frac{1}{\tau^*}\,\frac{\delta\ell\,\eta^*}{\pi\,\phi^{2/4}}\right) \qquad (2.54)$$

where n is the number of drops entering the element per second and d is the mean diameter of the drops.

Expanding equation (2.54) and considering first order terms only and assuming the drops as rigid spheres, they obtained

$$\frac{3}{d}\,\frac{dd}{d\ell} - \frac{1}{n}\,\frac{dn}{d\ell} + \frac{4}{\pi}\,\frac{\eta^*}{\tau^*}\,\frac{1}{nd^2} = 0 \qquad (2.55)$$

where η^* is the area packing efficiency of drops at the interface and τ^* is the mean drop interface coalescence time. A number balance of the drops over the increment was also carried out by assuming that the number of drops entering the element per second must be balanced by the number of drops leaving plus the number of drops coalescing at the interface and half the number of drops coalescing together by interdrop coalescence mechanism, thus

$$n = \left(n - \frac{dn}{d\ell}\,\delta\ell\right) + \left(\frac{\delta\ell}{\pi\,d^{2/4}} \cdot \frac{\eta^*}{\tau^*}\right) + \frac{1}{2}\,\frac{h\,\delta\ell\,\eta}{\left(\frac{\pi d^3}{6}\right)} \qquad (2.56)$$

where η is the volume packing efficiency of drops in the wedge.

2.5.3) contd.

d) contd.

Rearranging equation (2.56) gives

$$\frac{dn}{d\ell} = \frac{1}{d^2}\left(\frac{3}{\pi}\,\frac{\eta}{\tau}\,\frac{h}{d} + \frac{4}{\pi}\,\frac{\eta^*}{\tau^*}\right) \qquad (2.57)$$

where h is the depth of wedge and τ is the mean interdrop coalescence time.

They stipulated that the volume of dispersed phase entering the wedge per second must equal the dispersed phase coalescing at the interface over the entire wedge. Interdrop coalescence will influence only the average drop diameter, packing efficiencies and mean coalescence time at the interface. Thus, by assuming a small angle of inclination (θ) of the wedge i.e. the interface approximate to the wedge length (L), they derived an equation for the overall volume balance of the dispersed phase:-

$$n_o\, d_o^3 = \frac{4}{\pi}\int_0^L \frac{\eta^*}{\tau^*}\, d\, d\ell \qquad (2.58)$$

where n_o is the number of drops of mean diameter d_o entering the wedge.

By taking mean values they showed that

$$V_o = \frac{1}{3}\,\eta^* \int_0^L \frac{d}{\tau^*}\, d^* \qquad (2.59)$$

where V_o is volumetric flowrate of the dispersed phase in the settler.

The boundary conditions for equations (2.55),(2.57) and (2.59) are

$$\ell = 0 \quad n = n_o \text{ and } d = d_o$$

and in the limit $\ell \to L$ $n = 0$, $d = d_L$ and $h = d_L$.

2.5.3) contd.

d) contd.

$h = d_L$ expresses the condition at the end of the wedge, single row of drops of mean diameter ϕ_L exists. The general equation for the analysis of gravity settlers was obtained by combining equation (2.55) and (2.57)

$$\frac{dd}{d\ell} = \frac{\eta h}{\pi \tau n d^2} \qquad (2.60)$$

To solve the above equation they assumed that

$$\tau = f\, d^{1.5} \qquad (2.61)$$

and integrating between the limits (ℓ, d) and $(0, d_o)$ gave

$$d^{1.5} - d_o^{1.5} = \frac{1}{4\nu f} \qquad (2.62)$$

where f can be obtained from equation (2.5) listed in paragraph (2.1.2) and ν is axial velocity of the drops.

Finally by combining equation (2.5), (2.59) and (2,62) and integrating between the limits $\ell = 0$ to $\ell = L$ they obtained

$$V_o = 2\, \eta^* \nu \left[\left(d_o^{3/2} + \frac{L}{4\nu f} \right)^{2/3} - d_o \right] \qquad (2.63)$$

In the derivation of the above model certain assumptions were made which could limit its application. They assumed the drops to be rigid spheres which restrict it to the application of liquid-liquid froths. Another assumption was that rearrangement of drops in the vicinity of a coalescence step is instantaneous and that local disturbances in the vicinity of a coalescence step do not seriously affect the coalescence mechanism. It was found in the course of this study that after interdrop coalescence the arrangement of the drops is disturbed. This is then

2.5.3) contd.

d) contd.

followed by rearrangement of the drops with the continuous phase, which is not instantaneous. The assumption that τ is some function of $d^{-1.5}$ (equation 2.61) was based on results obtained in monolayers. This is not valid since the forces acting on drops in a monolayer are different from those acting on drops in dispersion bands which could result in different values of the mean interdrop coalescence time τ. Further they used the mean coalescence time for single drops at an interface (t) as expressed by equation (2.5) as equivalent to τ^* the mean drop interface coalescence time in a dispersion, again the validity of this is doubtful for the same reasons expressed above.

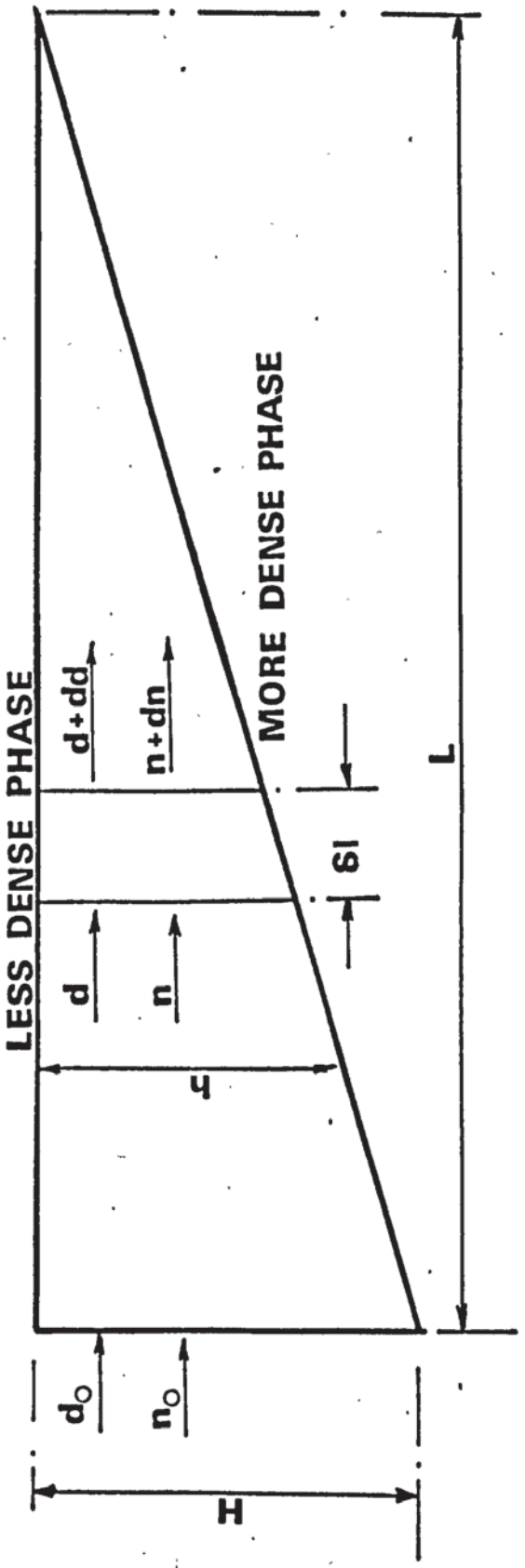

FIG 2.2 PARAMETER OF THE DIFFERENTIAL MODEL

2.5.3) contd.

e) Smith's Model.

Smith proposed a model which described the behaviour of drops in a dispersion band formed in a vertical settler. In the deviation of the model the following assumptions were made.

i) The drops travel through the bed towards the coalescence interface in approximately plug flow, moving relative to neighbouring drops as the result of drop-drop coalescence with adjacent drops or in the vicinity of a solid boundary by coalescence on the surfaces.

ii) The probability of drop-drop coalescence occurring in which three or more drops simultaneously take part is negligible.

iii) The rate of coalescence taking place between drops of a particular size depends on their diameters. Furthermore the average rate of coalescence at a given position within a bed will depend on the average diameter of drops at that position.

The flowrate of the dispersed phase in the bed V_d was related to the local mean drop diameter d by the following

$$V_d = \frac{\pi}{6} n d^3 \qquad (2.64)$$

where n is the rate of drop arrival per unit cross section area at position h. The change in V_d over the element dh was given by

$$\frac{dV_d}{dh} = \frac{\pi}{6}\left(d^3 \frac{dn}{dh} + 3n d^2 \frac{dd}{dn}\right) = 0 \qquad (2.65)$$

a number balance for the drop led to

2.5.3) contd.

e) contd.

$$\frac{dn}{dh} = \frac{36}{\pi} \frac{\eta}{d^3} \cdot \frac{1}{T} + \frac{16}{\pi} \frac{\eta^*}{T^* D d^2} \qquad (2.66)$$

where η and η^* are the volumetric and area packing efficiencies in the bed and at phase boundary respectively. D is the vessel diameter. T and T* are the mean interdrop and drop interface coalescence times respectively.

Solutions of the above differential equations with boundary conditions were derived by overall volume balances at steady state. The general solution was given for two cases,

a) for the case of the dispersed phase wetting the column wall

$$V_d = \frac{2}{3} \eta^* \frac{d}{T^*} + \frac{4}{D} \frac{2}{3} \eta^* \int_0^4 \frac{d}{T^*} \, dh \qquad (2.67)$$

b) for the case of the dispersed phase not wetting the column wall

$$V_d = \frac{2}{3} \eta^* \frac{d}{T^*} \qquad (2.68)$$

It is evident from the above that particular solutions of equations (2.67) and (2.68) depend upon the nature of the interdrop and drop interface coalescence times which represent a major obstacle for the application of the model. Various theoretical forms of the coalescence times functions were discussed, and approximate solutions were obtained by considering that

a) T and T* are independent of drop size

b) T and T* are a function of drop diameter

c) T and T* are a function of drop diameter and residence time in the bed.

2.5.3) contd.

e) contd.

No general conclusions were drawn regarding agreement between the model and experimental data.

An objection that can be raised against Smith's model is that, similar to the other models which have been described, the coalescence times have not been evaluated for drops inside the dispersion and the coalescence times based on single drops and monolayers were applied which is not valid as was argued previously. In fact Smith stated that the drop interface coalescence time was the same as the drop-drop coalescence time, although his own experimental results showed that this was not the case.

In this study it has not been possible to evaluate an interdrop coalescence time, even though it has been possible to observe the coalescence behaviour throughout the band. Each drop is surrounded with approximately 12 neighbours and the probability of coalescence with each of these is the same since each pair will have a distribution of coalescence times. The observed coalescence appears to be completely random. Hence some other criterion appears to be preferable e.g. critical film thickness.

f) Hittit Model.

Hittit recently studied the behaviour of drops and holdups in vertical dispersion bands under steady state conditions. He derived the velocity of a drop in the bed in terms of the holdup and the flowrate V_d of the dispersed phase:-

$$\frac{dh}{d\theta} = \frac{V_d}{1 - \varepsilon_c} \qquad (2.69)$$

where h is the position from bed entry and θ is the residence

2.5.3) contd.

f) contd.

time in the bed.

The variation of the holdup ε_c along the bed was found experimentally and was expressed by the general equation

$$(1 - \varepsilon_c) = mx + c \qquad (2.70)$$

The slope of the line m depends on the section of the bed. By integrating equation (1) between the limits

$$\theta = 0,\ h = 0 \text{ at bed entry}$$

and $\theta = \theta_r$, h = H at the interface he obtained

$$\frac{V_d\ \theta_r}{1-1} = K \quad \text{where } K = f(mx + c)$$

The model was based on overall material and volume balances and did not consider the elementary units in the bed. This has led to an over simplification of the situation resulting in an over simplified model.

CHAPTER 3

TECHNIQUES.

3) Techniques.

Previously most of the information obtained on dispersion bands was based on studying the overall picture of the bed and by observations made on individual drops residing at the column wall or at the coalescing interface. In both situations the true picture of the behaviour of the drops and the continuous phase inside the dispersion could not be seen. Important criteria for the design of gravity settlers such as film drainage, packing efficiency of the drops, interdrop, drop interface and drop wall coalescences have either been ignored or assumed to be identical with that of a single drop residing at an interface. Therefore, before an effective correlation can be produced to predict phase separation the mechanism must be observed inside a dispersion band. The refractive index matching technique developed in this study meets the above criteria. It further facilitates the application of other techniques such as flow visualization, holography and Christiansen effect which extends the amount of information obtainable. All of these techniques will be discussed.

3.1) Refractive Index matching technique.

The opacity of the drops in normal dispersion bands due to differences in the refractive indices of the phases, restrict observation to the first layer of drops. If however the refractive indices of the two phases are matched, the lens effect of the drops is eliminated, the drops become invisible and consequently so does the band they form. By introducing one or several discriminated drops into the bed, their behaviour can be studied without the influence of either the vessel wall or the coalescing interface.

Several investigators have studied the flow of liquids

3.1) contd.

in porous media by matching the refractive indices of saturating liquids to that of the granular component. By local injections of a coloured tracer Van Meurs[83] studied the displacement of one liquid by another. De Jong[86] used an analine dye in crushed optical glass saturated with an ammonia salt solution to study molecular diffusion in porous media. Heller[84] suggested the use of crystalline calcium fluoride for the solid component because of its low refractive index (n = 1.4338) making accessible a large assortment of matching liquids. Also calcium fluoride is relatively insoluble, chemically inert and nontoxic. Finally, Cloupeau and Klarsfeld[87] used several organic components for the liquid phase with various types of commonly used glasses in the form of microballs, filters or powder for the study of two dimensional thermal phenomena in saturated porous media. The refractive index matching enabled the visualization of a certain number of isotherms as bright lines of different colours.

3.2) Flow Visualization.

Having rendered the bed transparent by matching the refractive indices one or several drops can be discriminated from the rest as mentioned previously. The discriminating agents used were a phototropic dye or an ordinary dye. Both were now surfactants.

A phototropic dye is one that changes from a colourless to a coloured form by exposure to light. After the irridiation source is removed the dye reverts to its original colour. Generally the forward reaction is instantaneous but the reverse reaction is slower and depends on the concentration of the dye and the intensity of irridiation. Most dyes were

3.2) contd.

found to be activated by light in the region of the Ultra Violet. Finally some dyes are phototropic in the solid state only and others are phototropic when dissolved in a solvent. A good survey of these dyes was conducted by Exelby and Grinter[89] which lists various types, properties and their phototropic behaviour.

Hummel et al.[88] claimed to have utilized the phototropic properties of 2-(2',4'-dinitrobenzyl) pyridine (DNBP) to measure the mean velocity profiles in a vertical glass tube of 1.226 sq.cm. cross section. The dye was dissolved in 95% alcohol and was activated using a pulse ruby laser with a second harmonic generator to reduce the wave length of the laser light from 6943A to 3471.5A. A micronikon camera was used to record the event. More recently, employing the same technique as described above and using the same dye, they[90] studied the flow profiles of water alcohol solutions containing a drag reducing polemer. It must be mentioned however that when a sample of (DNBP) was obtained from Eastman Chemicals, dissolved in 95% alcohol and irridiated with U.V. light in these laboratories, no phototropic reaction occurred. Neither was there any activation when the dye was dissolved in other organic solvents, but it was found to be phototropic in the solid state, that is, the pale yellow crystals changed to blue after exposure to U.V. light.

Zolotrofe and Scheele[108] used an ultra violet sensitive photochromic spiropyran to measure the velocity profiles of organic liquids in pipes using high speed photography.

Other methods have been used for flow visualization. Takeo Yano et al.[91] utilized the electrolysis of sodium bromide

3.2) contd.

solution with methylorange. The Bromine generated was used as the tracer which was measured colorimetrically by measuring the concentration of methyl orange in the solution. Finally Adler et al.[92] used flash photolysis for introducing a non-disturbing tracer. The method uses a light sensitive dilute aqueous solution formed from a premixed concentrated solution, Sulphuric acid and water. The solution was irridiated with an electronic flash lamp and selenium photocells were used to measure the intensity of the tracer generated.

Unlike the phototropic dye techniques, the methods of Takeo Yano and Adler are non-reversible and accumulation of colour after several exposures occurs which is a major disadvantage to their techniques.

3.3) Recording techniques.

It is desirable that a permanent record be obtained of the observations made. Still and cine photograph has been the method preferred in chemical engineering. The use of photography in the field of liquid-liquid extraction has been adequately dealt with and described by several authors[38,28].

Whilst photography remains a very useful tool, the information obtained is limited to two dimensions. To overcome this limitation, holography seems to provide the answer. Unlike photography, holography records the pattern of wave fronts of light from the subject. This recorded information is then used to reconstruct an image of the subject in a three dimensional manner.

Although these basic principles of holography were described as early as 1947 by Gavor, it was only after the introduction of the laser that this novel technique became truly

3.3) contd.

practical. The basic principle for obtaining a hologram (equivalent to a photograph in photography) is that the coherent source of light from the laser is split into a signal beam which passes to the object and on to the holographic plate. The other part of the beam (reference beam) is directed to the holographic plate without any interference. The holographic plate then records the interaction of the wave fronts of the reference and the signal beam. If the hologram is then illuminated by a light source similar to that used to obtain the hologram, the original wave fronts are reconstructed. This causes the image to be produced in a truly three dimensional manner.

There are numerous types of holography now available but they can be categorized in four major sections

i) Direct transmission holography

ii) Diffuse transmission holography

iii) Reflection holography

iv) Fourier holography

More detailed information about the subject can be found in[93,94,95].

It is evident that holography can provide very useful information which normal photography cannot. This technique has so far been used to a limited extent.

A major application of holography has been for the use of particle size analysis. Thompson et al.[96] measured the size distribution of fog particles by taking a hologram of a sample of fog. After reconstructing the hologram a T.V. Camera attached to a T.V.Monitor was used to focus at different levels of the hologram thus studying a cross section

3.3) contd.

of size distribution of the fog particles. A similar technique was described by Fletcher[97] to measure the particle size of fast moving aerosols. Finally, Thompson[98] described the application of the Fraunhofer holography for the measurement of particle sizes of naturally occurring fog, laboratory aerosols and small rocket engine studies.

CHAPTER 4

MATHEMATICAL MODEL

4) Mathematical Model.

Several attempts have been made to develop mathematical models to predict the bed height in a dispersion in terms of the physical properties of the system, drop diameter, and coalescence times as discussed in paragraph (2.5.2). However, the interdrop and drop interface coalescence times in dispersion bands have remained unknown, and it has not been possible to relate these to the coalescence times of drop-drop pairs and single drops at a plane interface. In fact in this work it has been found that pairs of drops can coalesce in at least 12 different ways in a random manner. Hence it is believed that an alternative analytical procedure would be more fruitful.

To overcome the above difficulties a mathematical model is presented below based on the rate of drainage of the continuous phase from in between the drops.

4.1) Drainage of the continuous phase film.

It is assumed that the drainage of the film may be represented by the radial drainage of liquid from between two flat discs of radius (R) such that the area of the discs is equal to the area of one face of the dodecahedral bubble as shown in Fig.(4.1).

Considering the forces acting on element (ABCDEFGH)

4.1) contd.

1) Force on BCGF :- $r\ \delta\theta\ \delta z\ P$

2) Force on ABFE :- $\frac{1}{2}\delta r\ \delta z\ \delta\theta\left(P + \frac{1}{2}\frac{\partial P}{\partial r}\ \delta r\right)\sin\frac{\theta}{2}$

3) Force on DCGH :- $\frac{1}{2}\delta r\ \delta z\ \delta\theta\left(P + \frac{1}{2}\frac{\partial P}{\partial r}\ \delta r\right)\sin\frac{\theta}{2}$

4) Force on ADHE :- $(r+\delta r)\,\delta\theta\ \delta z\left(P + \frac{\partial P}{\partial r}\ \delta r\right)$

5) Shear force on EFGH :- $r\ \delta\theta\ \delta r\ \tau$

6) Shear force on ABCD:- $r\ \delta\theta\ \delta r\left(\tau + \frac{\partial \tau}{\partial z}\ \delta z\right)$

At steady state

$$1 + 2 + 3 + 5 = 4 + 6$$

Expanding the expressions and neglecting terms which contain δr^2 leads to

$$\frac{\partial P}{\partial r} + \frac{\partial \tau}{\partial z} = 0$$

or
$$\frac{\partial P}{\partial r} - \mu_c \frac{\partial^2 u}{\partial z^2} = 0 \qquad (4.1)$$

Since the film is thin the pressure does not vary in the z direction. Therefore, integrating equation (4.1) twice with respect to z gives

$$U = \frac{1}{\mu_c}\frac{\Delta P}{\Delta r}\frac{z^2}{2} + C_1 z + C_2 \qquad (4.2)$$

where C_1 and C_2 are the integration constants.

For liquid-liquid interfaces the surfaces of the approaching disc can be considered to be immobile. This was shown by Kintner[69] when he observed slow mixing when two drops coalesce. Similar observations have been made of the behaviour of coalescing drops in dispersion bandsphotograph (4.1). It can be seen that little or no mixing takes place after coalescence, which supports the existence of immobile surfaces. The following boundary conditions can therefore be used to

PLATE 4.1 SLOW MIXING AFTER INTERDROP COALESCENCE.

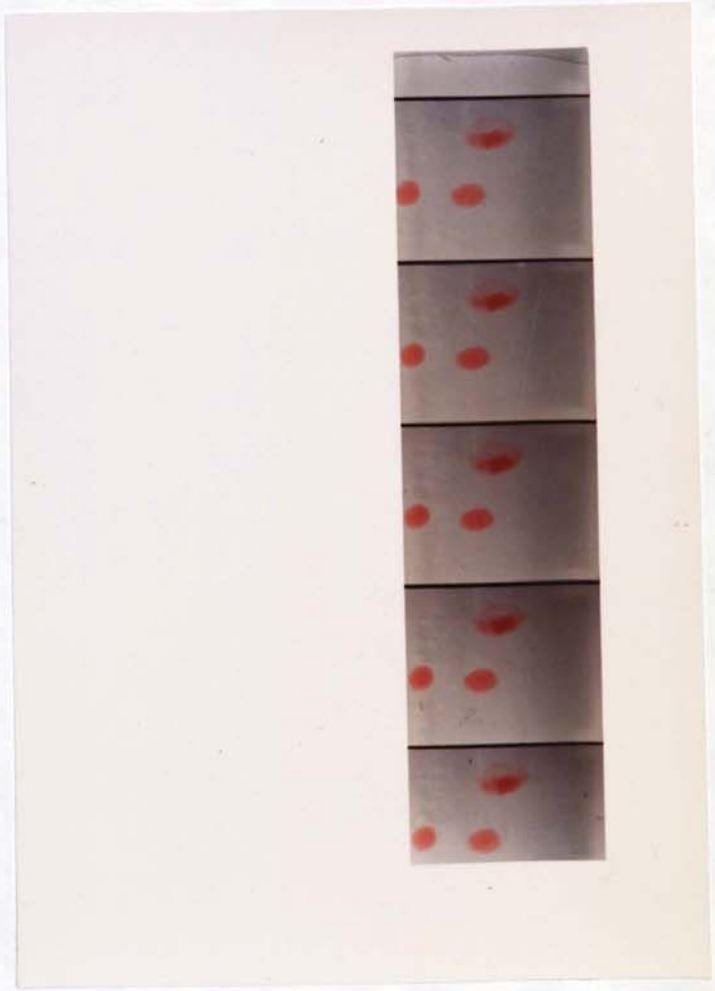

4.1) contd.

evaluate C_1 and C_2

1) $U = 0$ at $z = 0$ $\therefore$ $C_2 = 0$

2) $U = 0$ at $z = h$ $\therefore$ $C_1 = -\frac{1}{\mu_c}\frac{\Delta P}{\Delta r}\frac{h}{2}$

so that

$$U = \frac{1}{2\mu_c}\frac{\Delta P}{\Delta r}(z^2-hz) \qquad (4.3)$$

where U is the velocity profile in the film of thickness h.

An expression for the pressure gradiant, $\frac{\Delta P}{\Delta r}$ is required in order to proceed with the analysis. This may be obtained by considering the rate of approach of the two plane surfaces ν in terms of the rate of liquid flow in the film. The rate of reduction of the volume of the element shown in Figure (4.1) is $\pi r^2 \nu$ which may be equated to the volumentric rate of flow from the film at radius r. Thus

$$\pi r^2 \nu = 2\pi r \int_0^h U \, dz.$$

Substituting for U from equation (4.2)

$$\pi r^2 \nu = \frac{2\pi r}{2\mu_c}\frac{dP}{dr}\int_0^n (z^2-hz)$$

Integrating and rearranging yields the pressure gradient in the film $\frac{dP}{dr} = \frac{6\,\nu\mu_c r}{h^3}$ which in turn may be integrated with respect to r and using the boundary conditions that $P = 0$ at $r = R$ leads to

4.1) contd.

$$P = \frac{3\mu_c v}{h^3}(R^2 - r^2) \qquad (4.4)$$

The force acting on the film is given by

$$F = 2\pi \int_0^R r\,P\,dr$$

Substituting for P from equation (4.4) and integrating gives

$$F = \frac{3\pi\mu_c v R^4}{2h^3} \qquad (4.5)$$

since the velocity of approach of the two film surfaces v is equal to $-\frac{dh}{dt}$.

$$\text{Thus } \frac{dh}{dt} = -\frac{2h^3F}{3\pi\mu_c R^4} \qquad (4.6)$$

Equation (4.6) gives the rate of film thinning in terms of the force, the film dimensions and the liquid viscosity. In order to integrate equation (4.6) it is necessary to define the force F causing drainage. It will be shown below that the ratio of the interfacial tension forces is 15-350 times the gravity force and F must be expressed in terms of the interfacial tension. Thus F can be obtained from Laplace's equation

$$P = \gamma\left(\frac{1}{R_1} + \frac{1}{R_2}\right)$$

where R_1 and R_2 are the radii of curvature in the film and plateau border. Hence flow in the plateau borders must first be considered.

4.2) Flow in Plateau Borders.

Number of plateau borders per unit volume of dispersion is $\frac{60\ \varepsilon_d}{\pi d^3}$ (Appendix 1) where ε_d is the fractional hold up of the dispersed phase and d is the average drop diameter. The probability of a plateau border being inclined at any angle between θ and $(\theta+d\theta)$ to the horizontal is $\cos\theta\ d\theta$[103]. Therefore the number of plateau borders (n) per unit volume inclined between angle θ and $(\theta+d\theta)$ is

$$n = \frac{60\ \varepsilon_d}{\pi d^3}\ \cos\theta\ d\theta$$

The vertical projection of a plateau border of length ℓ inclined at an angle θ to the horizontal is $\ell \sin\theta$ or $0.41d \sin\theta$ (Appendix 1). The probability of this plateau border intersecting a horizontal plane per unit height of the dispersion is $0.41d \sin\theta$.

The cross sectional area of a plateau border shown in Figure (4.2a) is given by[104]

$$A_{pb} = 0.1612\ r_o^2 + 1.732\ r_o h$$

Since h is very small the area can be approximated to

$$A_{pb} = 0.1612\ r_o^2 \qquad (4.6a)$$

The continuous phase velocity through the plateau border is given by[105]

$$U = \frac{D_H^2}{2k\ \mu_c}\ \frac{dP}{d\ell}$$

where D_H is the hydraulic diameter and k is a constant. For immobile surfaces the values of D_H and k are $0.205r_o$ and 6.43 respectively. The volumetric flow rate in the plateau border q can be found from

$$q = U\ A_{pb}$$

4.2) contd.

$$\therefore\ q = \frac{0.0065}{12.86}\, r_o^4\ \frac{dP}{d\ell}$$

The pressure drop per unit length $\frac{dP}{d\ell}$ of the plateau border is the weight of the continuous phase minus the pressure drop across the dispersion in that section. For a plateau border at an angle of inclination θ from the horizontal

$$\frac{dP}{d\ell} = \varepsilon_d\ \rho_c g\ \sin\theta$$

The total flow rate of the continuous phase draining through the plateau borders can now be obtained from the following integration

$$Q_{down} = \int_o^{\pi/2} \left(\frac{0.000525\ r_o^4 \rho_c g \varepsilon \sin\theta}{\mu_c}\right)\left(0.41 d \sin\theta\right)\left(\frac{60\varepsilon\ \cos\theta}{\pi d^3}\ d\theta\right)$$

$$Q_{down} = \frac{0.0041\ r_o^4\ \rho_c g \varepsilon^2}{\mu\ d^2}\left[\frac{\sin^3\theta}{3}\right]_o^{\pi/2}$$

$$Q_{down} = \frac{0.0041\ r_o^4\ \rho_c g\ \varepsilon_d^2}{3\ \mu_c\ d^2} \qquad (4.7)$$

At steady state the amount of continuous phase draining through the plateau border at any plane must be equal to that being carried up.

4.3) <u>Upward flow of continuous phase.</u>

The rate of drops entering the bed per unit area

$$N = \frac{6\ V_d}{\pi\ d^3} \qquad (4.8)$$

where V_d is the superficial velocity of the dispersed phase.

4.3) contd.

The volume of the continuous phase attached to each drop

$$= \left(12 \times 0.29\ d^2 \times \frac{h}{2}\right) \qquad \text{(Appendix 1)}$$

$\therefore$ The upward flow of the continuous phase

$$Q_{up} = \left(\frac{6\ V_d}{\pi d^3}\right)\left(12 \times 0.29 d^2 \times \frac{h}{2}\right)$$

$$Q_{up} = \frac{3.32\ V_d h}{d} \qquad (4.9)$$

Q_{up} can also be expressed in terms of the fractional holdup

$$\therefore\ Q_{up} = \left(\frac{1-\varepsilon_d}{\varepsilon_d}\right) V_d \qquad (4.10)$$

from equations (4.9 and (4.10) the film thickness can be given in terms of the drop diameter and the fractional hold up

$$h = \left(\frac{1-\varepsilon_d}{3.32\varepsilon_d}\right) d \qquad (4.11)$$

4.4) Drainage time.

Before equation (4.6) can be integrated to yield the time taken for the film to drain from h_1 to h_2 an expression r_o was obtained from equation (4.9) and (4.7) since, at steady state for any plane in the dispersion $Q_{up} = Q_{down}$

$$\therefore\ r_o = \left(\frac{3 \times 3.32\ V_d\ h\mu_c d}{0.0041\ \rho_c\ g\ \varepsilon_d^2}\right)^{\frac{1}{4}} \qquad (4.12)$$

Consider Figure (4.26). Each border is bounded by three cylindrical surfaces and since the pressure difference ΔP across a curved surface is given by the Laplace equation -

4.4) contd.

$$\Delta P = \gamma\left(\frac{1}{r_1} + \frac{1}{r_2}\right)$$

the excess pressure in the drop over that in the border is given by

$$\Delta P = \gamma\left(\frac{1}{\infty} + \frac{1}{r_o}\right)$$

$$\Delta P = \frac{\gamma}{r_o}$$

The force acting on the film may be found from the equation

$$F = \Delta P \; a \qquad (4.13)$$

where a is the area of one pentagonal side of the dodecahedra and equals $0.29d^2$ (Appendix 1)

$$\therefore F = \frac{0.29d^2\gamma}{r_o}$$

Substituting for r_o gives

$$F = 0.29\, d^2\gamma\left(\frac{0.0041\ \rho_c g\varepsilon_d^2}{9.96\ V_d h\mu_c d}\right)^{\frac{1}{4}}$$

Substituting for F in equation (4.7) gives

$$\frac{dh}{dt} = \frac{-2h^3}{3\pi(0.303)^4\ \mu d^4} - \left(0.29d^2\gamma\left(\frac{0.0041}{3\times 3.32}\ \frac{\rho_c g\varepsilon^2 d}{V_d h\mu_c d}\right)^{\frac{1}{4}}\right)$$

Simplifying

$$\frac{dh}{dt} = -\ 1.04 \times 10^{-2} h^{\frac{11}{4}}\left(\frac{\rho_c g\gamma^4\varepsilon_d^2}{V_d\mu_c^5\ d^9}\right)^{\frac{1}{4}} \qquad (4.14)$$

Integrating equation (4.14) between the boundary condition

$t = 0$ at $h = h_1$ and

$t = t$ at $h = h_k$ where h_k is the critical film thickness before rupture gives

$$t = 55\left(\frac{V_d\mu_c^5 d^9}{\rho_c g\gamma^4\varepsilon_d^2}\right)^{\frac{1}{4}}\left(\frac{1}{h_k^{7/4}} - \frac{1}{h_1^{7/4}}\right) \qquad (4.15)$$

4.4) contd.

Since $h_1 >> h_k$ equation (4.15) can be simplified to

$$t = \frac{55}{981}\left(\frac{V_d \mu_c^5 d^9}{\rho_c g \gamma^4 \varepsilon_d^2 h_k^7}\right)^{\frac{1}{4}} \qquad (4.16)$$

4.5) Calculation procedure.

It is assumed that at the beginning of the bed the drops of diameter (d_o) trap some of the continuous phase which is calculated from equation (4.10). The initial film thickness (h_o) is then calculated from equation (4.11). As the drops travel through the bed the film thins and the critical film thickness is reached whereupon interdrop and drop wall coalescence takes place. The time taken (t_o) for the above to happen can be calculated from equation (4.15) or (4.16) since d_o, ε_{d_o} and V_{d_o} are known. Therefore the first increment of bed height can be calculated from

$$H_o = t_o V_{d_o} \qquad (4.17)$$

After coalescence, however, the drop diameter d_1, the fractional holdup ε_{d_1}, the superficial dispersed phase velocity V_{d_1}, the film thickness h_1 and the radius of the plateau border r_{o1} will vary. Therefore, before the next increment can be calculated the above quantities must be evaluated.

4.6) Superficial dispersed phase velocity V_d.

Since only drop wall coalescence affects V_d

$$V_{d_1} = \frac{\pi}{6} N_o (1-\beta) d_o$$

where β is the drop wall coalescence probability,

from equation (4.8) $N_o = \dfrac{6 V_{d_o}}{\pi d_o^3}$

4.6) contd.

$$\therefore\ V_{d_1} \quad \frac{\pi}{6}(1-\beta)d_o\left(\frac{6\ V_{d_o}}{\pi\ d_o^3}\right)$$

Simplifying

$$V_{d_1} = (1-\beta)V_{d_o} \tag{4.18}$$

4.7) Average Drop diameter.

The a verage drop diameter after coalescence has taken place can be calculated using the equation below

$$d_{ave} = \frac{\Sigma\, n_i\, d_i^3}{\Sigma\, n_i\, d_i^2}$$

where n_i is the number of drops of diameter d_i

$$\therefore\ d_{ave} = \frac{(N_o-N_I-N_W)d_o^3 + \frac{N_I}{2}\, d_I^3}{(N_o-N_I-N_W)d_o^2 + \frac{N_I}{2}\, d_I^2}$$

where N_I and N_W are the rate of interdrop and drop-wall coalescence per unit area respectively. d_I is the diameter of resulting drop after the coalescence of two drops of diameter d. The incident of three drops coalescing simultaneously is negligible. This is based on the numerous observations made of drops coalescing in the bed, where no such incident was observed, $N_I = \lambda N_o$ and $N_W = \beta N_o$ where λ is the probability of interdrop coalescence $d_I = \sqrt[3]{2}\, d_o$.

Substituting for N_I, N_W, and d_I

$$d_{a.ve} = \frac{N_o(1-\lambda-\beta)d_o^3+\frac{1}{2}\lambda N_o 2d_o^3}{N_o(1-\lambda-\beta)d_o^2+\frac{1}{2}\lambda N_o^3\sqrt{2}\ d_o^2}$$

Simplifying and using d_1 for d_{ane}

$$d_1 = \frac{(1-\beta)d_o}{(1-\beta-0.21\lambda)} \tag{4.19}$$

Finally from equation (4.11)

4.7) contd.

$$h_1 = \left(\frac{1 - \varepsilon_{d_1}}{3.32\varepsilon_{d_1}}\right) d_1 \qquad (4.20)$$

4.8) Estimation of ε_{d_1}

ε_1 can be calculated by considering the volume of the dispersed and the continuous phase. By definition

$$\varepsilon_{d_1} = \frac{V_{d_1}}{V_{d_1} + V_{c_1}} \qquad (4.21)$$

where V_{c_1} is the superficial velocity of the continuous phase.

V_{c_1} = Volume in plateau border + volume in film

$$V_{c_1} = 10\ N_1\ A_{pb}\ \ell_{pb} + 12 \times 0.29\ d_1^2 \times N_1 \frac{h_1}{2}$$

It can be seen from the drainage equation that the rate of film drainage and the establishment of the plateau borders is a fast process, further it can be safely stated that most of the continuous phase holdup is within the plateau borders. Therefore, neglecting the term $(12 \times 0.29\ d_1^2 \times N_1 \frac{h_1}{2})$

$$V_{c_1} = 10\ N_1\ A_{pb}\ \ell_{pb} \qquad \text{But } N_1 = \frac{6\ V_{d_1}}{\pi\ d_1^3}$$

Substituting for N_1, A_{pb} and ℓ_{pb}

$$V_{c_1} = 10\ N_1 \times 0.161\ r_{o_1}^2 \times 0.41 d_1$$

$$V_{c_1} = 0.66\ r_{o_1}^2 d_1 \left(\frac{6\ V_{d_1}}{\pi\ d_1^3}\right)$$

Substituting for V_{c_1} and V_{d_1} in equation (4.21)

$$\varepsilon_1 = \frac{V_{d_1}}{V_{d_1} + \frac{0.66 \times 6}{\pi} \frac{r_{b_1}^2}{d_1^2} V_{d_1}}$$

4.8) contd.

Simplifying $\varepsilon_1 = \dfrac{d_1^2}{d_1^2 + 1.26 r_{o1}^2}$ (4.22)

4.9) Determination of r_{o1}.

From equation (4.12) r_{o1} can be calculated since V_{d_1}, d_1 are known (equations 4.18, and 4.19.) Also h_1 can be substituted in terms of d_1 and ε_{d_1} (equation 4.20). Further ε_{d_1} can be obtained in terms of d_1 and r_{o1}.

Substituting for h_1 from equation (4.20) into equation (4.12)

$$r_{o1} = \left(\frac{2.43\times10^3 \mu_c V d_1 \left(\frac{1-\varepsilon_{d_1}}{3.32\,\varepsilon_{d_1}}\right) d_1}{\rho_c g \varepsilon_{d_1}^2} \right)^{\frac{1}{4}}$$

$$\therefore \quad r_{o1} = \left(\frac{2.43\times10^3 \mu_c V_{d_1} d_1^2}{3.32\,\rho_c g} \left(\frac{1-\varepsilon_{d_1}}{\varepsilon_{d_1}^3}\right) \right)^{\frac{1}{4}}$$

Substituting for ε_{d_1} in the expression

$$\left(\frac{1-\varepsilon_{d_1}}{\varepsilon_{d_1}^3}\right) = 1 - \frac{\left(\frac{d_1^2}{d_1^2+1.26r_{o1}^2}\right)}{\left(\frac{d_1^2}{d_1^2+1.26r_{o1}^2}\right)^3}$$

$$= \frac{1.26 r_{o1}^3 (d_1^2+1.26r_{o1}^2)^2}{(d_1^2)^3}$$

$$\therefore \quad r_{o1} = \left[\frac{2.43\times10^3}{3.32\,\rho_c g} \mu_c V_{d_1} d_1^2 \left(\frac{1.26 r_{o1}^2 (d_1^2+1.26r_{o1}^2)^2}{(d_1^2)^3} \right) \right]^{\frac{1}{4}}$$

$$r_{o1} = \left[\frac{920 \mu_c F_{d_1}}{\rho_c g\, d_1^4} \; r_{o1}^2 (d_1^2+1.26r_{o1}^2)^2 \right]^{\frac{1}{4}}$$

Let $K_1^2 = \dfrac{920 \mu_c V_{d_1}}{\rho_c g\, d_1^4}$

$$r_{o1} = \left[K_1^2 \; r_{o1}^2 (d_1^2+1.26r_{o1}^2)^2 \right]^{\frac{1}{4}}$$

$$r_{o1}^2 = K_1 \, r_{o1} (d_1^2 + 1.26\, r_{o1}^2)$$

4.9) contd.

$$\therefore\ 1.26\,K_1\,r_{o1}^2 + r_{o1} + K_1 d_1^2 = 0$$

$$r_{o1} = \frac{1 \pm \sqrt{1 - 4 \times 1.26 K_1^2 d_1^2}}{2 \times 1.26 K_1}$$

$$r_{o1} = \frac{1 \pm \sqrt{1 - 5.02\,K_1^2 d_1^2}}{2.52\,K_1} \qquad (4.28)$$

After the determination of r_{o1}, ε_{d_1} can be determined from equation (4.23) and t_1 from equation (4.16) and hence Q_1 equation (4.7), Finally the height of increment

$$H_1 = V_{d_1} t_1 \qquad (4.24)$$

The process is repeated using the values of $h_1, V_{d_1}, \varepsilon_{d_1}, d_1, r_{o1}, Q_1$ and K_1 as the initial values for increment 2. Until

$$Q_{up} - \Sigma\, Q_{i_{down}} = \text{zero}$$

where

ΣH_i represents the predicted bed height.

FIG 4.1

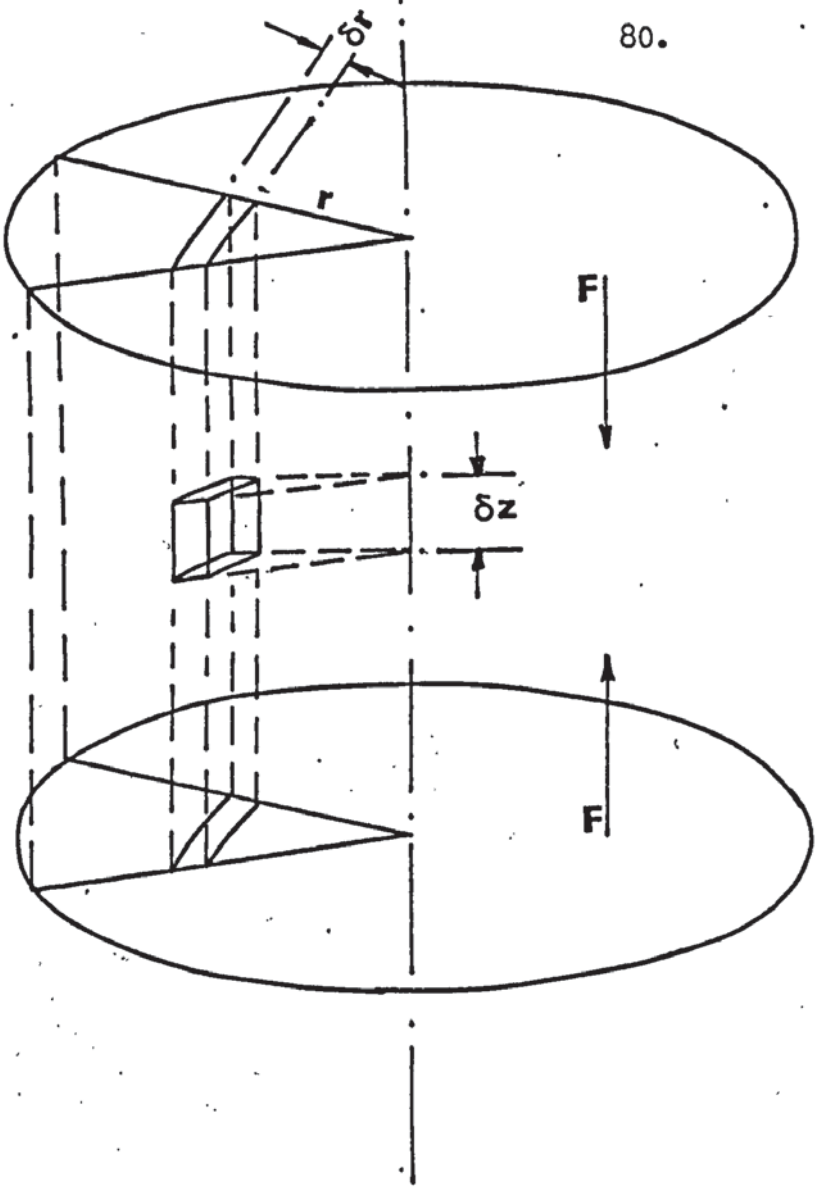

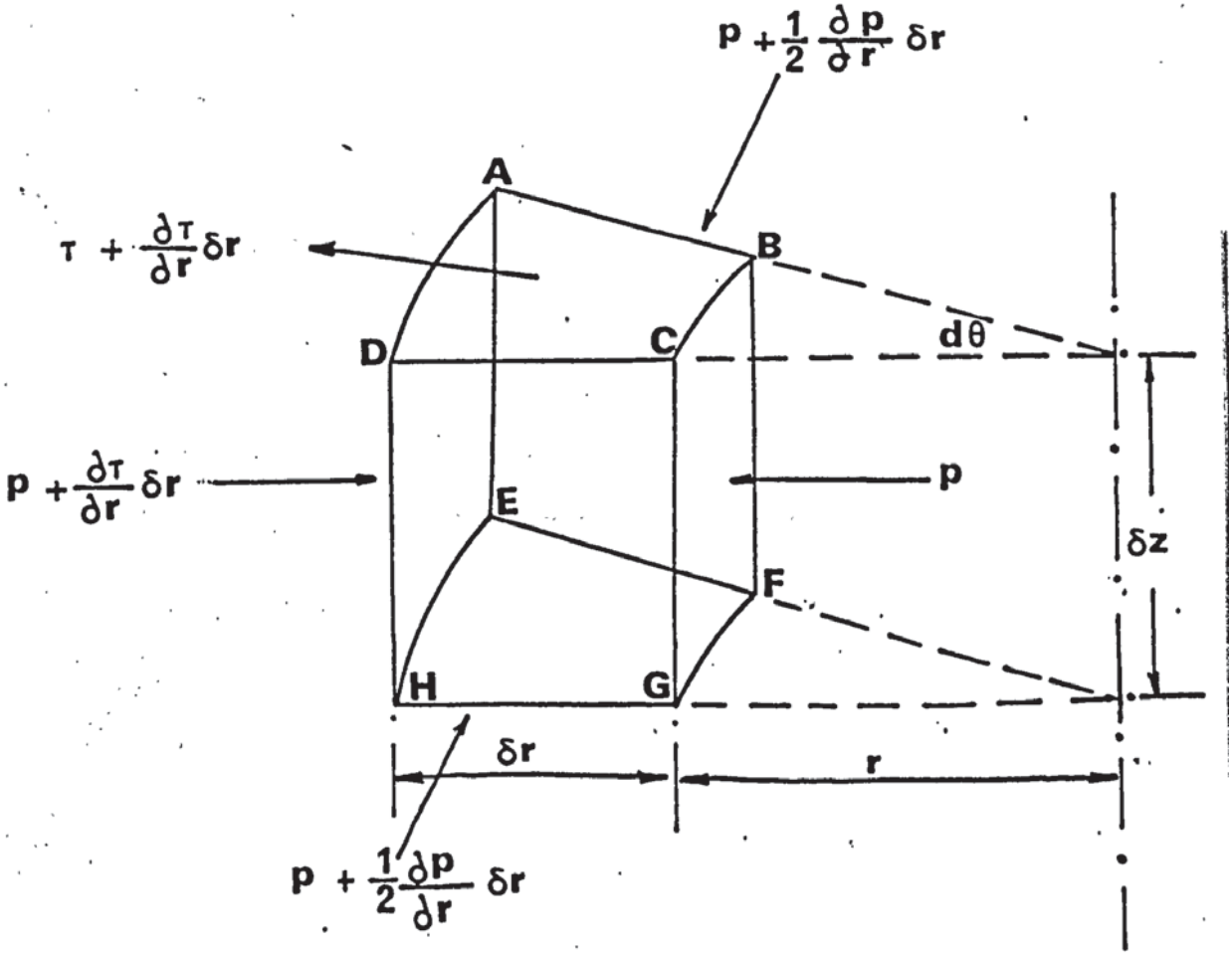

FIG 4·2a

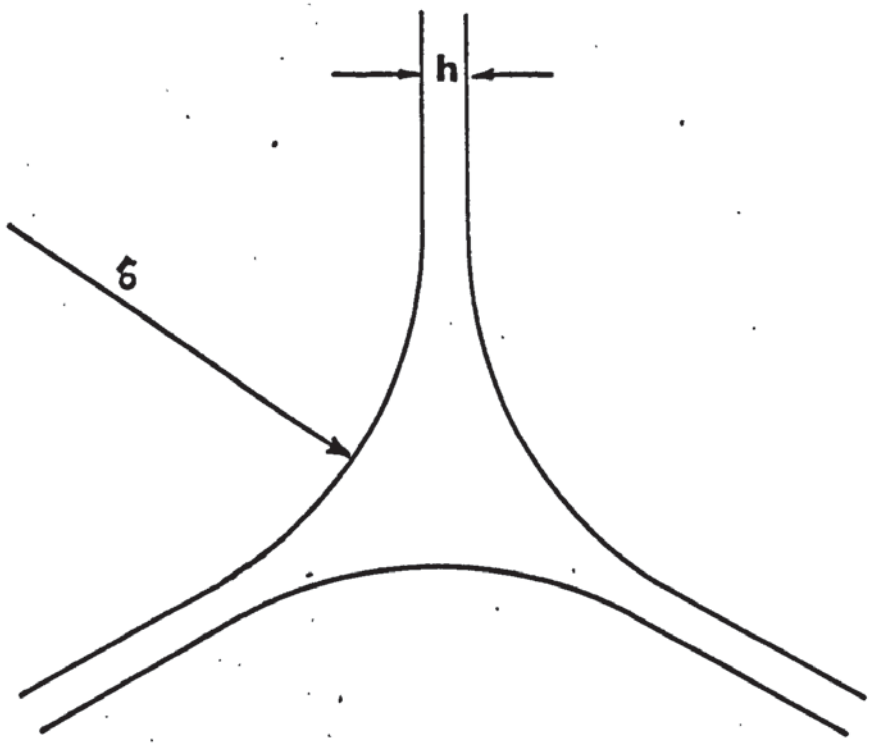

Cross Section of a Plateau Border

FIG 4·2b

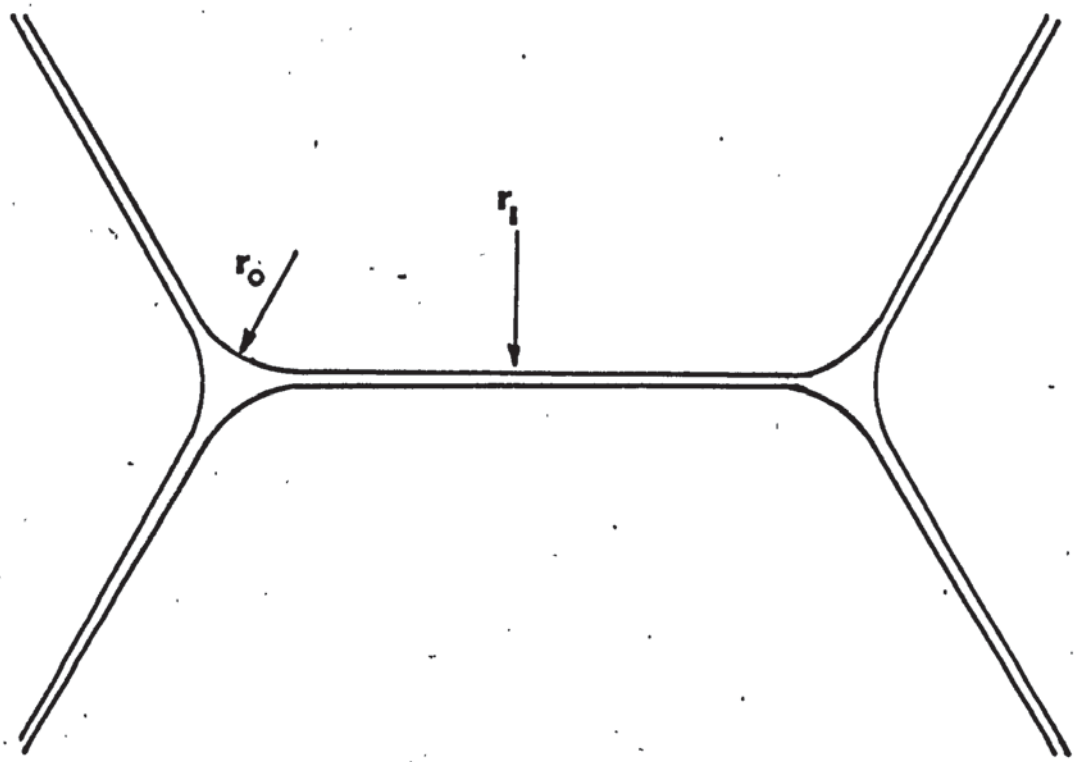

CHAPTER 5.

EXPERIMENTAL INVESTIGATIONS

5) Experimental Investigations.

Most of the experimental programmes for the study of drop behaviour in dispersion bands have been conducted in horizontal gravity settlers. More recently, a few investigations have been reported with a 2 in. and 3 in. diameter spray column[40,41]. Hittit[38] extended this work to pilot plant scale by using 6 in. and 9 in. glass column as the vertical gravity settler. However, in order to use the droplet visualisation technique, a smaller diameter column is desirable and consequently was preferred in this study.

5.1) Equipment.

The materials used for the equipment were restricted to glass, stainless steel and P.T.F.E. to minimize contamination to the systems. Figure (5.1) shows a schematic diagram and plate (5.1) the actual equipment. A 2" 10 Q.V.F. glass section (1) was used as the gravity settler where the dispersion band was formed by feeding the dispersed phase through the distributor(2). A 9 in. diameter Q.V.F.glass section(3) with stainless steel flanges was used as the storage tank which was connected to a Q.V.F. glass pump(4) with P.T.F.E. seals. A glass sintered filter(5) was used at the outlet of the pump to trap any solid particles that might be present in the liquid circulating. The dispersed phase was fed to one of a set of rotameters(7) to monitor the flow from a constant tank constructed from a 6" glass section with stainless steel flanges(6). This tank was provided with an overflow to the storage tank(3). The range of flow that the combination of the rotameters gave was from(0 to 5.0 ℓ/min) for water at 25°C. An important

5.1) contd.

feature of the design is that by manipulating the three way valves 8 and 9 the dispersed phase can be directed to the top or the bottom of the column. This provided a convenient way of inverting the system i.e. organics dispersed in aqueous or vice-versa by simply inverting the column without any other major alteration to the pipe work. The column was supported by rubber mountings and P.T.F.E. bellows were used for the pipe connected to the column to minimize the transmission of vibration. $\frac{5}{8}$ in. glass pipes with P.T.F.E. seals were used for the interconnecting pipe work. A mercury arc lamp fitted with an iris diaphragm(10) was used as the source of U.V. light.

Figure (5.2) shows the design of the distributor which was constructed from stainless steel. The main inlet tube (A) of the dispersed phase houses a small concentric tube (B) which leads to a single orifice in the middle of the distributor plate. This was sealed with P.T.F.E. thus isolating it from the main chamber and the rest of the nozzles in the distributor plate. Two sets of distributor plates were used depending on the preferential wettability of the dispersed phase. Stainless steel and P.T.F.E. for the aqueous and organic dispersed phases respectively. The size of the orifices ranged from 1 mm. to 4 mm. Plate (5.2) shows the actual distributor assembly.

5.2) Systems Employed.

It was not possible to obtain suitable pairs of liquids having identical refractive indices. Therefore, by using mixtures of glycerine and water as the aqueous phase

FIG 5.1

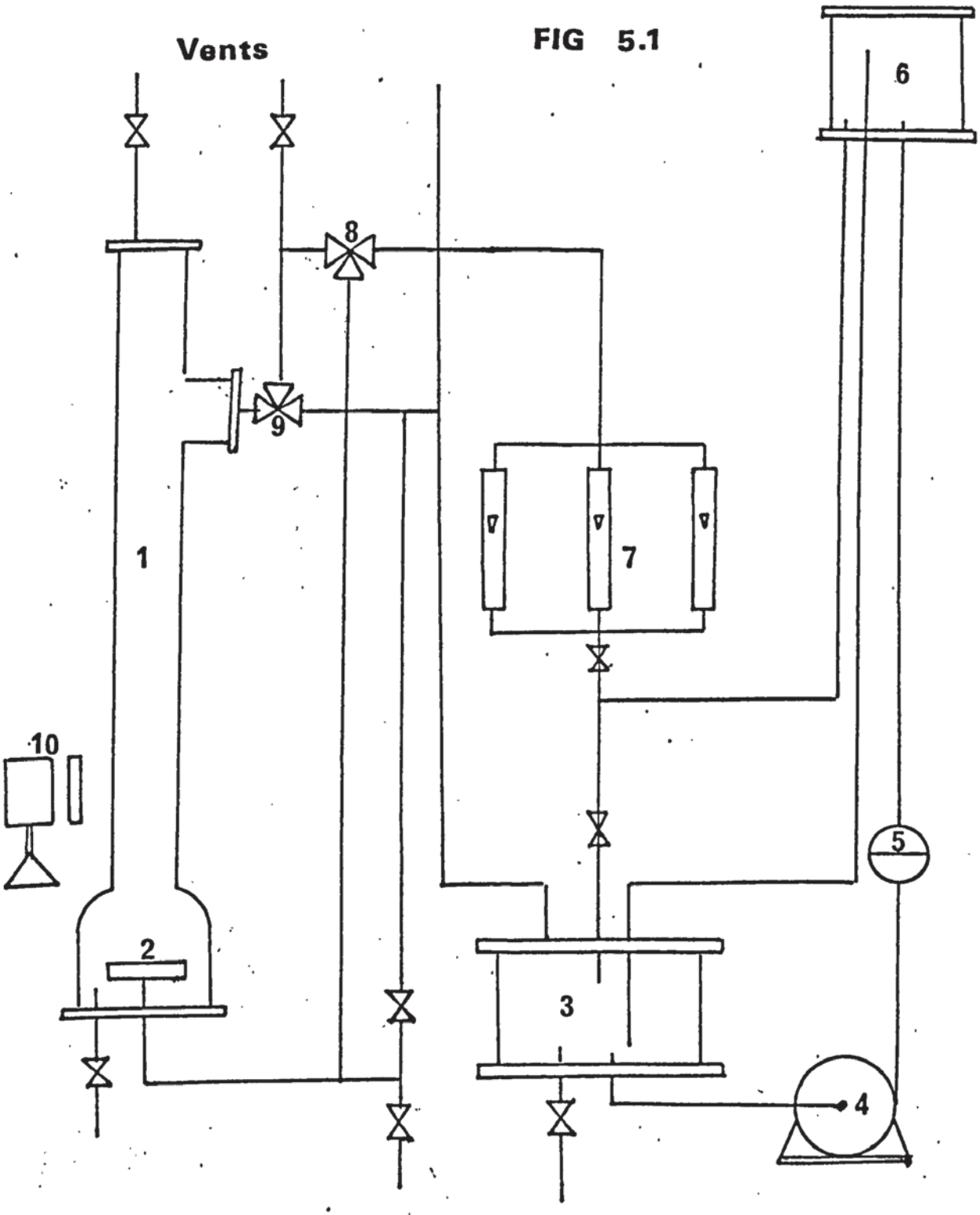

ARRANGEMENT OF THE COLUMN

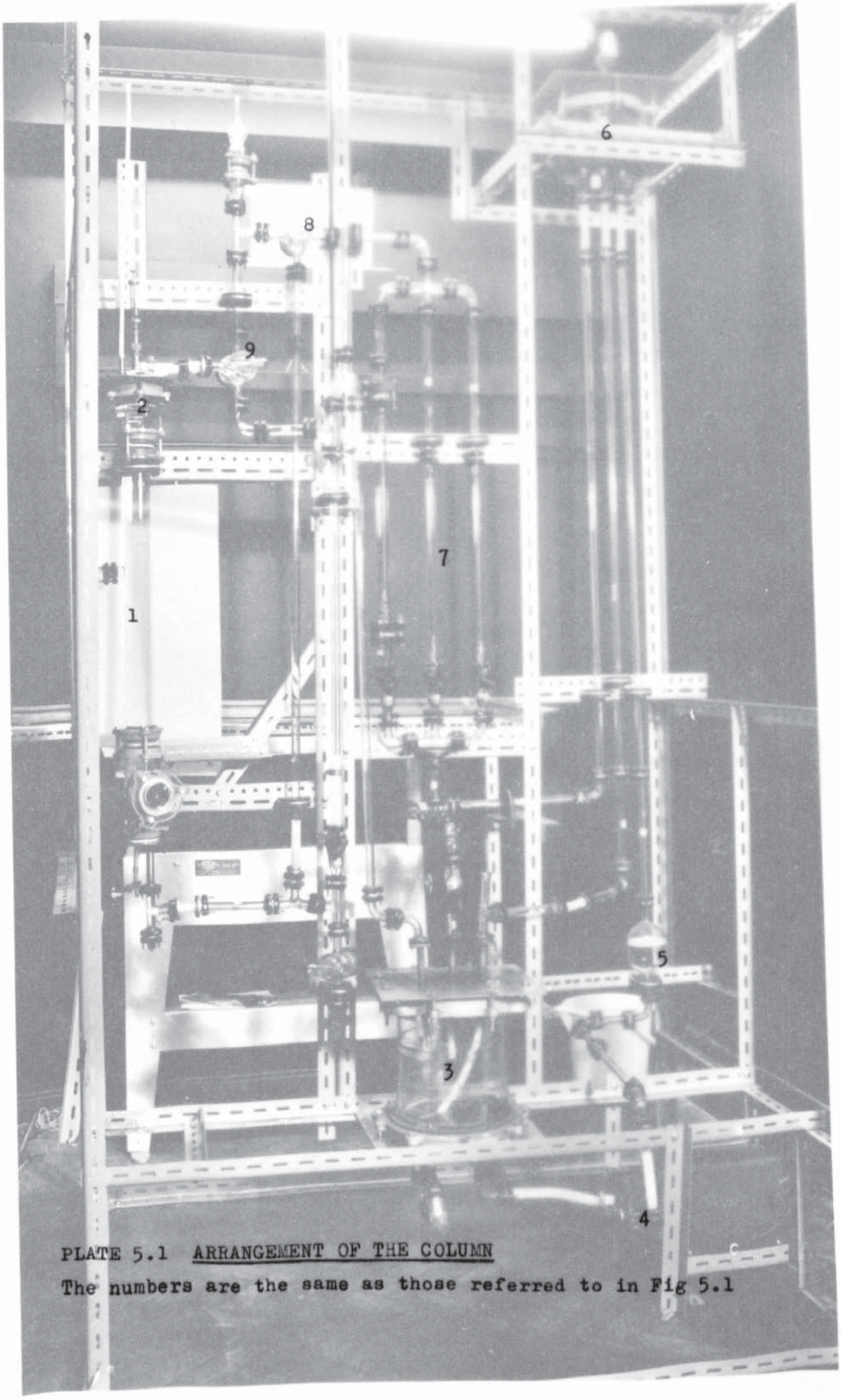

PLATE 5.1 ARRANGEMENT OF THE COLUMN

The numbers are the same as those referred to in Fig 5.1

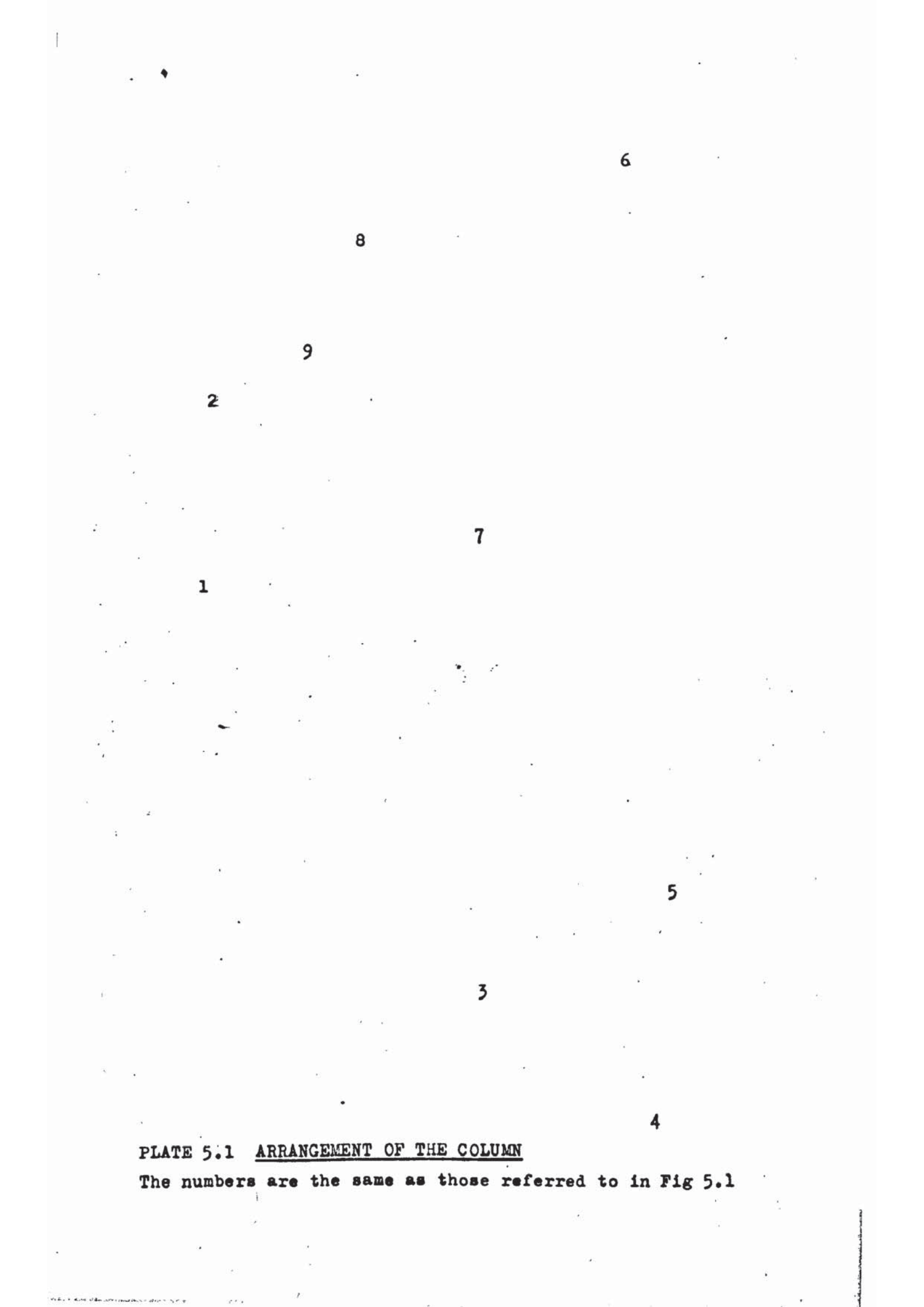

PLATE 5.1 ARRANGEMENT OF THE COLUMN

The numbers are the same as those referred to in Fig 5.1

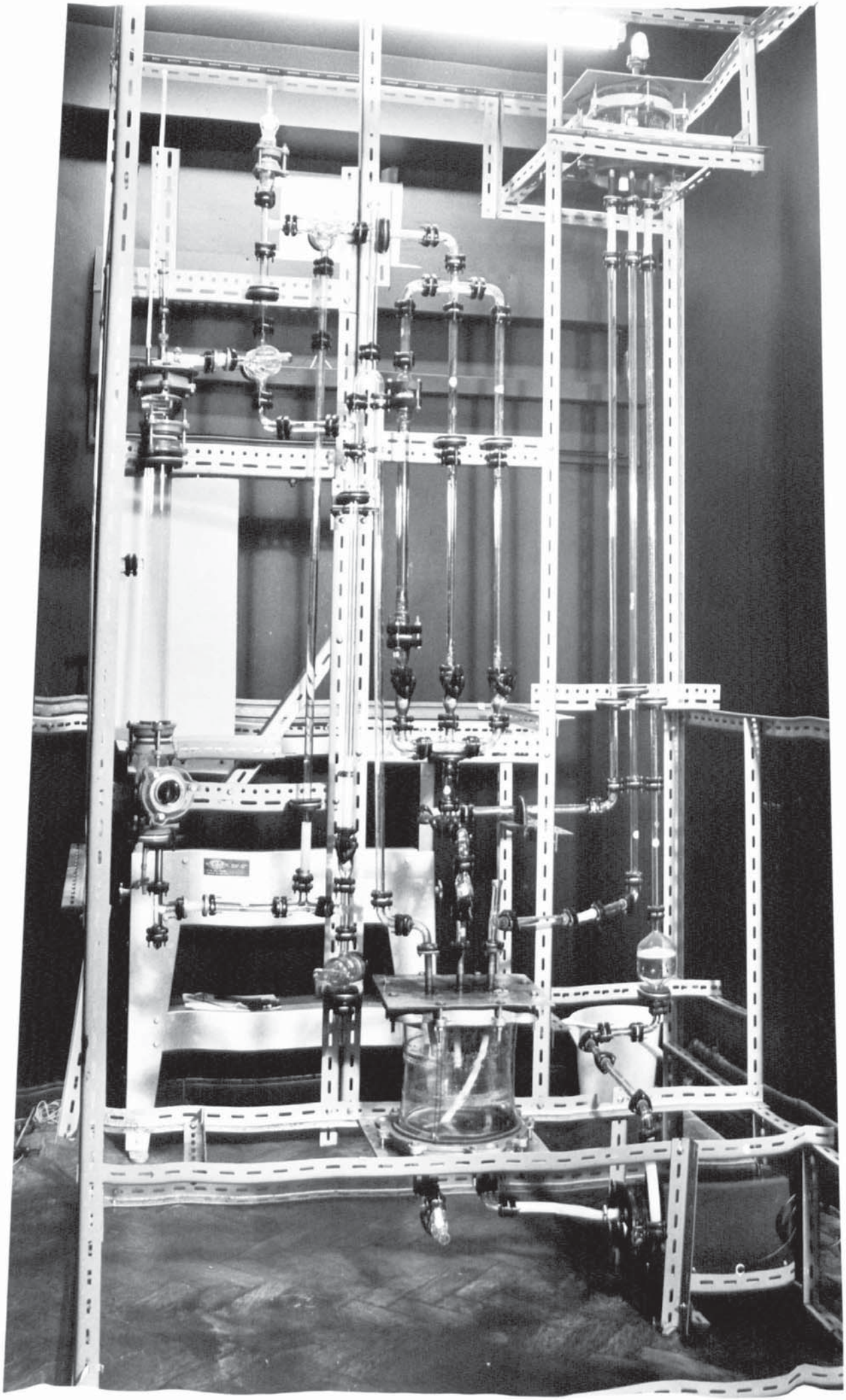

FIG 5.2

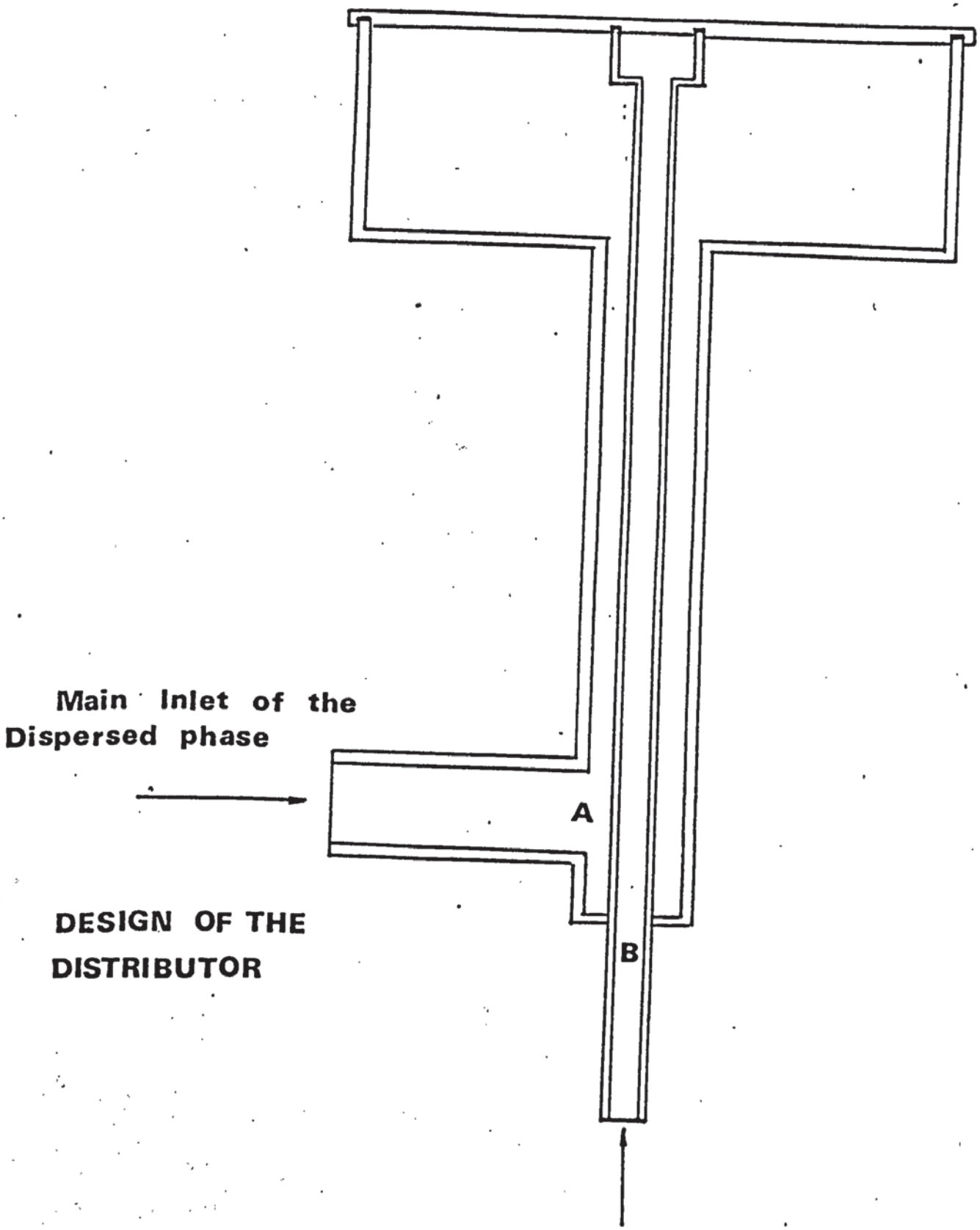

DESIGN OF THE DISTRIBUTOR

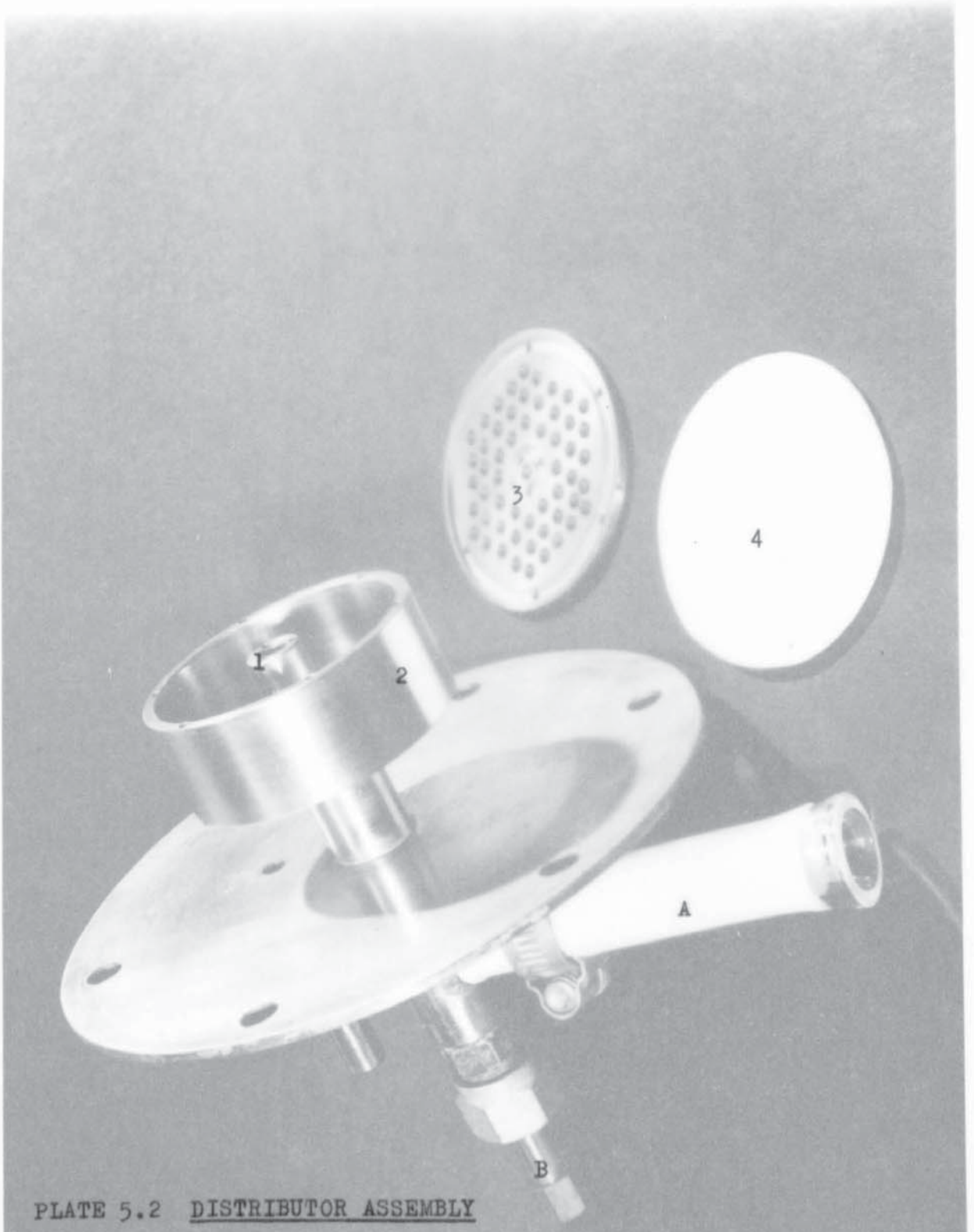

PLATE 5.2 DISTRIBUTOR ASSEMBLY

The letters are the same as those referred to in Fig 5.2

1. Isolated nozzle.
2. Main chamber.
3. Stainless steel distributor plate.
4. P.T.F.E. distributor plate.

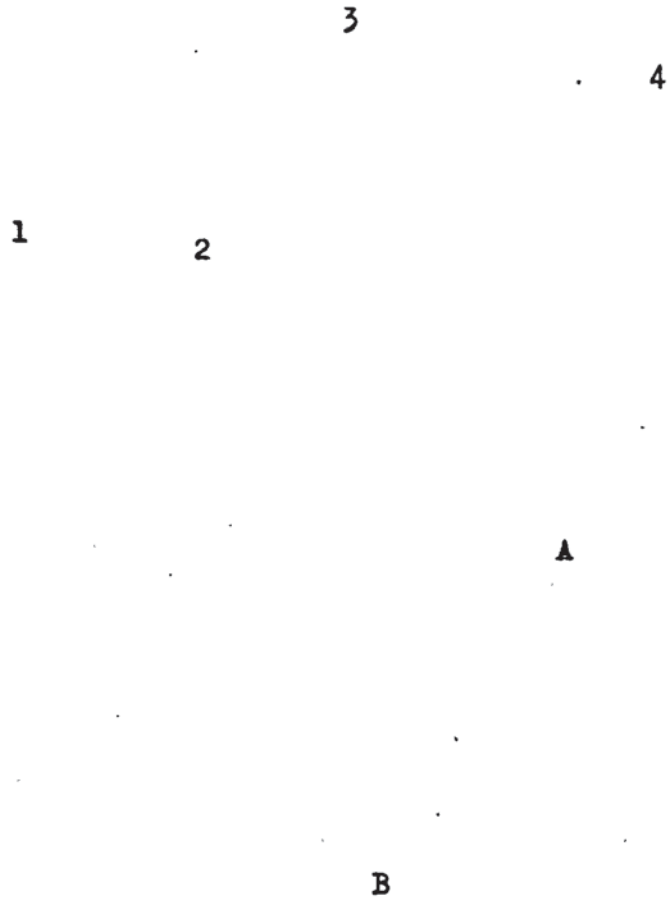

PLATE 5.2 DISTRIBUTOR ASSEMBLY

The letters are the same as those referred to in Fig 5.2

1. Isolated nozzle.
2. Main chamber.
3. Stainless steel distributor plate.
4. P.T.F.E. distributor plate.

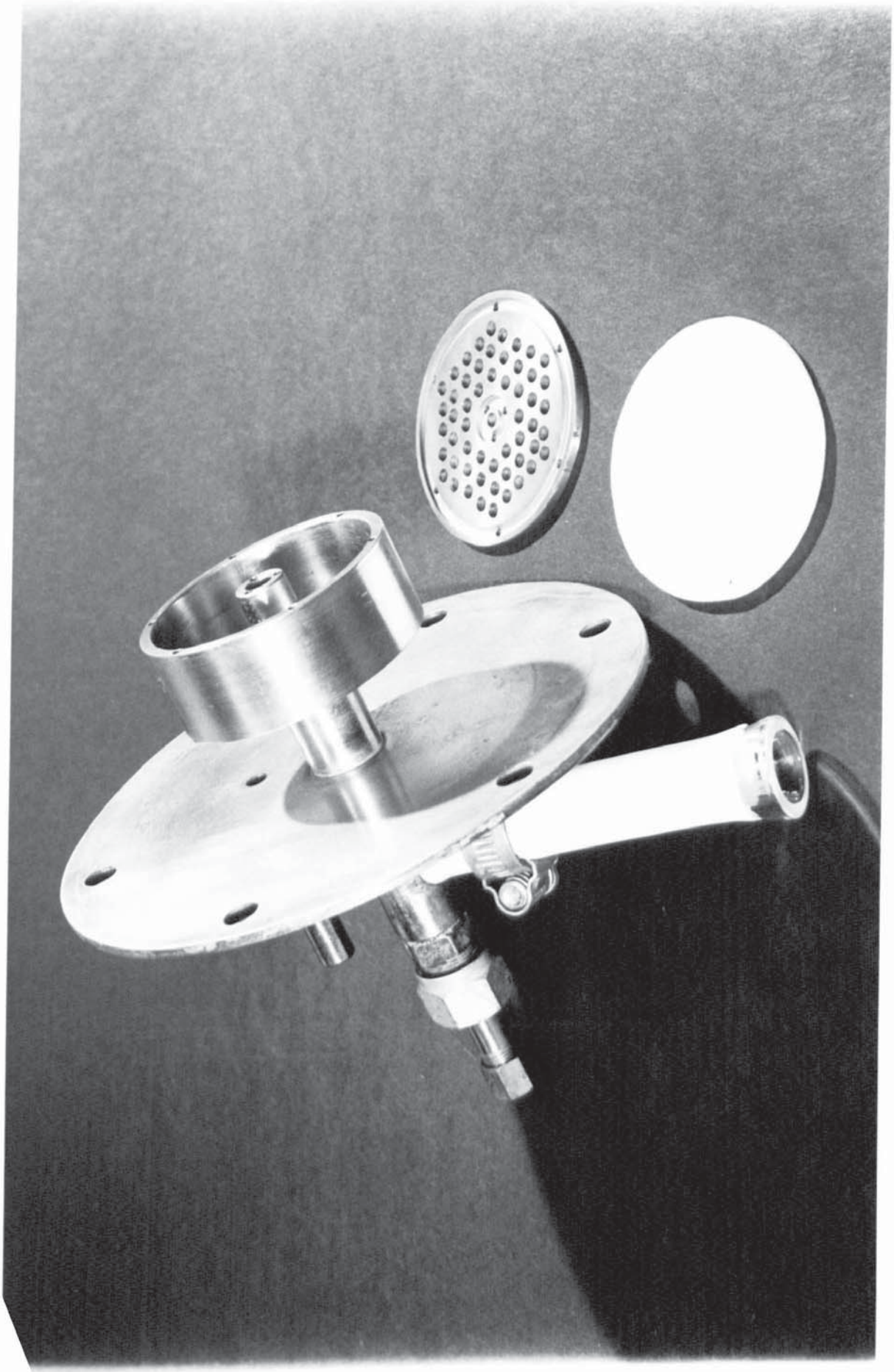

5.2) contd.

a refractive index range of 1.333 of water to 1.470 for glycerine can be obtained. Any organic liquid which is immiscible with water and glyerine and has a refractive index within the range of 1.333 to 1.47 can be used for the liquid pair. This enables a very close refractive index matching to be achieved.

Several organic liquids meet the above criteria, but as can be seen from Appendix (4) the viscosity of the glycerine water mixture increases rapidly after the concentration exceeds 50% by weight. The organic liquids chosen were therefore limited to correspond to a 50% glycerine water mixture. In Table (5.1) are presented a number of organic liquids that can be used. In systems I to IV the organic phase was dispersed whereas in systems V and VI the dispersed phase was the aqueous phase.

5.3) Experimental procedure.

From Appendix (2) the appropriate weight percentage of water and glycerine was determined. The refractive index of the water-glycerine mixture was checked, using an Abbe refractometer and a sodium light source, with that of the organic. The temperature of the equipment and of the refractometer were maintained at 20°C. After mutual saturation of the two phases the column(1) was filled to a predetermined height with the continuous phase. The rest of the equipment was then filled with the dispersed phase which was allowed to circulate through the equipment. The flow of the dispersed phase was then adjusted to the required rate and the operation was allowed to reach steady state. By using the phototropic dye or a discriminated single drop the bed height was noted. Measurements

TABLE 5.1

SYSTEM	DISPERSED PHASE	CONTINUOUS PHASE	REFRACTIVE INDEX	VISCOSITY cp DISP. μ_d	VISCOSITY cp CONT. μ_c	DENSITY gm/cm^3 DISP. ρ_d	DENSITY gm/cm^3 CONT. ρ_d	INTERFACIAL TENSION γ dynes/cm.
I	*AMYLACETATE	52% Wt.G	1.460	1.350	8.00	0.870	1.140	14.2
II	*ETHYLACETATE	37% Wt.G	1.372	0.455	3.60	0.900	1.090	7.0
III	*ISO OCTANE	48% Wt.G	1.395	0.433	5.45	0.692	1.122	35.6
IV	*HEXANE	37% Wt.G	1.372	0.326	3.60	0.660	1.090	34.5
V	*17% Wt.G	DIETHYLETHER	1.355	1.60	0.233	1.042	0.713	10.0
VI	*46% Wt.G.	ISOBUTYLACETATE	1.392	5.25	0.732	1.118	0.870	12.5
VII	ISOPROPYLETHER	27% G	1.367	0.470	2.15	0.730	1.065	15.0

*Systems that have been investigated.

5.3) contd.

of the probabilities of drop interface, drop wall and inter-drop coalescences were made. A Rustrack event recorder with an electrical clock calibrated to 100^{th} of a second was used to measure the residence times of single and layers of drops in the bed. The event recorder facilitated the measurement of several drops simultaneously.

The apparatus was cleaned before changing the systems. First the eqipment was flushed with water, then water with certain amounts of Decone concentrate was circulated through the equipment and was allowed to soak overnight. After draining the dilute Decone solution the equipment was then flushed with water continuously for several hours to remove all traces of the Decone. Finally the equipment was rinsed several times with distilled water and allowed to dry before fresh solution and organic liquids were introduced.

5.4) Phototropic dye technique.

A phototropic dye was used for the flow visualization for the following reasons:-

i) Only traces of the dye are normally required to bring about an effective colour change, and it does not cause any changes to the physical properties of the system.

ii) As the photochemical reaction is reversible, the process can be repeated as many times as is required without replacing the liquids because of contamination to the system.

5.4) contd.

The dye chosen was (1,3,3-TRIMETHYLINDOLINO-6'-NITROBENZOPYRYLOSPIRAN) which is the 6'-Nitro derivative of a family of compounds called the K spiro compounds. Other derivatives are (7'-Nitro), (7'-Chloro),(6',8'-Dibromo),(6'-Nitro-8'allyl) which causes a different colour change on irridiation. The dye is not commercially available but was synthesised using the procedure of Berman et al.[99] by refluxing a mixture of equimolar amounts of (5-NITROSALICYLALDEHYDE) and (2-METHYLENE-1,3,3-TRIMETHYLINDOLINE) in absolute ethonal in a steam bath for 5 hours. The resultant highly coloured mixture was cooled in an ice water bath, filtered, washed with cold ethonal and recrystallized from ethonal-water mixture.

The reversible reaction of the spiropiran dye requires ultraviolet radiation to break the carbon-oxygen bond in the spiropiran ring converting its structure to that of a merocyanine dye[100].

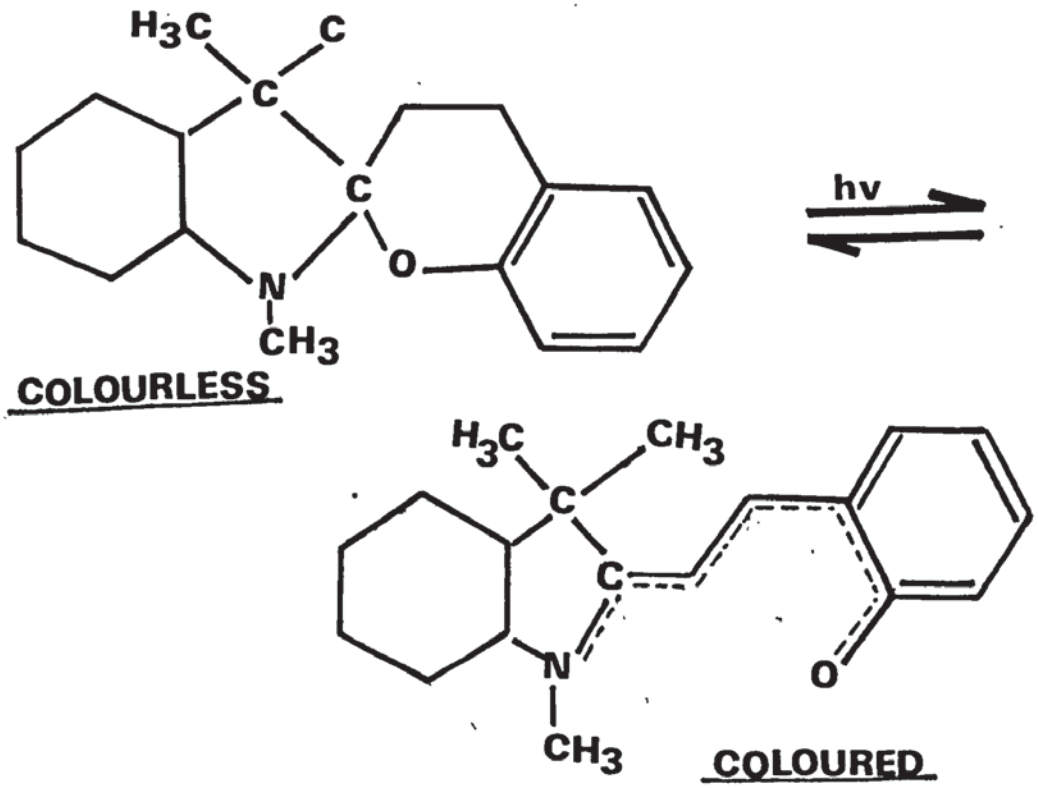

5.4) contd.

The equilibrium which exists between the colourless "closed" form and the coloured "open" form is dependent on the thermal and light radiation levels and also on solvent polarity, with non-polar solvents generally favouring the closed colourless form and vice-versa.

The dye is soluble in organic liquids only, and was found to be a satisfactory tracer when used in the organic liquids listed in Table (5.1). The forward reaction i.e. colourless to coloured, is instantaneous while the reverse takes several minutes for the colour to completely disappear. A small amount of the dye about 2×10^{-3}% by weight was dissolved in the organic liquid. A mercury arc lamp fitted with an iris diaphragm was used as the source of the U.V. light to effect the colour change.

In the case of systems I to IV where the organic liquids were the dispersed phase, the mercury arc lamp was situated in the free falling section of the column. A short pulse of the mercury arc lamp via the iris diaphragm caused the drops in the path of the U.V. light to change colour. They then formed a coloured layer of drops at the beginning of the bed and were studied as they passed through the bed, thereby giving the height of the bed and the average residence time of the drops in the bed. The U.V. beam could be narrowed so that one or several drops changed in colour rather than a layer. The coalescence phenomena of the drops in the bed were studied. The shape and the packing efficiency of the drops were also observed by this means.

When the organic liquids were the continuous phase as with systems V and VI, the mercury arc lamp was situated

5.4) contd.

at the desired level in the bed. Exposure to U.V. light caused the organic liquids in the plateau borders to change colour thereby exposing the network of plateau borders through which the continuous phase drains. The U.V. beam was collimated via a series of orifices which caused a coloured line to be drawn through the bed. Information regarding the behaviour of drops and drainage mechanism of the continuous phase were obtained by this method.

5.5) Frequency Doubler technique.

Another way of effecting a colour change in the phototropic dye was the use of a second harmonic generator to reduce the wavelength of the ruby laser used from 6943°A to 3471.5°A which is in the ultraviolet range.

A solid state ruby laser LU6 supplied from Barr and Stroud was used fitted with a QS1905 Dye cell Q Switch to give an output power of 5-10 MW, the pulse width being 20 nanosecs. The frequency doubling crystal was mounted on a spring loaded platform with screws for adjustment. An autocolimator was used for the final alignment of the frequency doubler with the laser. The laser was then focused at the required height of the bed and pulsed. Several blue spots appeared in the bed where the organic continuous phase had changed colour. Plate (5.3) shows the sequence of the event. It must be mentioned, however, that the frequency doubler is only 10% efficient and most of the laser light is not utilised. The technique has been reported to have been successful for very short tracer lengths (1-2)cm by

PLATE 5.3 INSTANTANEOUS COLOUR CHANGE IN THE CONTINUOUS PHASE INSIDE THE BED USING THE FREQUENCY DOUBLER TECHNIQUE.

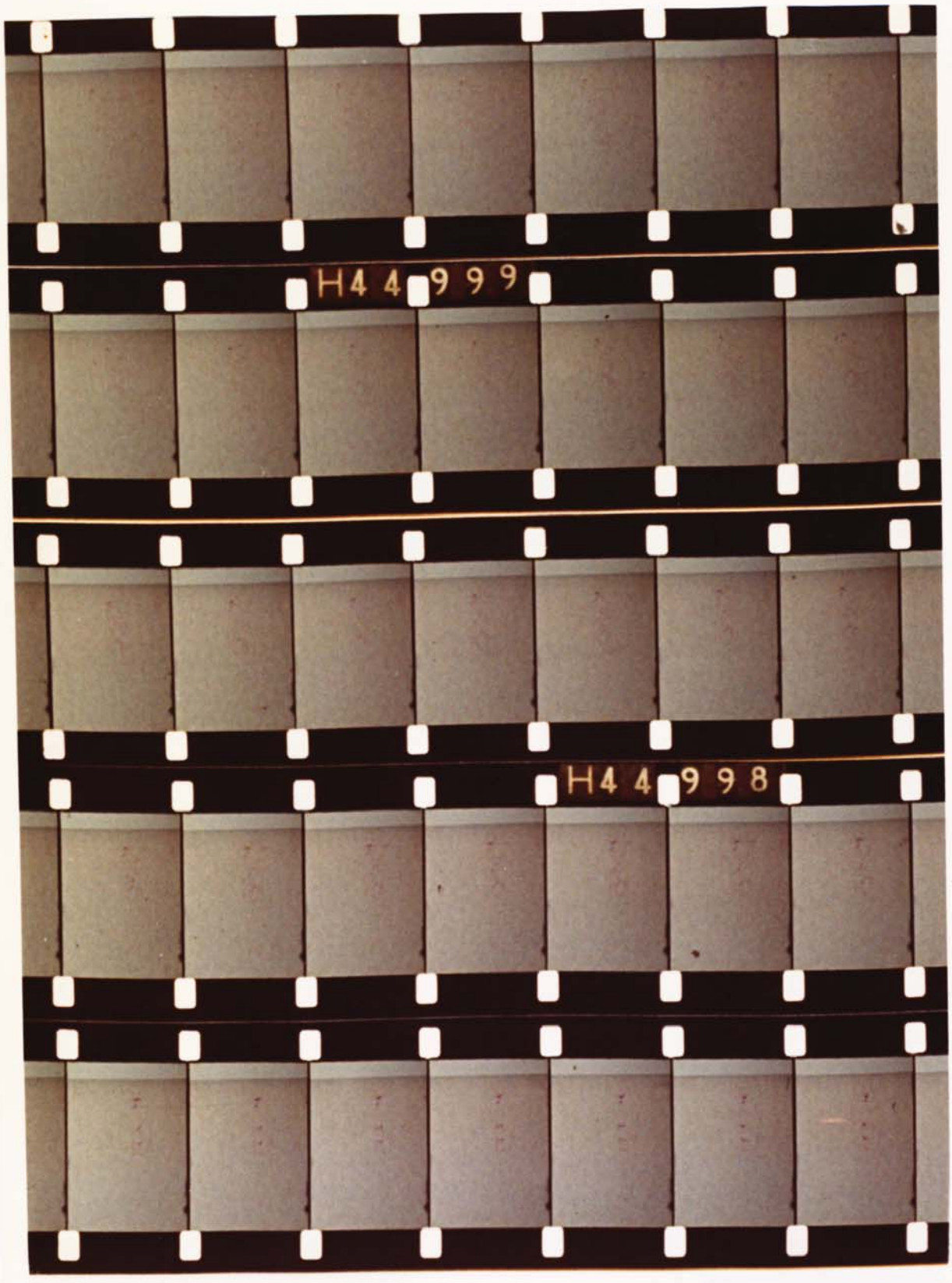
H4 4 9 9 9
H4 4 9 9 8

5.5) contd.

Hummel et al.[88,90]. A more efficient frequency doubler needs to be developed before the technique can be applied over longer distances.

5.6) Discriminated drop Method.

The isolated nozzle in the distributor described in paragraph (5.1) was used to introduce one or several coloured drops into the bed. The discriminating agent used was a non-surfactant dye "Red oil O". It was reported to be non-surfactant and was found to be so at low concentrations[89]. The dye, being insoluble in water and glycerine, was dissolved in a sample of the dispersed phase which was injected into the separate nozzle in the distributor to form the discriminated drops. These drops were identical to the rest of the drops except for their colour which made them visible. Their behaviour as they entered and propogated through the bed was observed and photographed for analysis. The type and number of the coalescences between the drops and the position in the bed at which the coalescence took place were noted. When a discriminated drop coalesced with an adjacent transparent drop the resultant drop became larger and surprisingly the dye slowly diffused from the coloured to the transparent section of the enlarged drop. This gave an indication about the internal circulation in the drops after coalescence. Finally residence times of single drops were also noted using this method.

5.7) Holographic Technique.

A Q switch pulsed laser was used as the coherent light source. The holographic method used was a form of diffused holography illustrated in Figure (5.3). The laser and the various optical accessories were fixed on an optical bench. The pinhole was produced by focusing the laser light through a 2 in. microscope objective lens on to a thin metal sheet. An optical flat and a front silvered mirror were used as the beam splitter and the reference beam reflector respectively. 10E 75 Agfa Geveart film was chosen as the holographic plate.

The technique was applied successfully to moving drops in a glass cell. However the success was limited when it was applied to moving drops in the column.

5.8) Christiansen effect.

The matching of the refractive indices of the liquids studied was based on the sodium D line. However, the indices are not identically matched for all other wave lengths. It is impossible to achieve equality of the refractive indices for all wavelengths simultaneously. This effect was studied by Chrisiansen[101] in 1884 by balancing the refractive index of quartz glass with mixtures of benzyl alcohol and carbon disulphide for different wavelengths thereby producing varying colour. The above principle, which is known as the Christiansen filter, has been applied in the construction of monochromatic light filters. Various authors have sought a theoretical expression of the bandwidth of the Christiansen filter as a function of a certain number of parameters. Most

5.8) contd.

notable amongst the results obtained are those of Raman[102]. He stipulated that blending of the two phases constituting the filter is a hetrogeneous medium for all wavelengths except the one for which the refractive indices of the solid and the liquid are equal. It is clear, therefore, that after balancing the refractive indices of the continuous and the dispersed phase the resulting bed acts as a form of a Christiansen filter. For any particular wavelength the difference in the refractive indices between the continuous and the dispersed phase causes the light rays to be bent away from the perpendicular to the medium with the higher refractive index thereby resulting in a demarcation line. This principle was employed to study closely the behaviour of the drops in the dispersion. The optical arrangement is shown in Figure (5.4). A light source was focused on to a pinhole by a 16 mm. microscope objective. A second 16 mm. microscope objective was used to colimate the beam to a few mm. in diameter which was then passed through the column. Finally a line was used to project the image on to a screen where it was photographed. A mercury arc lamp was used as the light source. This presented a difficulty when high speed motion pictures were taken because the film resolved the discharge cycle which resulted in cycles of under exposed frames making the analysis difficult. To overcome this difficulty a continuous burning gas laser was used as the light source. Plates (5.4) and (5.5) illustrate the two effects. Plate (5.6) shows a plateau border inside the dispersion. The size of the beam can be varied by moving the microscope objective lens after the pinhole. The elementary unit in the bed was photographed and studied and information regarding film drainage, the shape and the radius of curvature of the plateau border, packing

PLATE 5.4

PHOTOGRAPH OF PLATEAU BORDERS USING CHRISTIANSEN EFFECT AND MERCURY ARC LAMP AS THE LIGHT SOURCE.

The resolution of the light from the mercury arc lamp is illustrated.

PLATE 5.5

PHOTOGRAPH OF PLATEAU BORDERS USING A GAS LASER AS THE LIGHT SOURCE.

The sequence shows the formation of two plateau borders.

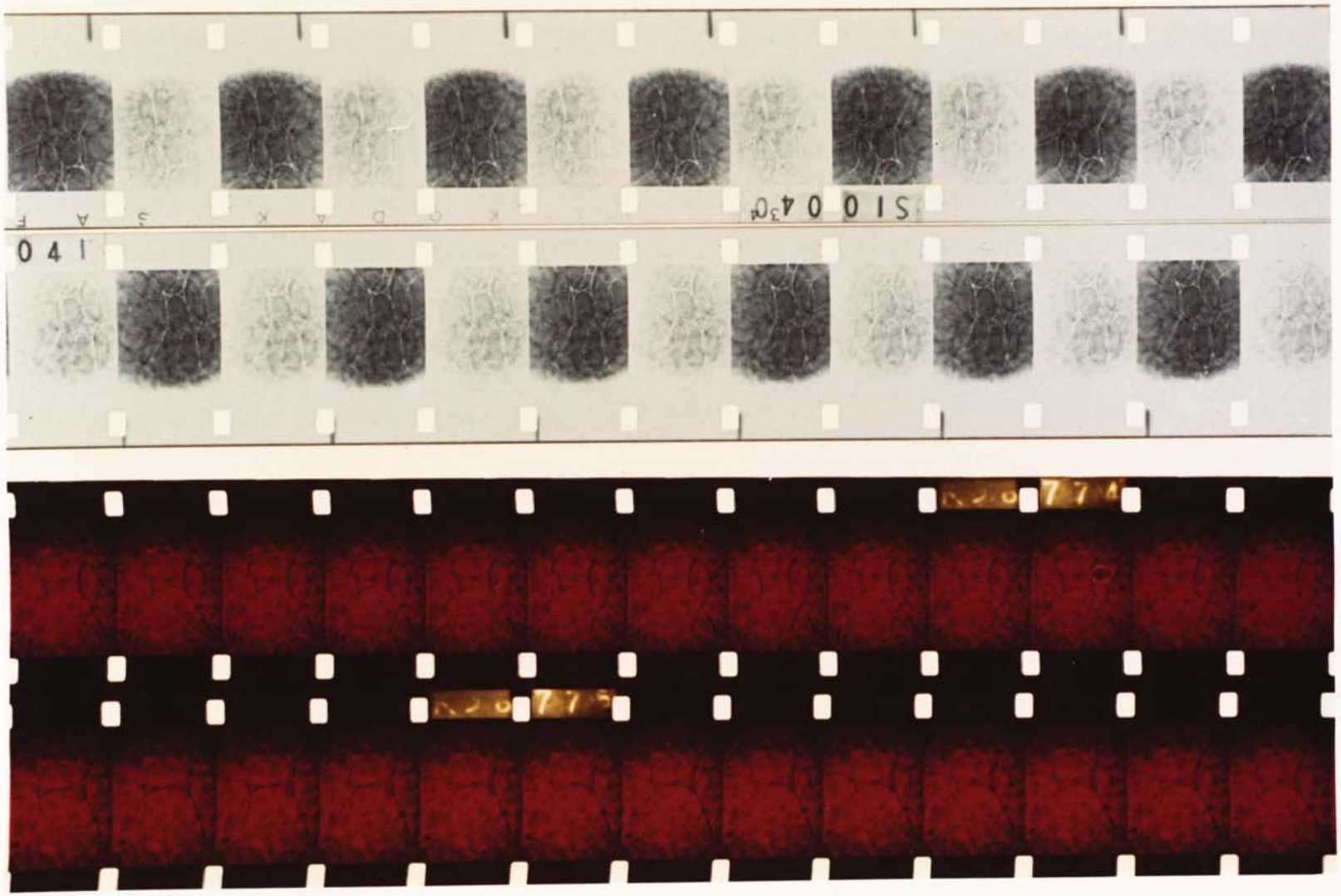

5.8) contd.

arrangement of the drops and interdrop coalescence mechansim was obtained using this technique.

PLATE 5.6 SHAPE OF PLATEAU BORDERS INSIDE THE BED.

Measurements of r_o were taken from this film.

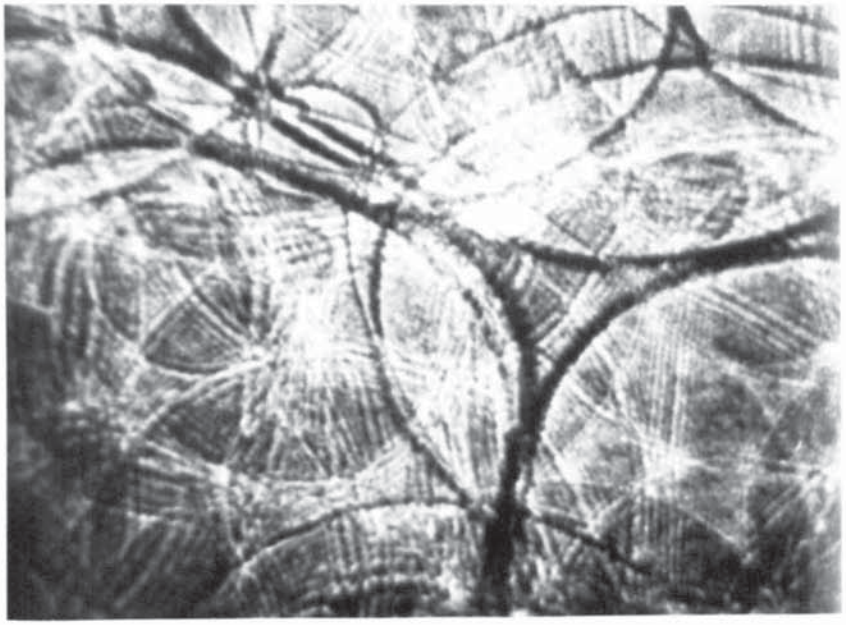

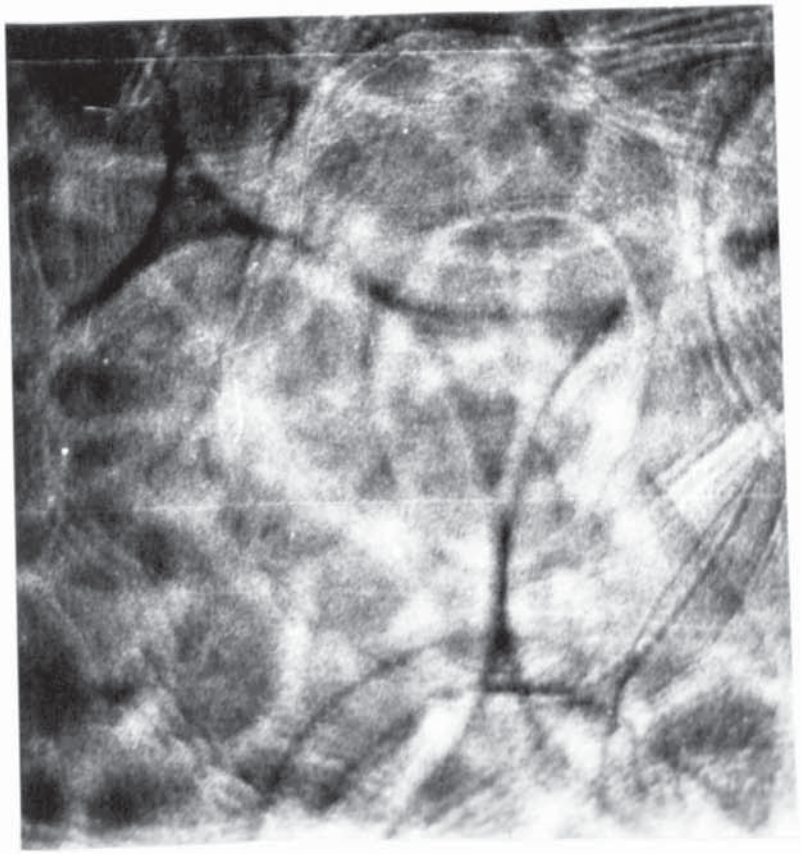

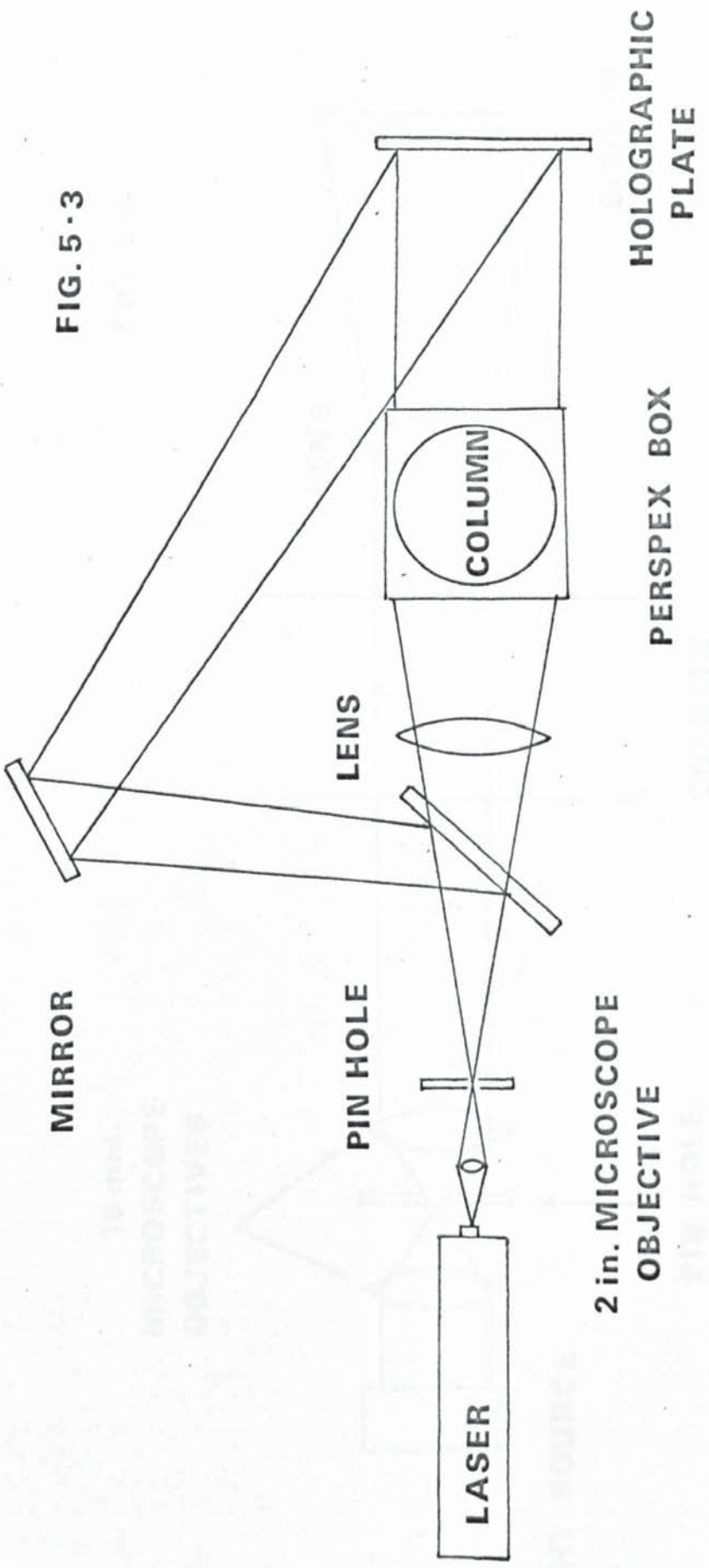
HOLOGRAPHIC PLATE
PERSPEX BOX
COLUMN
LENS
BEAM SPLITTER
MIRROR
PIN HOLE
2 in. MICROSCOPE OBJECTIVE
LASER

FIG. 5·3

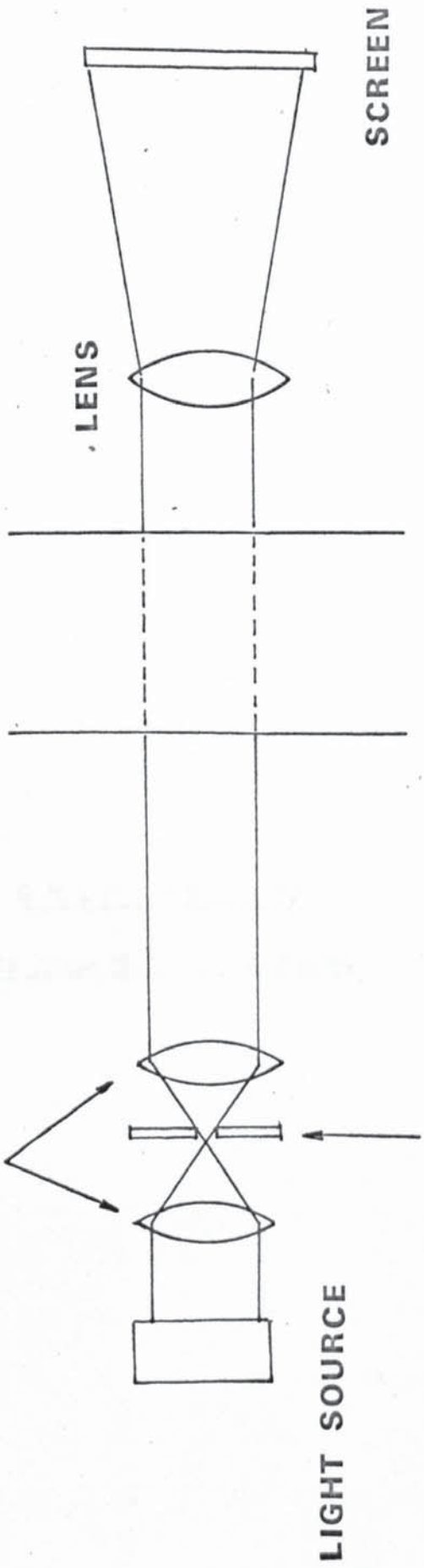
SCREEN
LENS
COLUMN
16 mm.
MICROSCOPE
OBJECTIVES
PIN HOLE
LIGHT SOURCE

FIG. 5·4

CHAPTER 6.

EXPERIMENTAL RESULTS.

6.0) Experimental Results.

As stated previously the techniques described in Chapter 5 revealed that velocity profile exists in the bed. In the past it was generally believed that the drops in the dispersion band moved in a plug flow. This was found to be so at low flow rates. The flow pattern then changes and a velocity gradient is generated as the flowrate increases. It will be discussed in greater detail below.

The bed height versus flowrate relationship are shown in Figures (6.1) to (6.5). From these it can be seen that for any particular drop size the bed height increases with increase in flowrate. Further, for any particular flowrate the bed height increases with a decrease in drop size. This confirms the findings of Ali[41], Smith[49] and more recently Hittit[38]. This has been attributed to the belief that in the dispersion band larger drops coalesce more rapidly than smaller drops. It has been established that before coalescence can take place the continuous phase film between the faces of adjacent drops must drain to a critical thickness. Therefore for the larger drops, a greater drainage time is necessary. There appears to be a contradiction between experimental observation and the theory of film drainage. Thus the dispersion band must be considered in terms of both the film between the faces and the continuous phase drainage rate in the plateau borders.

When the drops arrive in the bed, and before any deformation has taken place, they probably pack in the most efficient way to trap the continuous phase with the result that the dispersed phase is 74% i.e. Ostwald's ratio. When deformation has taken place large drops will deform more readily than the smaller drops. Consequently more of the continuous

6.0) contd.

phase will squeeze out from in between the drops than for the smaller drops. Further it can be seen from equation (4.12) that

$$r_o \propto d^{\frac{1}{4}}$$

where r_o is the radius of the plateau border and d is the drop diameter. So that when d is large r_o is large and, therefore, the flow area in the plateau border A_{pb} is large, equation (4.6a). This results in easier drainage of the continuous phase in the case of larger drops than smaller ones. Consequently it is the retention of the continuous phase and the difficulty of its drainage through the plateau borders in the case of smaller drops that results in greater bed height for the latter. The interfacial tension force causing drainage is expressed by equation (4.13) where

$F \propto \frac{d^2}{r_o}$.

If (d) increases by a factor of 2 from equation (4.12), r_o increases by a factor of 1.19 and the ratio of $\frac{d^2}{r_o}$ by 3.4. Therefore, the force is greater on large drops than on smaller drops which again contributes to a larger bed height in the case of smaller drops.

Consider Figure (6.4) for the system IV (Hexane), the portion of the curve OA shows a slow rate of increase of bed height with flowrate. This changes at B when the portion BC shows a greater rate of increase of bed height with flowrate. It was further noticed during the experiments that the flow pattern of the drops in the bed changes at point A and a velocity profile begins to exist which then becomes fully developed at point B. The velocity gradient causes smaller drops to be projected further into the bed which could account

FIG 6.1

SYSTEM I AMYL ACETATE

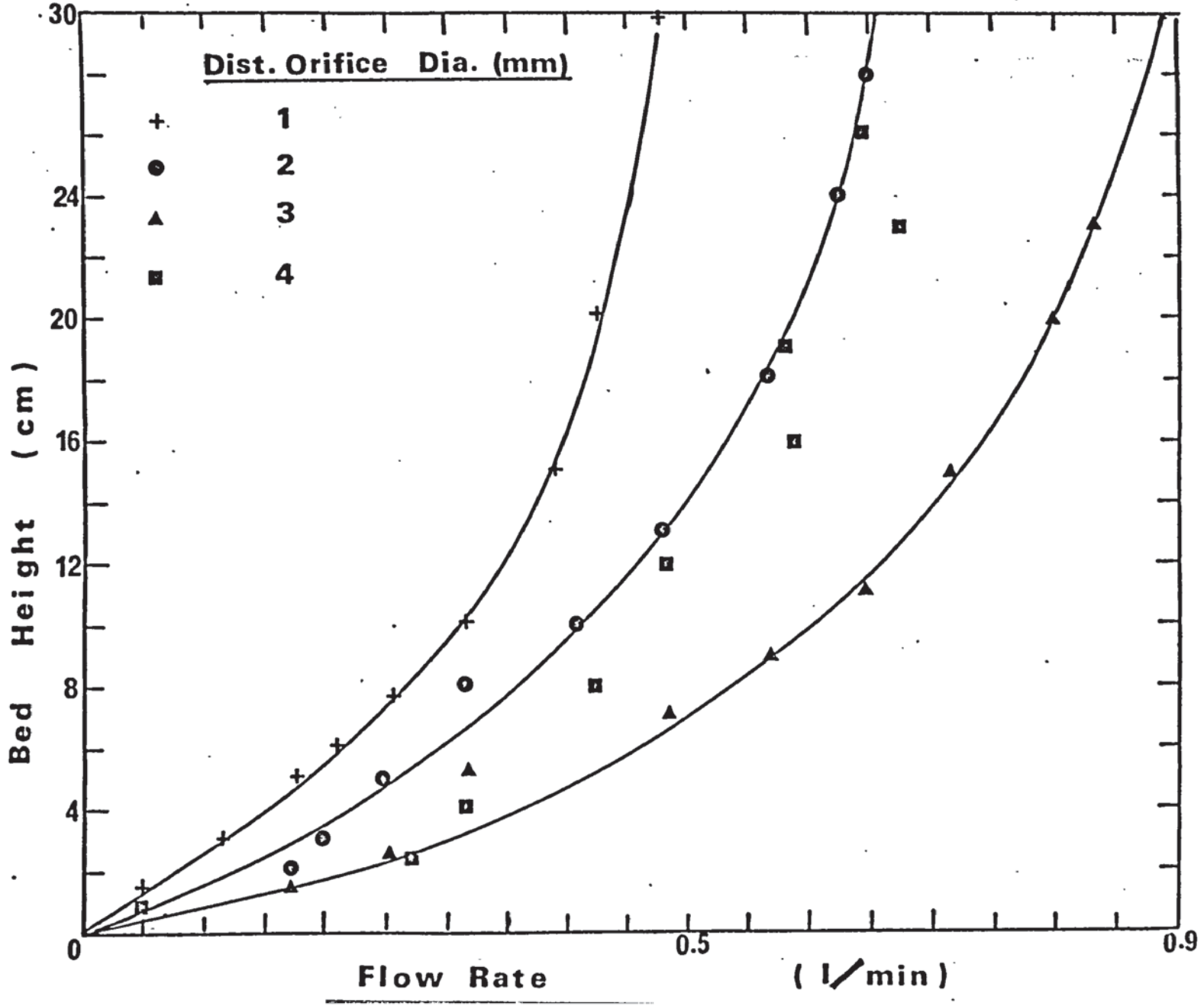

FIG 6.2

SYSTEM II ETHYL ACETATE

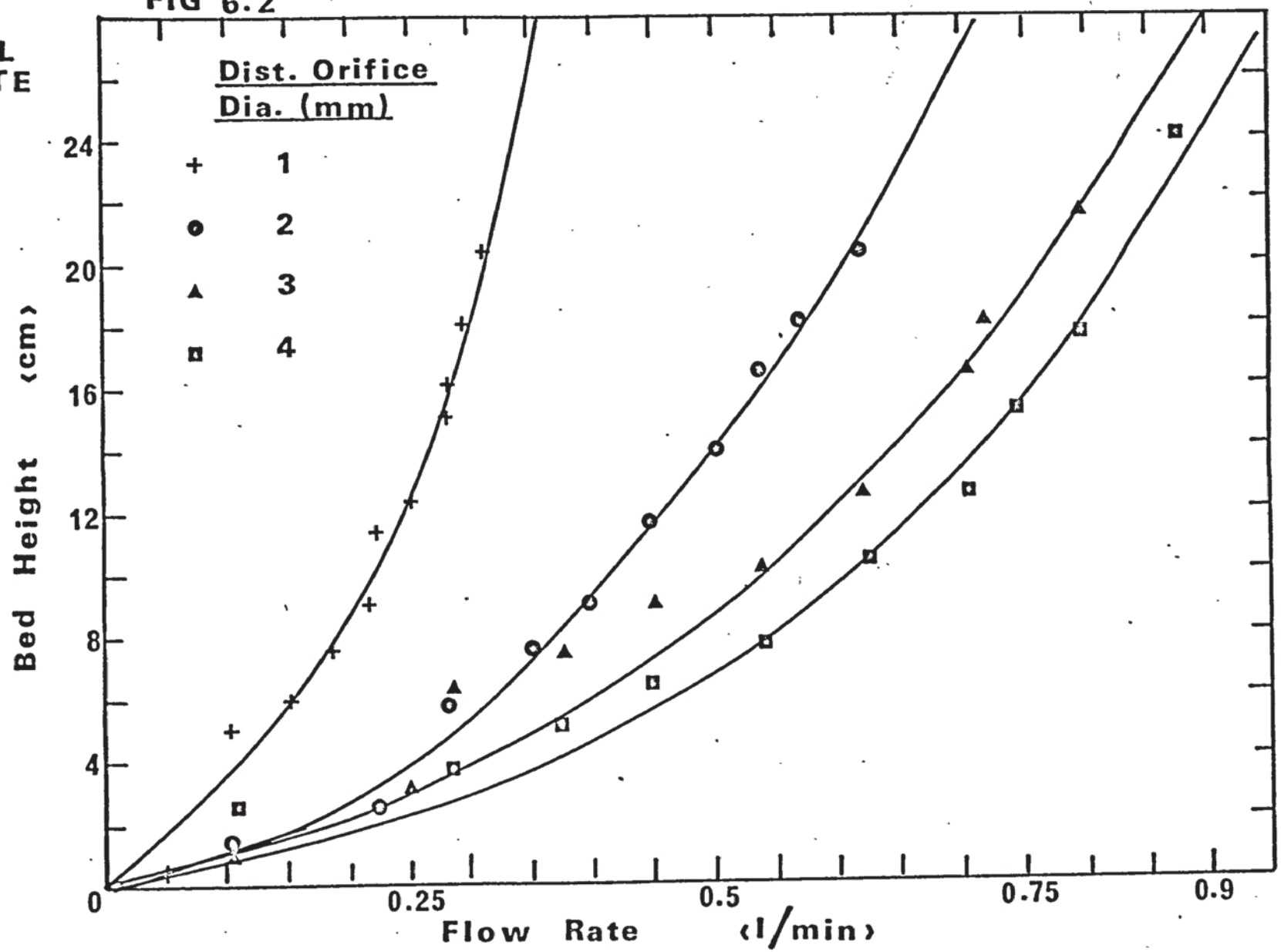

FIG 6.3

SYSTEM III ISO OCTANE

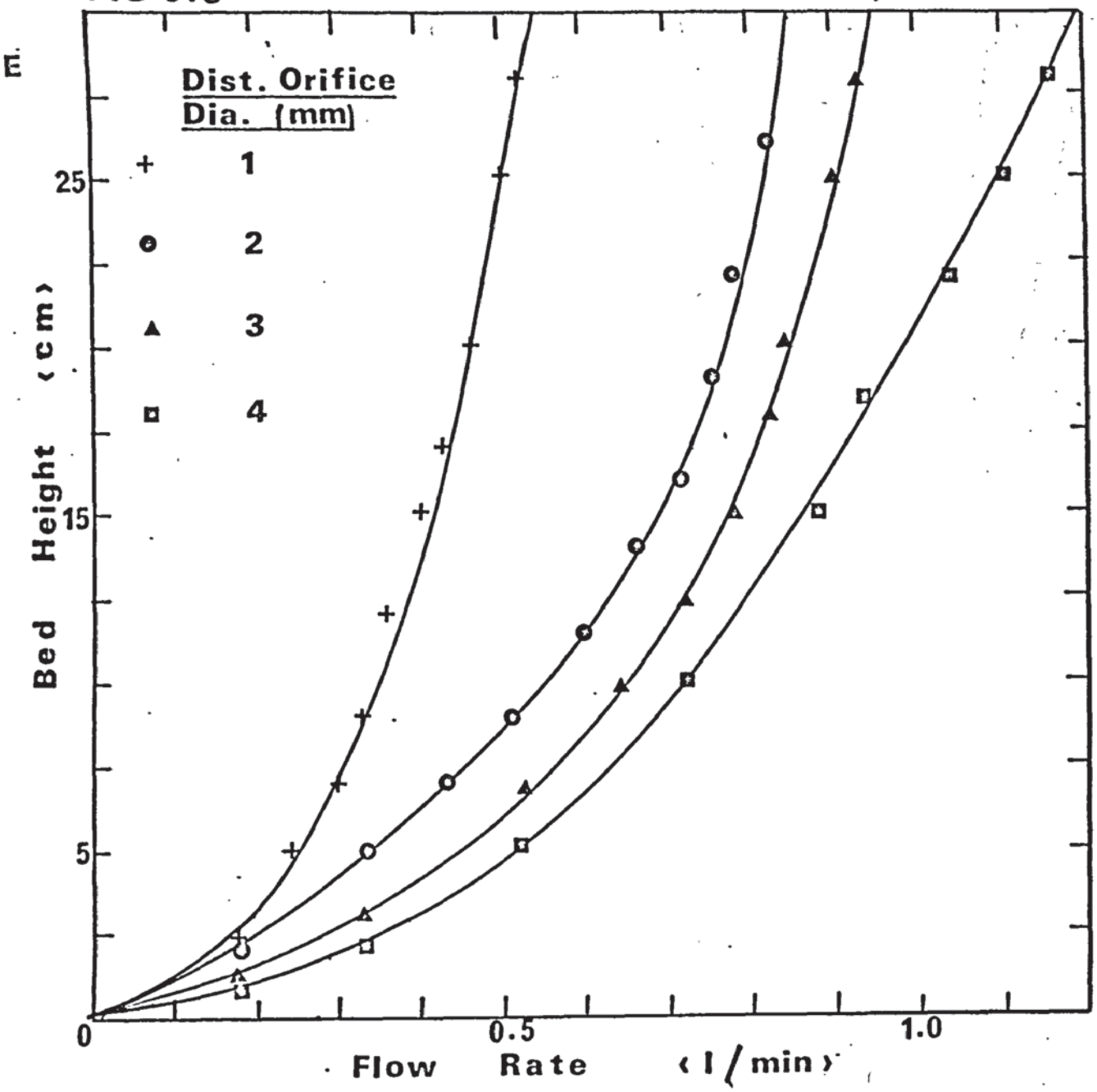

SYSTEM IV HEXANE

FIG 6.4

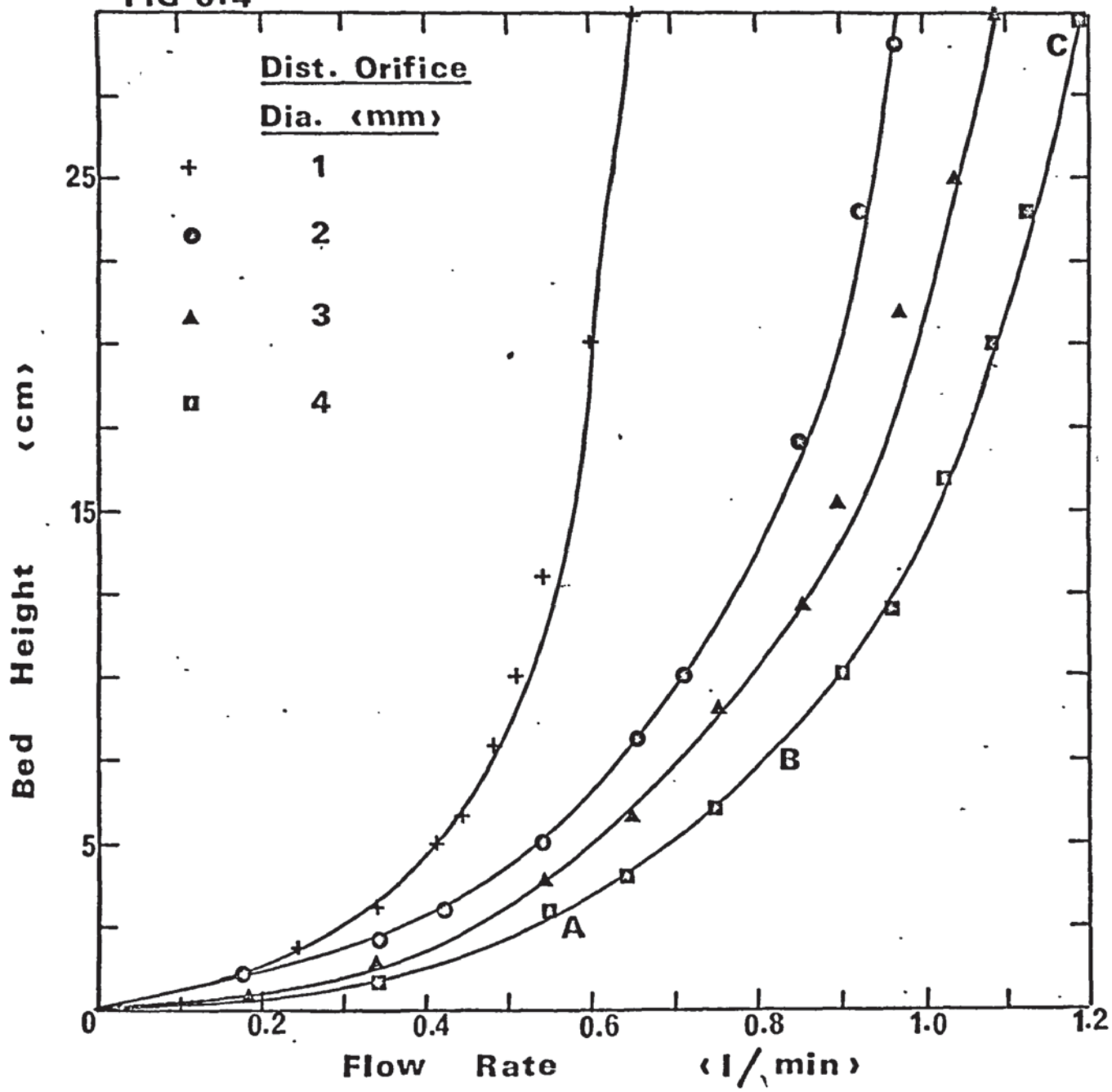

SYSTEM V
DIETHYL ETHER

FIG 6.5

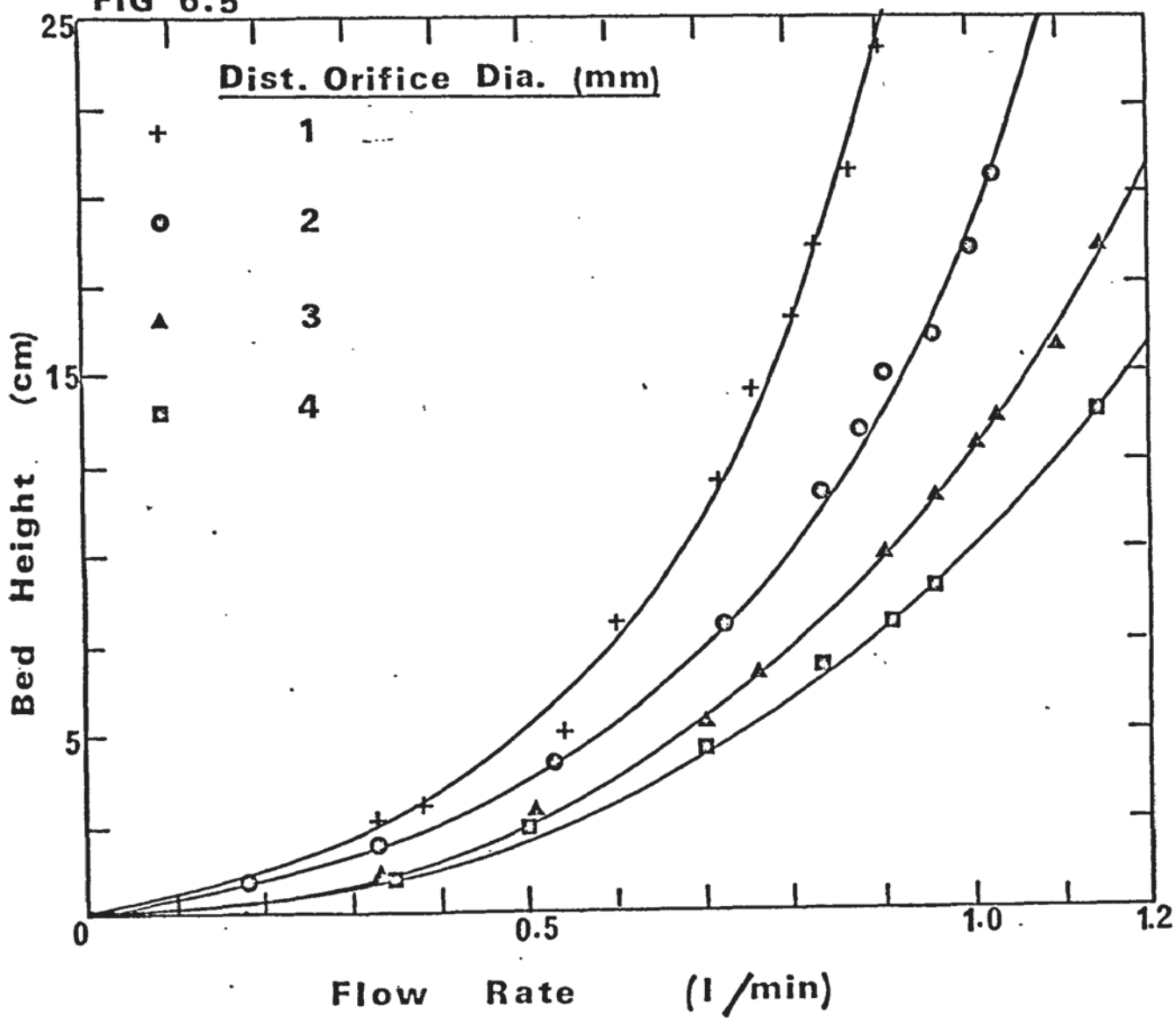

6.0) contd.

for the higher rate of increase of bed height after point B. The portion AB is the transition period. This behaviour was observed in all the systems.

Figures (6.6) to (6.10) show the relationship between the residence time of the drops with flowrate. The residence time increases with the increase in bed height for the same reasons as above. However, for any particular bed height the residence time decreases with the increase in drop size. This must be due to the buoyancy forces being greater on large drops than on smaller ones. Also the graph is in two sections, before and after the propagation of the velocity profile with a transition period similar to the behaviour of the bed height flowrate relationship. This is shown clearly in Figure (6.6) for the Amyl acetate system. It is worth noticing, however, that at low bed heights there is a noticeable scatter of points and the residence time is not consistent. This is due to the fact that the residence time can be regarded as a combination of

a) the time required for the drop to travel to the coalescing interface, and

b) the time taken for the drop to coalesce and disappear with the dispersed phase homophase.

At low bed height the predominant factor is the latter which proved to be inconsistent giving rise to the discrepancy. At large bed height, on the other hand, the first factor is the predominant one and the time measured becomes the true residence time rather than the inconsistent drop interface coalescence time.

Finally measurements of the probability of coalescence for systems I to III, for different bed heights, are presented in Figures (6.11) to (6.22). An average of 70 drops was measured

FIG 6.6

SYSTEM I
AMYL
ACETATE

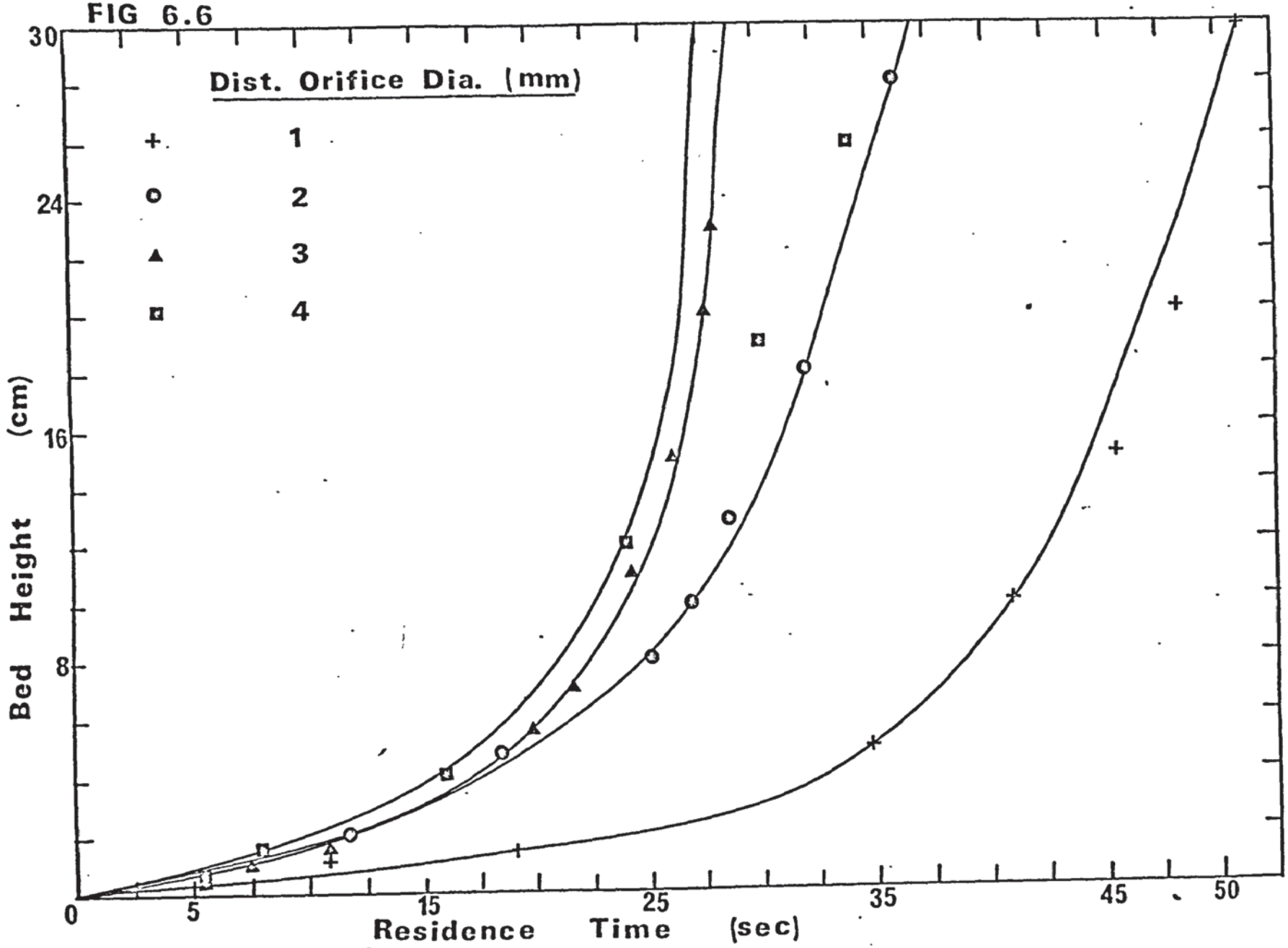

SYSTEM II
ETHYL ACETATE

FIG 6.7

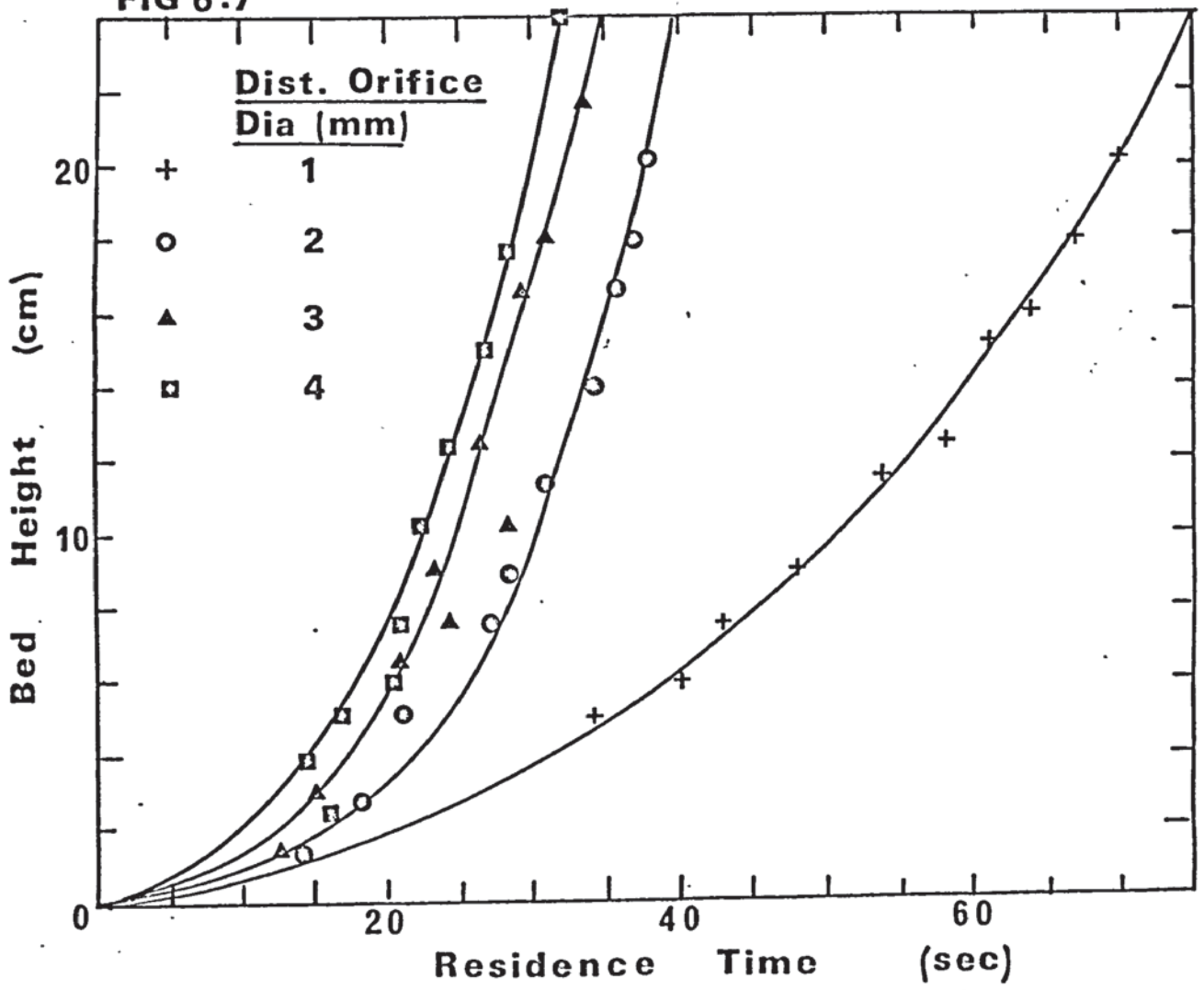

FIG 6.8

SYSTEM III

ISO OCTANE

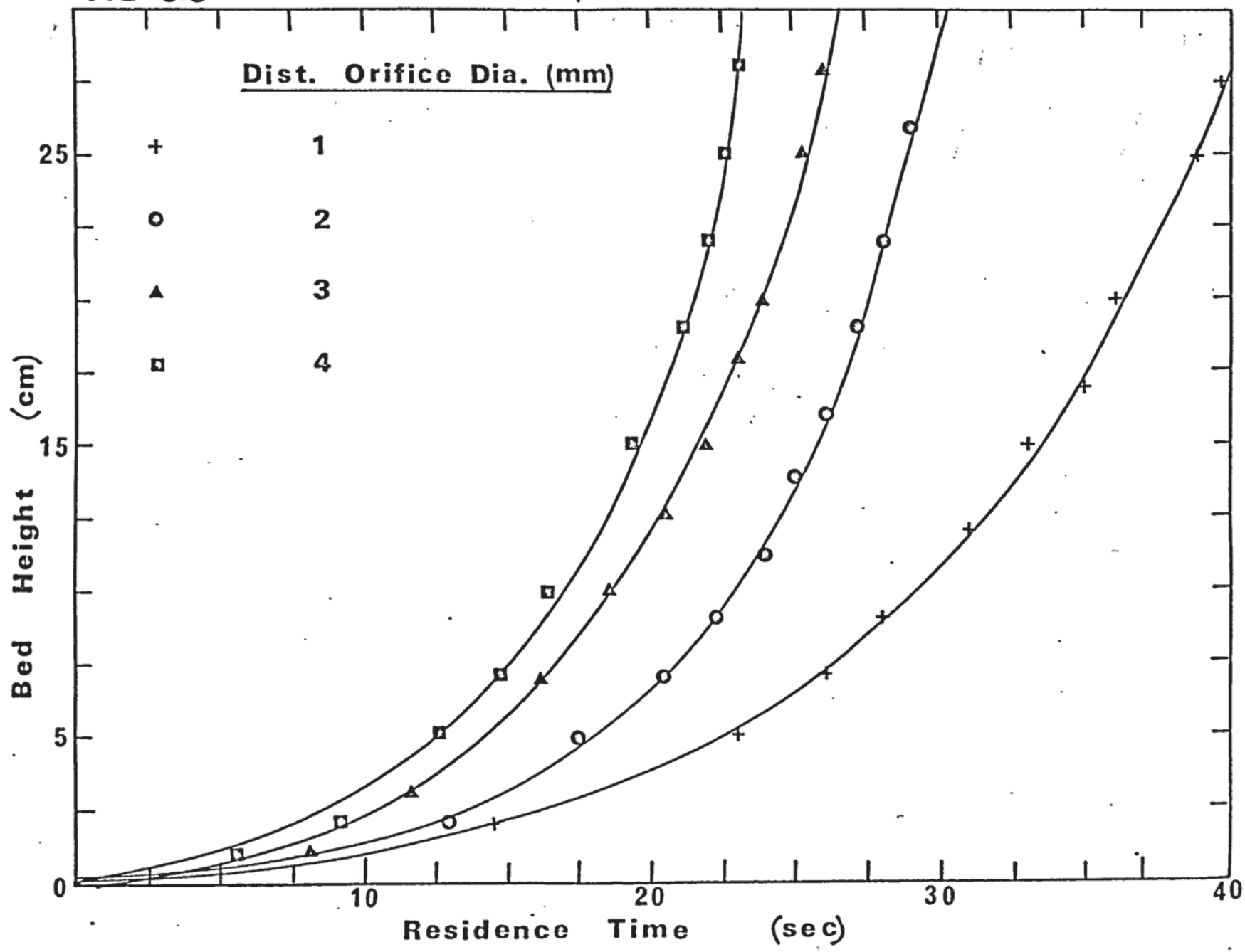

SYSTEM IV HEXANE

FIG 6.9

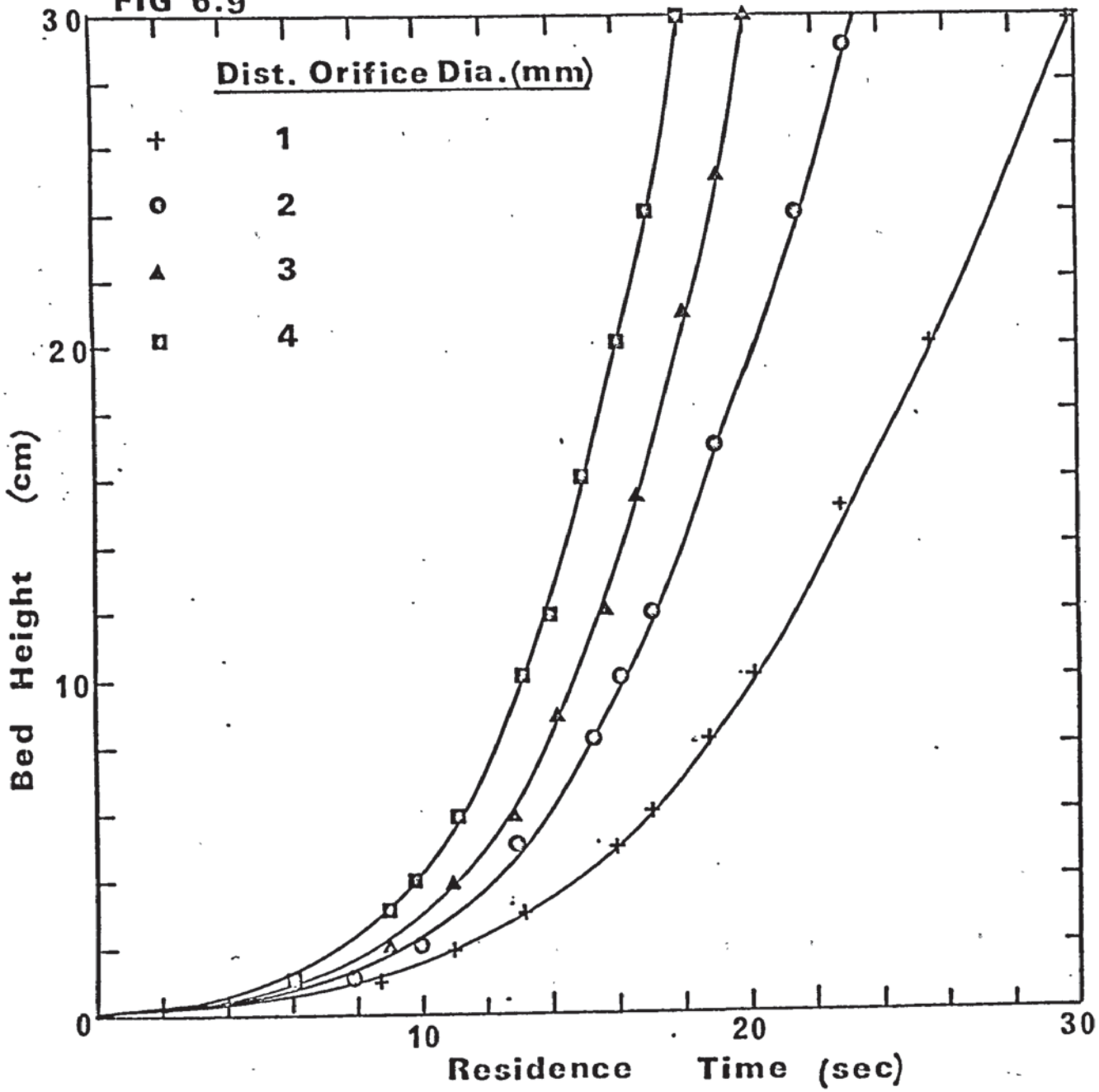

SYSTEM V
DIETHYL ETHER

FIG 6.10

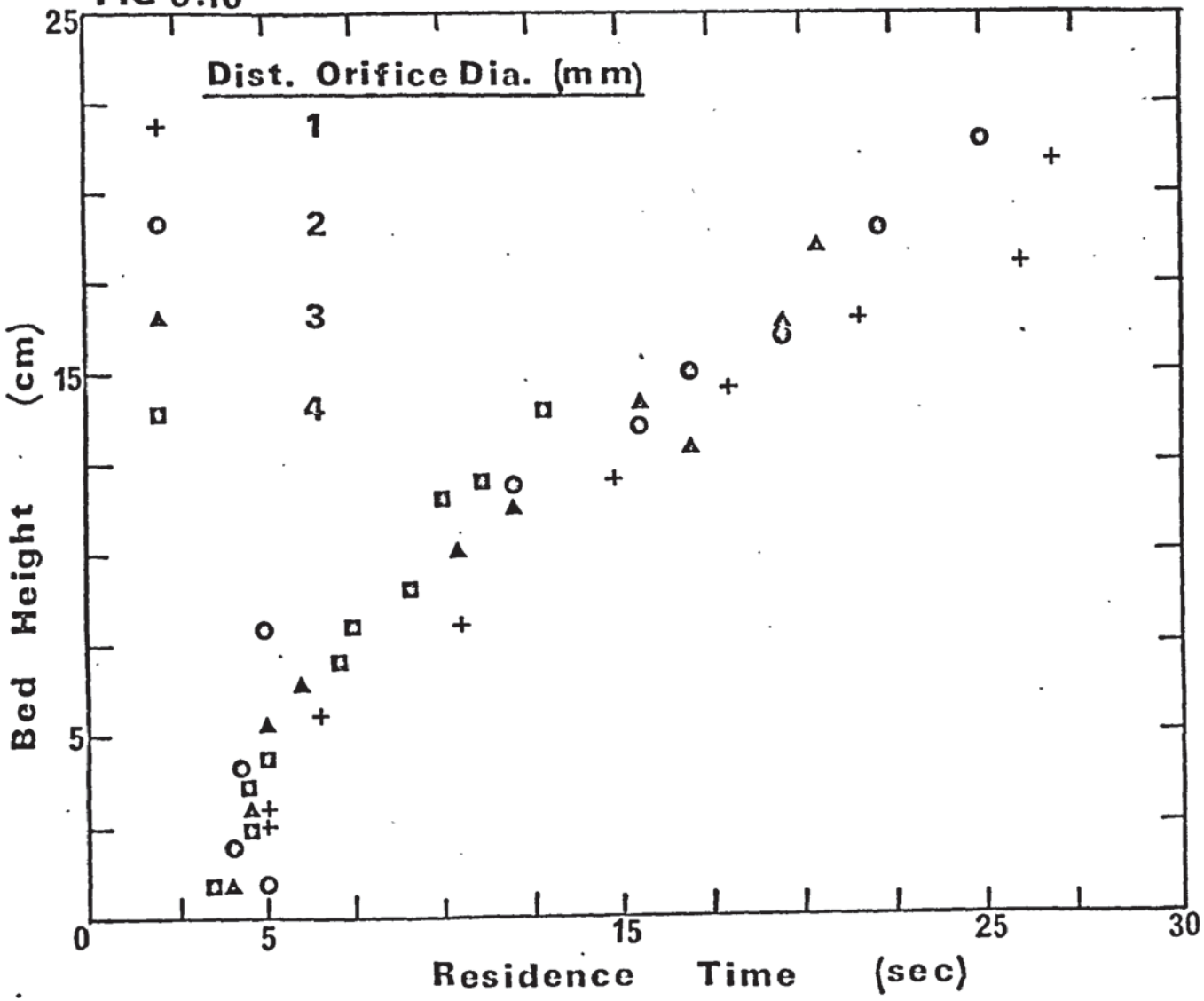

6.0) contd.

for each bed height. Figures (6.23) to (6.41), on the other hand, show the average coalescence probability for a complete bed e.g. in Figure (6.28), the abscissa value of 3,5 etc. represents the first 3 cm. and the first 5 cm. of a bed height of 24 cm. respectively. These are therefore the instantaneous coalescence probabilities at the planes within a particular bed. The significance of these curves is further discussed in Section 8 and is one of the basic concepts in the development of the model describing drainage.

6.1) Velocity profile.

The true mechanism of the velocity profile in a dispersion band is not yet fully understood, nor is the reason for its propagation. In fact, previous to this finding it was generally assumed that the flow of drops in a dispersion band was plug flow. The mechanism of such a flow was described by the successive replacements of the drops after one has disappeared at the coalescencing interface. If the same mechanism is assumed to occur when a velocity profile exists, this presupposes the fact that the rate of drop interface coalescence at the centre of the coalescence interface is greater than at the periphery causing the drops in the centre of the bed to move faster. Several facts support this hypothesis. It was noticed that the coalescence interface changes from a flat to a curved one. The curvature resembles that of the profile. Such a curvature suggests that a greater coalescing area is being exposed at the centre of the interface giving rise to a faster rate of drop disappearance at the centre than at the periphery. Hittit[38] observed large drops appearing at the centre of the coalescing interface. The disappearance

6.1) contd.

of such drops can also give rise to a faster movement of the drops at the centre of the bed.

An analogy can be drawn between the velocity profile of fluid flowing in a pipe and the profile in a dispersion band by assuming that the drops in the bed form concentric cylinders slipping past each other. The cylinder adjacent to the wall has the highest number of drops and the lowest velocity. The centre of this idealised situation is a single drop with the highest velocity. This,however, neglects the drop wall coalescence and the interdrop coalescence in the radial direction. The above type of coalescence must inevitably lead to radial movement of the drops.

The situation is clearly more complicated than described and before it can be expressed in mathematical terms more information is needed. Further studies must be conducted in the transition period to understand the mechanism and the reason for its propagation.

Table (6.1) lists the bed height at which the velocity profile is evident. It ranges from 5 cm. to 12 cm. bed height and seems to be independent of physical properties. This is probably due to the fact that there exists no clear dividing line between the plug flow and profile flow and the effect is dampened by the existence of the transition period. Plate (6.1) illustrates the propagation of the profile for the amylacetate system.

PLATE 6.1 PROPAGATION OF THE VELOCITY PROFILE IN THE BED.

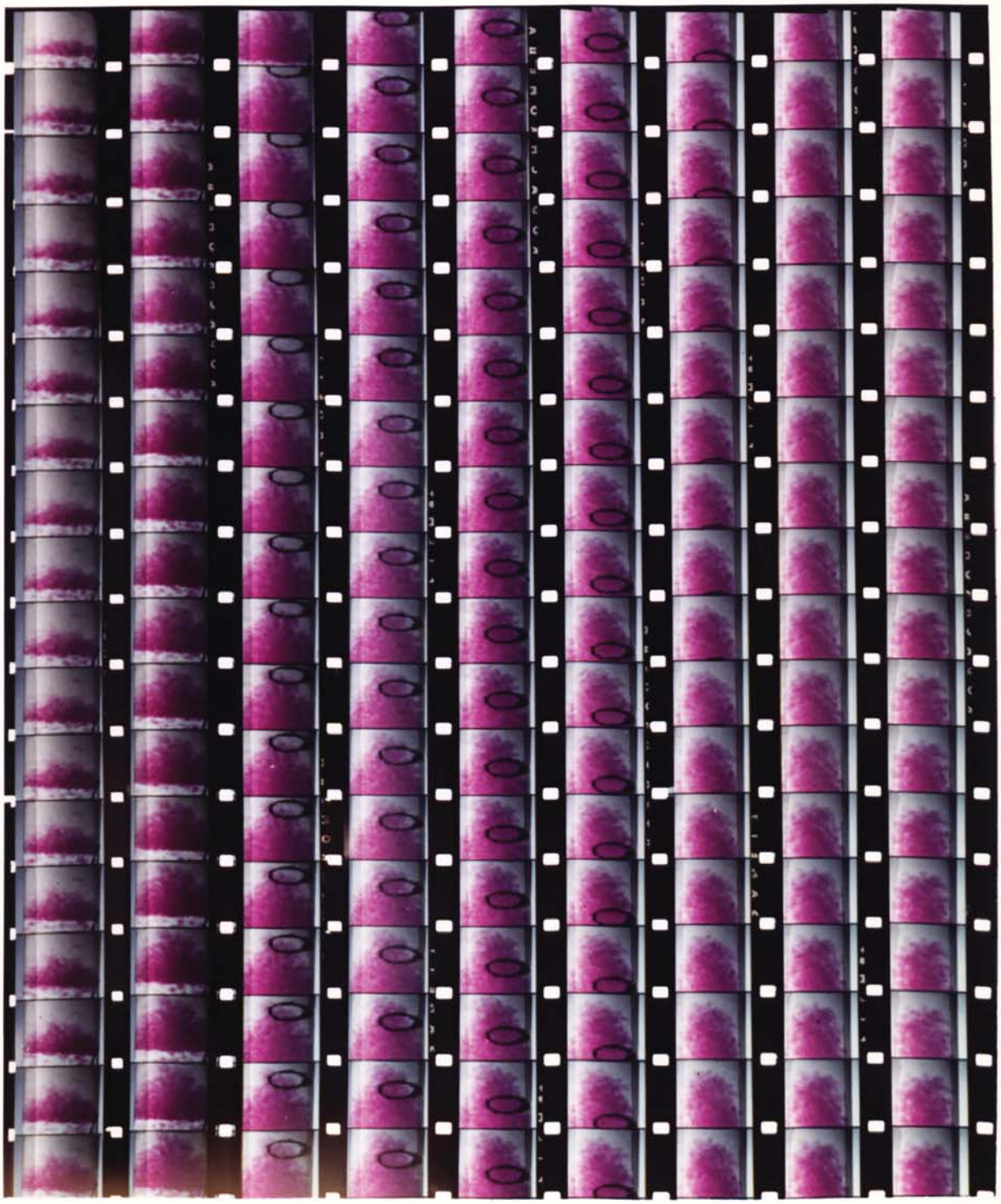

6.1) contd.

TABLE 6.1

BED HEIGHT AT WHICH VELOCITY PROFILE IS EVIDENT cm.

SYSTEM	DISTRIBUTOR ORIFICE DIA mm. 1	2	3	4
I (AMYLACETATE)	10.5	10.0	9.5	8.5
II (ETHYLACETATE)	11.4	9.0	7.6	5.0
III (ISOOCTANE)	10.0	9.5	8.5	8.0
IV (HEXANE)	11.0	10.0	9.0	7.5

6.2) Deformation and shape of drop.

Several authors have observed that drops in dispersion band undergo a certain amount of deformation as they pack and arrange themselves. Hartland[67] showed photographs of the deformation of drops in a two dimensional bed. Hittit[38] has also shown photographs of the deformation of the drops in dispersion bands taken at the column wall. None of the above represent the true deformation inside a dispersion band and therefore the packing efficiency inside the bed. Jeffreys et al.[46] assumed a face centred cubic configuration of spherical drops i.e. each drop is surrounded by 12 drops.

Plate (6.2) shows a discriminated drop inside a dispersion band. The deformation is quite evident and the drops have almost flat faces where the adjacent drops are pressing against it. Each face appears to have five sides i.e. a pentagon. The only stable configuration which satisfies

6.2) contd.

the above criteria is a "pentagonal dodecahedra". Plate (6.3) shows the phototropic dye in the continuous phase which acts as border lines of the drops and the dodecahedra shape is quite evident. The properties of a dodecahedron are shown in Appendix (1). It consists of 12 sides each side being a regular pentagon. Therefore each drop is surrounded by 12 other drops.

Rigid pentagonal dodecahedra cannot grow in three dimensions. The residual spaces amount to approximately 3% of the total volume and a certain amount of distortion of the drop from the regular dodecahedron takes place. Figure (6.1) shows two views of the dodecahedra.

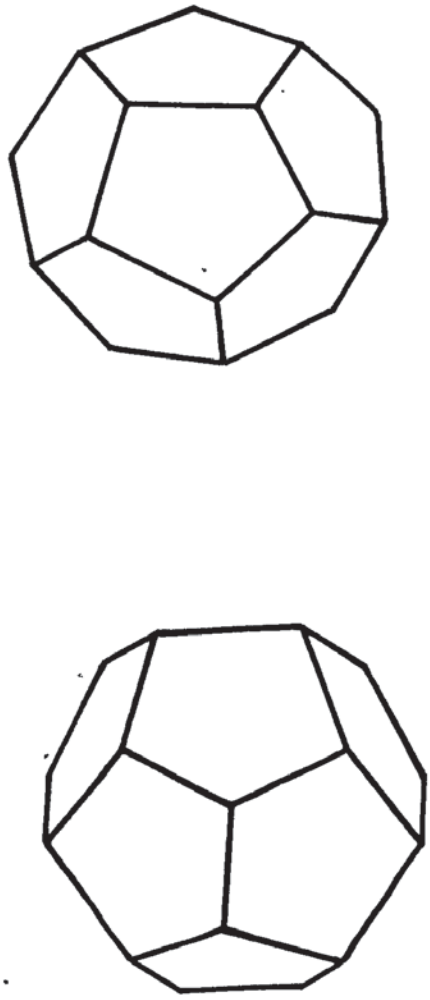

Figure (6.1)

PLATE 6.2 SHAPE OF DISCRIMINATED DROPS INSIDE THE BED SHOWING FLAT FACES.

Slow mixing after coalescence is also illustrated.

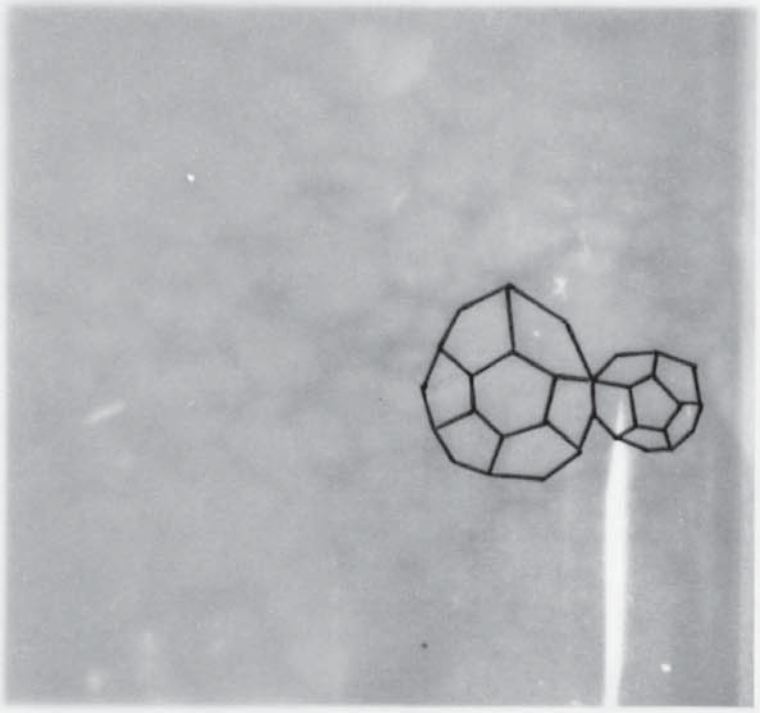

PLATE 6.3 PHOTOTROPIC DYE IN THE CONTINUOUS PHASE SHOWING THE SHAPE OF DROPS INSIDE THE BED. (DODECAHEDRAL)

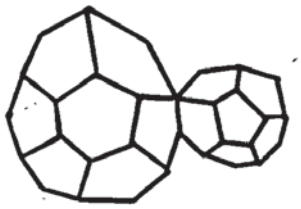

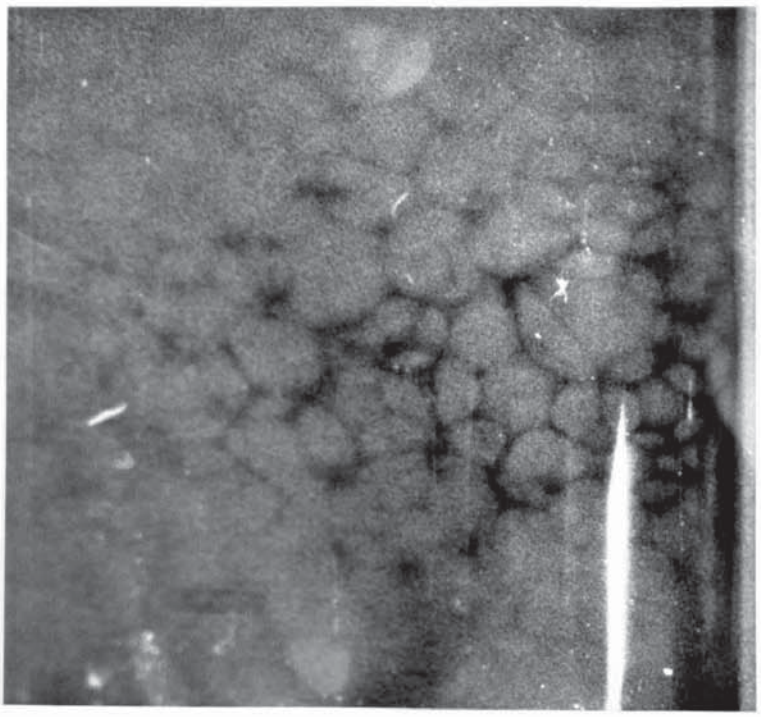

PLATE 6.3 PHOTOTROPIC DYE IN THE CONTINUOUS PHASE SHOWING THE SHAPE OF DROPS INSIDE THE BED. (DODECAHEDRAL)

6.3) Formation of secondary hazes.

During the experimental runs satellite drops were observed after the coalescing interface. These were small secondary drops of the continuous phase in the dispersed phase homophase. Lawson showed that when a single drop coalesces at an interface, some of the continuous phase film fragments are trapped in the dispersed phase homophase forming satellite drops. Such occurrences take place to an even greater extent in dispersion bands since the continuous phase in the bed is trapped in the form of plateau borders and a continuous film i.e. isolated"pockets". These pockets are then rejected into the dispersed phase homophase after coalescence of the drops takes place forming a secondary haze. Rejection of these pockets has not been observed when drop wall coalescence takesplace. This could be due to the fact that at the column wall the continuous phase is not in abundance, a necessary criterion for the formation of secondary drops. The formation of satellite drops at the coalescing boundary was also observed by Ali[41] in a vertical settler and by Jeffreys et al.[81] in a horizontal wedge.

In this study, when the continuous phase was an organic with the phototropic dye, exposure to U.V. light caused a change of colour in the satellite drops which definitely confirmed that these had been fragmentationsof the continuous phase. Some of the drops were observed to reside at the column wall and travel thus to the beginning of the bed. Plate (6.4) shows such action. This confirms the existence of a film of the dispersed phase at the column wall.

It was further observed that the fragmentation of the continuous phase increased with increasing bed height,

PLATE 6.4 PROPAGATION OF THE CONTINUOUS PHASE SATTELITE DROPS TO THE START OF THE BED.

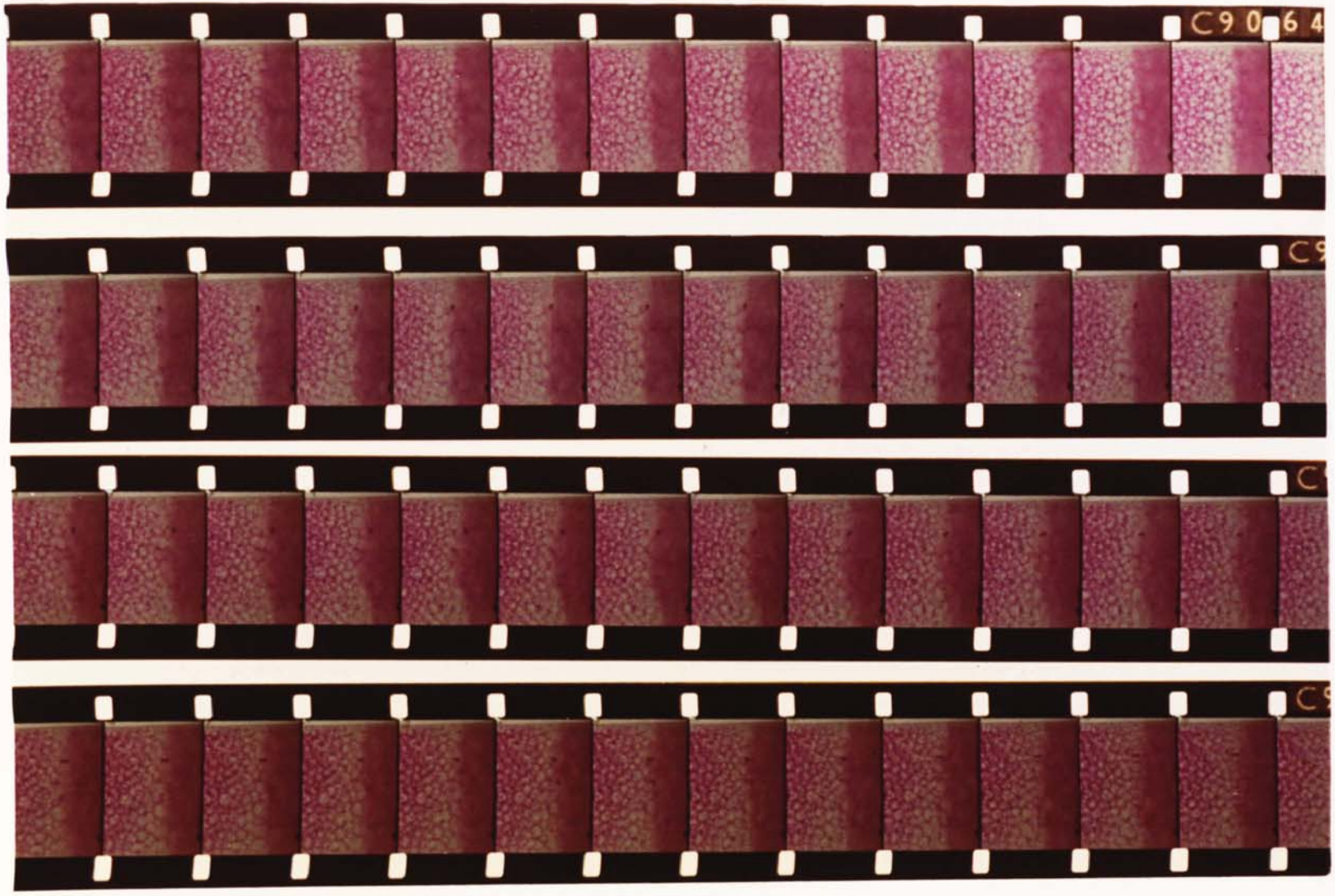
C9 0 6 4

6.3) contd.

and it also increased for systems with low interfacial tensions.

Despite the numerous observations made of the interdrop, drop interface and drop wall coalescences no satellite drop formation of the dispersed phase was observed. Further when several dyed drops were introduced repeatedly, an accumulation of secondary dispersed phase drops should have occurred after the coalescence of the dyed drops. It was not the case. This suggests that either the secondary drops coalesce immediately after formation, which cannot be the case since they would be very stable drops, or that the formation of such drops does not occur to an appreciable extent. Hence it is reasonable to assume that the formation of satellite drops in a disperson band is very rare or indeed non-existent. It is therefore believed that two conditions must exist before secondary drops of the dispersed phase are formed after coalescence.

1) Excess of the continuous phase
2) The vibrations generated by the coalescence remain undampened.

In the case of vertical beds it has been shown that the first condition does not apply. Moreover any vibration generated after coalescence is absorbed by the adjacent drops. Situations where the above conditions are satisfied and secondary drop formation has been observed are

a) Coalescence of single drops at an interface
b) Coalescence of a small drop with a large drop surrounded by the continuous phase. This resembles situation (a)
c) Horizontal wedges where the drops have a vertical and a horizontal velocity and where the wedge is a form of a liquid-liquid froth.

6.3) contd.

Jeffreys et al.[81] reported the formation of secondary drops of the dispersed phase in a horizontal mixer settler. It can, however, be argued that the formation of secondary drops in a horizontal wedge could have taken place in a mixer. Further, localised phase inversion can take place. This causes the dispersed phase to become the continuous phase and secondary drops are then formed by the fragmentation of the continuous film.

Finally, Davies et al.[67] showed a photograph with secondary drops residing at the coalescing interface for a vertical dispersion band which he stated to be of the dispersed phase. The formation of satellite drops leads to inefficient phase separation and is therefore undesirable.

6.4) Probability and type of coalescences.

Consider Figure (6.13) for system IV "Hexane" which gives a plot of the interdrop coalescence probability versus bed height. At low bed height the probability is relatively high because at this stage the bed has not fully developed. The drainage of continuous phase is not restricted and the probability of direct collision of the arriving drops with those having just entered the bed is high and this accounts for the high probability of interdrop coalescence. As soon as the bed begins to increase, however, the drops pack together and the continuous phase is trapped between the drops as a film. This film drains and not all of it is released until the coalescing interface is reached. Near the entrance of the bed a thick film is maintained between the drops, this inhibits interdrop coalescence, and therefore there is a sharp decrease in the

SYSTEM IV HEXANE

1 mm Dist. Orifice Dia.

○ Inter-drop Coal.

▲ Drop-wall Coal.

■ Drop-interface Coal.

FIG 6.11

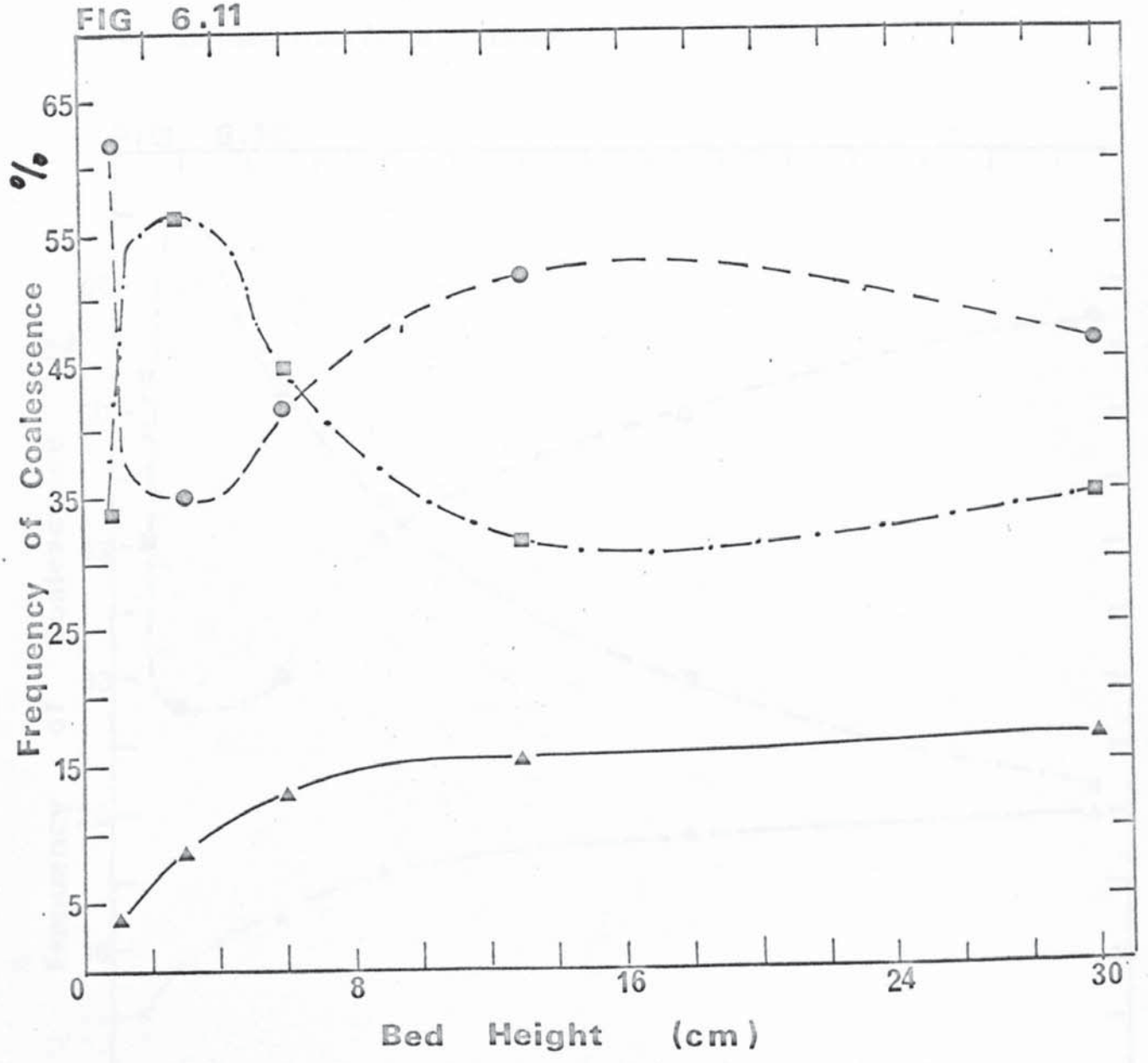

SYSTEM IV HEXANE

2 mm Dist. Orifice Dia.

○ Inter-drop Coal.

▲ Drop-wall Coal.

■ Drop-interface Coal.

FIG 6.12

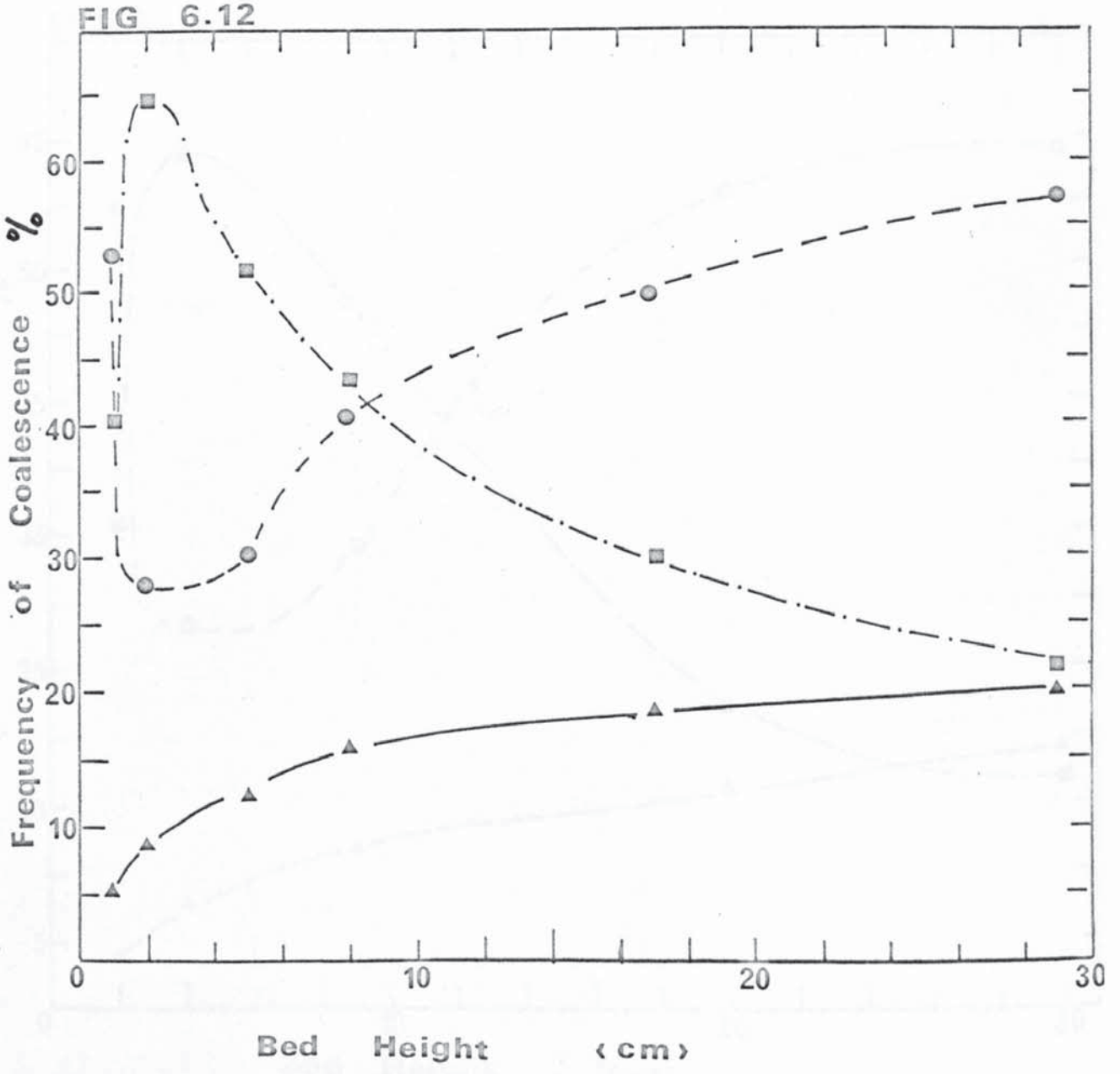

SYSTEM IV HEXANE

3 mm Dist. Orifice Dia.

○ Inter-drop Coal.

△ Drop-wall Coal.

□ Drop-interface Coal.

FIG 6.13

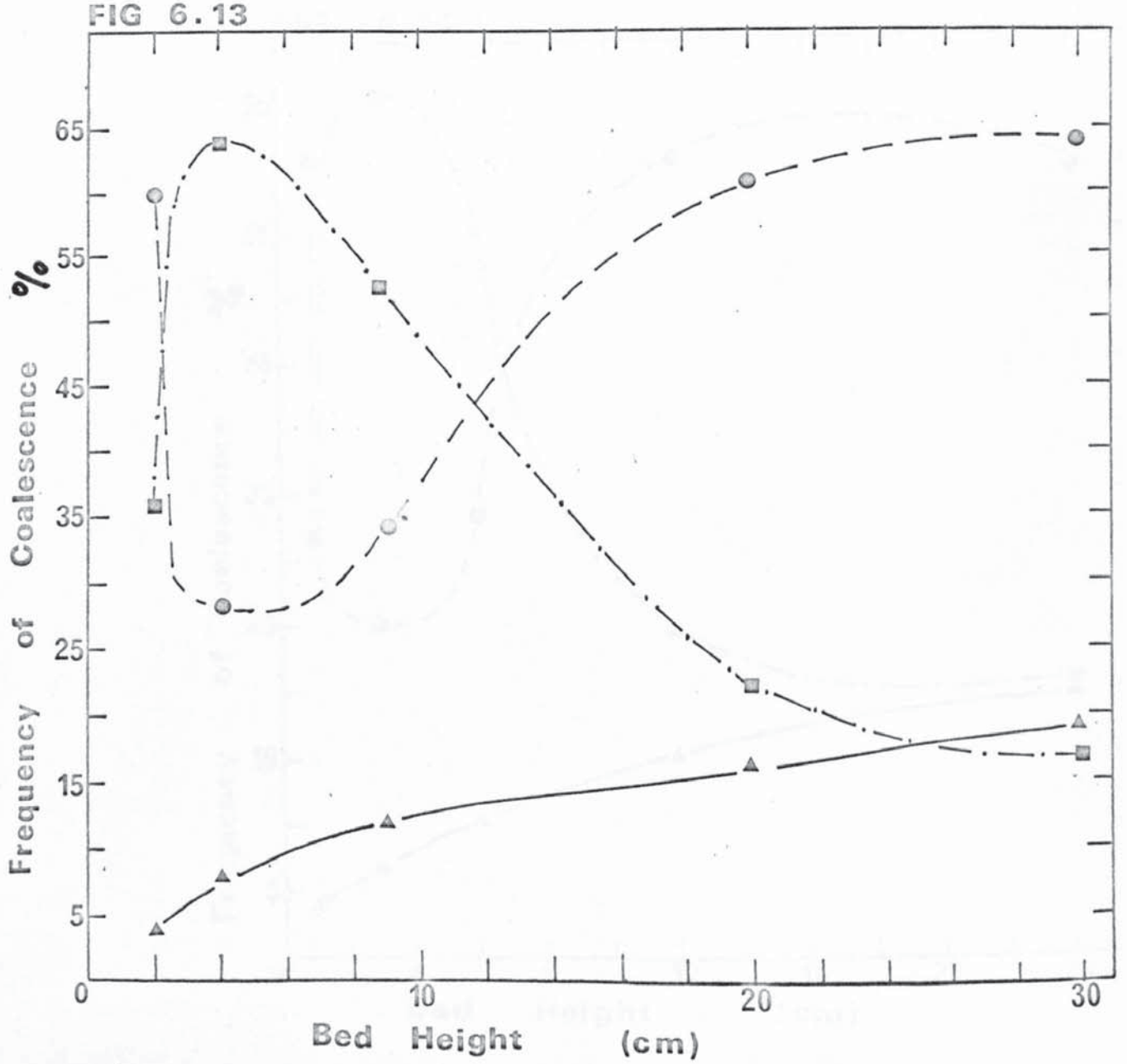

SYSTEM IV HEXANE

4 mm Dist. Orifice Dia.

○ Inter - drop Coal.

▲ Drop - wall Coal.

■ Drop - interface Coal.

FIG 6.14

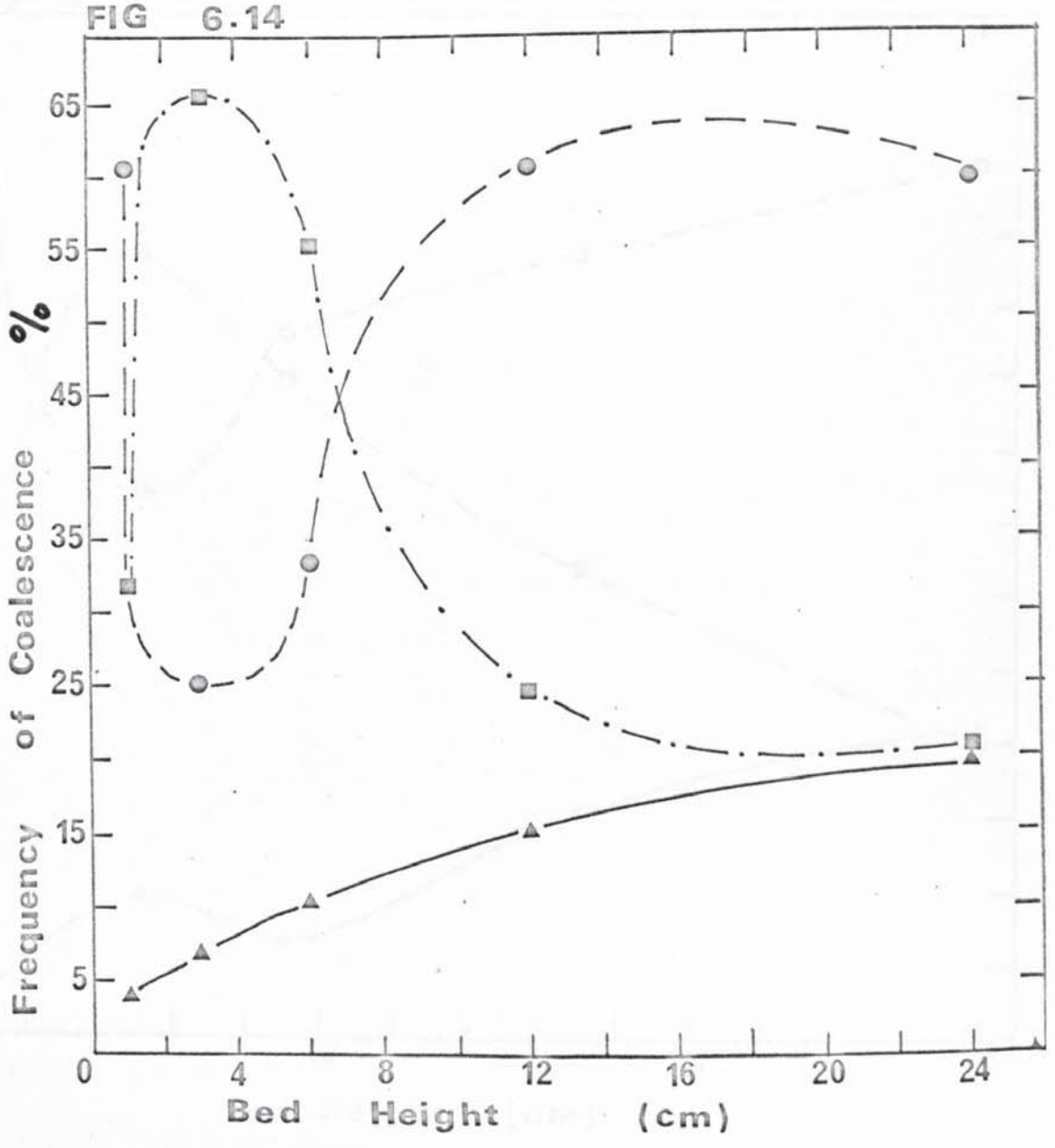

SYSTEM III ISO-OCTANE

1 mm Dist. Orifice Dia.

○ Inter-drop Coal.

△ Drop-wall Coal.

□ Drop-interface Coal.

FIG 6.15

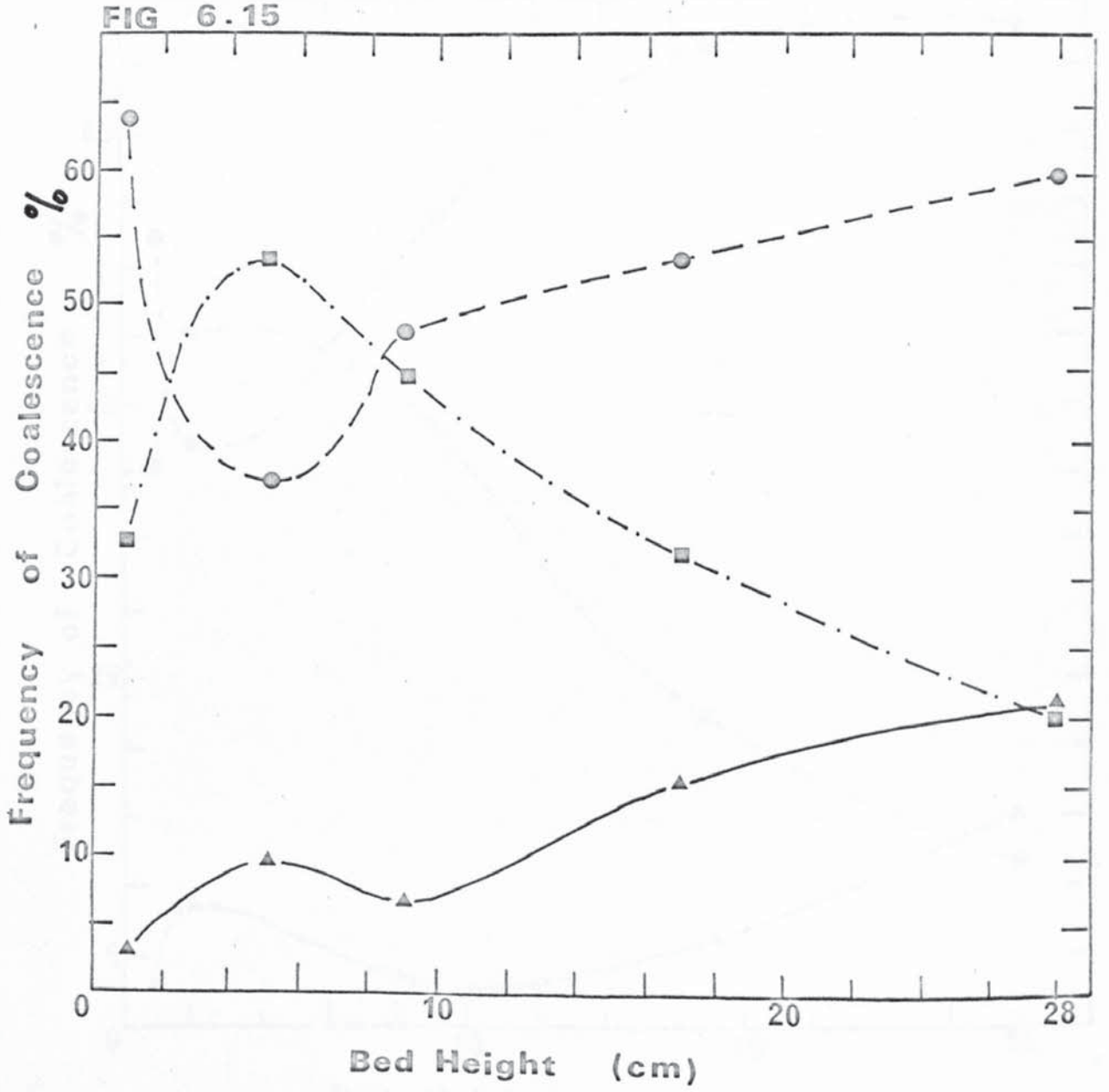

SYSTEM III ISO-OCTANE

2 mm Dist. Orifice Dia.

○ Inter-drop Coal.

△ Drop-wall Coal.

□ Drop-interface Coal.

FIG 6.16

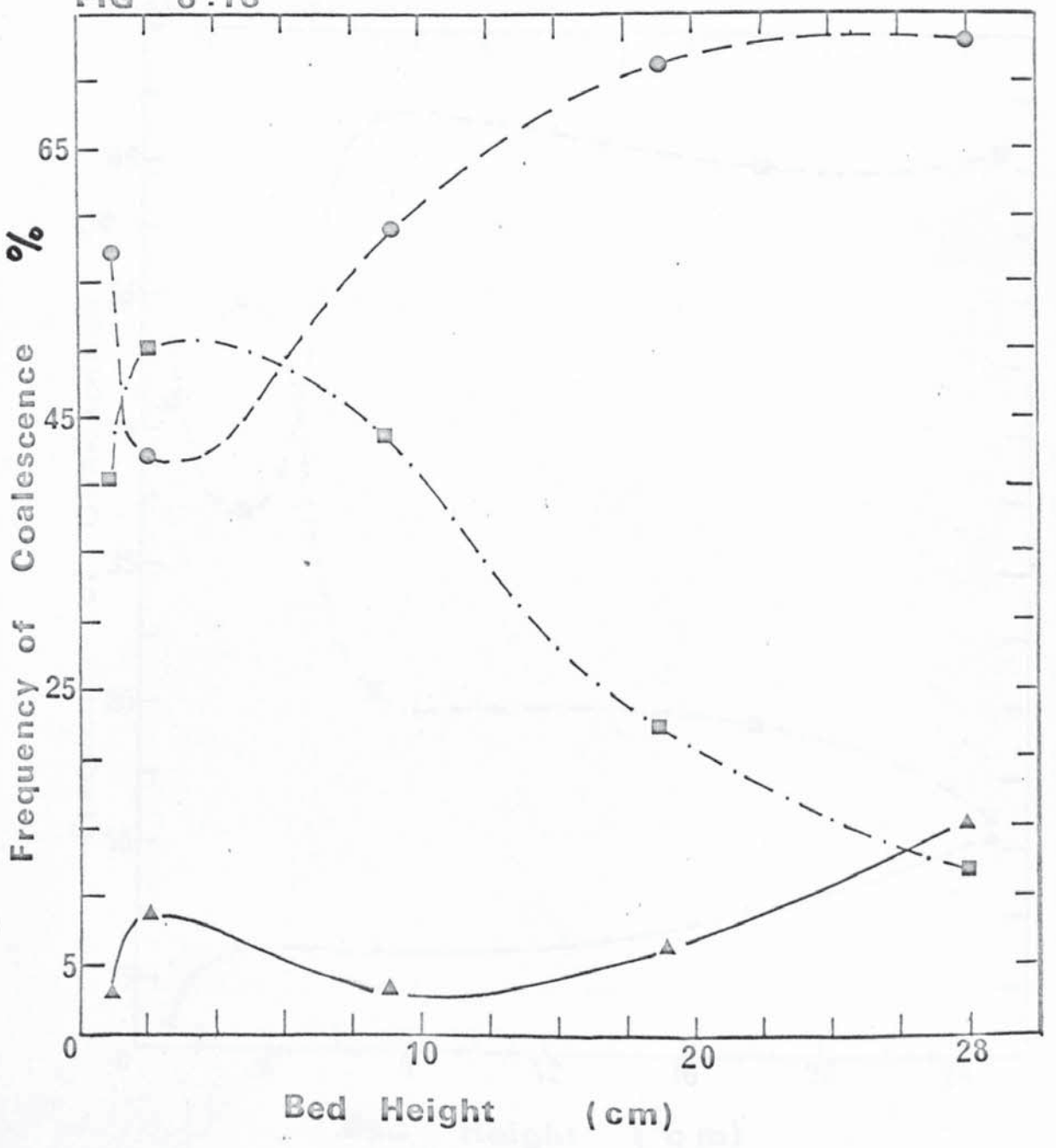

SYSTEM III ISO-OCTANE

3 mm Dist. Orifice Dia.

○ Inter-drop Coal.

▲ Drop-wall Coal.

□ Drop-interface Coal.

FIG 6.17

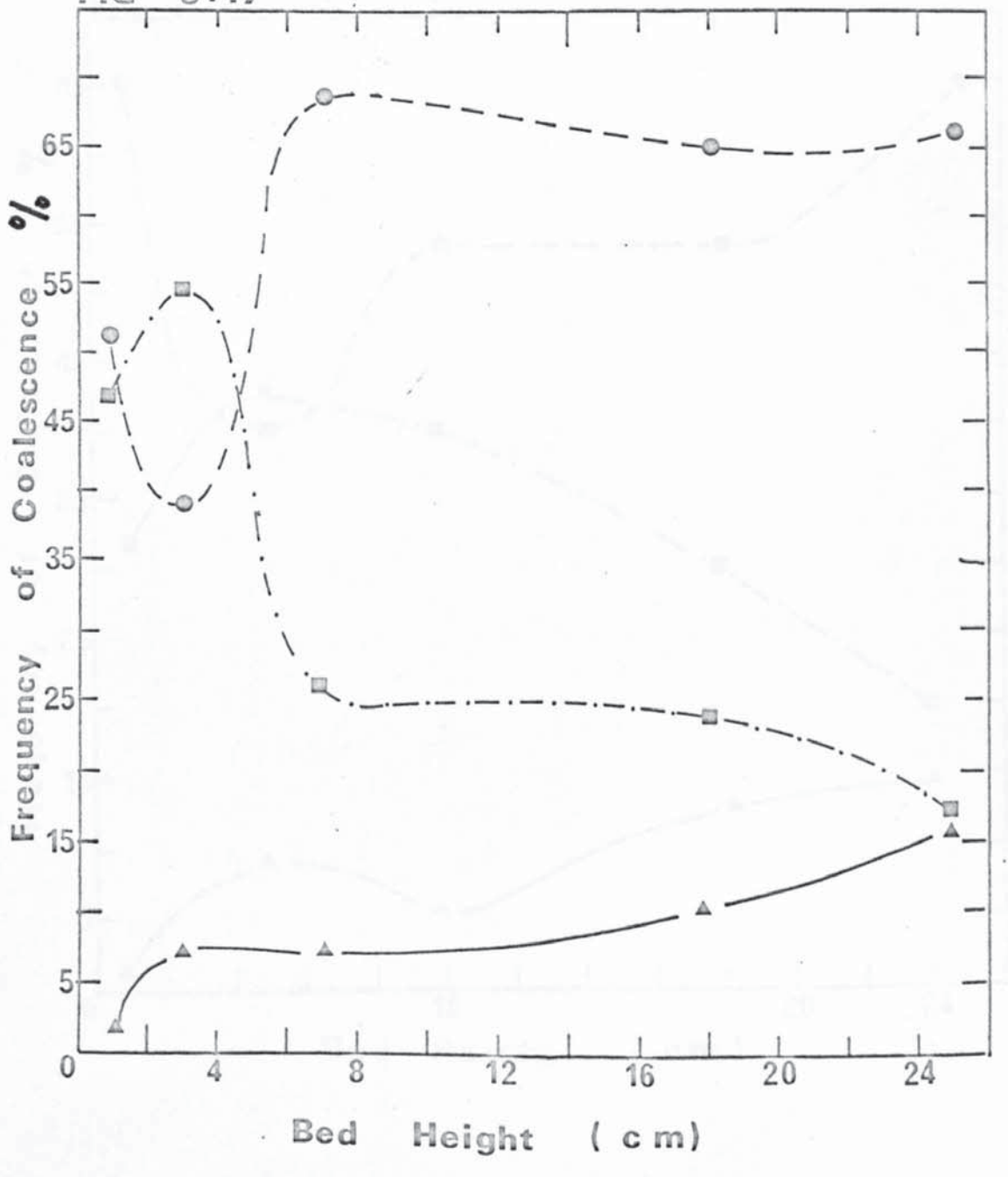

SYSTEM III ISO-OCTANE

4 mm Dist. Orifice Dia.

○ Inter-drop Coal.

▲ Drop-wall Coal.

■ Drop-interface Coal.

FIG 6.18

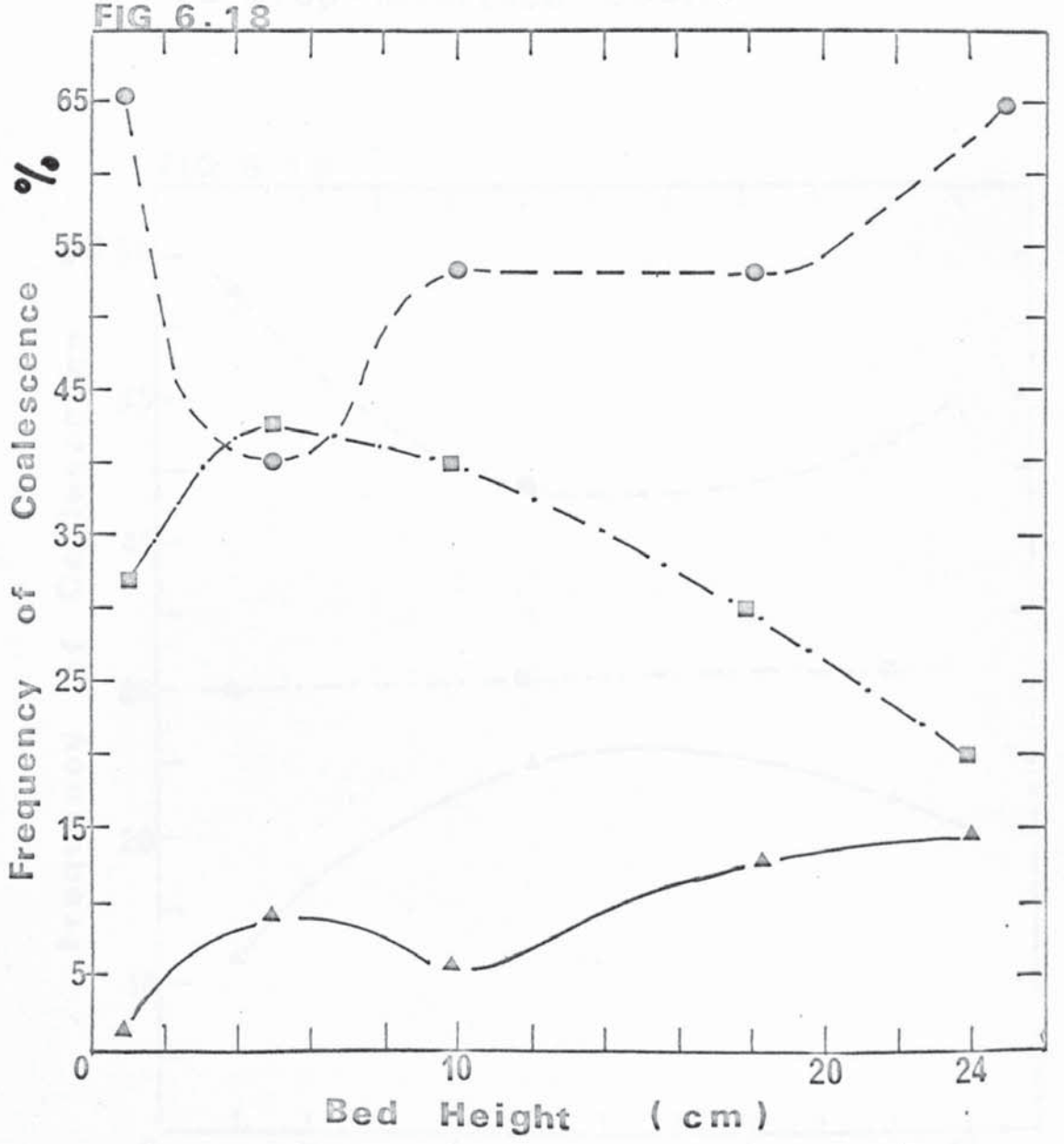

SYSTEM I AMYL ACETATE

1 mm Dist. Orifice Dia.

○ Inter-drop Coal.

△ Drop-wall Coal.

□ Drop-interface Coal.

FIG 6.19

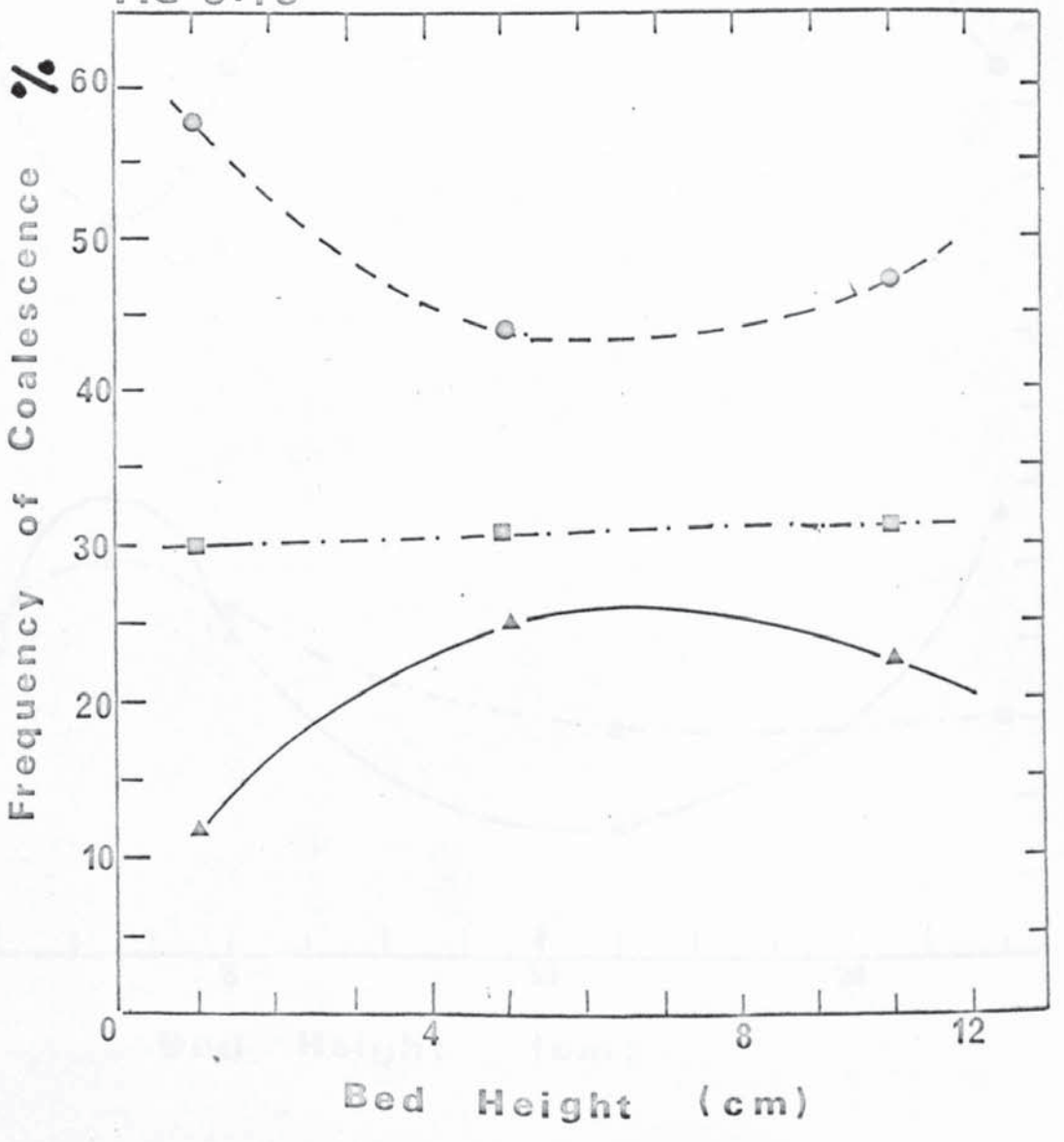

SYSTEM I AMYL ACETATE

2 mm Dist. Orifice Dia.

○ Inter-drop Coal.

△ Drop-wall Coal.

□ Drop-interface Coal.

FIG 6.20

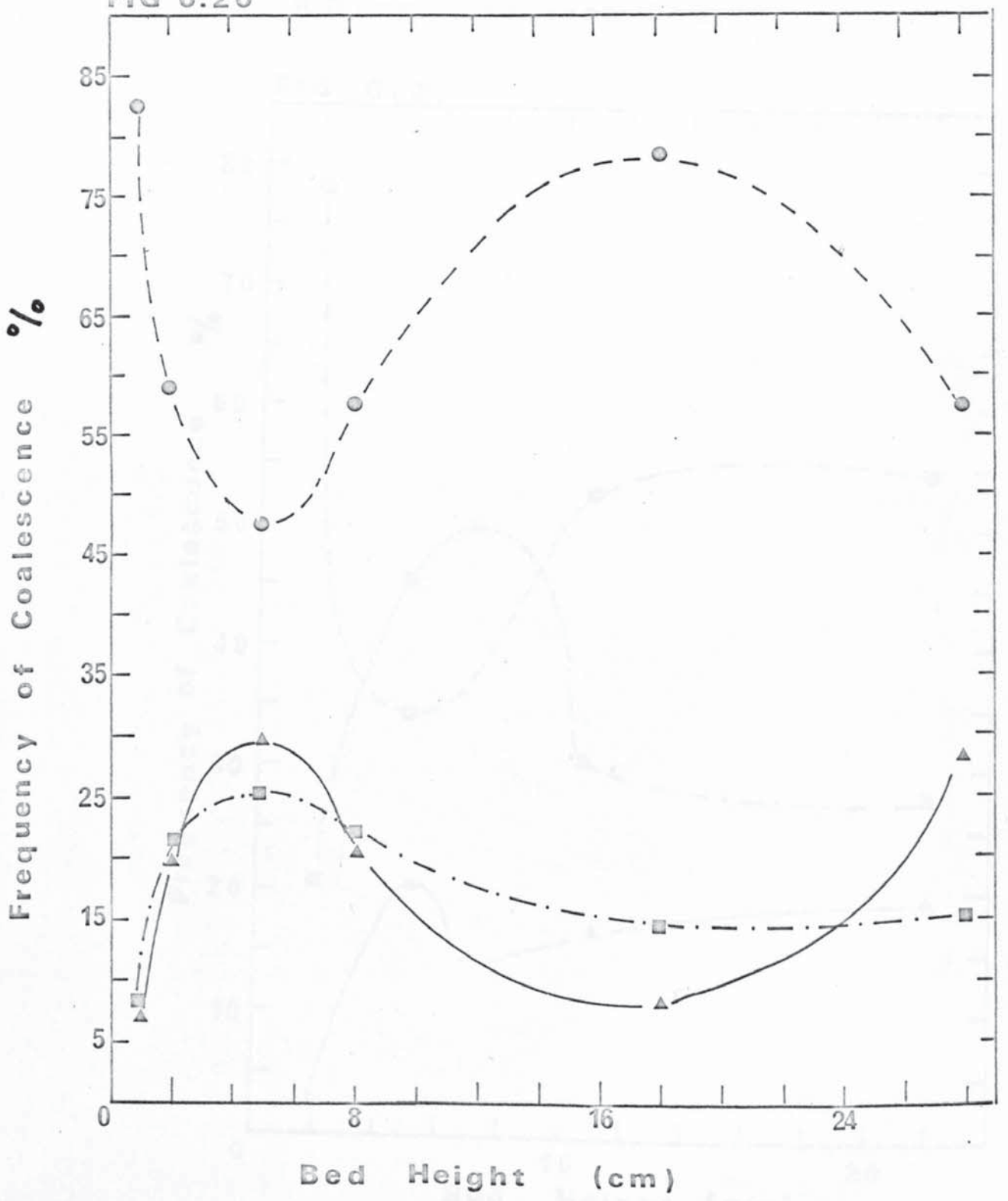

SYSTEM I AMYL ACETATE
3 mm Dist. Orifice Dia.

○ Inter-drop Coal.

△ Drop-wall Coal.

□ Drop-interface Coal.

FIG 6.21

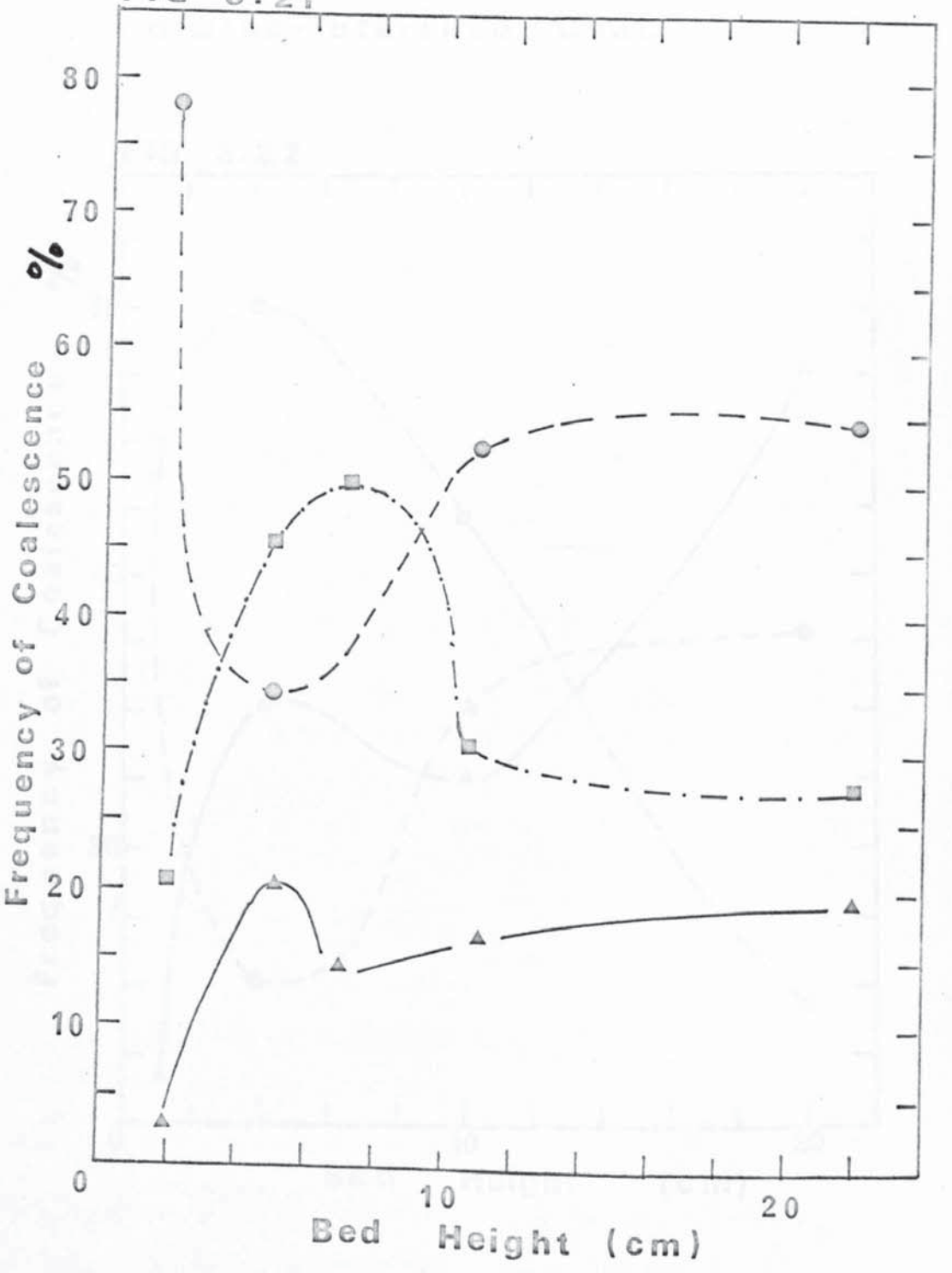

SYSTEM I AMYL ACETATE

4 mm Dist. Orifice Dia.

○ Inter-drop Coal.

△ Drop-wall Coal.

□ Drop-interface Coal.

FIG 6.22

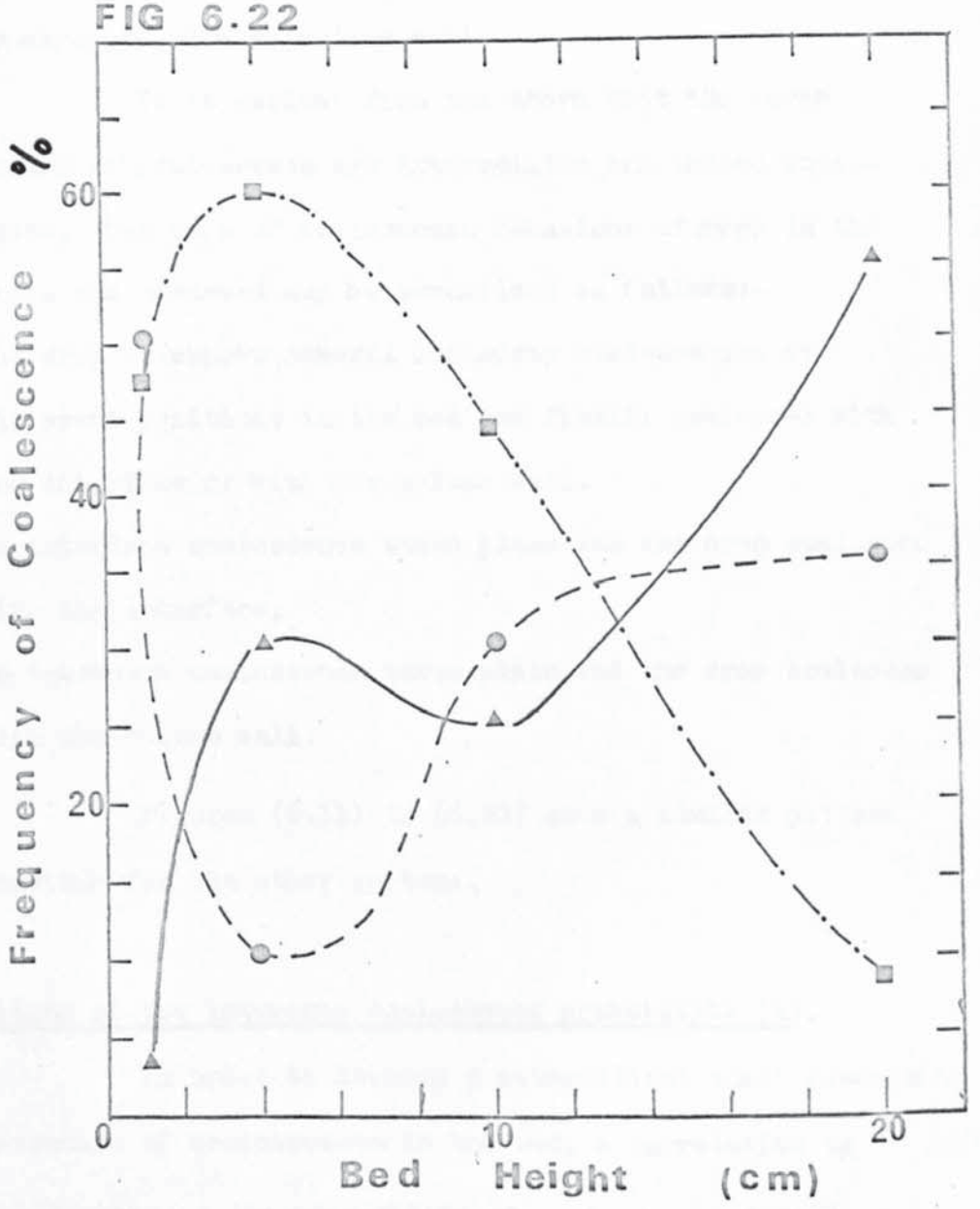

6.4) contd.

coalescence probability as seen in Figure (6.13). Further increases in bed height result in higher probability which is enhanced by the generation of the velocity profile. It is clear from the previous definitions of the coalescence phenomena that an increase in drop interface coalescence will result in a decrease in interdrop coalescence. Dropwall coalescence can be regarded as a form of drop interface coalescence since, as explained previously, the drop coalesces with the film at the phase boundary residing at the column wall. It increases gradually with increasing bed height. This is undoubtedly due to the exposure of more column wall.

It is evident from the above that the three mechanisms of coalescence are interrelated and indeed inter-dependent. The type of coalescence behaviour of drops in the bed which was observed may be summarized as follows:-

a) The drop undergoes several interdrop coalescences at different positions in the bed and finally coalesces with the interface or with the column wall.

b) No interdrop coalescence takes place and the drop coalesces with the interface.

c) No interdrop coalescence takes place and the drop coalesces with the column wall.

Figures (6.11) to (6.22) show a similar pattern of behaviour for the other systems.

6.5) Estimation of the interdrop coalescence probability (λ).

In order to develop a mathematical model describing the mechanism of coalescences in the bed, a correlation is required to predict the probability of coalescence at various

SYSTEM IV (HEXANE)

4mm DISTRIBUTOR ORIFICE DIA.

FIG 6.23

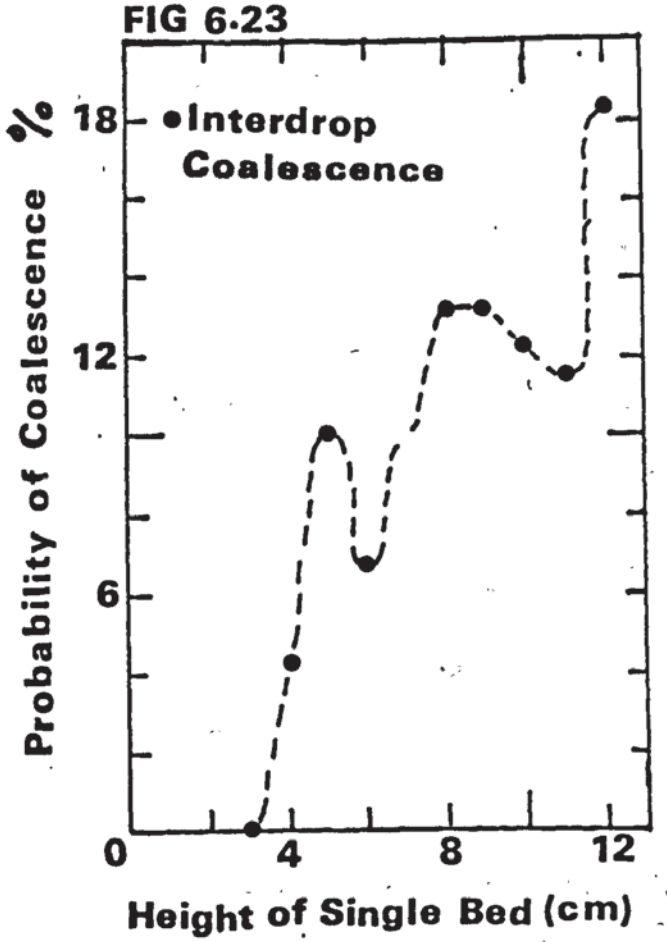

FIG 6.24

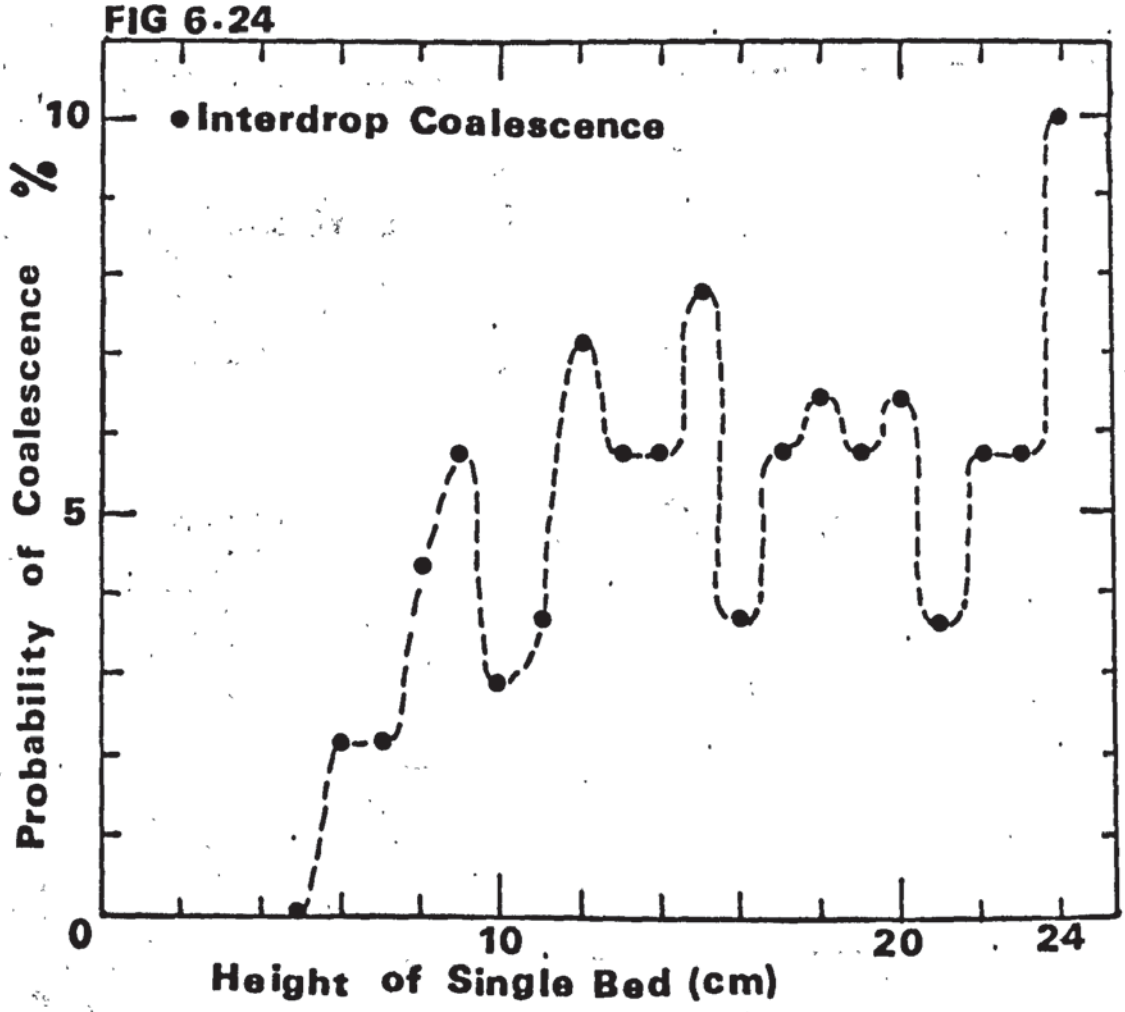

FIG 6.25

SYSTEM IV (HEXANE)

3mm DISTRIBUTOR ORIFICE DIA.

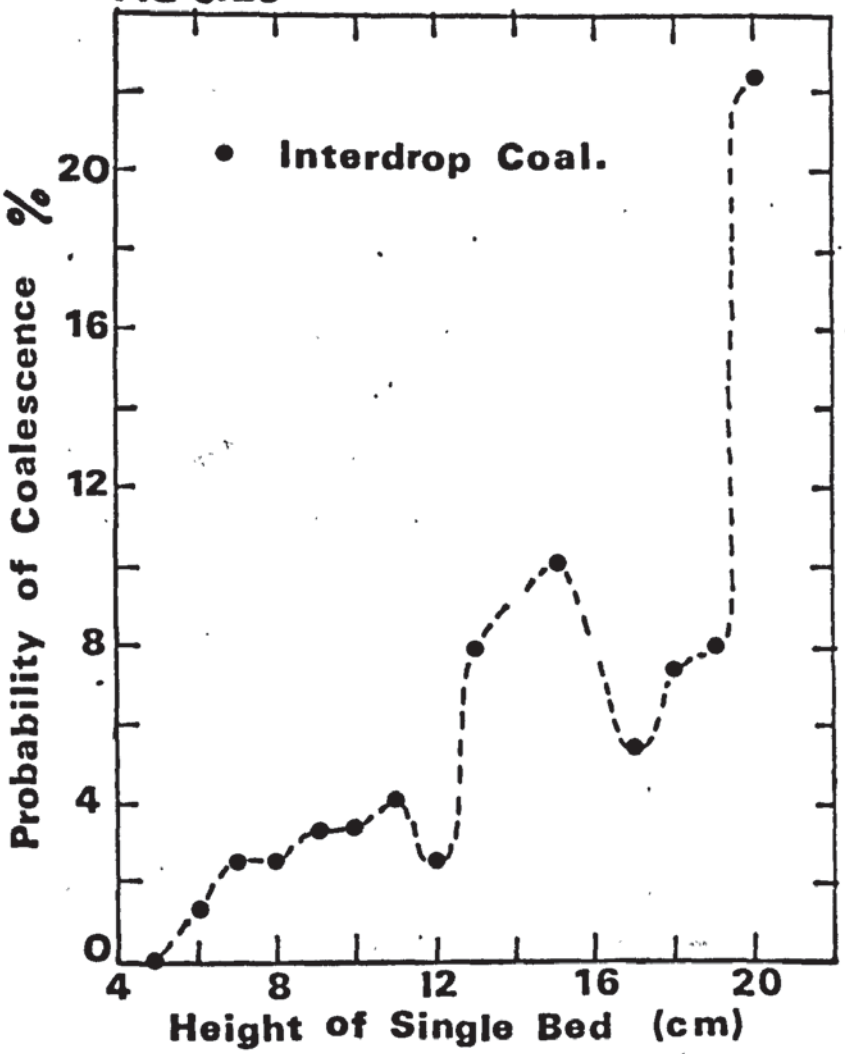

FIG 6.26

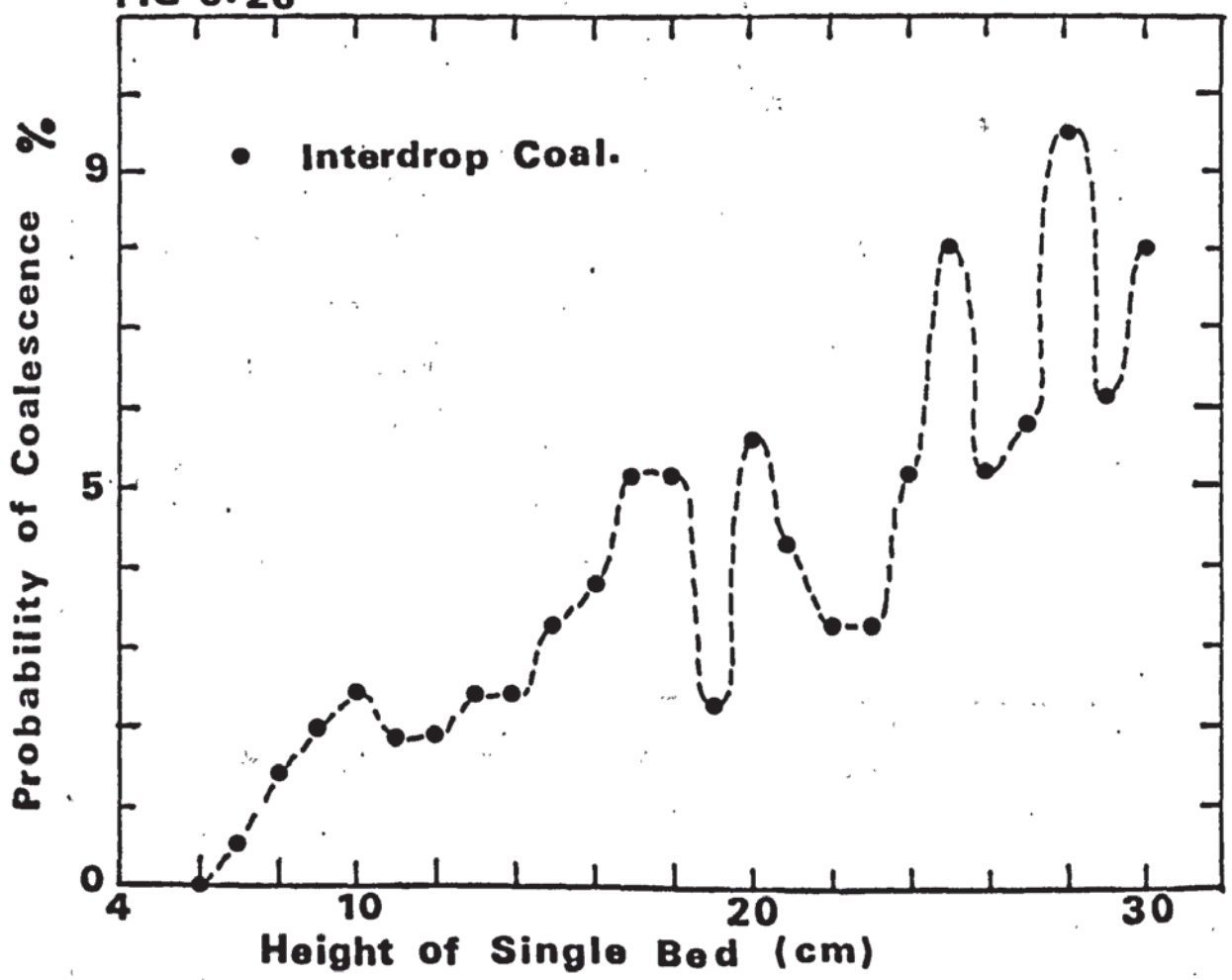

SYSTEM IV HEXANE

2mm DISTRIBUTOR
ORIFICE DIA.

FIG 6.27

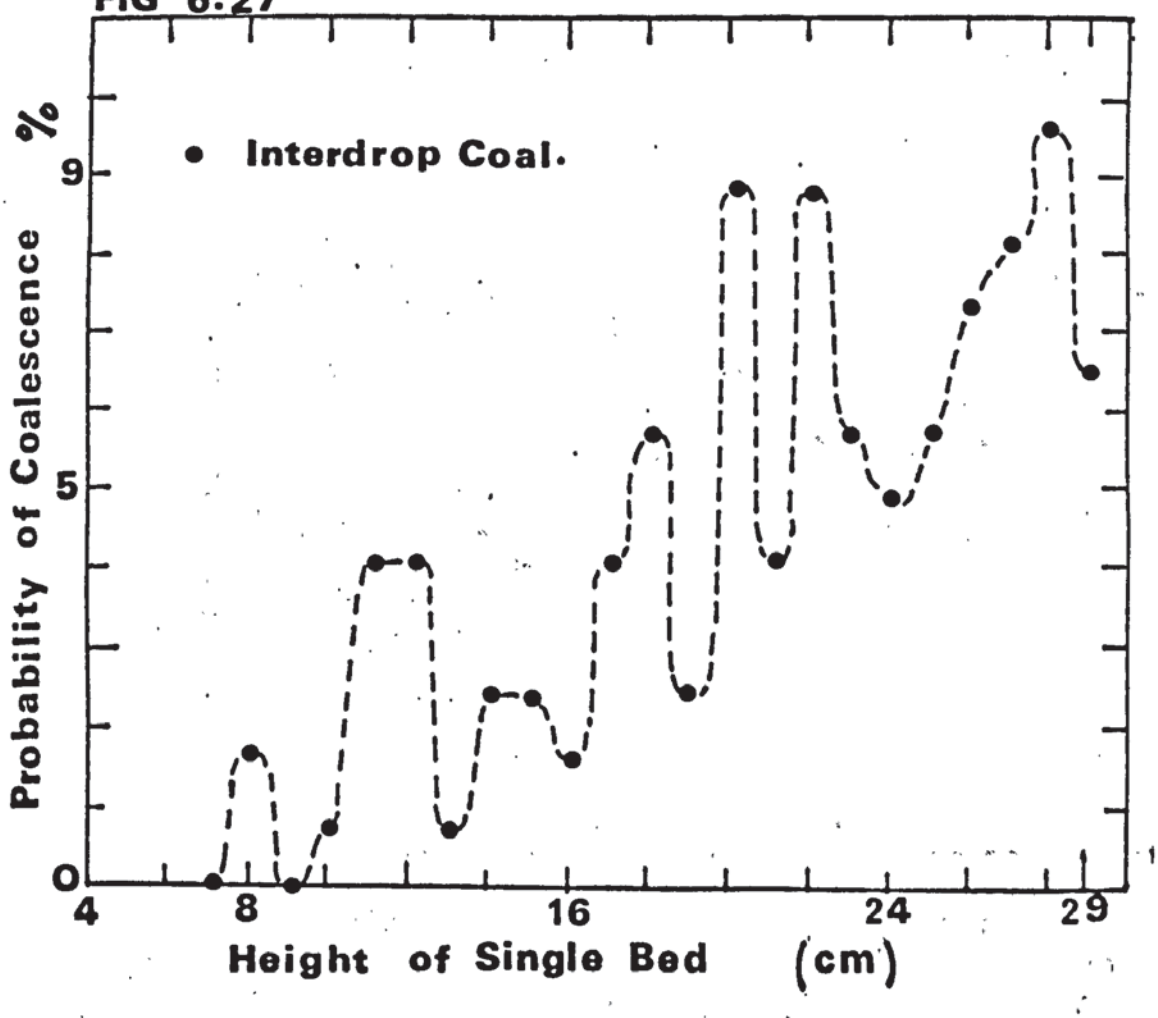

SYSTEM IV HEXANE

1 mm DISTRIBUTOR ORIFICE DIA.

FIG 6.28

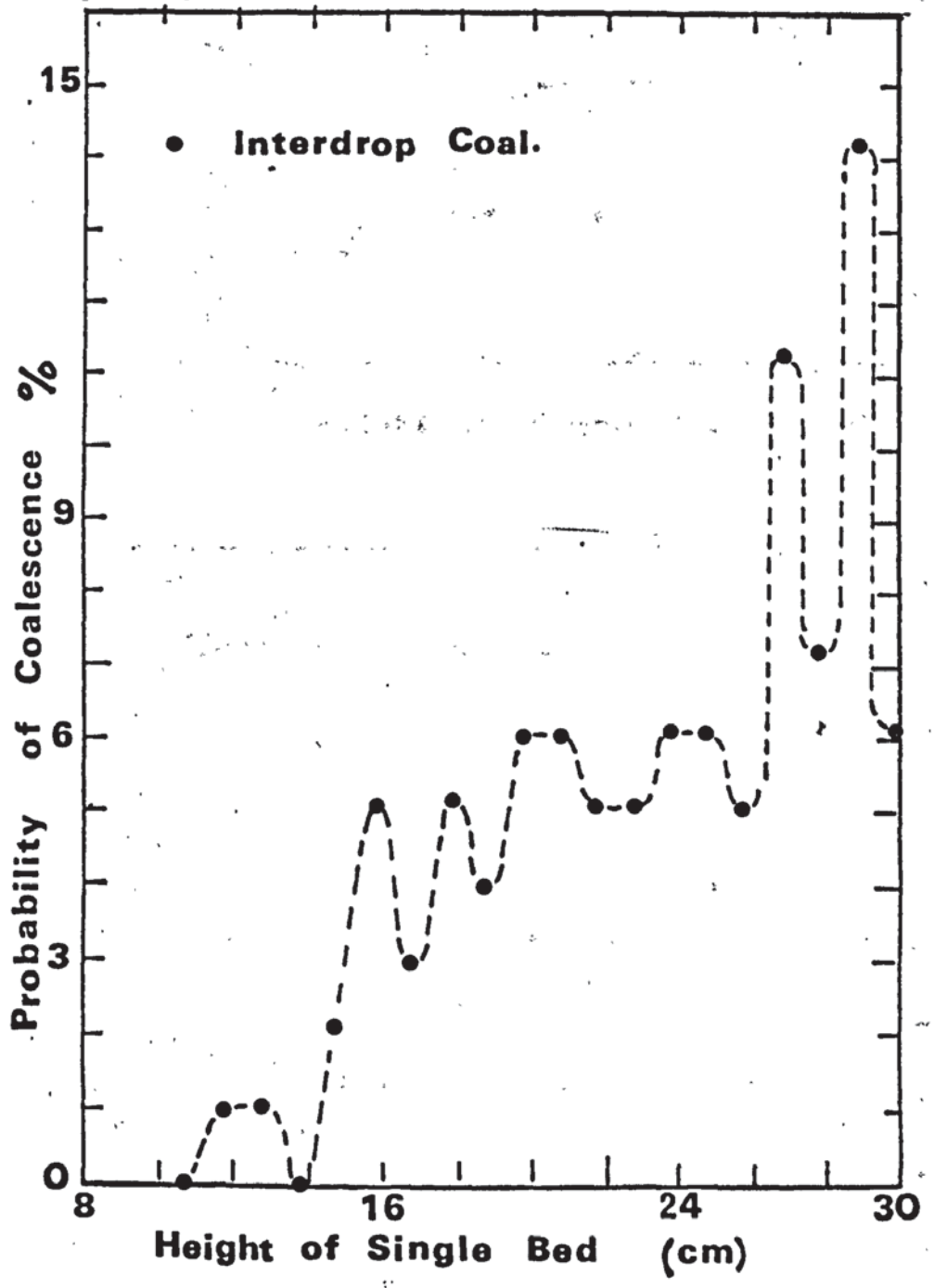

SYSTEM III
ISO OCTANE

1mm DIST.
ORIFICE DIA.

FIG 6.29

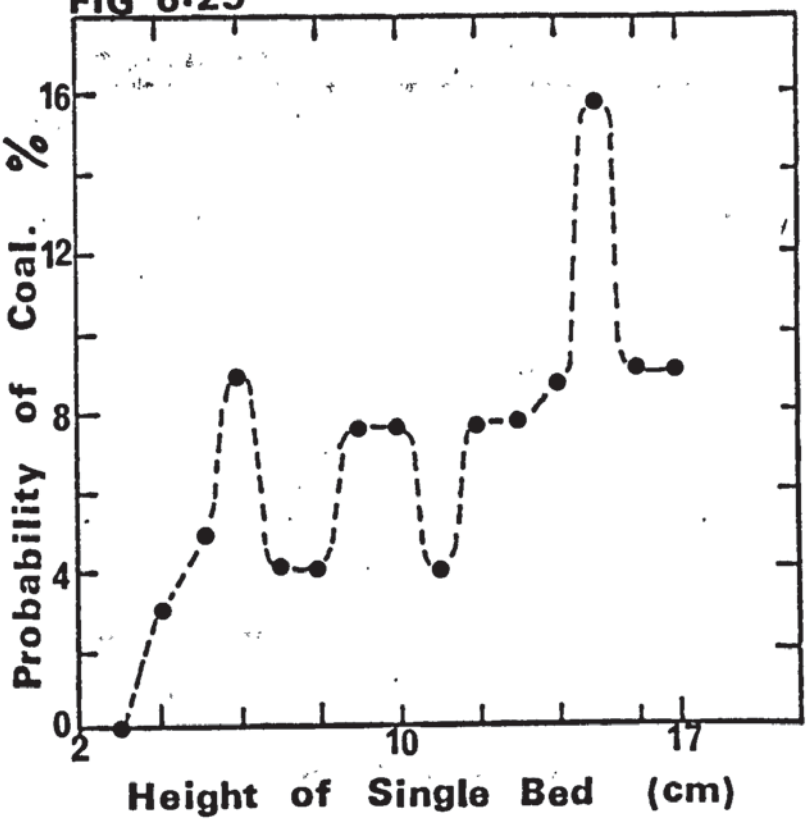

FIG 6.30

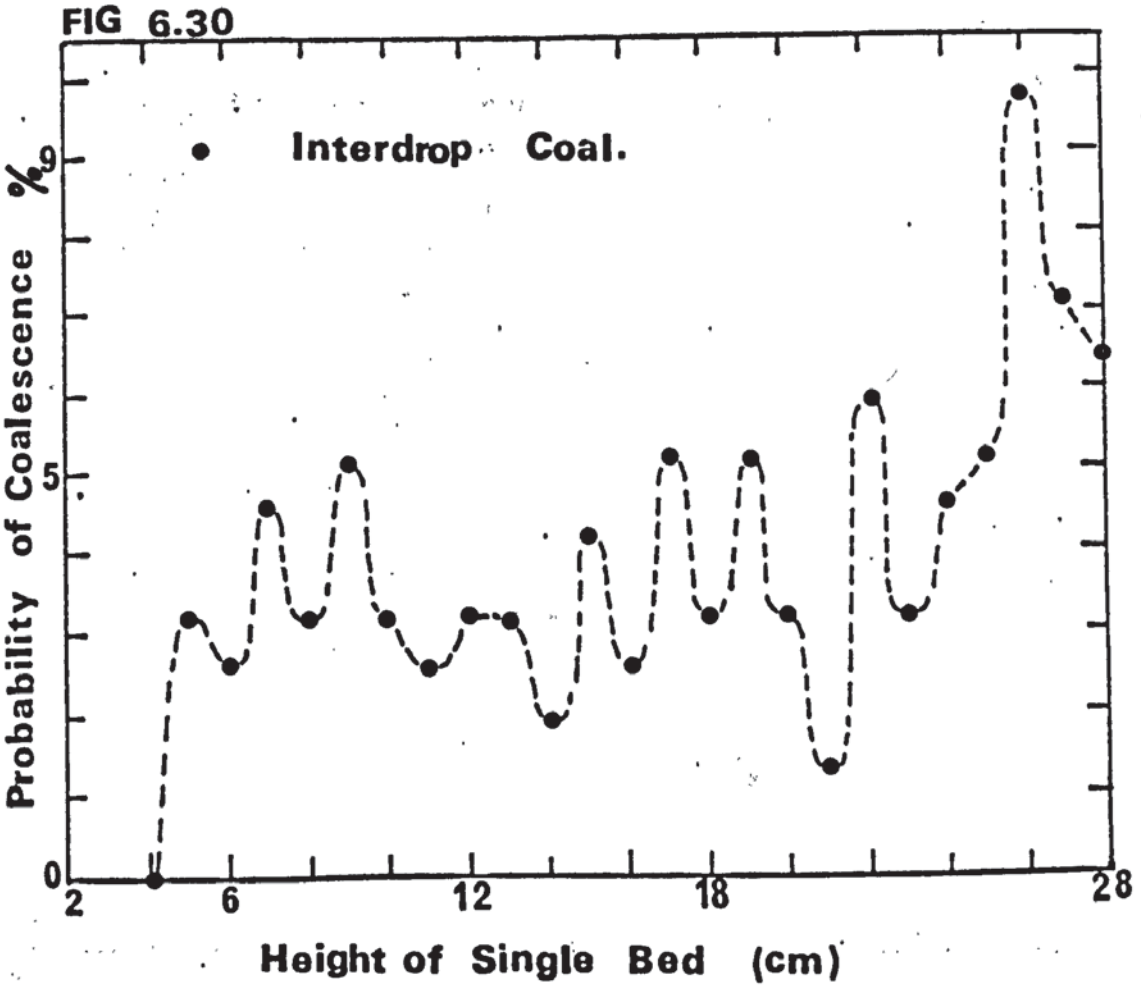

SYSTEM III

ISO OCTANE

2 mm DIST.
ORIFICE DIA.

FIG 6.31

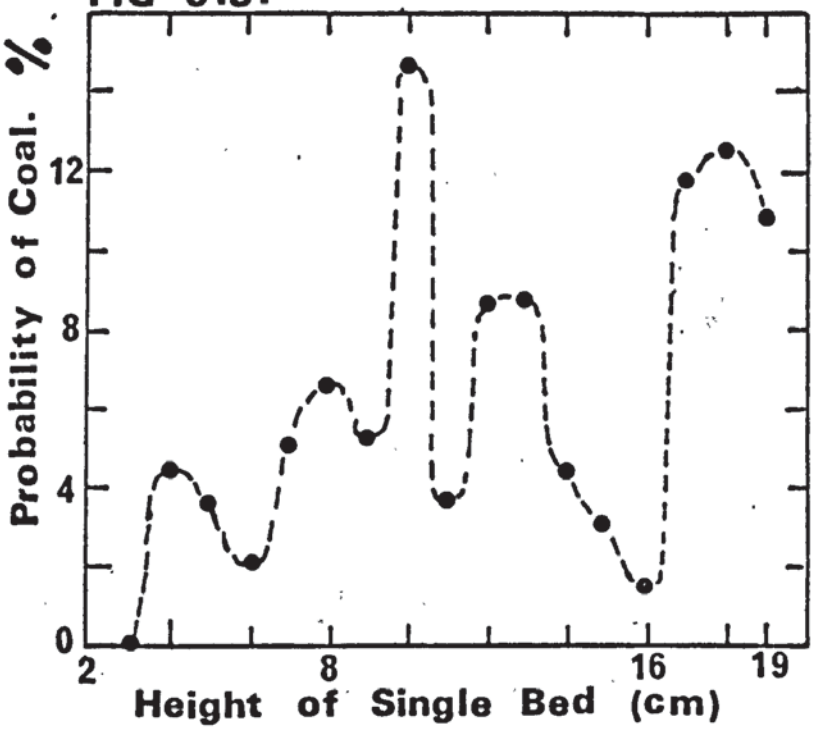

FIG 6.32

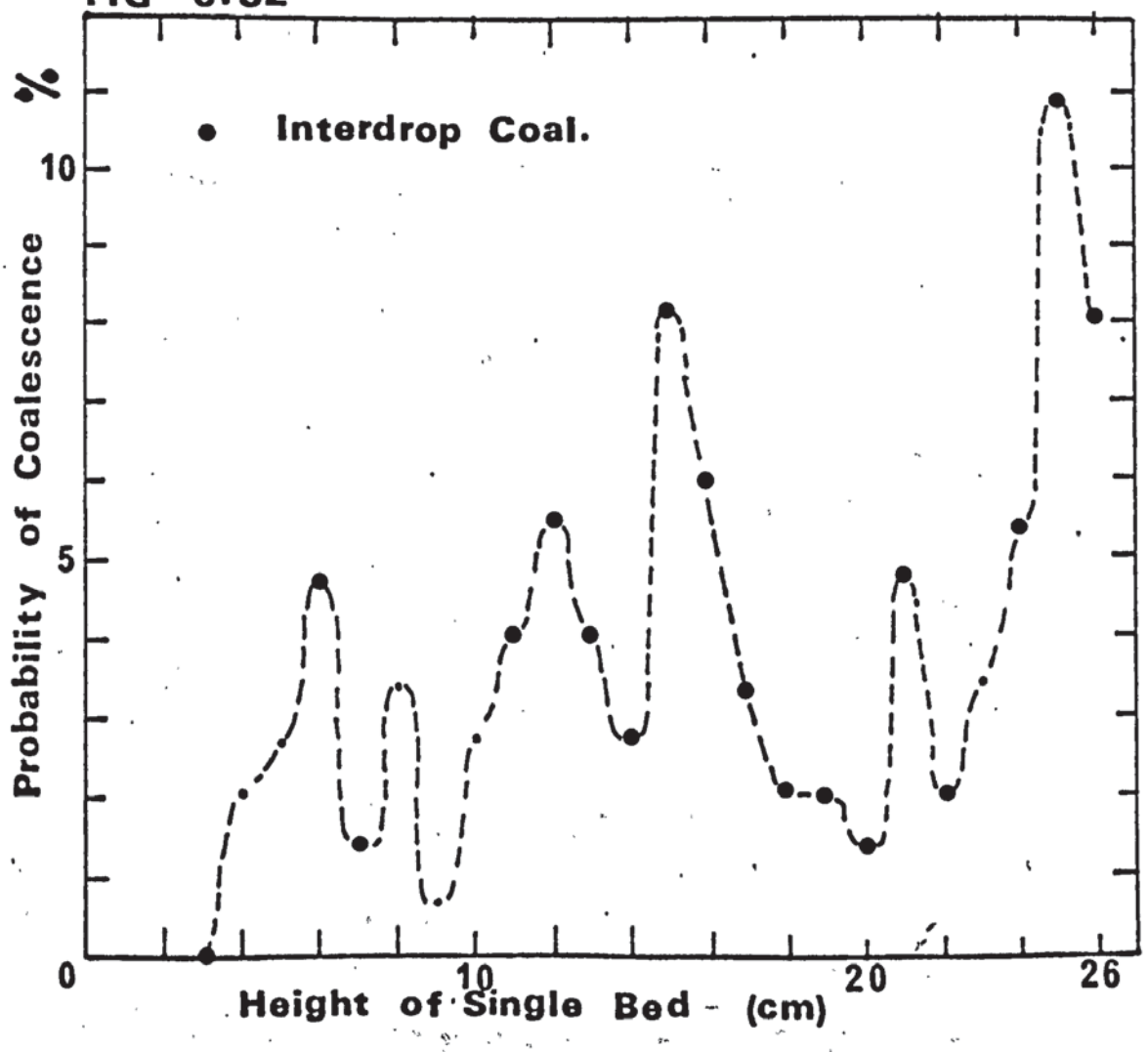

SYSTEM III
ISO OCTANE

3 mm DIST.
ORIFICE DIA.

FIG 6.33

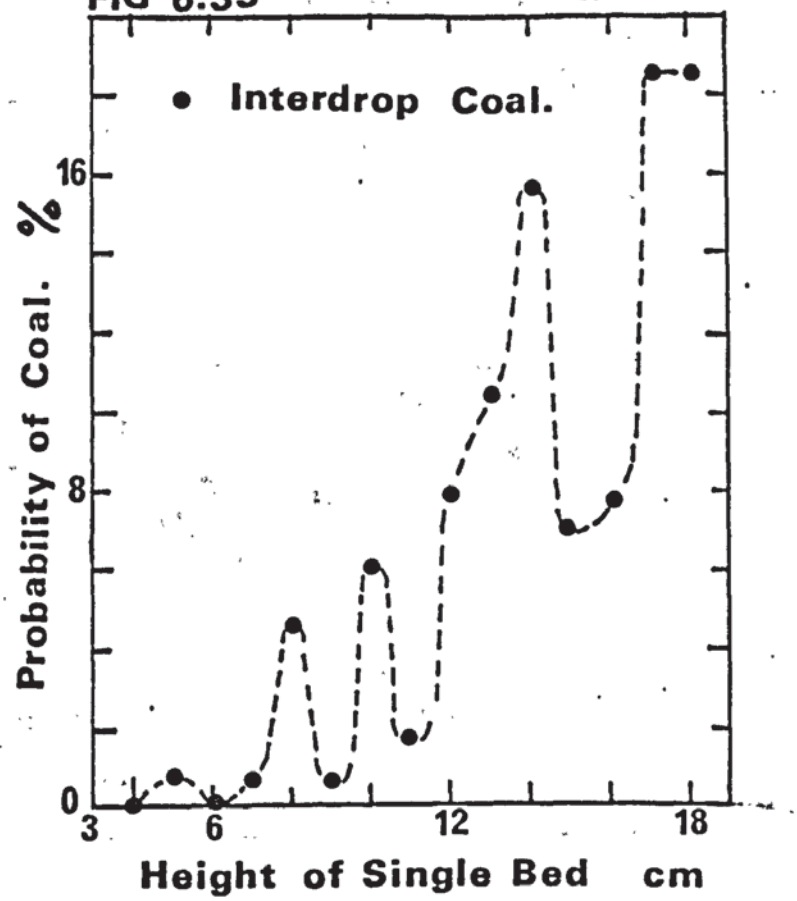

FIG 6.34

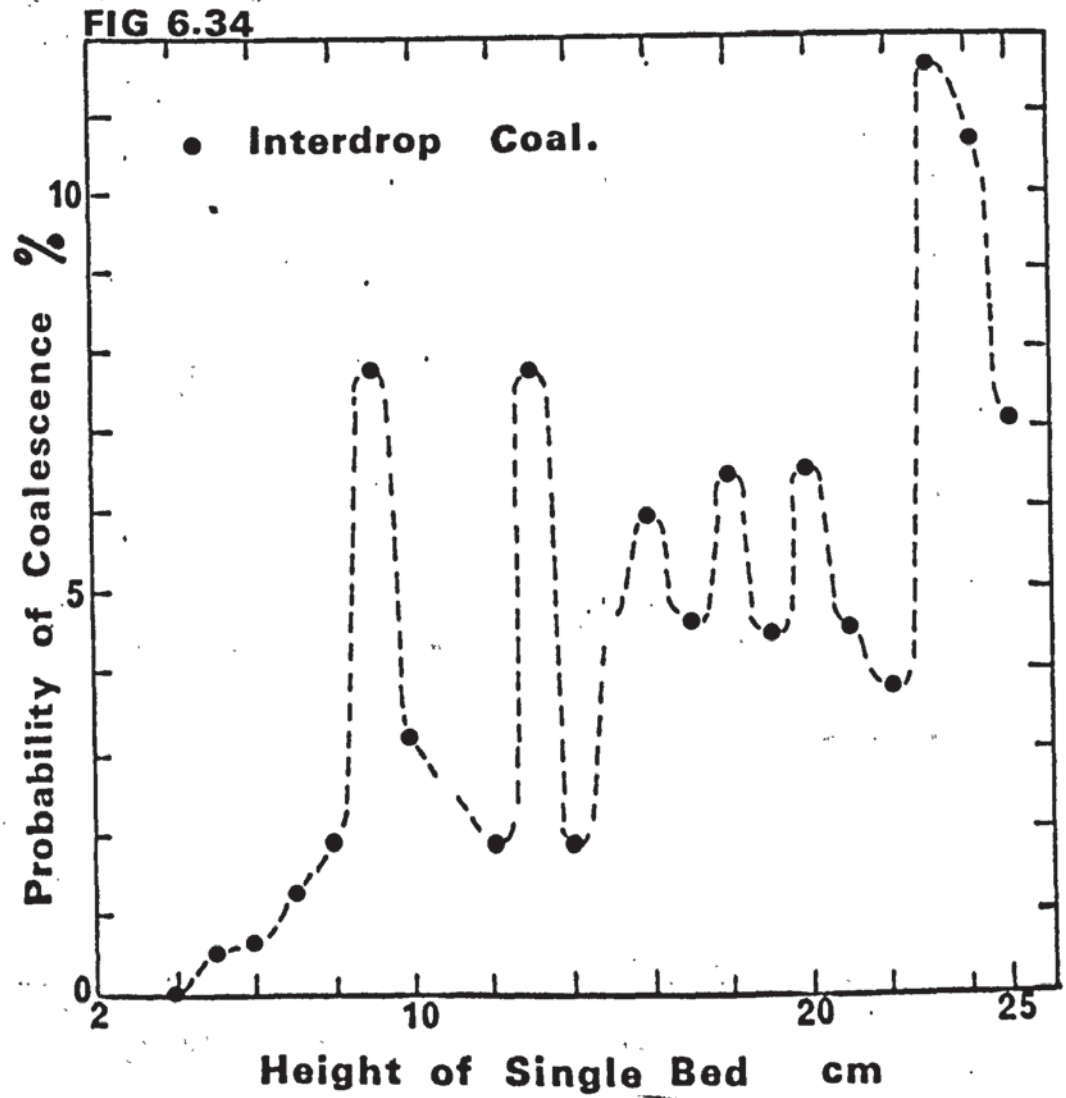

SYSTEM III

ISO OCTANE

4 mm DIST.
ORIFICE DIA.

FIG 6.35

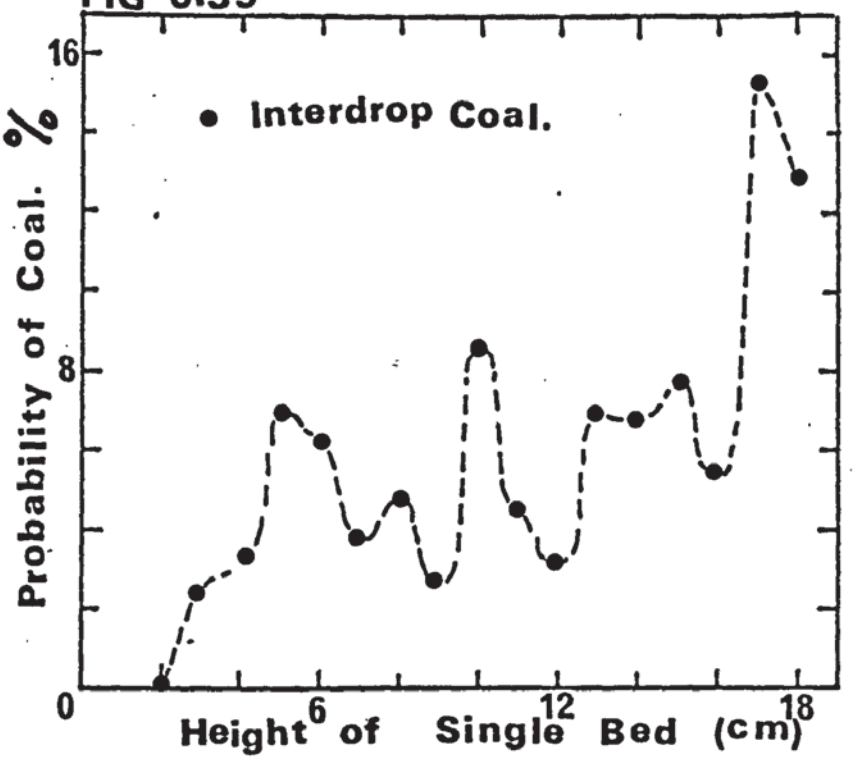

FIG 6.36

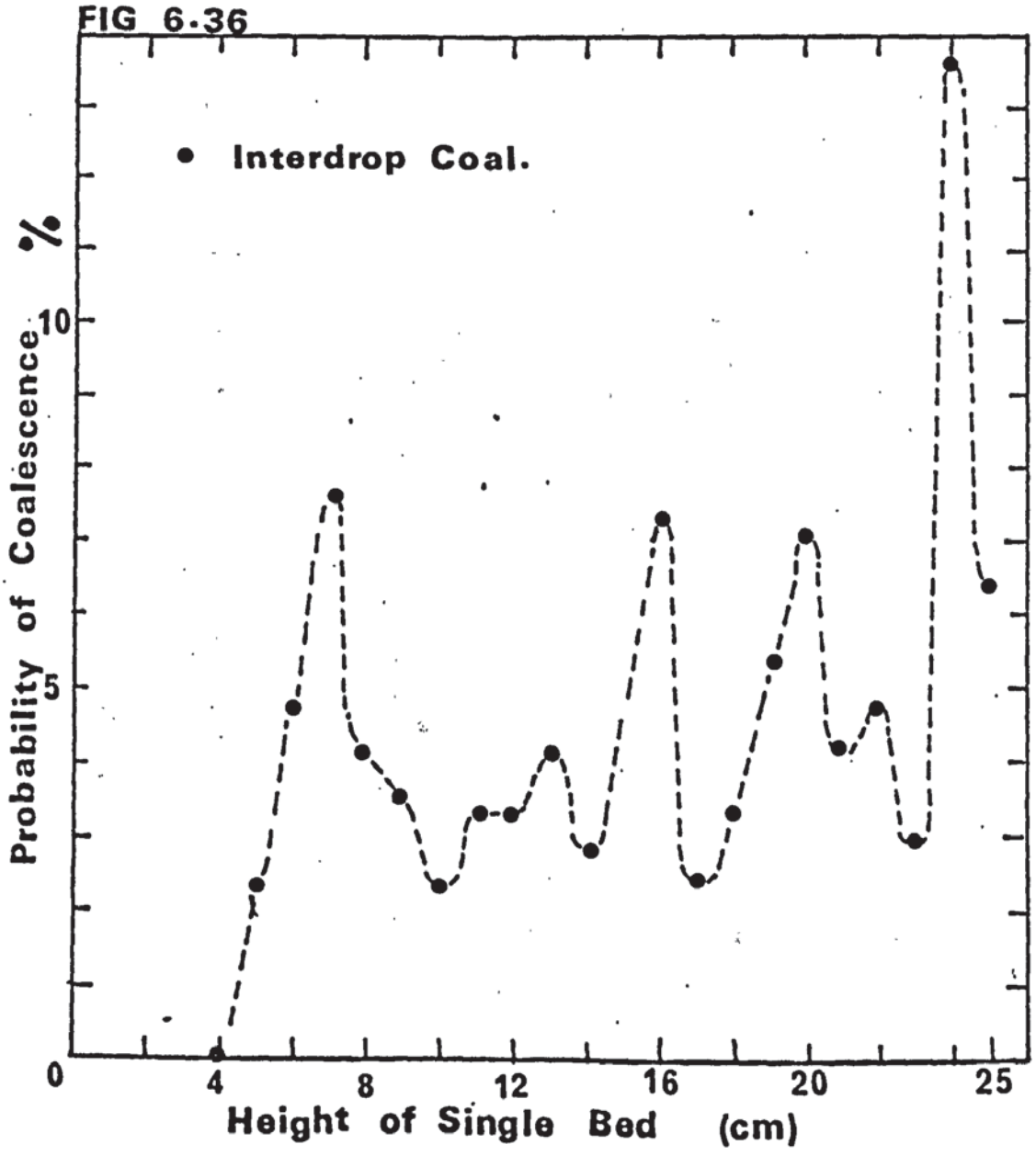

SYSTEM I AMYL ACETATE

1 mm DISTRIBUTOR

ORIFICE DIA.

FIG 6.37

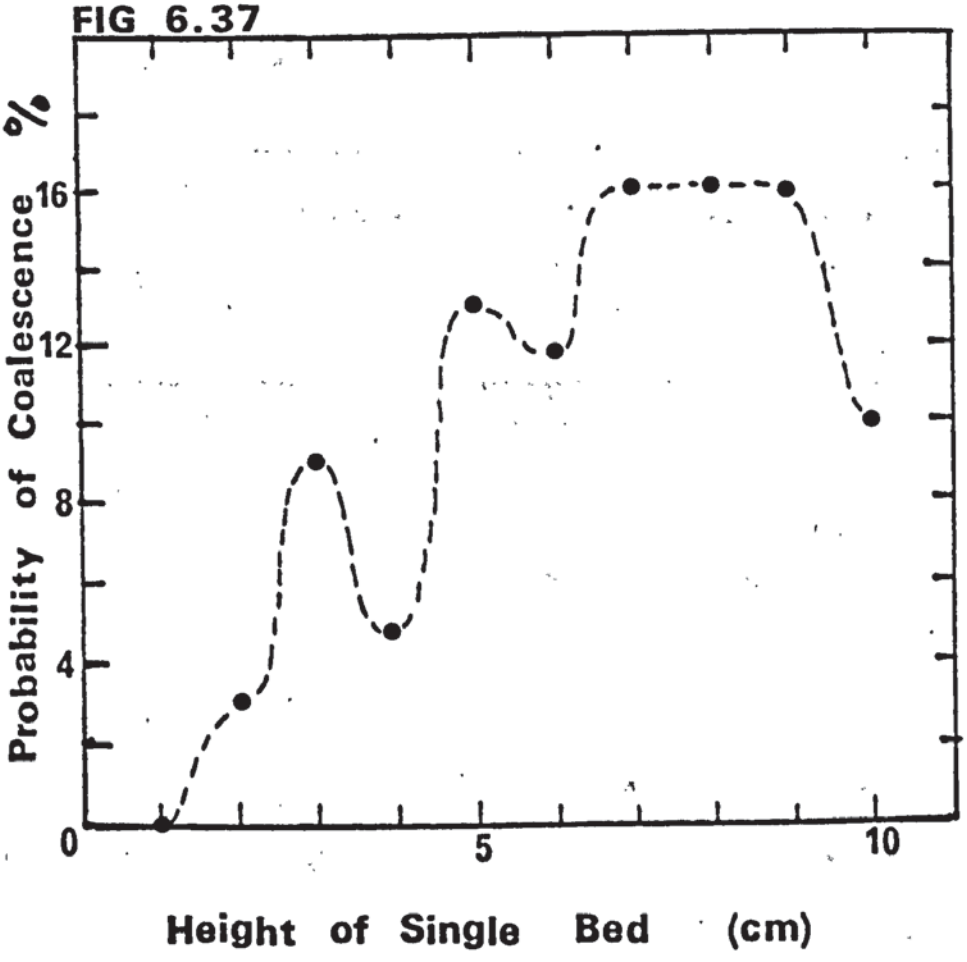

SYSTEM I
AMYL ACETATE

2mm DISRIBUTOR
ORIFICE DIA.

FIG 6.38

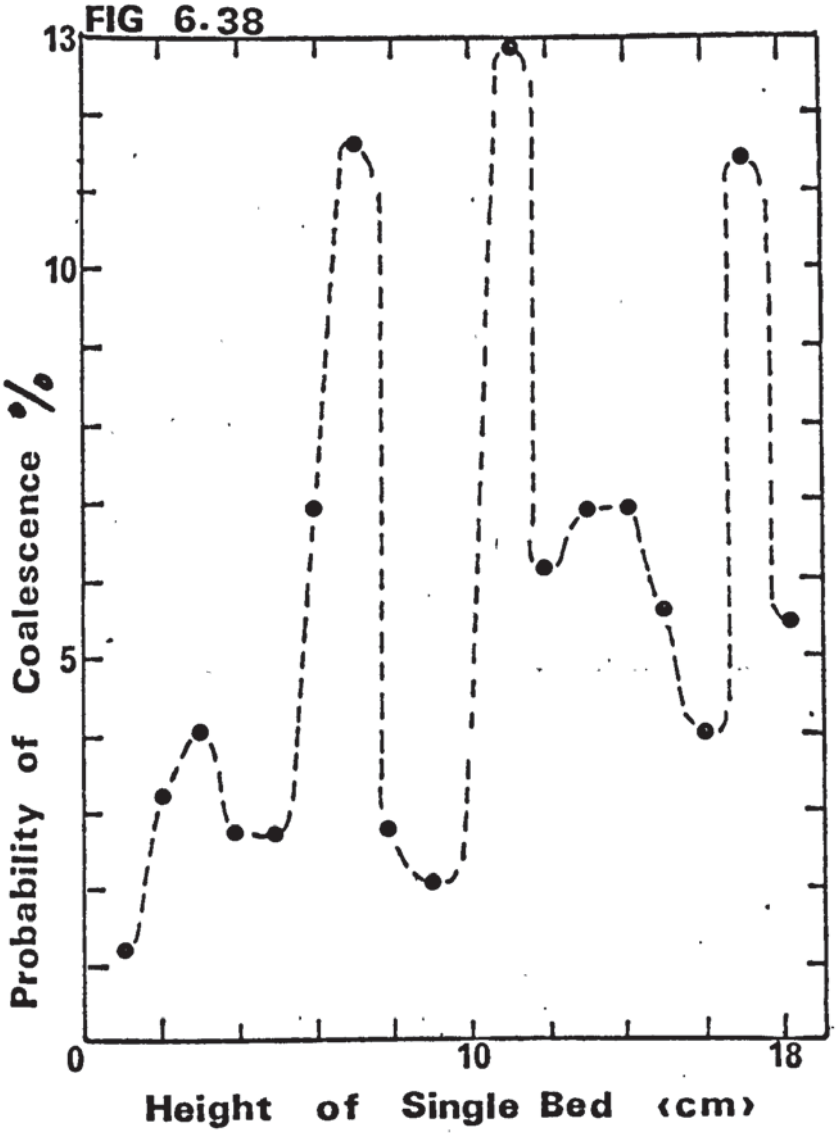

FIG 6.39

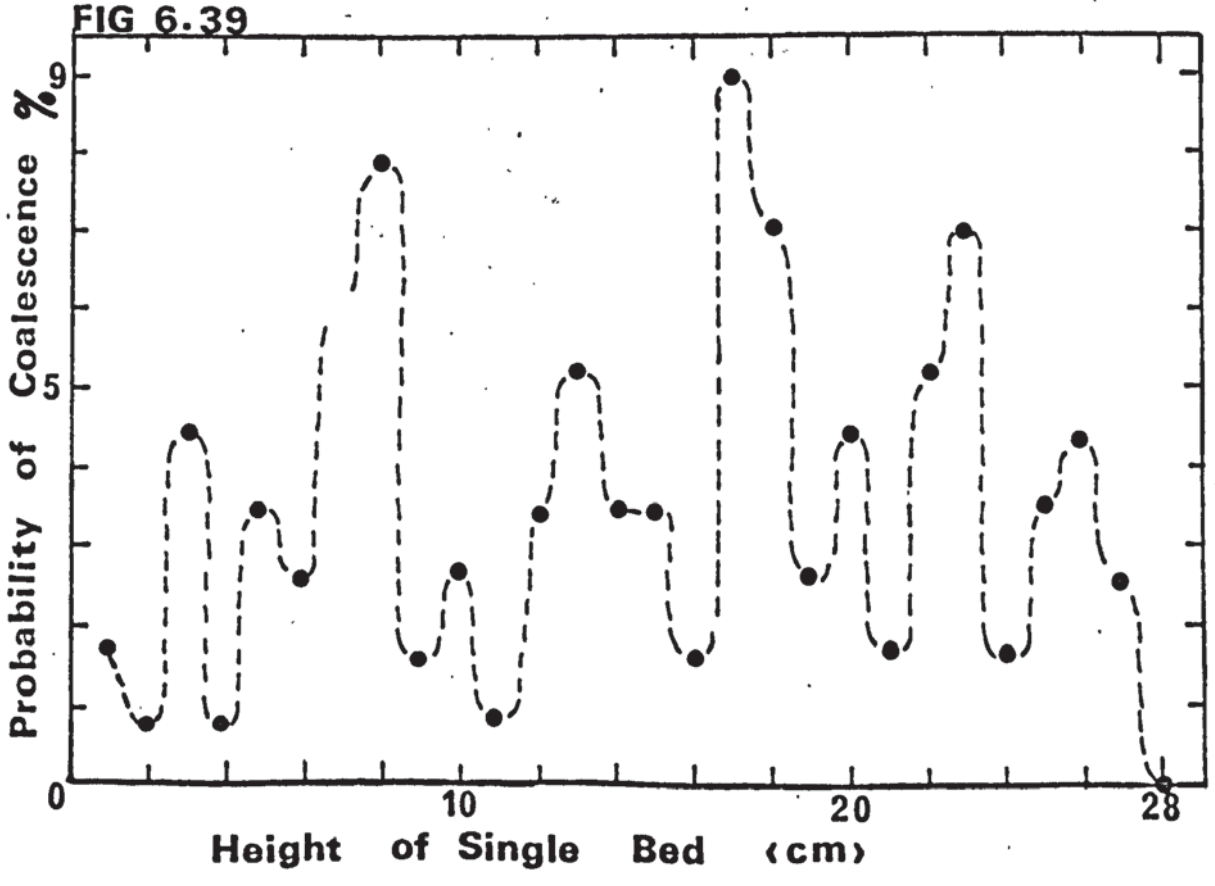

SYSTEM I AMYL ACETATE

3 mm DISTRIBUTOR ORIFICE DIA.

FIG 6.40

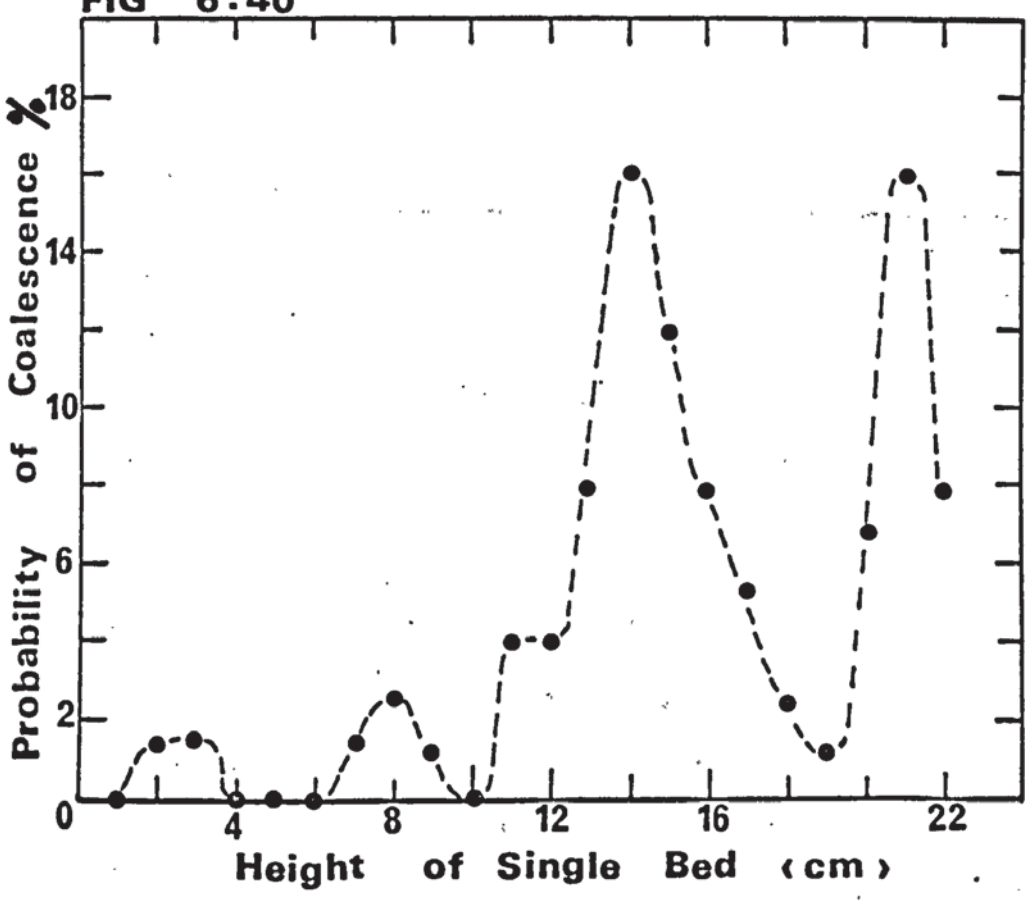

SYSTEM I AMYL ACETATE

4 mm DISTRIBUTOR ORIFICE

FIG 6.41

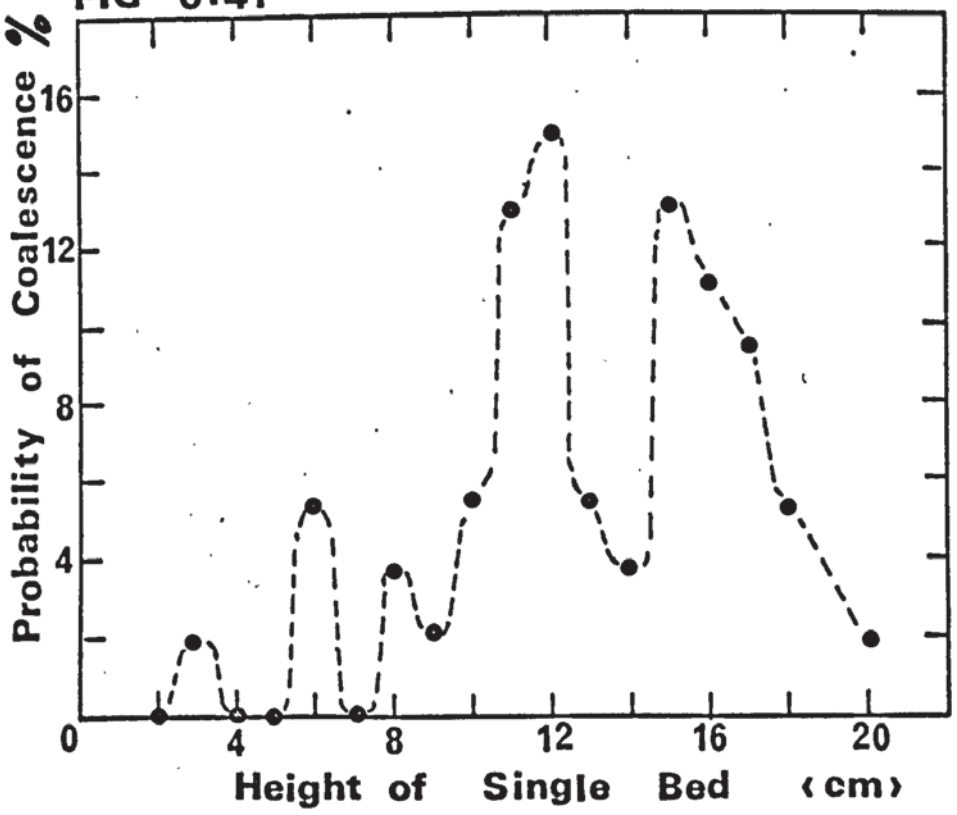

6.5) contd.

bed heights. Based on the results shown in the graphs in Figures (6.11) to (6.22) a correlation is proposed in terms of the capillary number which is an expression of the forces causing drainage and the ratio of bed height and drop diameter

$$\lambda = 1 - a\left(\frac{\gamma}{\mu_c V_d}\right)^b \left(\frac{d}{H}\right)^c$$

The constants a,b and c were evaluated using the least square method presented in Appendix 10. Experimental values of bed height below 3 cm. were not included since, as stated above, they do not represent a fully developed packed bed. The values of the constants were

$$a = 0.559, \quad b = 0.0536, \quad c = 0.19$$

This leads to the final correlation

$$\lambda = 1-0.559\left(\frac{\gamma}{\mu_v V_d}\right)^{0.0536} \left(\frac{d}{H}\right)^{0.19} \qquad (6.1)$$

It can be seen from equation (6.1) that λ will increase as the superficial velocity V_d and, consequently, the bed height increases. Equation (6.1) further shows that as d decreases λ increases. This suggests that smaller bed height is expected for smaller drop sizes contrary to the experimental findings. It was argued in paragraph 6, however, that in the case of smaller drops, more of the continuous phase is retained, the plateau boarders are smaller and the force causing drainage is less. Consequently, the time taken for the coalescence of smaller drops inside a dispersion band is greater. Therefore while the probability of coalescence increases for smaller drops the time taken for the probability to occur is greater, resulting in higher beds.

Calculated values of λ from equation (6.1) were

FIG 6.42 COALESCENCE PROBABILITY

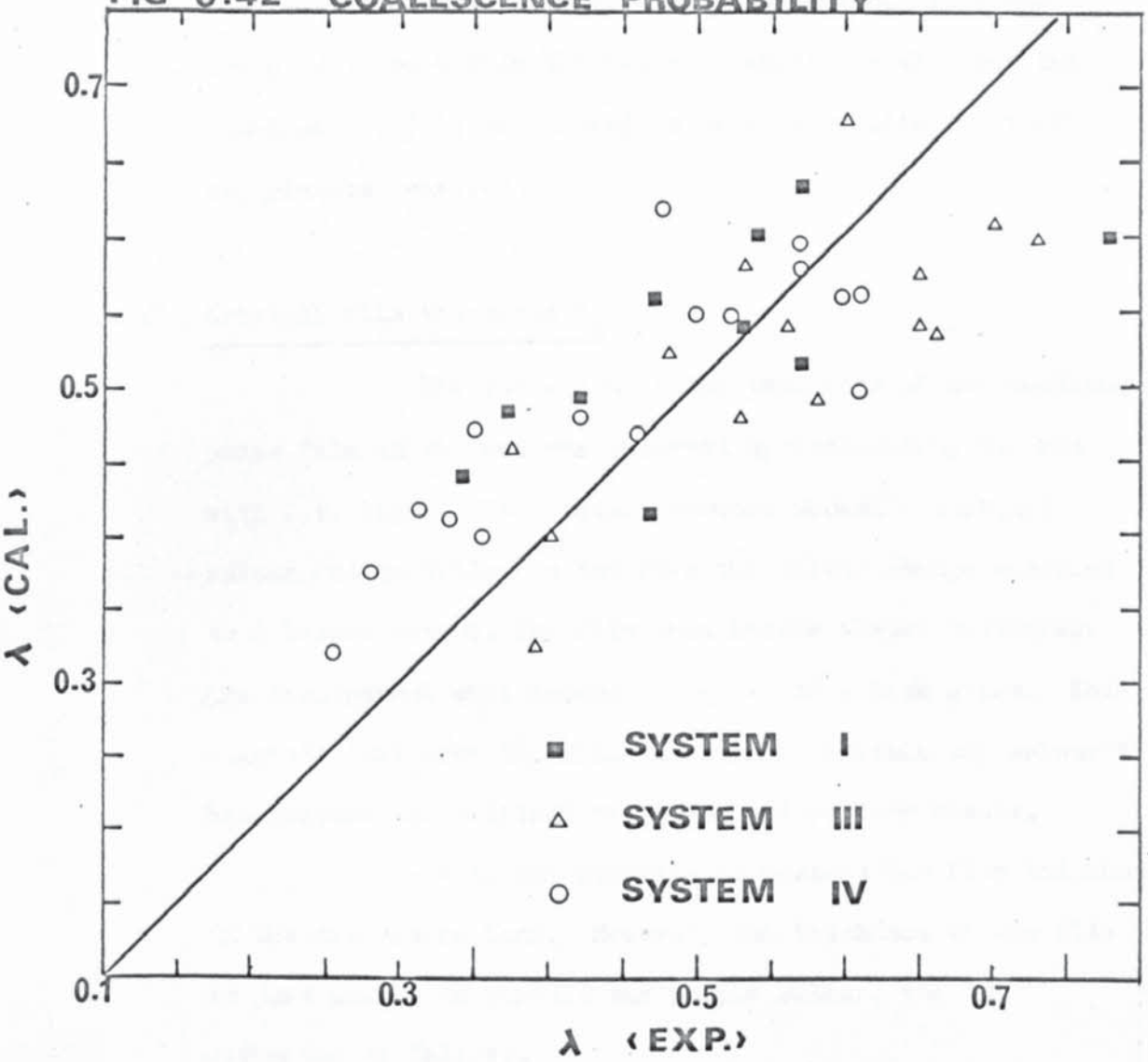

FOR DATA SEE APPENDIX (11)

6.5) contd.

plotted against the experimental values of λ Figure (6.42). A certain amount of scatter will be observed. This was accepted to be within the range of experimental error and equation (6.1) is considered to be a satisfactory fit of experimental results.

6.6) Critical film thickness h_k

The variation in the thickness of the continuous phase film in the bed was observed by irridiating the bed with U.V. light. The plateau borders showed a distinct colour change whilst in the film the colour change occurred to a lesser extent. The film then became almost colourless and transparent when interdrop coalescence took place. This suggests that when the film just cannot sustain any colour it has reached its critical thickness and rupture ensues.

It is not possible to measure the film thickness in the dispersion band. However, the thickness of the film that is just unable to sustain the purple colour, may be estimated as follows.

Three cells 50.0; 25.0 and 7.0 microns were used to measure the absorption of light by the solution in the excited and the unexcited state. The absorption was plotted versus cell thickness. Figure (6.43) shows that when the two curves were extrapolated they intersected at about 2 microns. To verify the extrapolated value of 2 microns two optical flats were made into a cell. The space between the optical flats was measured by counting the fringes produced from a sodium lamp. A sample of the organic liquids with the phototropic dye was taken from the columnand placed in the

Film Thickness (microns)	Absorbance Unirridiated ●	Irridiated ■
7	0.035	0.038
25	0.036	0.047
50	0.060	0.094

FIG 6.43

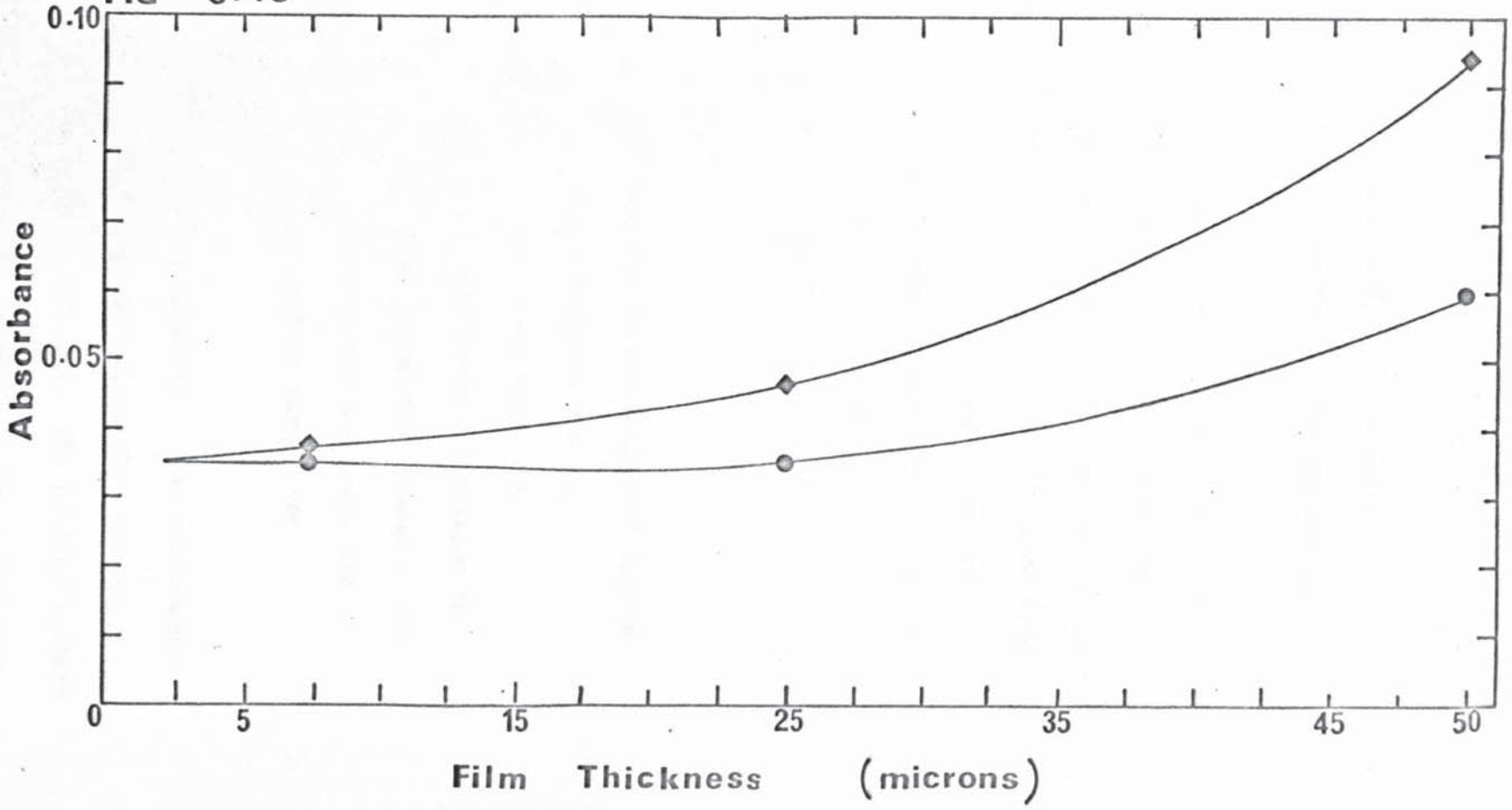

6.6) contd.

cell. It was then irridiated with U.V. light and the space was reduced until the colour disappeared. The gap was found to be about 2 microns.

The experimental evidence leads to the conclusion that the film between the drops is approximately 2 microns thick at the point of rupture. This appears to be less than the thickness estimated for the case of single drop at a plane interface i.e. 4.0 microns. It must, however, be stressed that the technique is approximate and only gives an indication of the order of magnitude of the critical thickness of the film in the dispersion band.

6.7) Bed Zones.

Experimental observation has confirmed that a vertical dispersion band has three distinct zones.

1) At the beginning of the bed where the drops are approximately spherical and little or no deformation to the shape of the drops has taken place. The holdup of the continuous phase is relatively high and the drops are loosely packed. This section will be termed the flocculating zone.

2) After the flocculating zone the majority of the continuous phase is squeezed out, the drops are closely packed and the deformation of the drops is evident. The plateau borders are formed at this stage and the drainage of the continuous phase becomes more restricted. This section will be termed the packing zone.

3) The drops, having travelled through the packing zone finally coalesce at the interface. This will be termed the coalescence zone. Hittit[88] reported the same observation

6.7) contd.

3) contd.

when studying dispersion bands in vertical settlers of 3", 6" and 9" diameters respectively.

For low bed height the flocculating zone is the predominant one and the dispersion band behaves as a liquid-liquid froth. The probability of interdrop coalescence is very low. The coalescing interface at this stage is flat.

For bed height values of about 10 cm. the packing zone becomes more evident and a slight curvature in the coalescence interface appears. The probability of interdrop coalescence has increased at this stage. However, the flocculating zone still constitutes an appreciable part of the bed. The packing zone continues and the probability of interdrop coalescence continues to increase with increasing bed height until values of 20 cm. and over are reached. At such bed heights the packing zone becomes the predominant one and the flocculating zone constitutesa small part of the bed. The curvature of the coalescing interface has also increased. The dispersion band now behaves as a true liquid-liquid foam.

6.8) Radius of the Plateau border r_o.

It can be seen from equation (4.12) that r_o appears to be independent of bed height i.e. its position in the dispersion band. This is to be expected since the forces causing drainage, which in turn affect the value of r_o are interfacial. However, for any particular bed height the average diameter of the drops d, and the superficial velocity of the dispersed phase V_d changes within the dispersion band due to interdrop and drop wall coalescences respectively. The fractional hold up of the dispersed phase also changes along the bed. This causes the value of r_o to change along the dispersion band. Moreover after regrouping of the drops due to disturbances caused by interdrop coalescence, the plateau borders are reformed and as drainage of the continuous phase proceeds, the radius of the plateau border changes until further disturbances are caused, new plateau borders are formed and the process is repeated.

The Christiansen effect described in paragraph 5.8 has enabled the measurement of r_o inside a dispersion band. A comparison of the measured value and the predicted one from equation (4.12) for system VI are shown in Appendix (14). There are numerous difficulties in making these measurements; the greatest of which was that the plateau border could be inclined at any angle to the horizontal and it is impossible to state with certainty that the plateau border being photographed is absolutely parallel with the photographic film. Small inclinations are difficult to detect and can cause large distortions to the curves forming the plateau borders. When photographed these can introduce a large error in the measured value. Good agreement however was obtained between the measured and the predicted value of r_o.

6.8) contd.

The mean measured value of r_o for system VI was 3.1 mm. whilst the predicted one was 3.9 mm.

CHAPTER 7.

DIMENSIONAL ANALYSIS.

7.0) Dimensional Analysis.

An initial attempt was made to correlate the parameters affecting the height of a bed by a dimensional analysis on Systems I to IV.

The factors that were considered to affect the bed height (H) were:-

$$H = f\left[d^a(\Delta\rho g)^b(\mu_c)^c(\gamma)^e(V_d)^h(T)^q\right] \qquad (7.1)$$

where d = the drop diameter (L)

$\Delta\rho g$ = the gravitational force ($ML^{-2}T^{-2}$)

μ_c = the viscosity of the continuous phase ($ML^{-1}T^{-1}$)

γ = the interfacial tension (MT^{-2})

V = the superficial velocity of the dispersed phase (LT^{-1})

T = the residence time of the drops in the bed (T)

Substituting the dimensions in equation (7.1) gives

$$L = f\left[L^a(ML^{-2}T^{-2})^b(ML^{-1}T^{-1})^c(MT^{-2})^e(LT^{-1})^n(T)^q\right]$$

Summing the length, time and mass units gives

$$\sum L = 0 \qquad 1 = a - 2b - c + h \qquad (7.2)$$

$$\sum M = 0 \qquad 0 = b + c + e \qquad (7.3)$$

$$\sum T = 0 \qquad 0 = -2b - c - 2e - h + q \qquad (7.4)$$

Solving equations (7.2)(7.3) and (7.4) in terms of a,b and q leads to the following groups

$$\frac{T\gamma}{\mu_c H} = k\left(\frac{d}{H}\right)^a\left(\frac{\Delta\rho g H^2}{\gamma}\right)^b\left(\frac{\mu_c V_d}{\gamma}\right)^q \qquad (7.5)$$

where $\left(\frac{\mu_c V_d}{\gamma}\right)$ is the capillary number which is the ratio of the

7.0) contd.

viscous and the interfacial forces, $\left(\frac{\Delta\rho g H^2}{\gamma}\right)$ is Bond number which is the ratio of the gravitational and the interfacial forces and $\frac{T\gamma}{\mu_c H}$ is the ratio of the interfacial and viscous forces.

The constants k,a,b and q were evaluated using ICL 1900 STATISTICAL ANALYSIS library programme. Their values were

$k = 11.22$, $a = -0.331$, $b = -0.276$, $q = -0.768$

equation (7.5) becomes

$$\frac{T\gamma}{\mu_c H} = 11.22\left(\frac{d}{H}\right)^{-0.331}\left(\frac{\Delta\rho g H^2}{\gamma}\right)^{-0.276}\left(\frac{\mu_c V_d}{\gamma}\right)^{-0.768} \qquad (7.6)$$

The values of $\frac{T\gamma}{\mu_c H}$ calculated from the experimental results and the estimated one showed good agreement and are presented in Figure 7.1 and Appendix (12).

By a closer inspection of equation (7.6) the following points can be made

1) $T \propto H^{0.78}$ i.e. when the bed height increases the residence time increases.
2) $H \propto V_d^{0.985}$ i.e. an increase in the superficial velocity will result in an increase in bed height.
3) For any particular bed height $T \propto \frac{1}{V^{0.768}}$ i.e. if the superficial velocity increases the residence time decreases.
4) $T \propto \frac{1}{d^{0.381}}$ i.e. when the drop size is small the residence time is high.
5) From (1) and (4)

$$H^{0.78} \propto \frac{1}{d^{0.33}} \quad \therefore \quad H \propto \frac{1}{d^{0.423}}$$

i.e. when the drop size is small for any particular flowrate the bed height increases.

FIG 7.1

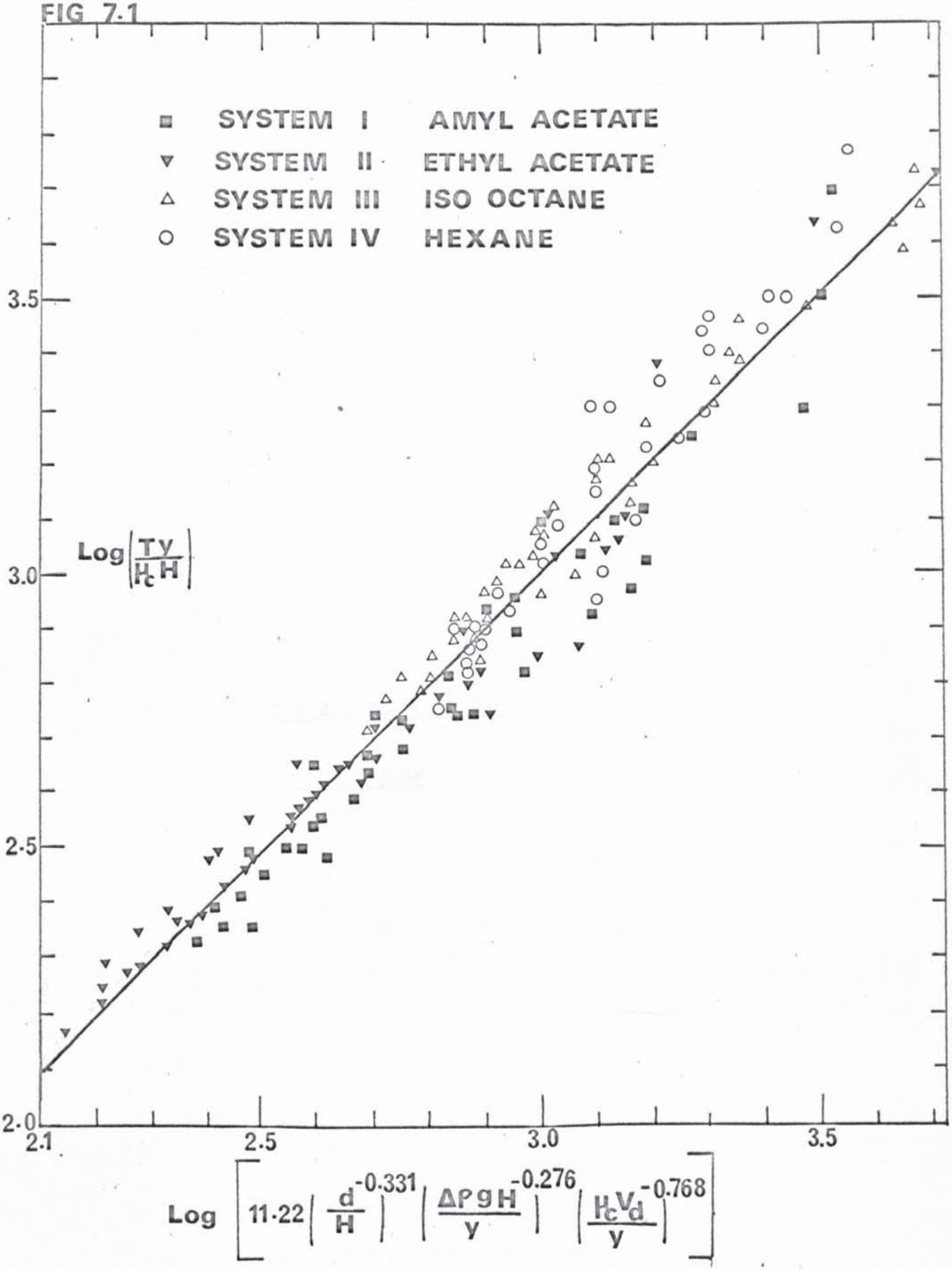
SYSTEM I AMYL ACETATE
SYSTEM II ETHYL ACETATE
SYSTEM III ISO OCTANE
SYSTEM IV HEXANE
3.5
3.0
2·5
2·0
2.1
2.5
3.0
3.5
Log (Ty / μc H)
Log [11·22 (d/H)^-0.331 (ΔρgH/y)^-0.276 (μc Vd/y)^-0.768]

CHAPTER 8

DISCUSSION

8.0) Discussion.

The experimental results were considered in two ways:-

1) A correlation was developed using dimensional analysis in order to identify the relevant parameters affecting dispersion bands. The predominant group appeared to be the capillary number $\left(\frac{\mu_c V_d}{\gamma}\right)$. This is to be expected since it describes the forces causing flow into "capillary tubes" which is the case when the dispersed phase flows into the plateau borders.

The capillary number also appeared in the correlation describing interdrop coalescing probability; paragraph (6.5). The Bond number $\left(\frac{\Delta\rho_g H^2}{\gamma}\right)$ and the drop diameter to bed height ratio $\left(\frac{d}{H}\right)$ have approximately the same index (-0.276) and (-0.331) respectively and, therefore, their effect on the correlation is similar. Good agreement was obtained between the experimental and the correlated results.

It can be seen from Figure 7.1 that 97.5% of the points are within $\pm$ 10% and 85% are within $\pm$ 5%.

2) A mathematical model was developed based on the drainage of the continuous phase through the network of the plateau borders.

The incremental treatment of the model described in Chapter 4 was based on the experimental findings shown in Figures (6.23) to (6.41). These illustrate that on interdrop coalescence, at a plane within the bed, there appears to be a disruption locally and the droplets reorient themselves to again pack together. Following this there is a period of calm where the probability of coalesence is low. This is followed by a high rate of interdrop coalescence and subsequent calm, after which the cycle is repeated throughout the bed.

8.0) contd.

These fluctuations are due to the regrouping of the drops and a redistribution of the continuous phase after interdrop coalescence has taken place. New plateau borders are formed and the process of film drainage continues once more. When the critical film thickness for rupture is reached, interdrop coalescence occurs and is once again followed by the regrouping of the drops and the redistribution of the film.

In the computer application of the model the film thickness was adjusted until the predicted bed height agreed with the experimental findings. It confirmed that the critical film thickness varies with drop size. As the drop size increases so does the critical film thickness. This is to be expected since smaller drops share smaller faces i.e. areas of contact within which the continuous film is trapped. Smaller areas approximate to their behaviour to rigid plates, so that when the film drains these faces remain flat enabling the film to drain to its critical thickness for rupture. When bigger face areas are involved however, it is probable that a dimple is formed which traps the continuous phase and a form of the "barrier ring" is created at which the film prematurely ruptures analagous to the single drop at an interface situation. This leads to a greater average value of the critical film thickness when considered in conjunction with holdup.

8.0) contd.

The criteria

$$Q_{up} - \sum_{i=1}^{i=n} Q_{i\ down} = 0$$

where initially used to terminate the calculation on the computer. However, it was found to be impractical since after several iterations, the value of the amount of the continuous phase draining $Q_{i\ down}$ for the subsequent increments was very small and did not affect the sum appreciably. This resulted in excessively high values for the bed height and in some instances the computer programme ran to infinity.

A more practical criterion for the termination of the programme was found to be the fractional holdup of the dispersed phase ε_d. A value of $\varepsilon_d = 0.98$ was used implying that 98% of the continuous phase initially trapped had drained. The other 2% accounts for the loss of the continuous phase due to the fragmentation of the film and the formation of satellite drops of secondary haze found in the coalesced phase. As mentioned in paragraph (6.3) the formation of the secondary haze increased for systems with low interfacial tension e.g. systems I, II and V.

From figures (8.1) to (8.5) it can be seen that good agreement is obtained at low bed heights.

Two factors play an important part in the prediction of such bed heights:

1) For low values of bed heights the dispersion band approximates in its behaviour to a liquid-liquid froth as stated in paragraph 6.6; this is expected to produce inaccuracies in the calculation since the model is based on the drainage through liquid-liquid foam.

2) In the model an average velocity is used in the calculation

SYSTEM I
AMYL ACETATE

FIG 8.1

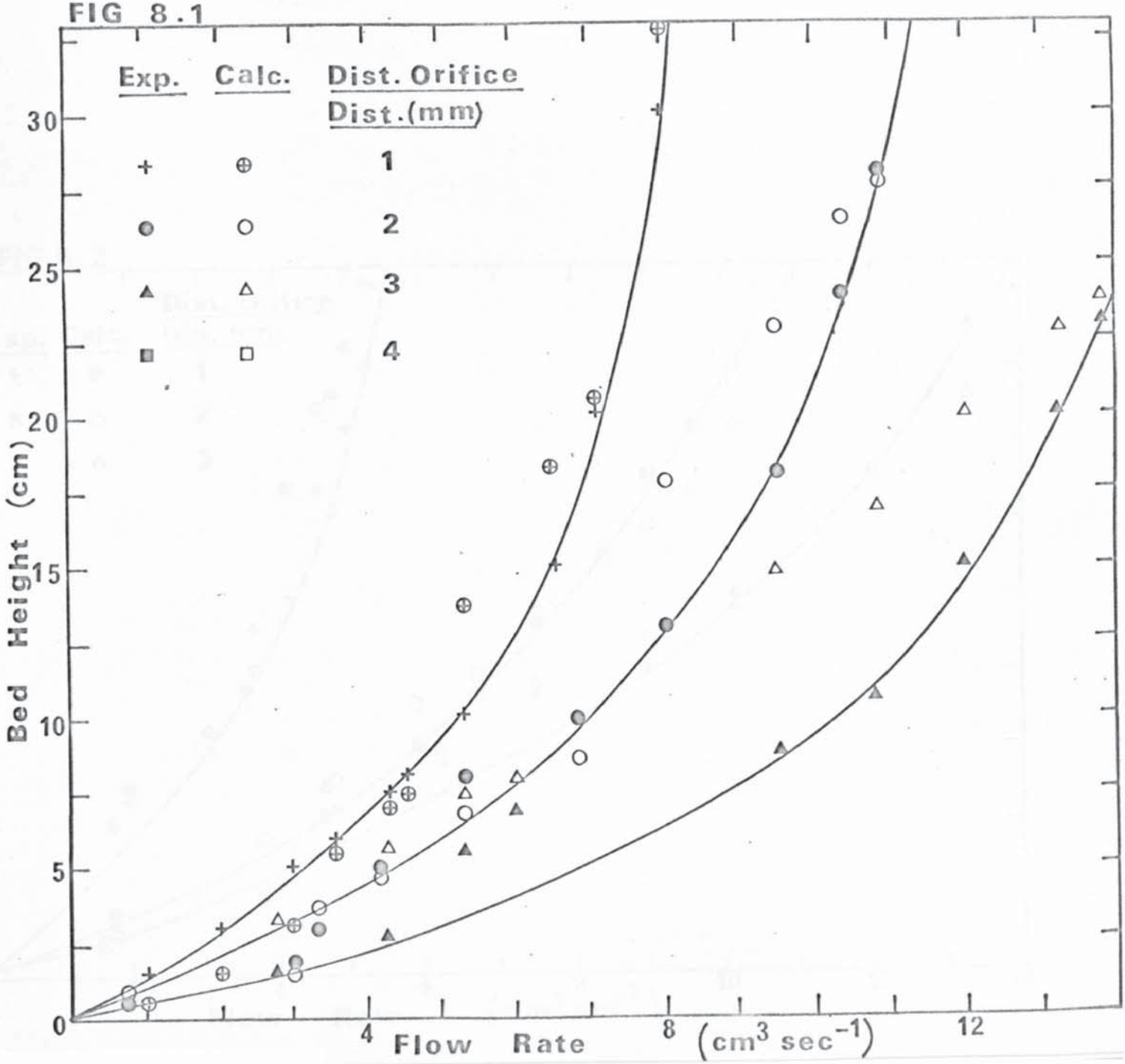

SYSTEM II
ETHYL ACETATE

FIG 8.2

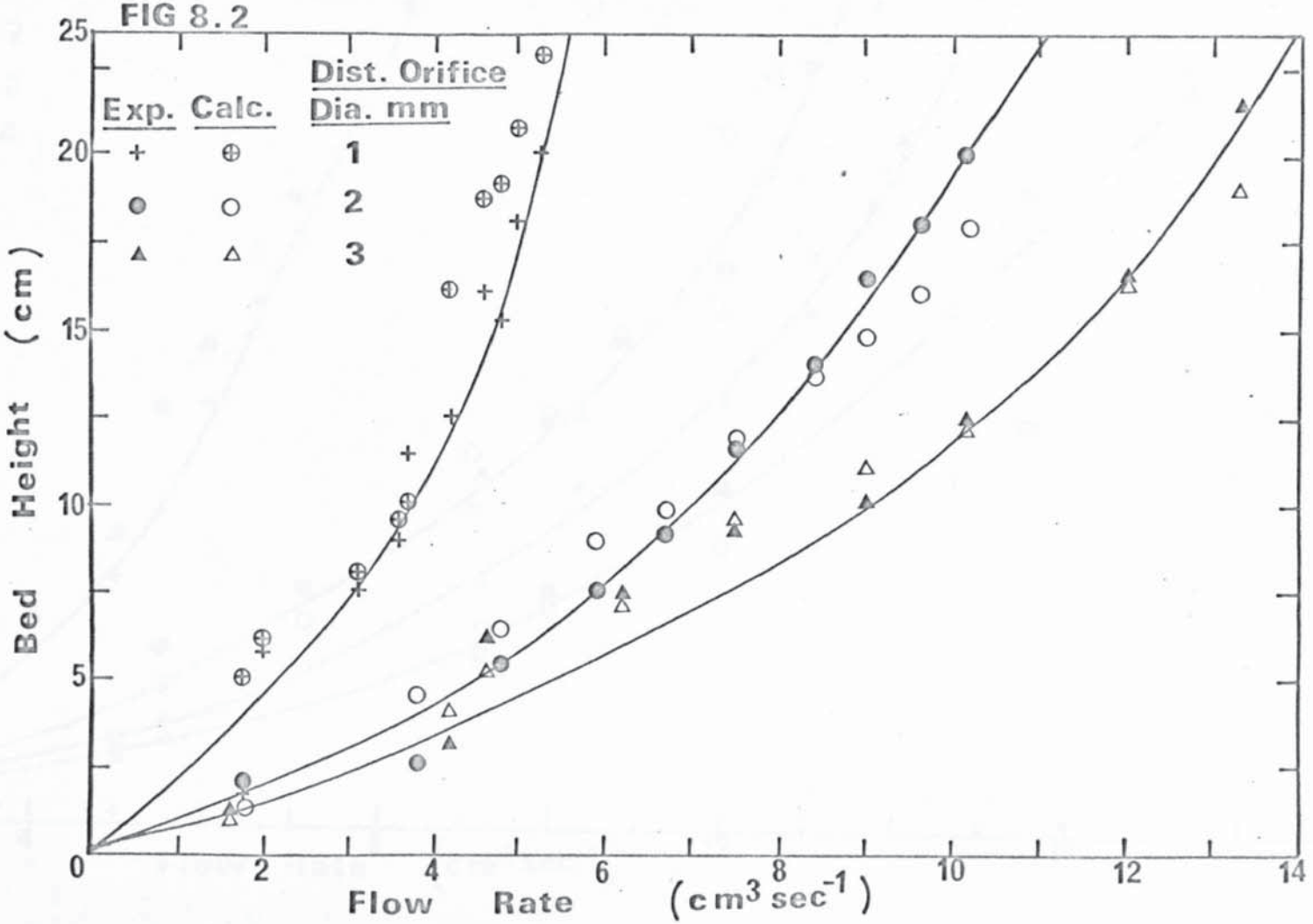

FIG 8.3

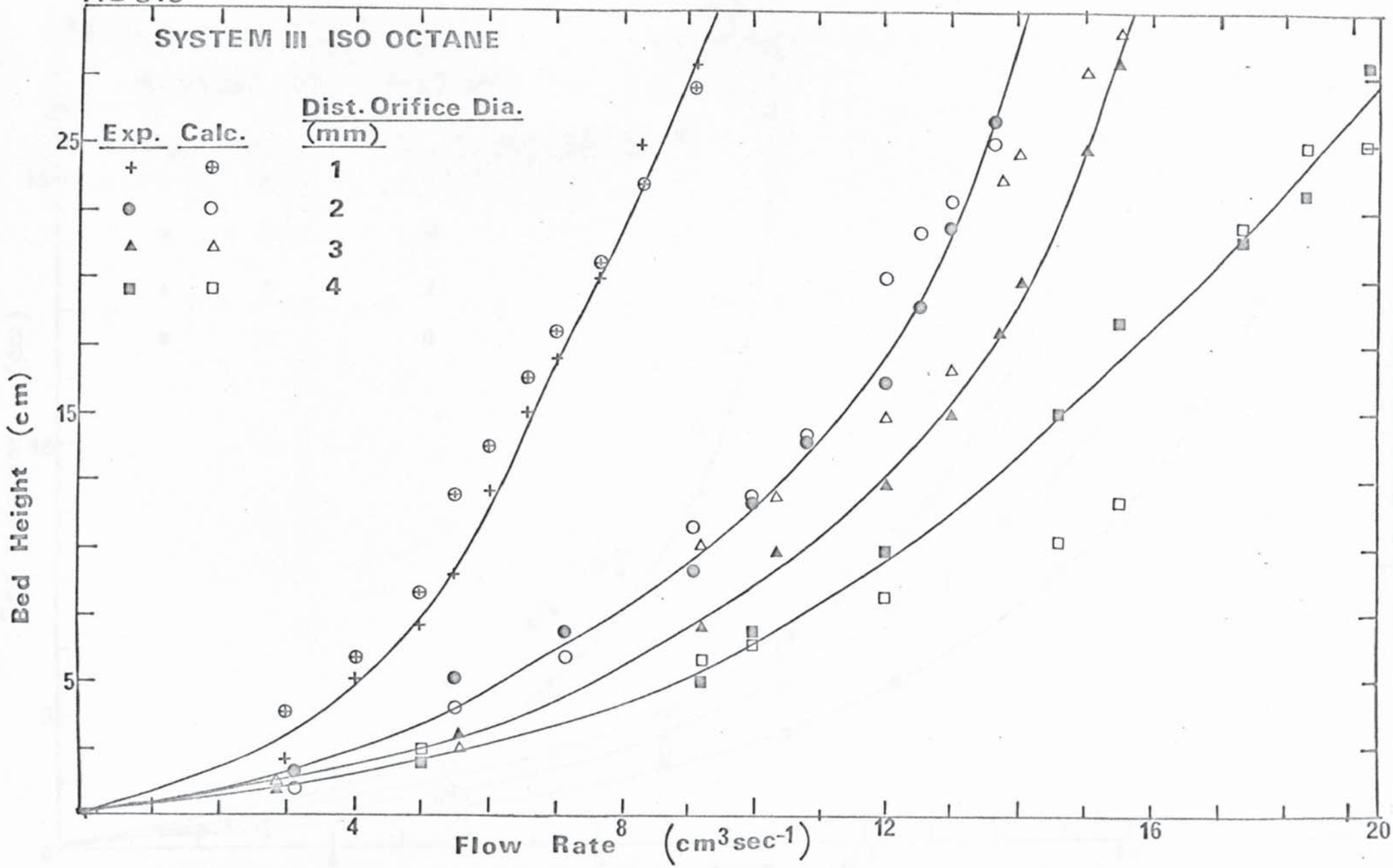
SYSTEM III ISO OCTANE
Exp.
Calc.
Dist. Orifice Dia. (mm)
1
2
3
4
Bed Height (cm)
25
15
5
4
8
12
16
20
Flow Rate (cm3sec-1)

FIG 8-4

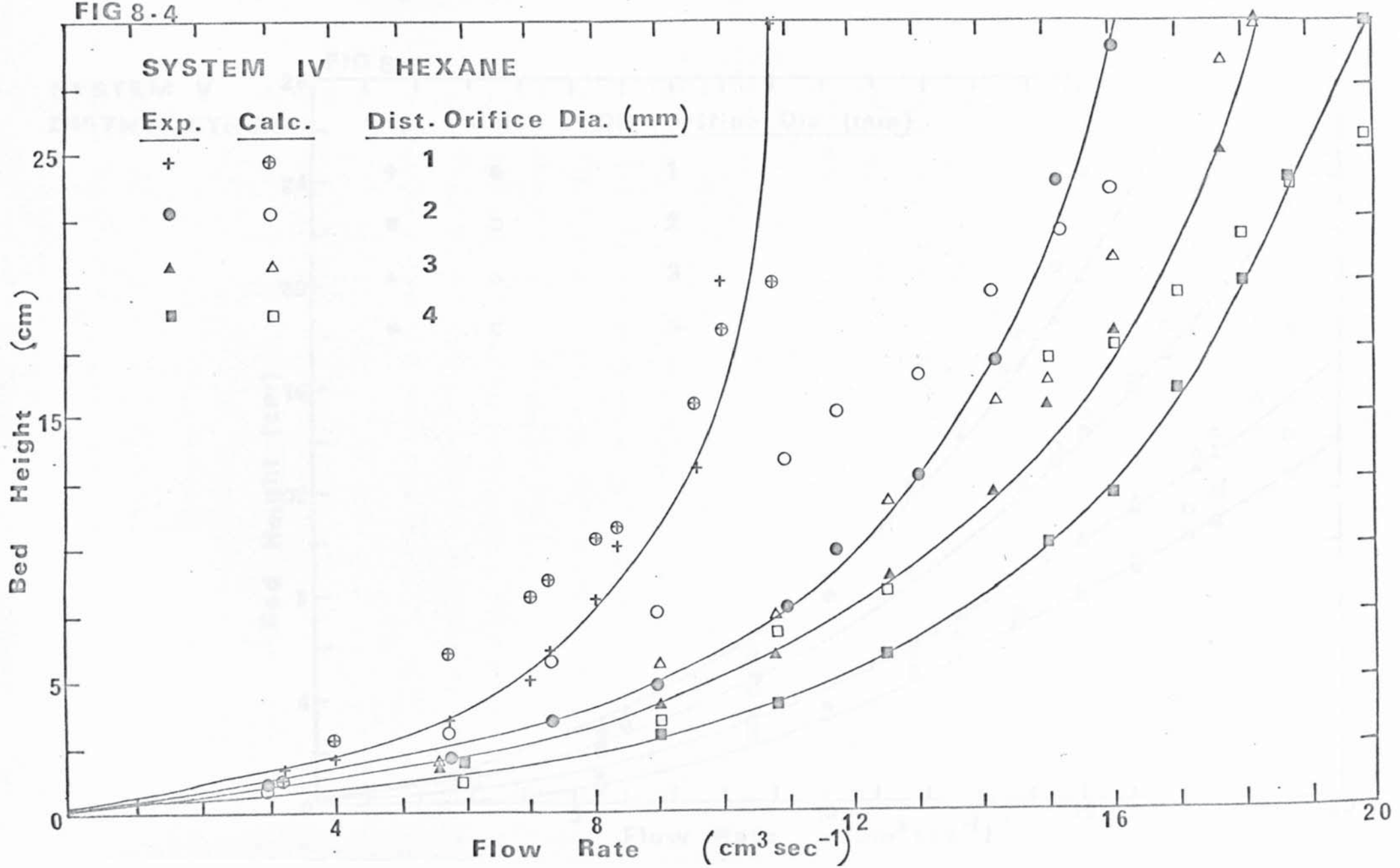
SYSTEM IV HEXANE
Exp.
Calc.
Dist. Orifice Dia. (mm)
1
2
3
4
Bed Height (cm)
0
5
15
25
4
8
12
16
20
Flow Rate (cm³ sec⁻¹)

FIG 8.5

SYSTEM V
DIETHYL ETHER

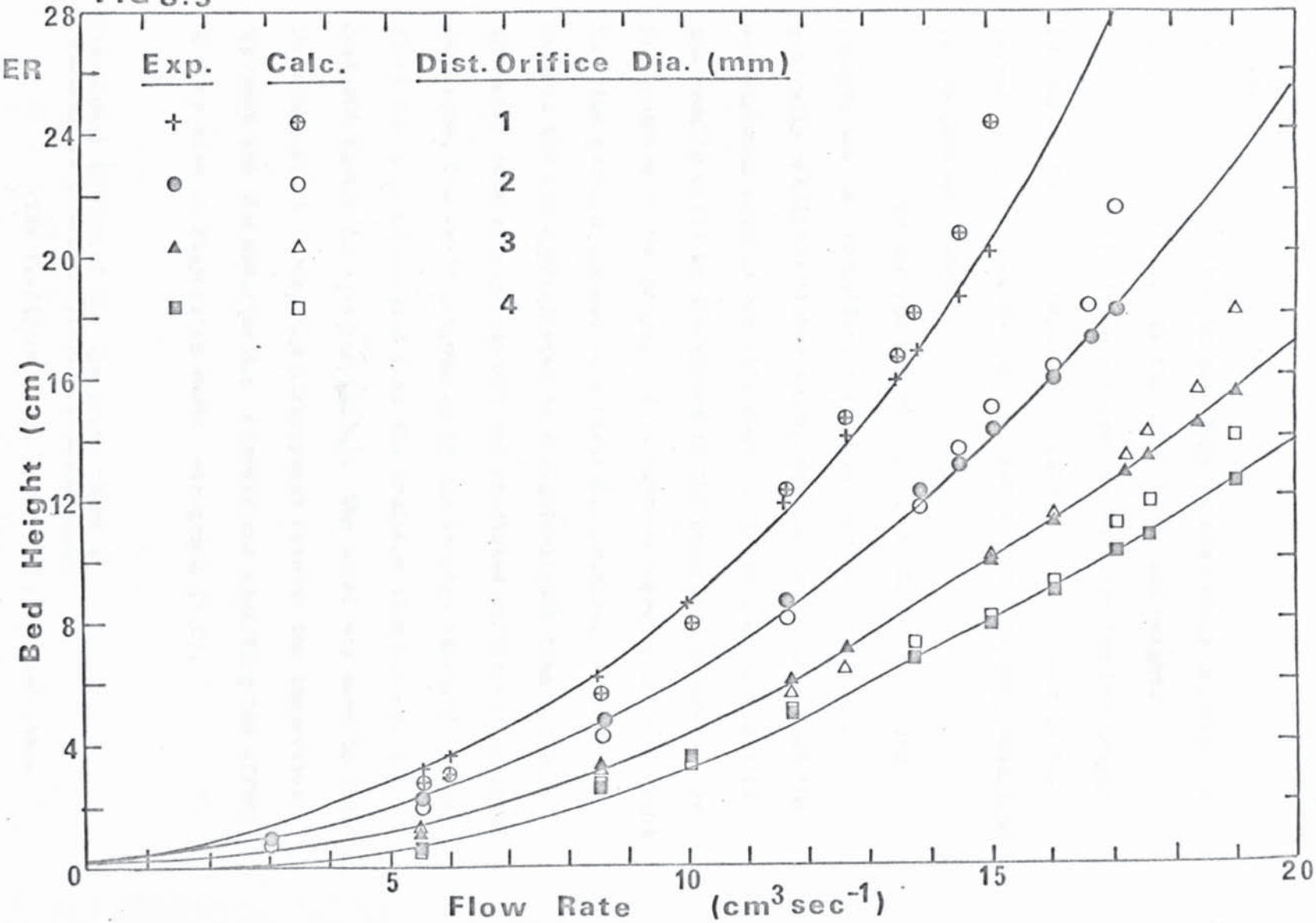

8.0) contd.

of the incremental bed height. This is absolutely correctwhen plug flow exists which is the case at low bed height.

It is evident therefore that for low bed height the former factor is expected to introduce some error in the calculation. This however is superseded in the latter, resulting in the good agreement.

As the bed height increases the flow pattern changes and the transition region is reached. The model generally predicted higher values for the bed heights than the experimental heights for this region. These discrepancies in the results could be attributed to the undefined nature of the flow pattern of the drops. At a further increase in bed height the flow pattern changed to a parabolic profile. At such bed heights the bed approximates to a liquid-liquid foam and good agreement between experimental and predicted values was achieved once more. The error introduced by the average velocity is small since for a liquid-liquid foam the drainage time becomes the dominant factor in equation (4.24). The model was used to explain, in mathematical terms, the discrepancy between the theoretical approach and the experimental observations regarding the effect of drop size on dispersion bands, paragraph (6.0).

8.1) Fractional hold up of the dispersed phase ε_d

The fractional hold up of the dispersed phase is governed by the amount of the continuous phase trapped which is unable to drain. This is due to the loss of the continuous phase via the fragmentation of the continuous film at the coalescing interface, as stated previously, and the amount of the continuous phase in the films and the plateau borders. It is evident from the above definition that when the majority

8.1) contd.

of the trapped continuous phase drains and the losses due to fragmentation are low, the hold up of the continuous phase is low, resulting in a high hold up of the dispersed phase and vice-versa.

The model was used to demonstrate the effect of bed height on the fractional hold up at the coalescing interface. Consider Appendix (13) System I (Amylacetate). It can be seen that for small values of bed height the hold up of the dispersed phase is approximately 99% for the 2 mm. diameter nozzle. It was stated in paragraph 6.6 that for low bed heights the drops are approximately spherical, the rate of drainage is relatively easy and the loss of the continuous phase due to fragmentation is low, which accounts for the high hold up of the dispersed phase. As the bed thickens, drainage of the continuous phase becomes more restricted. Moreover the loss of the continuous phase due to fragmentation and the formation of the satellite drops increases. Consequently the amount of the trapped continuous phase draining decreases resulting in a higher hold up of the continuous phase, and therefore a lower hold up value for the dispersed phase. This is shown in Appendix (13) where the hold up of the dispersed phase for a bed of 28 cm. thick is 93%.

8.2) Critical film thickness.

As stated in paragraph 8 the critical film thickness varies with drop diameter. The variations predicted by the model are listed in Appendix (6). It shows that for systems I to IV the critical film thickness varied from 1.5 to 2.0 microns for a variation in drop size 0.4 to 0.45 cm. 2.5 to 3.5 microns for a variation in drop size from 0.6 to

8.2) contd.

0.73 cm. and 3.0 to 4.0 microns for a variation in drop size from 0.8 to 0.98 cm. System V (Diethylether) was used as a further test of the model by inverting the phases. It showed smaller values for the critical film thickness. This could be attributed to the fact that in System V the water/glycerine mixture is the dispersed phase. This causes the faces of the drops to approximate more closely in the behaviour to rigid plates enabling the continuous phase film to drain to its smaller values before rupture.

Consequently any losses of the continuous phase due to fragmentation after coalescence will also be small. This was confirmed in the experimental work where very little secondary haze was observed after the coalescing interface. In addition it will be seen that for System V high values of hold up were predicted by the model (Appendix 13).

8.3) Coalescence probability.

Two types of coalescence probability have been incorporated in the model, drop wall (β) and interdrop coalescence (λ). The former affects the bed by removing a certain amount of the dispersed phase with the phase boundary residing at the column wall. This causes the incremental superficial velocity to change in equation (4.18). It also affects the average drop diameter equation (5.19). Drop wall coalescence was found to occur under all the conditions and for all the systems studied. Figures (6.11) to (6.22) show that the value of drop wall coalescence probability generally rises slowly with bed height and an average value of 10% was employed in the model.

Interdrop coalescence however is more sensitive

8.3) contd.

to bed height. Paragraph (6.5) shows the correlation developed to predict such variations. The interdrop coalescence probability predicted by the model for low values of bed height was found to be very low. This was based on the experimental observations. Figures (6.23) to (6.41) illustrate that little or no interdrop coalescence takes place for bed height below 4 cm.

8.4) Drainage times.

Equation (4.15) can be rewritten as follows:-

$$t = \phi\left(\frac{1}{h_k^{7/4}} - \frac{1}{h^{7/4}}\right) \qquad (8.1)$$

where ϕ is a constant for any particular system with a specific flowrate and hold up. Figure (8.6) illustrates the effect of the critical film thickness in the drainage time. It is evident that the time taken for the film to drain from an initial value of 1 mm. to 0.1 mm. is negligible compared with the time taken for the film to drain to its critical thickness. This indicates that after interdrop coalescence and regrouping of the drops has taken place the initial value of the film has little effect on the drainage time so that an error introduced in the selection of the initial film thickness at each increment has little or no effect on the predicted bed height.

FIG 8.6

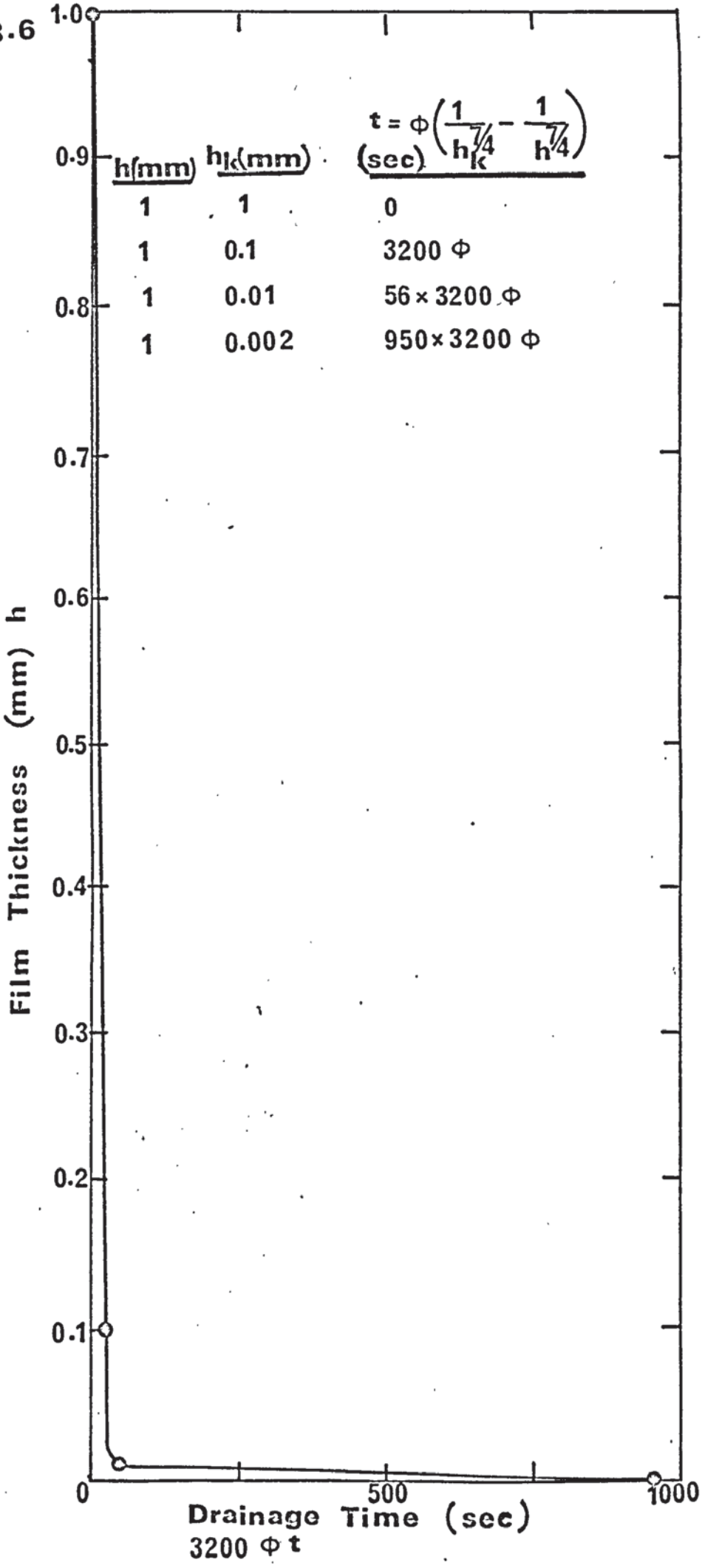

h(mm)	h_k(mm)	$t = \Phi\left(\frac{1}{h_k^{7/4}} - \frac{1}{h^{7/4}}\right)$ (sec)
1	1	0
1	0.1	3200 Φ
1	0.01	56 × 3200 Φ
1	0.002	950 × 3200 Φ

CONCLUSIONS.

Several conclusions are presented from this investigation.

1) The use of the refractive index matching and the photctropic dye technique has enabled analysis to be made inside a dispersion band.

2) The flow of drops in dispersion bands changes from plug flow to a velocity gradient after a certain critical flow rate is reached. Further, a transition period exists between the change from plug to profile flow.

3) The types of coalescence phenomena in a dispersion band i.e. Drop interface, Interdrop and drop wall coalescence are inter-related and indeed interdependent.

4) The critical film thickness in dispersion bands was found to be of the order of 2 microns, which is lower than the estimated value for the single drop at a plane inferface; 4 microns.

5) The profile of the plateau border inside the bed was studied and photographed using the Christiansen effect, and the radius of curvature of the wall of the plateau border was measured. This gave very good agreement with the calculated value considering the difficulties in the measurements.

6) The deformation of the drops inside a dispersion band was photographed and the shape of the drops was found to be pentagonal dodecahedra. The resulting packing arrangement approach was that of a "face centred cube" structure; i.e. each drop is surrounded by 12 drops.

7) A mathematical model has been developed to predict bed height in terms of the drainage of the continuous phase. This approach has eliminated the need to use coalescence

7) contd.

times in dispersion bands, a quantity which is difficult to define and impossible to measure realistically.

RECOMMENDATION FOR FURTHER WORK.

The recommendations for further work can be categorised as follows:-

1) To study the effect of different size drops packing together at different points in the bed in order to assess how the packing arrangement and consequently the film thickness affect continuous phase drainage. This will introduce distribution functions in the model presented. There was insufficient time to pursue this approach in this investigation.

2) The model can be further tested using systems having more extreme physical properties. This has been touched upon with the system diethylether/17" glycerine water mixture which indicated the existence of very thin films.

3) The application of the Christiansen effect needs to be exploited further to examine the behaviour of drops inside the bed.

4) To study the mechanism and the reason causing the velocity gradient and the transition period in close packed dispersions.

5) Investigation of the effect of mass transfer on the parameters that determine band thickness would be of interest; even though this is a somewhat artificial problem since most of the mass transfer would have been accomplished before phase separation.

APPENDIX 1.

PROPERTIES OF A REGULAR PENTAGONAL DODECAHEDRON.

Number of faces = 12

Number of edges per face = 5

Total number of edges = 30

In terms of a sphere of diameter d having the same value V:

Volume V $= \pi d^3/6$

Length of edge = 0.41d

Area of face $= 0.29\ d^2$

Diameter of an equivalent circle of one face = 0.61d

Each face is shared by two drops, so that number of faces per dop is 6.

Each edge is shared by three drops, so that the effective number of edges per drop is 10.

Angle between the edges in any one face is 72°

Angle between the faces is 116°32'

A P P E N D I X 2.

REFRACTIVE INDEX OF GLYCERINE/WATER SOLUTION.

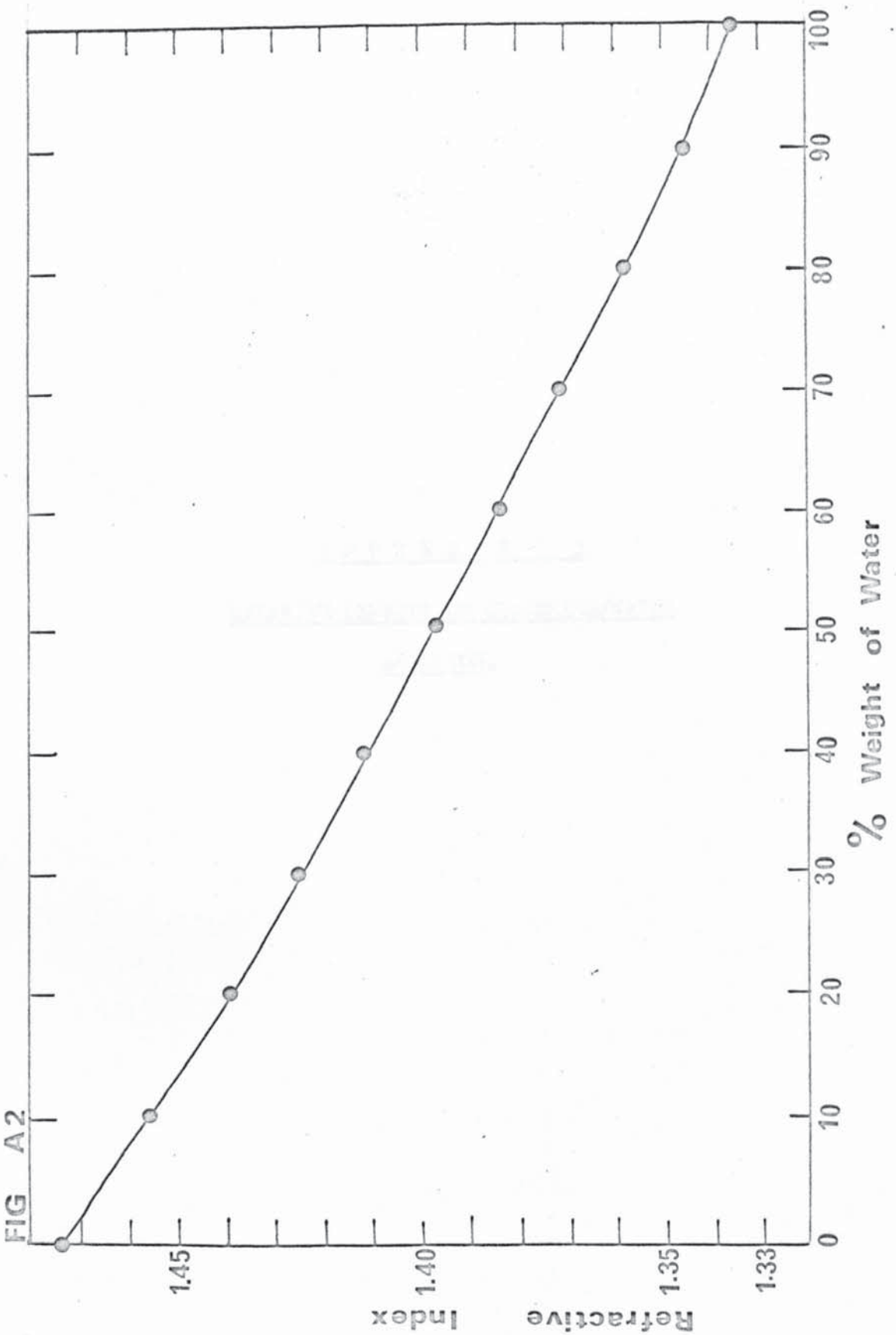
Refractive Index
1.45
1.40
1.35
1.33
0
10
20
30
40
50
60
70
80
90
100
% Weight of Water

FIG A2

APPENDIX 3

RELATIVE DENSITY OF GLYCERINE/WATER SOLUTION.

FIG A 3

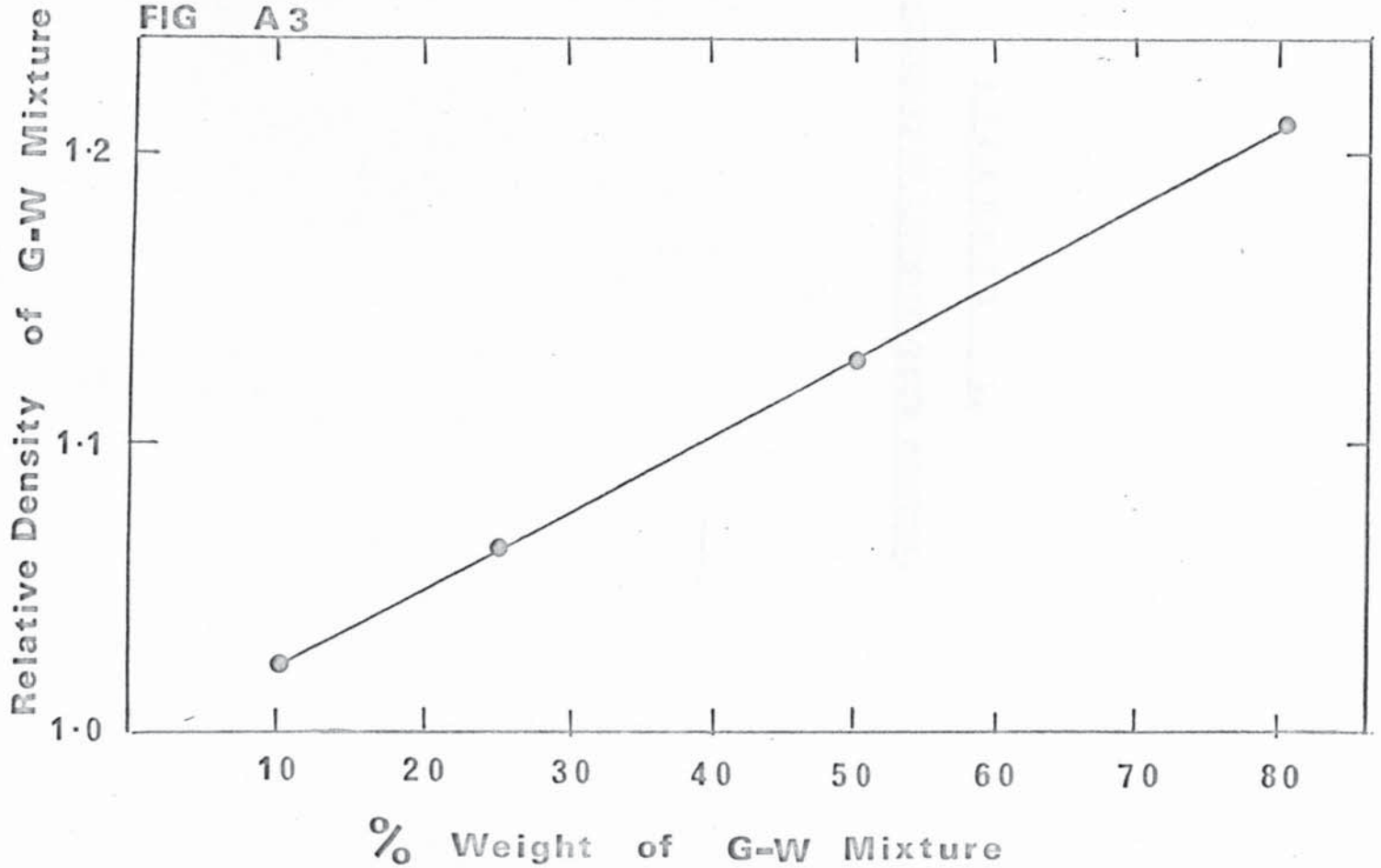
Relative Density of G-W Mixture
1·2
1·1
1·0
10
20
30
40
50
60
70
80
% Weight of G-W Mixture

A P P E N D I X 4.

VISCOSITY OF GLYCERINE/WATER SOLUTION.

FIG A4

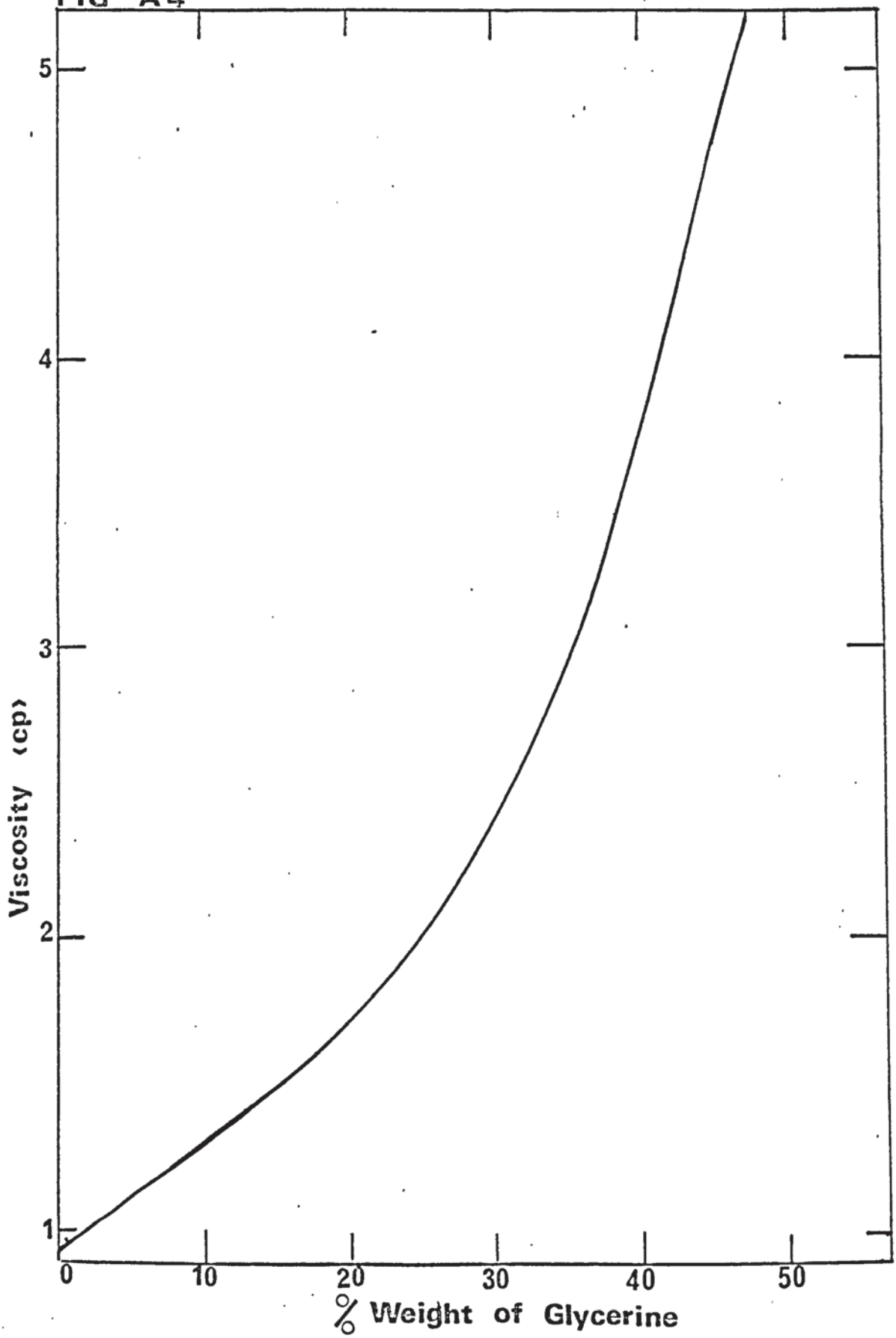

APPENDIX 5.

FLOWRATE CALIBRATION CHART.

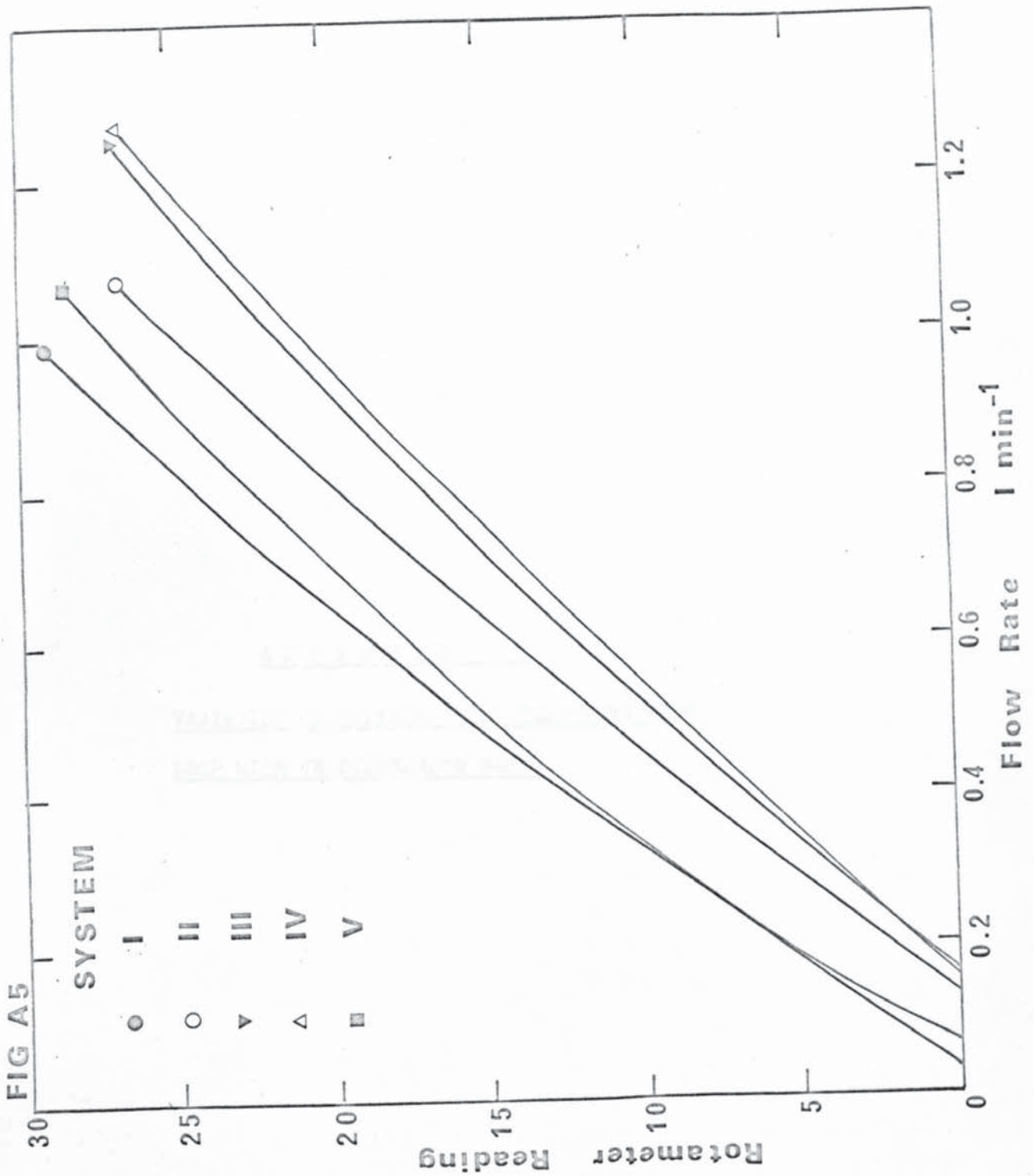
FIG A5
SYSTEM
I
II
III
IV
V
Rotameter Reading
Flow Rate l min⁻¹
0
5
10
15
20
25
30
0.2
0.4
0.6
0.8
1.0
1.2

APPENDIX 6

VARIATION OF CRITICAL FILM THICKNESS WITH DROP SIZE IN DISPERSION BANDS.

SYSTEM	CRITICAL FILM THICKNESS (MICRONS)	DROP SIZE cm.	DISTRIBUTOR'S NOZZLE DIA.cm.
I			
AMYLACETATE	2.0	0.41	0.1
	3.0	0.60	0.2
	4.0	0.77	0.3
	4.0	0.84	0.4
II			
ETHYLACETATE	1.5	0.40	0.1
	2.5	0.62	0.2
	4.0	0.80	0.3
	4.0	0.95	0.4
III			
ISO OCTANE	1.5	0.43	0.1
	3.5	0.73	0.2
	4.0	0.90	0.3
	4.0	0.98	0.4
IV			
HEXANE	1.5	0.45	0.1
	2.5	0.70	0.2
	3.0	0.83	0.3
	3.5	0.95	0.4
V			
DIETHYL ETHER	1.0	0.5	0.1
	1.5	0.7	0.2
	2.0	0.8	0.3
	2.5	0.9	0.4

APPENDIX 7.

SYSTEM I (AMYLACETATE)

1 mm.DISTRIBUTOR ORIFICE DIA.

FLOW RATE		BED HEIGHT	RESIDENCE TIME
ℓ/min.	cc/sec.	cm.	sec.
0.050	0.833	1.5	19.0
0.120	2.000	3.0	30.0
0.175	2.967	5.0	35.0
0.215	3.583	6.0	36.0
0.260	4.333	7.5	38.0
0.275	4.583	8.0	39.0
0.320	5.333	10.0	41.0
0.395	6.583	15.0	46.0
0.425	7.083	20.0	48.0
0.480	8.000	30.0	51.0
		2 mm. DISTRIBUTOR ORIFICE DIA.	
0.050	0.833	0.5	9.7
0.175	2.967	2.0	12.0
0.200	3.333	3.0	14.0
0.250	4.167	5.0	18.5
0.320	5.333	8.0	25.5
0.410	6.833	10.0	27.0
0.480	8.000	13.0	28.5
0.570	9.500	18.0	32.0
0.625	10.417	24.0	34.0
0.650	10.833	28.0	36.0
		3 mm. DISTRIBUTOR ORIFICE DIA.	
0.050	0.833	1.0	7.5
0.175	2.967	1.5	11.0
0.255	4.250	2.5	17.0
0.320	5.333	5.5	20.0
0.480	6.000	7.0	22.0
0.570	9.500	9.0	23.0
0.650	10.833	11.0	24.0
0.720	12.000	15.0	26.0
0.800	13.333	20.0	27.5
0.830	13.833	23.0	28.0

4 mm. DISTRIBUTOR ORIFICE DIA.

0.050	0.833	0.5	5.3
0.175	2.967	1.5	8.0
0.275	4.583	2.5	11.0
0.320	5.333	4.0	15.8
0.425	7.083	8.0	21.0
0.480	6.000	12.0	24.0
0.580	9.667	16.0	28.5
0.570	9.500	19.0	30.0
0.650	10.833	26.0	34.0
0.675	12.500	23.0	33.0

SYSTEM II (ETHYLACETATE)

1 mm. DISTRIBUTOR ORIFICE DIA.

FLOW RATE		BED HEIGHT	RESIDENCE TIME
ℓ/min	cc/sec.	cm.	sec.
0.106	1.77	5.08	34.0
0.160	2.68	6.00	40.0
0.190	3.18	7.62	43.0
0.220	3.68	9.00	48.0
0.225	3.75	11.40	54.0
0.255	4.15	12.40	58.3
0.285	4.79	15.20	61.0
0.280	4.68	16.00	64.0
0.300	5.00	18.00	67.0
0.320	5.35	20.30	70.0

2 mm. DISTRIBUTOR ORIFICE DIA.

0.106	1.77	1.27	14.2
0.225	3.75	2.54	18.0
0.285	4.79	5.08	21.2
0.355	5.94	7.62	27.0
0.400	6.69	9.00	28.0
0.450	7.51	11.42	31.0
0.505	8.44	14.00	34.0
0.537	9.00	16.47	35.4
0.575	9.60	18.00	37.0
0.625	10.05	20.30	38.4

3 mm. DISTRIBUTOR ORIFICE DIA.

0.106	1.77	1.27	12.5
0.250	4.17	3.00	15.0
0.285	4.79	6.35	20.7
0.375	6.25	7.62	24.4
0.450	7.51	8.89	23.5
0.537	9.00	10.16	28.0
0.625	10.05	12.40	26.0
0.710	11.87	16.47	29.0
0.720	12.01	18.00	31.0
0.800	13.39	21.57	33.6

4 mm. DISTRIBUTOR ORIFICE DIA.

0.106	1.77	2.54	15.96
0.285	4.79	3.81	14.40
0.375	6.25	5.08	17.30
0.450	7.51	6.35	20.42
0.537	9.00	7.62	21.60
0.625	10.05	10.16	22.60
0.715	11.93	12.40	24.80
0.800	13.39	17.70	28.70
0.750	12.51	15.20	36.50
0.875	14.60	24.11	32.20

SYSTEM III (ISO-OCTANE)

1 mm. DISTRIBUTOR ORIFICE DIA.

FLOW RATE		BED HEIGHT	RESIDENCE TIME
ℓ/min	cc/sec.	cm.	sec.
0.180	3.00	2.0	14.45
0.240	4.00	5.0	23.80
0.300	5.00	7.0	26.00
0.330	5.50	9.0	28.00
0.360	6.00	12.0	31.10
0.400	6.67	15.0	33.50
0.425	7.08	17.0	35.00
0.460	7.67	20.0	36.50
0.500	8.33	25.0	39.00
0.520	9.17	28.0	40.00
	2 mm. DISTRIBUTOR ORIFICE DIA.		
0.180	3.00	2.0	13.60
0.330	5.50	5.0	17.40
0.430	7.17	7.0	20.40
0.520	9.17	9.0	22.20
0.600	10.00	11.5	24.00
0.660	11.00	14.0	25.00
0.720	12.00	16.0	26.00
0.750	12.50	19.0	27.00
0.780	13.00	22.0	28.00
0.820	13.67	26.0	28.90
	3 mm. DISTRIBUTOR ORIFICE DIA.		
0.180	3.00	1.0	8.30
0.330	5.50	3.0	11.60
0.526	9.17	7.0	16.10
0.620	10.33	10.0	18.60
0.720	12.00	12.5	20.50
0.780	13.00	15.0	21.80
0.820	13.67	18.0	23.00
0.840	14.00	20.0	23.80
0.900	15.00	25.0	25.20
0.930	15.50	28.0	26.10

4 mm. DISTRIBUTOR ORIFICE DIA.

0.180	3.00	1.0	6.00
0.330	5.00	2.0	9.00
0.520	9.17	5.0	12.50
0.600	10.00	7.0	14.30
0.720	12.00	10.0	16.10
0.880	14.67	15.0	19.20
0.930	15.50	18.5	21.10
1.040	17.33	22.0	21.90
1.100	18.33	25.0	22.50
1.160	19.33	28.0	23.00

SYSTEM IV. (HEXANE)

1 mm. DISTRIBUTOR ORIFICE DIA

FLOW RATE		BED	RESIDENCE TIME
ℓ/min.	cc/sec.	cm.	sec.
0.180	3.00	1.0	8.84
0.240	4.00	2.0	11.00
0.340	5.70	3.0	13.10
0.420	7.00	5.0	16.00
0.440	7.30	6.0	17.10
0.480	8.00	8.0	18.60
0.500	8.30	10.0	20.00
0.54	9.00	13.0	23.10
0.600	10.00	20.0	23.80
0.650	10.80	30.0	30.00
	2 mm. DISTRIBUTOR ORIFICE DIA.		
0.180	3.0	1	8.00
0.340	5.7	2	10.00
0.440	7.3	3	11.00
0.540	9.0	5	13.02
0.655	10.9	8	15.20
0.705	11.8	10	16.10
0.750	12.5	12	17.02
0.850	14.2	17	18.80
0.910	15.2	24	21.40
0.960	16.0	29	23.10
	3 mm. DISTRIBUTOR ORIFICE DIA.		
0.180	3.0	0.5	5.0
0.340	5.70	2.0	8.9
0.540	9.0	4.0	11.2
0.650	10.8	6.0	12.6
0.750	12.5	9.0	14.1
0.850	14.2	12.0	15.13
0.890	14.9	15.4	16.6
0.960	16.0	21.0	18.10
1.060	17.7	25.0	19.0
1.090	18.2	30.0	20.0

4 mm. DISTRIBUTOR ORIFICE DIA.

0.340	5.7	1.0	6.00
0.540	9.0	3.0	9.10
0.645	10.8	4.0	9.80
0.750	12.5	6.0	12.22
0.900	15.0	10.0	13.00
0.960	16.0	12.0	13.90
0.102	17.0	16.0	15.00
0.108	18.0	20.0	16.00
1.120	18.7	24.0	16.90
1.190	19.9	30.0	18.01

SYSTEM V (DIETHYLETHER)

1 mm. DISTRIBUTOR ORIFICE DIA.

FLOW RATE		BED HEIGHT	RESIDENCE TIME
ℓ/min.	cc/sec.	cm.	sec.
0.330	5.50	2.50	5.00
0.505	8.40	5.50	6.40
0.700	11.67	12.00	14.70
0.830	13.83	18,00	26.00
0.905	15.08	24.20	30.50
0.870	14.50	20.75	27.70
0.810	13.50	16.50	21.50
0.760	12.67	14.50	18.00
0.600	10.00	8.00	10.50
0.380	6.33	3.00	5.00
	2 mm. DISTRIBUTOR ORIFICE DIA.		
0.180	3.00	1.00	5.0
0.330	5.50	2.00	4.1
0.505	8.42	4.30	4.1
0.700	11.67	8.00	5,0
0.905	15.08	15.00	17.0
0.830	13.83	11.75	12.0
1.030	17.17	21.50	25.0
1.000	16.67	18.50	22.7
0.960	16.00	16.00	19.6
0.870	14.50	13.50	15.5
	3 mm. DISTRIBUTOR ORIFICE DIA.		
0.330	5.50	1.00	4.0
0.505	8.42	3.00	4.5
0.700	11.67	5.50	5.0
0.905	15.08	10.00	10.3
1.030	17.17	14.25	15.5
1.140	19.00	18.50	20.5
1.100	18.33	15.75	19.5
1.050	17.50	13.20	17.0
0.960	16.00	11.50	12.0
0.760	12.67	6.50	6.0

4 mm. DISTRIBUTOR ORIFICE DIA.

0.330	5.50	1.00	3,6
0.505	8.42	2.50	5.0
0.700	11.67	4.50	5.0
0.905	15.08	8.00	7.5
1.140	19.00	14.00	12.8
1.030	17.17	11.50	10.0
1.050	17.50	12.00	11.0
0.830	13.83	7.00	7.0
0.600	10.00	3.50	4.5
0.960	16.00	9.00	9.0

APPENDIX 8.

COALESCENCE PROBABILITY OF COMPLETE BEDS.

In this appendix

I.D.C. refers to interdrop coalescence

D.I.C. refers to drop interface coalesence

D.W.C. refers to drop wall coalesence

The percentage is based on the total number of drops observed.

SYSTEM I (AMYLACETATE)

1mm. DISTRIBUTOR ORIFICE DIA.

BED HEIGHT cm.	I.D.C. No.	%	D.I.C. No.	%	D.W.C. No.	%	TOTAL NUMBER OF DROPS.
1	39	58	20	30	7	12	66
5	39	44	21	30	16	25	66
10	34	47	22	31	14	22	70
2 mm. DISTRIBUTOR ORIFICE DIA.							
1	51	85	5	8	4	7	60
2	35	58	14	22	11	20	60
5	30	47	16	25	18	28	64
8	38	57	14	22	14	21	66
18	49	78	9	14	5	8	63
28	35	57	9	15	17	28	61
3 mm. DISTRIBUTOR ORIFICE DIA.							
2	42	78	11	20	1	2	54
5	25	34	34	46	15	20	74
7	28	37	37	49	10	14	75
11	37	53	21	30	12	17	70
22	38	54	19	27	16	19	71
4 mm. DISTRIBUTOR ORIFICE DIA.							
1	38	50	34	47	2	3	72
4	5	10	31	60	15	30	51
12	16	30	24	44	14	26	54
23	18	36	4	8	28	56	50

SYSTEM III (ISO-OCTANE)

1 mm. DISTRIBUTOR ORIFICE DIA.

BED HEIGHT cm	I.D.C. No.	%	D.I.C. No.	%	D.W.C. No.	%	TOTAL NUMBER OF DROPS.
2	48	64.0	25	33.3	2	2.7	75
5	28	37.3	40	53.3	7	9.3	75
9	36	48.0	34	45.3	5	6.7	75
17	40	53.3	24	32.0	11	14.7	75
28	45	60.0	15	20.0	15	20.0	75
2 mm. DISTRIBUTOR ORIFICE DIA.							
1	40	57.1	28	40.0	2	2.9	70
2	30	42.9	35	50.0	5	7.1	70
9	41	58.6	27	38.6	2	2.9	70
19	30	71.4	16	22.9	4	5.7	70
26	51	72.9	9	12.9	10	14.3	70
3 mm. DISTRIBUTOR ORIFICE DIA.							
1	37	51.4	34	47.2	1	1.4	72
3	28	38.9	39	34.1	5	6.9	72
7	49	68.1	18	25.0	5	6.9	72
18	49	65.3	18	24.0	8	10.7	75
25	50	66.7	13	17.3	12	16.0	75
4 mm. DISTRIBUTOR ORIFICE DIA.							
1	50	66.7	24	32.0	1	1.3	75
5	30	40.0	38	42.7	7	9.3	75
10	40	53.3	31	41.3	4	5.4	75
18	42	56.0	23	30.7	10	13.3	75
25	49	65.3	15	20.0	11	14.7	75

SYSTEM IV (HEXANE)

1 mm. DISTRIBUTOR ORIFICE DIA.

BED HEIGHT cm.	I.D.C. No.	%	D.I.C. No.	%	D.W.C. No.	%	TOTAL NUMBER OF DROPS
1	45	61.6	25	34.2	3	4.2	73
3	26	35.6	41	56.2	6	8.2	73
6	32	42.1	34	44.7	10	13.2	76
13	42	52.5	26	32.5	12	15.0	80
30	36	47.4	27	35.5	13	17.1	76
2 mm. DISTRIBUTOR ORIFICE DIA.							
1	37	52.9	29	41.4	4	5.7	70
2	19	27.1	45	62.3	6	8.6	70
5	22	31.4	37	52.9	9	12.9	70
8	29	41.4	30	42.9	11	15.7	70
17	35	50.0	22	31.8	13	18.6	70
29	40	57.14	16	22.86	14	20.0	70
3 mm. DISTRIBUTOR ORIFICE DIA.							
2	45	60.0	27	36.0	3	4.0	75
4	21	28.0	48	64.0	6	8.0	75
9	26	34.7	40	53.3	9	12.0	75
20	46	61.3	17	22.7	12	16.0	75
30	48	64.0	13	17.3	14	18.7	75
4 mm. DISTRIBUTOR ORIFICE DIA.							
1	46	61.3	26	34.7	3	4.0	75
3	19	25.3	50	66.7	5	6.7	75
6	25	33.3	42	56.0	8	10.7	75
12	46	61.3	18	24.0	11	14.7	75
24	43	60.0	15	20.0	15	20.0	75

APPENDIX 9

COALESCENCE PROBABILITY AT DIFFERENT PLANES IN THE BED. (Instantaneous coalesence probability).

I.D.C. and D.W.C. have a similar meaning as in Appendix 9.

The percentage in this Appendix is based on the number of I.D.C. and D.W.C. observed e.g. in a bed height of 5 cm. the figure of 24% for I.D.C. refers to the percentage of I.D.C. that has occurred in a plane 3 cm. from the entrance of the bed.

SYSTEM I (AMYLACETATE)

1 mm. DISTRIBUTOR ORIFICE DIA.

BED HEIGHT cm.	PLANES IN THE BED. cm	I.D.C. No.	I.D.C. %	D.W.C. No.	D.W.C. %
5	1	5	7	6	35
	2	19	28	4	23
	3	16	24	2	12
	4	20	30	3	18
	5	8	11	2	12
	TOTAL	68		17	
10	1	0	0	0	0
	2	3	3	0	0
	3	9	9	1	7
	4	5	5	2	14
	5	13	13	2	14
	6	12	12	1	7
	7	16	16	3	22
	8	16	16	3	22
	9	16	16	3	14
	10	10	10	0	0
	TOTAL	100		14	
2 mm. DISTRIBUTOR ORIFICE DIA.					
5	1	3	4.5	1	5
	2	5	7.5	0	0
	3	13	20.0	5	25
	4	26	40.0	7	35
	TOTAL	66		20	

		No.	%	No.	%
8	1	2	2.5	0	0
	2	4	5.5	3	21
	3	8	11.5	0	0
	4	11	15.5	0	0
	5	12	16.5	3	21
	6	22	30.5	3	21
	7	12	16.5	5	37
	8	1	1.5	0	0
	TOTAL	72		14	
18	1	2	1.3	0	0
	2	5	3.4	0	0
	3	6	4.0	0	0
	4	4	2.7	0	0
	5	4	2.7	0	0
	6	10	6.8	0	0
	7	17	11.5	0	0
	8	4	2.7	0	0
	9	3	2.0	1	20
	10	6	4.0	0	0
	11	18	12.0	0	0
	12	9	6.1	0	0
	13	10	6.8	3	60
	14	10	6.8	0	0
	15	8	5.5	1	20
	16	6	4.0	0	0
	17	17	11.5	0	0
	18	8	5.5	0	0
	TOTAL	147		5	
28	1	2	1.7	1	6
	2	1	0.9	0	0
	3	5	4.4	0	0
	4	1	0.9	1	6
	5	4	3.5	0	0
	6	3	2.6	0	0
	7	7	6.1	1	6
	8	9	7.9	1	6
	9	2	1.7	1	6
	10	3	2.6	1	6
	11	1	0.9	0	0

	12	4	3.5	1	6
	13	6	5.2	0	0
	14	4	3.5	0	0
	15	4	3.5	0	0
	16	2	1.7	0	0
	17	10	9.0	2	12
	18	8	7.0	1	6
	19	3	2.6	0	0
	20	5	4.4	1	6
	21	2	1.7	0	0
	22	6	5.2	1	6
	23	8	7.0	2	12
	24	2	1.7	1	6
	25	4	3.5	1	6
	26	5	4.4	0	0
	27	3	2.6	1	6
	28	0	0	0	0
	TOTAL	114		17	

3 mm. DISTRIBUTOR ORIFICE DIA.

5	1	0	0	0	0
	2	0	0	0	0
	3	1	8	6	40
	4	2	16	8	53
	5	10	76	1	7
	TOTAL	13		15	
7	1	0	0	1	10
	2	0	0	0	0
	3	2	6	1	10
	4	4	12	1	10
	5	4	12	1	10
	6	12	40	5	50
	7	10	30	1	10
	TOTAL	32		10	

4 mm. DISTRIBUTOR ORIFICE DIA.

			No.	%	No.	%
4	1		0	0	1	6.5
	2		1	20	3	20.0
	3		2	40	6	38.5
	4		2	40	5	35.0
		TOTAL	5		15	
10	1		0	0	1	7.1
	2		0	0	0	0
	3		0	0	0	0
	4		1	5	0	0
	5		1	5	0	0
	6		3	15	1	7.1
	7		5	25	1	7.1
	8		2	10	5	35.7
	9		3	15	6	42.8
	10		5	25	0	0
		TOTAL	20		14	
20	1		0	0	0	0
	2		0	0	0	0
	3		1	2.0	0	0
	4		0	0	0	0
	5		0	0	0	0
	6		3	5.5	1	4
	7		0	0	0	0
	8		2	3.7	1	4
	9		1	2.0	1	4
	10		3	5.5	2	8
	11		7	13.0	0	0
	12		8	15.0	2	8
	13		3	5.5	2	8
	14		2	3.7	3	11.5
	15		7	13.0	4	15.0
	16		6	11.0	5	19.0
	17		5	9.3	3	11.5
	18		3	5.5	0	0
	19		1	2.0	1	4
	20		2	3.7	1	4
		TOTAL	54		26	

			No.	%	No.	%
11	1		0	0	0	0
	2		2	4	2	16
	3		0	0	0	0
	4		1	2	0	0
	5		1	2	0	0
	6		2	4	0	0
	7		1	2	0	0
	8		10	20	2	16
	9		14	25	1	8
	10		11	21	5	44
	11		13	24	2	16
		TOTAL	55		12	
22	1		0	0	0	0
	2		1	1.3	0	0
	3		1	1.3	0	0
	4		0	0	0	0
	5		0	0	0	0
	6		0	0	1	6
	7		1	1.3	1	6
	8		2	2.6	0	0
	9		1	1.3	0	0
	10		0	0	0	0
	11		3	4.0	0	0
	12		3	4.0	0	0
	13		6	7.9	0	0
	14		12	16.0	1	6
	15		9	12.0	0	0
	16		7	7.9	0	0
	17		4	5.3	1	6
	18		2	2.6	2	12
	19		1	1.3	1	6
	20		5	6.7	7	46
	21		12	16.0	1	6
	22		6	7.9	1	6
		TOTAL	76		16	

SYSTEM III (ISO-OCTANE)

1 mm. DISTRIBUTOR ORIFICE DIA.

BED HEIGHT	PLANES IN THE BED	I.D.C.		D.W.C.	
cm.	cm.	No.	%	No.	%
5	1	0	0	0	0
	2	3	6.5	0	0
	3	12	26.1	2	286
	4	13	28.2	3	42.8
	5	18	39.2	2	28.6
	TOTAL	46		7	
9	1	0	0	0	0
	2	2	3.1	0	0
	3	3	4.6	0	0
	4	6	9.2	1	20
	5	8	12.3	1	20
	6	6	9.2	0	0
	7	15	23.1	1	20
	8	8	12.3	2	40
	9	17	26.1	0	0
	TOTAL	65		5	
17	1-3	0	3.3	0	0
	4	4	3.3	0	0
	5	6	4.9	0	0
	6	11	9.1	1	9.1
	7	5	4.1	2	18.2
	8	5	4.1	0	0
	9	9	7.4	0	0
	10	9	7.4	2	18.2
	11	5	4.1	0	0
	12	7	5.8	1	9.1
	13	7	5.8	2	18.2
	14	8	6.6	0	0
	15	14	15.7	3	27.3
	16	11	9.1	0	0
	17	11	9.1	0	0
	TOTAL	121		11	

		No.	%	No.	%
28	1-4	0	0	0	0
	5	5	3.2	0	0
	6	4	2.6	0	0
	7	7	4.5	0	0
	8	5	3.2	0	0
	9	8	5.2	2	13.3
	10	5	3.2	1	6.7
	11	4	2.6	0	0
	12	5	3.2	0	0
	13	5	3.2	1	6.7
	14	3	1.9	2	13.3
	15	7	4.5	1	6.7
	16	4	2.6	2	13.3
	17	8	5.1	1	6.7
	18	5	3.2	0	0
	19	8	5.1	0	0
	20	5	3.2	2	13.3
	21	2	1.3	0	0
	22	9	5.8	2	13.3
	23	5	3.2	0	0
	24	7	4.5	0	0
	25	8	5.1	0	0
	26	15	9.7	0	0
	27	11	7.1	0	0
	28	10	6.5	0	0
	TOTAL	155		15	
2 mm. DISTRIBUTOR ORIFICE DIA.					
9	1-3	0	0	0	0
	4	11	14.9	0	0
	5	9	12.1	0	0
	6	12	16.2	0	0
	7	5	6.7	1	50
	8	16	21.6	1	50
	9	21	28.4	0	0
	TOTAL	74		2	

		No.	%	No.	%
19	1.3	0	0	0	0
	4	6	4.4	0	0
	5	5	3.6	0	0
	6	3	2.2	0	0
	7	7	5.1	0	0
	8	9	6.6	0	0
	9	7	5.1	0	0
	10	2	1.4	0	0
	11	5	3.7	0	0
	12	12	8.7	0	0
	13	12	8.7	0	0
	14	6	4.4	1	25
	15	4	2.9	1	25
	16	2	1.4	2	50
	17	16	11.7	0	0
	18	17	12.4	0	0
	19	15	10.9	0	0
	TOTAL	137		4	
26	1.3	0	0	0	0
	4	3	2.0	0	0
	5	4	2.7	0	0
	6	7	4.7	0	0
	7	2	1.4	1	10
	8	5	3.4	1	10
	9	1	0.6	0	0
	10	4	2.7	0	0
	11	6	4.0	0	0
	12	8	5.4	0	0
	13	6	4.0	0	0
	14	4	2.7	0	0
	15	12	8.1	1	10
	16	9	6.1	1	10
	17	5	3.4	0	0
	18	4	2.7	0	0
	19	4	2.7	0	0
	20	2	1.3	1	10
	21	7	4.7	4	40

	22	4	2.7	0	0
	23	5	3.38	1	10
	24	8	5.4	0	0
	25	16	10.8	0	0
	26	12	8.1	0	0
	TOTAL	148		10	

3 mm. DISTRIBUTOR ORIFICE DIA.

		No.	%	No.	%
3	1	4	10	0	0
	2	8	20	0	0
	3	28	70	5	100
	TOTAL	40		5	
7	1.2	0	0	0	0
	3	1	1.3	0	0
	4	8	10.8	0	0
	5	10	13.5	1	20
	6	19	25.7	1	20
	7	36	47.3	3	60
	TOTAL	74		5	
18	1.4	0	0	0	0
	5	1	0.9	0	0
	6	0	0	0	0
	7	1	0.9	0	0
	8	5	4.3	0	0
	9	1	0.9	0	0
	10	7	6.1	0	0
	11	2	1.7	0	0
	12	9	7.8	0	0
	13	12	10.4	0	0
	14	18	15.6	0	0
	15	8	7.0	1	12.5
	16	9	7.8	5	62.5
	17	21	18.3	2	25.0
	18	21	18.3	0	0
	TOTAL	115		8	

			No.	%	No.	%
25	1.4		0	0	0	0
	5		1	0.6	0	0
	6		1	0.6	0	0
	7		2	1.3	0	0
	8		3	1.9	0	0
	9		12	7.7	0	0
	10		5	3.2	0	0
	11		4	2.6	0	0
	12		3	1.9	1	8.3
	13		12	7.7	2	16.7
	14		3	1.93	1	8.3
	15		7	4.5	2	16.7
	16		9	5.8	0	0
	17		7	4.5	1	8.3
	18		10	6.5	0	0
	19		7	4.5	3	25.0
	20		10	6.5	0	0
	21		7	4.5	0	0
	22		6	3.9	1	8.3
	23		18	11.6	0	0
	24		17	11.0	1	8.3
	25		11	7.1	0	0
		TOTAL	155		12	
4 mm. DISTRIBUTOR ORIFICE DIA.						
5	1		0	0	0	0
	2		14	28.6	0	0
	3		11	22.4	3	43
	4		15	30.6	2	28.8
	5		19	18.4	2	28.8
		TOTAL	49		7	
10	1.2		0	0	0	0
	3		9	9.5	0	0
	4		10	10.5	0	0
	5		14	14.7	0	0
	6		10	10.5	1	25
	7		11	11.6	0	0

		No.	%	No.	%
	8	6	6.3	1	25
	9	20	21.1	1	25
	10	15	15.8	1	25
	TOTAL	95		4	
18	1-2	0	0	0	0
	3	3	2.3	0	0
	4	4	3.0	0	0
	5	9	6.8	0	0
	6	8	6.1	1	10
	7	5	3.8	0	0
	8	6	4.6	1	10
	9	3	2.3	0	0
	10	11	8.4	1	10
	11	6	4.6	0	0
	12	4	3.0	3	30
	13	9	6.8	1	10
	14	9	6.8	2	20
	15	10	7.6	0	0
	16	7	5.3	1	10
	17	20	15.2	0	0
	18	17	13.0	0	0
	TOTAL	131		10	
25	1-4	0	0	0	0
	5	4	2.3	0	0
	6	8	4.7	0	0
	7	12	7.1	0	0
	8	7	4.1	0	0
	9	6	3.5	0	0
	10	4	2.3	0	0
	11	6	3.5	0	0
	12	6	3.5	0	0
	13	7	4.1	2	18.2
	14	5	3.0	3	22.7
	15	8	4.7	0	0
	16	12	7.1	1	9.1
	17	4	2.3	1	9.1
	18	6	3.5	1	9.1
	19	9	5.3	0	0
	20	12	7.1	0	0

	No.	%	No.	%
21	7	4.1	1	9.1
22	8	4.7	2	18.2
23	5	3.0	0	0
24	23	13.5	0	0
25	11	6.5	0	0
TOTAL	170		11	

SYSTEM IV (HEXANE)

1 mm. DISTRIBUTOR ORIFICE DIA.

BED HEIGHT cm.	PLANES IN THE BED cm.	I.D.C. No.	I.D.C. %	D.W.C. No.	D.W.C. %
3	1	0	0	0	0
	2	24	92.3	0	0
	3	2	7.7	6	100
	TOTAL	26		6	
6	1	0	0	0	0
	2	1	2.6	0	0
	3	6	15.8	1	10
	4	11	28.9	3	30
	5	15	39.5	6	60
	6	5	13.2	0	0
	TOTAL	38		10	
13	1-5	0	0	0	0
	6	2	1.8	0	0
	7	4	5.9	0	0
	8	2	1.8	0	0
	9	10	14.9	1	8.3
	10	11	16.5	2	16.7
	11	10	14.9	8	66.7
	12	22	32.9	1	8.3
	13	6	8.9	0	0
	TOTAL	67		12	
30	1-10	0	0	0	0
	11	0	0	0	0
	12	1	1.0	0	0
	13	1	1.0	0	0
	14	0	0	0	0
	15	2	2.1	0	0
	16	5	5.1	0	0
	17	3	3.0	0	0
	18	5	5.1	1	7.8
	19	4	4.1	0	0
	20	6	6.1	0	0
	21	6	6.1	3	25

			No.	%	No.	%
	22		5	5.1	0	0
	23		5	5.1	0	0
	24		6	6.1	2	15
	25		6	6.1	1	7.8
	26		5	5.1	2	15
	27		11	11.3	1	7.8
	28		7	7.2	1	7.8
	29		14	14.3	2	15.0
	30		6	6.1	0	0
		TOTAL	98		13	
2 mm. DISTRIBUTOR ORIFICE DIA.						
2	1		0	0	0	0
	2		19	100	6	100
		TOTAL	19		6	
5	1		0	0	0	0
	2		3	12.5	0	0
	3		7	29.2	0	0
	4		10	41.7	8	89
	5		4	16.6	1	11
		TOTAL	24		9	
8	1-3		0	0	0	0
	4		1	2.3	0	0
	5		13	25.7	1	10
	6		13	25.7	5	45
	7		7	15.9	5	45
	8		10	22.5	0	0
		TOTAL	44		11	
17	1		3	2.7	0	0
	2		2	1.9	0	0
	3-7		0	0	0	0
	8		3	2.7	0	0
	9		5	4.6	0	0
	10		9	8.2	0	0
	11		14	12.9	0	0
	12		120	18.3	1	8.5
	13		25	22.9	2	17.0
	14		19	17.4	4	34.0
	15		6	5.5	3	25.0

			No.	%	No.	%
	16		3	2.8	2	17.0
	17		0	0	1	8.5
		TOTAL	109		13	
29	1-7		0	0	0	0
	8		2	1.6	0	0
	9		0	0	0	0
	10		1	0.8	0	0
	11		5	4.0	0	0
	12		5	4.0	0	0
	13		1	0.8	0	0
	14		3	2.5	0	0
	15		3	2.5	0	0
	16		2	1.6	0	0
	17		5	4.0	0	0
	18		7	5.7	1	7.1
	19		3	2.5	0	0
	20		11	8.9	3	21.3
	21		5	4.0	0	0
	22		11	8.9	1	7.1
	23		7	5.7	2	14.2
	24		6	4.9	1	7.1
	25		7	5.7	2	14.2
	26		9	7.3	2	14.2
	27		10	8.1	1	7.1
	28		12	9.5	1	7.1
	29		8	6.5	0	0
		TOTAL	123		14	
3 mm. DISTRIBUTOR ORIFICE DIA.						
2	1		0	0	0	0
	2		45	100	3	100
		TOTAL	45		3	

		No.	%	No.	%
4	1	0	0	0	0
	2	0	0	0	0
	3	8	36.2	3	50
	4	14	63.8	3	50
	TOTAL	22		6	
9	1-3	0	0	0	0
	4	2	3.5	0	0
	5	4	3.4	0	0
	6	9	16.7	1	11.5
	7	9	16.7	3	33.0
	8	9	16.7	4	44.0
	9	21	38.9	1	11.5
	TOTAL	54		9	
20	1-5	0	0	0	0
	6	2	1.3	0	0
	7	4	2.6	0	0
	8	4	2.6	0	0
	9	5	3.3	0	0
	10	5	3.3	0	0
	11	6	6.0	0	0
	12	4	2.6	1	6.6
	13	12	8.0	2	13.2
	14	14	9.2	1	6.6
	15	15	9.9	3	19.8
	16	12	7.9	1	6.6
	17	8	5.3	1	6.6
	18	11	7.26	2	13.2
	19	12	7.92	1	6.6
	20	34	22.5	0	0
	TOTAL	147		12	
30	1-6	0	0	0	0
	7	1	0.5	0	0
	8	3	1.4	0	0
	9	4	1.9	0	0
	10	5	2.4	0	0
	11	4	1.9	1	9
	12	4	1.9	1	9

			No.	%	No.	%
	13		5	2.4	0	0
	14		5	2.4	0	0
	15		7	3.3	0	0
	16		8	3.8	0	0
	17		11	5.2	0	0
	18		11	5.2	0	0
	19		5	2.4	1	9
	20		12	5.7	2	18
	21		9	4.3	0	0
	22		8	3.8	2	18
	23		8	3.8	1	9
	24		10	5.2	1	9
	25		17	8.1	2	18
	26		11	5.2	1	9
	27		12	5.7	2	18
	28		20	9.5	0	0
	29		13	6.2	0	0
	30		17	8.1	0	0
		TOTAL	210		14	
4 mm. DISTRIBUTOR ORIFICE DIA.						
3	1		5	19.2	0	0
	2		6	23.0	0	0
	3		15	57.8	5	100
		TOTAL	26		5	
6	1		1	2.4	0	0
	2		2	4.9	0	0
	3		7	17.1	1	12.5
	4		5	12.2	2	25.0
	5		11	26.8	3	37.5
	6		15	36.7	2	25.0
		TOTAL	41		8	
12	1-3		0	0	0	0
	4		5	4.2	0	0
	5		12	10.0	1	9.1
	6		8	6.7	0	0
	7		12	10.0	1	9.1

			No.	%	No.	%
	8		16	13.3	0	0
	9		16	13.3	4	36.4
	10		15	12.5	3	27.3
	11		14	11.7	1	9.1
	12		22	18.3	1	9.1
		TOTAL	120		11	
24	1-5		0	0	0	0
	6		3	2.1	0	0
	7		3	2.1	0	0
	8		6	4.3	0	0
	9		8	5.7	0	0
	10		4	2.9	1	6.7
	11		5	3.6	1	6.7
	12		10	7.1	0	0
	13		8	5.7	1	6.7
	14		8	5.7	1	6.7
	15		11	7.9	0	0
	16		5	3.6	0	0
	17		8	5.7	0	0
	18		9	6.4	3	20.0
	19		8	5.7	1	6.7
	20		9	6.4	3	20.0
	21		5	5.6	2	13.3
	22		8	5.7	1	6.7
	23		8	5.7	1	6.7
	24		14	10.0	0	0
		TOTAL	140		15	

APPENDIX 10.

LEAST SQUARE FIT FOR THE COALESCENCE PROBABILITY λ.

$$\lambda = 1 - a\left(\frac{\gamma}{\mu V}\right)^{b}\left(\frac{d}{H}\right)^{c} \qquad (1)$$

$$\lambda = 1 = a\left(\frac{\gamma}{\mu V}\right)^{b}\left(\frac{d}{H}\right)^{c}$$

Taking $\log_e$

$$\log_e(\lambda-1) = \log_e a + b\log_e\left(\frac{\gamma}{\mu V}\right) + c\log_e\left(\frac{d}{H}\right) \qquad (2)$$

Let $\log_e(\lambda-1) = L$

$$\log_e a = A \quad \text{and} \quad \log_e \frac{d}{H} = K$$

$$\log_e\left(\frac{\gamma}{\mu V}\right) = T$$

$\therefore$ equation (2) becomes

$$L = A + bT + cK \qquad (3)$$

$$(A+bT + cK - L)^2 = R^2 \qquad (4)$$

where R is the residual.

Expanding equation (4) and reducing the residual R to zero gives

$$(A^2+b^2T^2+c^2K^2+L^2 + 2AbT + 2AcK - 2AL + 2bTcK-2bTL-2cKL) = 0$$

$$\therefore \sum_{i=1}^{i=n} (A^2+b^2T^2+c^2K^2+L^2+2AbT+2AcK-2AL+2bTck-2bTL-2cKL) = \phi$$

Differentiating with respect to A,b and c

$$\frac{\partial\phi}{\partial A} = \sum_{i=1}^{i=n} (A + bT + cK - L) \qquad (5)$$

$$\frac{\partial\phi}{\partial b} = \sum_{i=1}^{i=n} (AT + bT^2 + cTK - TL) \qquad (6)$$

$$\frac{\partial \phi}{\partial c} = \sum_{i=1}^{i=n} (AK + bTK + cK^2 - KL) \qquad (7)$$

$$\frac{\partial \phi}{\partial c} = \sum_{i=1}^{i=n} (AK + bTK + cK^2 - KL) \qquad (7)$$

Substituting for the values of L,A,T and K in equations 5, 6 and 7

$$\sum_{i=1}^{i=n} \left[\log_e a + b \log_e\left(\frac{\gamma}{\mu V}\right) + c \log\left(\frac{d}{H}\right) - \log(\lambda-1) \right] = 0 \qquad (8)$$

and $$\sum_{i=1}^{i=n} \left[\log_e a \log_e\left(\frac{\gamma}{\mu V}\right) + b\left(\log_e \frac{\gamma}{\mu V}\right)^2 + c\left(\log \frac{\gamma}{\mu V}\right)\left(\log \frac{d}{H}\right) - \left(\log \frac{\gamma}{\mu V}\right)\left(\log(\lambda-1)\right) \right] = 0 \qquad (9)$$

and $$\sum_{i=1}^{i=n} \left[(\log a)\left(\log \frac{d}{H}\right) + b\left(\log \frac{\gamma}{\mu V}\right)\left(\log \frac{d}{H}\right) + c\left(\log \frac{d}{H}\right)^2 - \left(\log \frac{d}{H}\right)(\log(\lambda-1)) \right] = 0 \qquad (10)$$

Expanding equations 8, 9 and 10

$$n \log a + b \sum_{i=1}^{i=n} \log_e\left(\frac{\gamma}{\mu V_i}\right) + c \sum_{i=1}^{i=n} \log_e\left(\frac{d_i}{H_i}\right) - \sum_{i=1}^{i=n} \log_e(\lambda_i - 1) = 0 \qquad (11)$$

and $$\log_e a \sum_{i=1}^{i=n} \log_e\left(\frac{\gamma}{\mu V_i}\right) + b \sum_{i=1}^{i=n} \left(\log_e \frac{\gamma}{\mu V_i}\right)^2 + c \sum_{i=1}^{i=n} \log_e\left(\frac{\gamma}{\mu V_i}\right) \log_e\left(\frac{d_i}{H_i}\right) - \sum_{i=1}^{i=n} \log_e\left(\frac{\gamma}{\mu V_i}\right) \log_e(\lambda_i - 1) = 0 \qquad (12)$$

$$\text{and } \log a \sum_{i=1}^{i=n} \log\left(\frac{d_i}{H_i}\right) + b \sum_{i=1}^{i=n} \log\left(\frac{\gamma}{\mu V_i}\right) \log_e\left(\frac{d_i}{H_i}\right) + c \sum_{i=1}^{i=a} \left(\log_e\left(\frac{d_i}{H_i}\right)\right)^2$$

$$+ \sum_{i=1}^{i=n} \log_e\left(\frac{d_i}{H_i}\right) \log_e(\lambda_i - 1) = 0 \qquad (13)$$

The matrix below was solved via a matrix inversion for the values of a, b and c

$$\begin{bmatrix} n & \sum_{i=1}^{i=n} \log_e\left(\frac{\gamma}{\mu V_i}\right) & \sum_{i=1}^{i=n} \log_e\left(\frac{d_i}{H_i}\right) \\ \sum_{i=1}^{i=n} \left(\log_e \frac{\gamma}{\mu V_i}\right) & \sum_{i=1}^{i=n} \left(\log_e \frac{\gamma}{\mu V_i}\right)^2 & \sum_{i=1}^{i=n} \log_e\left(\frac{\gamma}{\mu V_i}\right) \log_e\left(\frac{d_i}{H_i}\right) \\ \sum \log_e\left(\frac{d_i}{H_i}\right) & \sum_{i=1}^{i=n} \log_e\left(\frac{\gamma}{\mu V_i}\right) \log_e\left(\frac{d_i}{H_i}\right) & \sum_{i=1}^{i=n} \log_e\left(\frac{d_i}{H_i}\right) \end{bmatrix} \begin{bmatrix} \log_e a \\ b \\ c \end{bmatrix} =$$

$$\begin{bmatrix} \sum_{i=1}^{i=n} \log_r(\lambda_i - 1) \\ \sum_{i=1}^{i=n} \log_e\left(\frac{\gamma}{\mu V_i}\right) \log_e\left(\lambda_i - 1\right) \\ \sum_{i=1}^{i=n} \log_e\left(\frac{d_i}{H_i}\right) \log_e\left(\lambda_i - 1\right) \end{bmatrix}$$

A P P E N D I X 11.

DATA FOR THE COALESCENCE PROBABILITY (λ)

SYSTEM	λ CAL	λ EXP	FLOWRATE $cm^3/sec.$	BED HEIGHT cm.	DROP DIA. cm.
I (AMYL ACETATE)	0.492	0.44	2.967	5.0	0.41
	0.598	0.47	5.330	10.0	0.41
	0.350	0.58	2.970	2.0	0.60
	0.464	0.47	4.170	5.0	0.60
	0.516	0.57	5.330	8.0	0.60
	0.598	0.78	9.500	18.0	0.60
	0.633	0.57	10.833	28.0	0.60
	0.445	0.34	5.330	5.0	0.77
	0.483	0.37	6.000	7.0	0.77
	0.540	0.53	10.833	11.0	0.77
	0.602	0.54	13.830	22.0	0.77
	0.411	0.10	5.33	4.0	0.84
	0.525	0.30	6.00	12.0	0.84
	0.56823	0.36	12.5	23.0	0.84
IV (HEXANE)	0.398	0.36	5.700	3.0	0.45
	0.479	0.42	7.300	6.0	0.45
	0.555	0.53	9.000	13.0	0.45
	0.624	0.47	10.80	30.0	0.45
	0.420	0.32	9.00	5.0	0.70
	0.475	0.42	10.90	8.0	0.70
	0.551	0.50	14.2	17.0	0.70
	0.597	0.571	16.0	29.0	0.70
	0.375	0.28	9.0	4.0	0.83
	0.473	0.34	12.5	9.0	0.83
	0.554	0.61	16.0	20.0	0.83
	0.587	0.57	18.2	29.0	0.83
	0.322	0.25	9.0	3.0	0.95
	0.495	0.61	16.0	12.0	0.95
	0.561	0.60	18.7	24.0	0.95
	0.417	0.33	12.5	6.0	0.95

III	0.459	0.373	4.000	5.0	0.43
(ISO-OCTANE)	0.524	0.480	5.500	9.0	0.43
	0.584	0.533	7.080	17.0	0.43
	0.627	0.600	9.170	28.0	0.43
	0.488	0.586	9.170	9.0	0.73
	0.563	0.714	12.50	19.0	0.73
	0.591	0.730	13.670	26.0	0.73
	0.326	0.389	5.50	3.0	0.90
	0.441	0.680	9.170	7.0	0.90
	0.543	0.653	13.670	18.0	0.90
	0.535	0.667	13.000	16.0	0.90
	0.395	0.400	9.170	5.0	0.98
	0.541	0.560	15.5	18.5	0.98
	0.477	0.533	12.0	10.0	0.98
	0.571	0.650	18.33	25.0	0.98

APPENDIX 12

DATA FOR THE DIMENSIONAL ANALYSIS

Experimental values of $\log\left[\frac{T\,\gamma}{\mu_c H}\right]$ will be referred to as Y(EXP).

Estimated value of $\log\left[\frac{T\,\gamma}{\mu_c H}\right]$ which is $\log\left[11.22\left(\frac{d}{H}\right)^{0.331}\left(\frac{\Delta\rho g\,H^2}{\gamma}\right)^{-0.276}\left(\frac{\mu_c V_d}{\gamma}\right)^{-0.768}\right]$ will be referred to as Y(CAL).

SYSTEM I (AMYLACETATE)

Y(EXP)	Y(CAL)	Y(EXP)	Y(CAL)
3.352	3.737	3.124	3.701
3.249	3.269	3.114	3.184
3.094	3.146	2.809	2.835
2.954	2.950	2.746	2.680
3.027	3.067	2.588	2.535
2.862	2.855	2.335	2.387
2.937	2.904	3.094	2.981
2.735	2.748	2.657	2.586
2.629	2.693	2.488	2.470
2.489	2.616	2.387	2.413
3.537	3.530	2.406	2.459
3.027	3.198	2.500	2.548
2.917	2.976	2.668	2.689
2.749	2.837	2.892	2.959
2.680	2.750	2.365	2.430
2.590	2.664	2.447	2.507
2.499	2.573	2.550	2.607
2.358	2.484	2.845	2.846
2.746	2.873	2.976	3.165
2.918	3.097	3.274	3.476

SYSTEM II (ETHYLACETATE)

Y(EXP)	Y(CAL)	Y(EXP)	Y(CAL)
2.287	2.224	2.431	2.439
2.171	2.154	2.538	2.557
2.255	2.209	2.322	2.332
2.347	2.283	2.377	2.399
2.393	2.343	2.480	2.485
2.496	2.417	2.599	2.599
2.552	2.485	2.664	2.707
2.576	2.568	2.896	2.859

SYSTEM II (contd)

Y(EXP)	Y(CAL)	Y(EXP)	Y(CAL)
2.624	2.679	3.094	3.151
2.845	3.024	2.616	2.613
2.282	2.265	2.648	2.648
2.745	2.912	2.773	2.823
2.238	2.215	2.824	2.885
2.291	2.282	2.583	2.588
2.367	2.349	2.649	2.653
2.486	2.415	2.718	2.706
2.468	2.478	2.721	2.766
2.551	2.554	2.869	3.068
2.559	2.655	2.798	2.875
3.039	3.120		
2.358	2.368		

SYSTEM III (ISO-OCTANE)

Y(EXP)	Y(CAL)	Y(EXP)	Y(CAL)
3.647	3.633	3.468	3.357
3.357	3.313	3.213	3.117
3.207	3.105	3.022	2.941
3.259	2.941	2.858	2.797
2.861	2.858	2.729	2.964
3.279	3.188	3.125	3.029
3.067	2.992	2.922	2.842
2.992	2.919	2.813	2.752
2.919	2.891	2.769	2.722
2.894	2.870	3.674	3.686
3.734	3.675	3.492	3.477
3.402	3.337	3.308	3.308
3.177	3.105	3.128	3.163
3.030	2.940	2.970	3.050
2.921	2.868	3.228	3.218
2.796	2.780	3.164	3.168
3.084	2.999	3.076	3.107
2.890	2.841	3.008	3.063
2.977	2.901	3.385	3.358
2.818	2.797		
3.593	3.656		

SYSTEM IV (HEXANE)

Y(EXP)	Y(CAL)	Y(EXP)	Y(CAL)
3.898	3.844	3.773	3.539
3.694	3.523	3.477	3.300
3.410	3.300	3.304	3.122
3.147	3.105	3.059	2.977
3.039	3.034	2.773	2.822
2.896	2.905	2.843	2.854
2.945	3.100	2.898	2.887
3.165	3.143	3.109	3.012
3.232	3.194	3.384	3.216
3.509	3.410	2.967	2.933
3.941	3.889	3.643	3.491
3.735	3.712	3.442	3.289
3.635	3.529	3.190	3.100
3.450	3.392	3.096	3.036
3.245	3.253	2.930	2.942
3.106	3.176	2.819	2.871
2.995	3.118	2.867	2.896
3.296	3.292	3.028	2.989
3.361	3.335	3.317	3.183
3.500	3.443		

APPENDIX 13

SYSTEM I (AMYLACETATE)

1 mm. DISTRIBUTOR ORIFICE DIA.

BED HEIGHT (cm.) EXP.	CAL.	FRACTIONAL HOLD UP OF DISPERSED PHASE. (ε_d)	COALESENCE PROBABILITY (λ)
1.5	0.51	0.98	0.05
3.0	1.62	0.95	0.27
5.0	2.72	0.93	0.34
6.0	5.50	0.94	0.45
7.5	7.12	0.93	0.48
8.0	7.23	0.93	0.48
10.0	13.69	0.95	0.54
15.0	18.38	0.94	0.57
20.0	20.35	0.93	0.58
30.0	33.78	0.95	0.61
2 mm. DISTRIBUTOR ORIFICE DIA.			
0.5	0.58	0.99	0.001
2.0	1.94	0.98	0.24
3.0	3.63	0.97	0.34
5.0	4.86	0.96	0.38
8.0	6.70	0.95	0.42
10.0	8.38	0.94	0.45
13.0	18.58	0.95	0.54
18.0	23.41	0.94	0.57
24.0	26.48	0.93	0.58
28.0	27.91	0.93	0.58
3 mm. DISTRIBUTOR ORIFICE DIA.			
1.0	0.62	0.99	0.00
1.5	3.28	0.98	0.29
2.5	5.25	0.97	0.36
5.5	7.05	0.96	0.40
7.0	8.22	0.96	0.42
9.0	14.94	0.94	0.49
11.0	17.72	0.94	0.51
15.0	20.23	0.93	0.53
20.0	23.18	0.92	0.54

SYSTEM I (contd)

4 mm. DISTRIBUTOR ORIFICE DIA.

0.5	0.73	0.99	0
1.5	3.89	0.98	0.30
2.5	6.88	0.97	0.38
4.0	8.38	0.97	0.41
8.0	12.12	0.96	0.46
12.0	9.77	0.97	0.43
16.0	18.15	0.95	0.50
19.0	17.75	0.95	0.50
23.0	25.32	0.94	0.54
26.0	21.05	0.95	0.52

SYSTEM II (ETHYLACETATE)

1 mm. DISTRIBUTOR ORIFICE DIA.

BED HEIGHT (cm.) EXP.	BED HEIGHT (cm.) CAL.	FRACTIONAL HOLD UP OF DISPERSED PHASE (ε_d)	COALESENCE PROBABILITY (λ)
5.08	1.64	0.980	0.26
6.00	6.20	0.985	0.45
7.62	7.92	0.983	0.48
9.00	9.74	0.981	0.50
11.40	10.05	0.980	0.50
12.40	16.36	0.986	0.54
15.20	19.23	0.984	0.55
16.00	18.74	0.985	0.55
18.00	20.72	0.984	0.56
20.30	22.75	0.983	0.57
2 mm. DISTRIBUTOR ORIFICE DIA.			
1.27	1.77	0.991	0.21
2.54	4.75	0.984	0.36
5.08	6.46	0.980	0.41
7.62	8.61	0.975	0.44
9.00	10.05	0.972	0.46
11.42	11.71	0.969	0.48
14.00	13.60	0.965	0.50
16.47	14.73	0.963	0.51
18.00	16.10	0.960	0.52
20.30	17.93	0.957	0.53
3 mm. DISTRIBUTOR ORIFICE DIA.			
1.27	1.35	0.995	0.13
3.00	4.17	0.989	0.32
6.35	4.95	0.987	0.35
7.62	7.09	0.984	0.40
8.89	8.98	0.981	0.43
10.16	11.31	0.977	0.46
12.40	13.77	0.974	0.48
16.47	16.36	0.971	0.50
18.00	16.54	0.971	0.50
21.57	18.96	0.967	0.52

SYSTEM III (ISO-OCTANE)

1 mm. DISTRIBUTOR ORIFICE DIA.

BED HEIGHT (cm.) EXP.	CAL.	FRACTIONAL HOLD UP OF DISPERSED PHASE. (ε_d)	COALESCENCE PROBABILITY (λ)
2.0	3.78	0.984	0.35
5.0	5.92	0.982	0.41
7.0	8.36	0.980	0.44
9.0	12.05	0.985	0.47
12.0	13.85	0.984	0.48
15.0	16.39	0.983	0.50
17.0	18.02	0.983	0.51
20.0	20.47	0.982	0.52
25.0	23.32	0.981	0.53
28.0	27.14	0.980	0.54

2 mm. DISTRIBUTOR ORIFICE DIA.

2.0	0.87	0.984	0.04
5.0	3.92	0.983	0.32
7.0	5.73	0.980	0.37
9.0	10.71	0.983	0.44
11.5	12.17	0.982	0.46
14.0	14.00	0.980	0.47
16.0	20.56	0.986	0.49
19.0	21.88	0.985	0.50
22.0	23.23	0.985	0.51
26.0	25.08	0.984	0.52

3 mm. DISTRIBUTOR ORIFICE DIA.

1.0	1.10	0.989	0.05
3.0	2.44	0.982	0.20
7.0	10.35	0.984	0.42
10.0	12.25	0.983	0.44
12.5	15.15	0.981	0.46
15.0	16.96	0.980	0.48
18.0	24.54	0.985	0.50
20.0	25.41	0.985	0.51
25.0	28.11	0.984	0.52
28.0	29.49	0.984	0.52

SYSTEM III (contd)

4 mm. DISTRIBUTOR ORIFICE DIA.

1.0	1.34	0.991	0.07
2.0	2.62	0.986	0.19
5.0	5.81	0.976	0.32
7.0	6.51	0.974	0.34
10.0	8.25	0.969	0.38
15.0	10.73	0.962	0.41
18.5	11.52	0.960	0.42
22.0	21.48	0.969	0.50
25.0	23.17	0.968	0.51
28.0	24.90	0.967	0.52

SYSTEM IV (HEXANE)

1 mm. DISTRIBUTOR ORIFICE DIA.

BED HEIGHT (cm.) EXP.	BED HEIGHT (cm.) CAL	FRACTIONAL HOLD UP OF DISPERSED PHASE. (ε_d)	COALESCENCE PROBABILITY (λ)
1.0	0.85	0.988	0.03
2.0	2.97	0.983	0.27
3.0	5.72	0.984	0.37
5.0	7.71	0.982	0.40
8.0	13.41	0.985	0.46
10.0	15.07	0.985	0.47
12.0	16.40	0.984	0.48
17.0	19.79	0.983	0.50
24.0	21.86	0.982	0.51
29.0	23.57	0.981	0.52

2 mm. DISTRIBUTOR ORIFICE DIA.

1.0	1.50	0.981	0.23
2.0	2.87	0.982	0.32
3.0	6.09	0.984	0.40
5.0	8.37	0.982	0.43
6.0	8.93	0.982	0.44
8.0	10.28	0.981	0.46
10.0	10.88	0.980	0.47
13.0	15.45	0.986	0.49
20.0	18.27	0.985	0.50
30.0	20.65	0.984	0.51

3 mm. DISTRIBUTOR ORIFICE DIA.

0.5	0.90	0.991	0.06
2.0	2.09	0.985	0.17
4.0	5.88	0.983	0.35
6.0	7.54	0.980	0.39
9.0	12.06	0.984	0.45
12.0	15.52	0.982	0.47
15.4	16.61	0.981	0.48
21.0	18.37	0.980	0.49
25.0	28.70	0.985	0.523
30.0	29.90	0.985	0.527

SYSTEM IV (contd)

4 mm. DISTRIBUTOR ORIFICE DIA.

1.0	2.16	0.988	0.16
3.0	3.94	0.982	0.26
4.0	7.75	0.85	0.38
6.0	9.45	0.983	0.40
10.0	17.16	0.986	0.47
12.0	18.80	0.985	0.48
16.0	20.48	0.984	0.49
20.0	22.20	0.983	0.49
24.0	23.42	0.983	0.50
30.0	25.57	0.982	0.51

SYSTEM V (DIETHYLETHER)

1 mm. DISTRIBUTOR ORIFICE DIA.

BED HEIGHT (cm.)		FRACTIONAL HOLD UP OF DISPERSED PHASE (ε_d)	COALESCENCE PROBABILITY (λ)
EXP.	CAL.		
2.50	3.19	0.999	0.22
3.00	3.66	0.999	0.23
5.50	6.10	0.999	0.30
8.00	8.65	0.999	0.34
12.00	11.86	0.999	0.37
14.50	14.03	0.999	0.38
16.50	15.97	0.999	0.40
18.00	16.78	0.999	0.40
20.75	18.48	0.999	0.41
24.20	20.01	0.999	0.42
2 mm. DISTRIBUTOR ORIFICE DIA.			
1.00	0.80	0.999	0.04
2.00	2.46	0.999	0.17
4.30	4.68	0.999	0.25
8.00	8.69	0.999	0.32
11.75	12.00	0.999	0.36
13.50	13.13	0.999	0.37
15.00	14.14	0.999	0.38
16.00	15.82	0.999	0.39
18.50	17.10	0.999	0.40
21.50	18.08	0.999	0.41
3 mm. DISTRIBUTOR ORIFICE DIA.			
1.00	1.65	0.999	0.11
3.00	3.38	0.999	0.21
5.50	6.15	0.999	0.28
6.50	7.19	0.999	0.30
10.00	10.01	0.999	0.33
11.50	11.20	0.999	0.35
13.20	13.28	0.999	0.37
14.25	12.81	0.999	0.36
15.75	14.50	0.999	0.37
18,5	15.50	0.999	0.38

SYSTEM V (contd)

4 mm. DISTRIBUTOR ORIFICE DIA.

1.0	1.32	0.999	0.07
2.5	2.76	0.999	0.17
3.5	3.72	0.999	0.21
4.5	4.90	0.999	0.24
7.0	6.76	0.999	0.28
8.0	7.97	0.999	0.30
9.0	8.91	0.999	0.31
11.5	10.19	0.999	0.33
12.0	10.56	0.999	0.33
14.0	12.35	0.999	0.35

APPENDIX 14.

ESTIMATING THE VALUES OF r_o

From equation 4.12, it can be seen that for any particular plane in the bed (i)

$$r_{oi} = \left(\frac{9.96\ V_{di}\ h_i\ \mu_c\ d_i}{0.004\ \rho_c\ g\ \varepsilon_{di}^2}\right)^{\frac{1}{4}} \qquad (4.12)$$

and from equation (4.22)

$$\varepsilon_{di} = \frac{d_i^2}{d_i^2 + 1.26\ r_{oi}^2} \qquad (4.22)$$

Substituting (4.22) in (4.12)

$$r_{oi} = \frac{L_i\ d_i}{(1 + 1.26\ L_i^2)^{\frac{1}{2}}}$$

where $$L_i = \left(\frac{9.96\ V_{di}\ h_i\ \mu_c}{0.004 \rho_c\ g\ d_i^3}\right)^{\frac{1}{4}}$$

Measurements of r_o for system VI were taken from a cine film at about 4 cm. from the start of a bed 12 cm. thick. It can therefore be assumed that little or no interdrop coalescence has taken place i.e. $V_{di} = V_{do}$

and $d_i = d_o$

The superficial velocity of the dispersed phase was 0.675 cm./sec. The film thickness of the continuous phase h_i and the drop diameter d_i were measured from the film. The average values were found to be 0.01 cm. and 0.5 cm. respectively.

Therefore for system VI

$$L_i = \left(\frac{9.96 \times 0.675 \times 0.01 \times 0.00732}{0.87 \times 981 \times 0.004 \times (0.5)^3}\right)^{\frac{1}{2}}$$

$$L_i = 1.8$$

since $$r_{oi} = \frac{L\ d_i}{(1 + 1.26L^2)^{\frac{1}{2}}}$$

$$= \frac{1.8 \times 0.5}{(1+1.26(1.8)^{\frac{1}{2}}}$$

$$= 0.39 \text{ cm.}$$

Thus the c alculated value of r_{oi}

$$r_{oi\ CAL.} = 3.9 \text{ mm.}$$

Two methods of measuring r_o were employed

1) Two tangents were drawn to the curvature of the plateau border and the intersection of the two perpendicular to the tangents was taken as the centre of the circle.

2) From simple geometrical consideration $r_o = a\sqrt{3}$ where (a) is the distance shown in the illustration below(104)

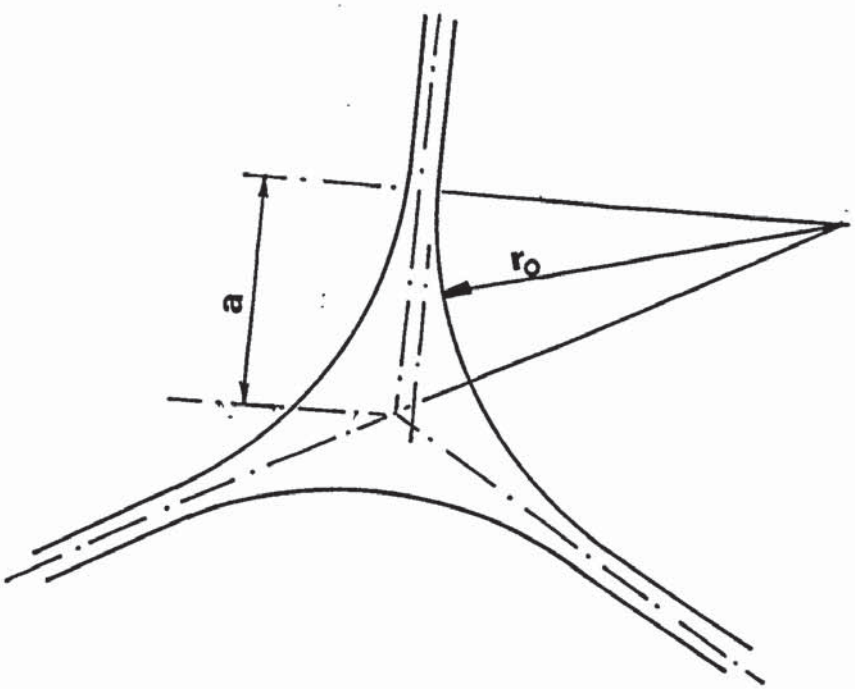

The measurements are listed in the table below

1st Radius (cm.)	2nd Radius (cm.)	3rd Radius (cm.)	Average r_o for one plateau border (cm.)
15.0	17.0	21.5	17.8
20.0	19.4	12.5	17.3
14.0	22.0	17.0	17.7
17.7	16.7	23.0	18.8
28.0	16.0	15.0	19.7
15.5	20.5	17.8	17.9
21.0	16.5	26.0	21.5
15.0	24.5	20.0	19.7
23.5	18.5	35.0	21.1
18.5	18.5	18.5	18.5
19.7	19.1	20.0	19.5
18.3	17.7	16.0	17.5
17.3	18.2	16.5	20.6
15.0	25.0	15.7	18.5
			266.1

$\therefore$ Average value for $r_o = \frac{266.1}{14} = 19.0$

The magnification factor = 61

$\therefore$ Measured value for $r_o = \frac{19.0}{61} = 0.31$ cm.

or measured value of r_o

$r_{oi\ MEAS.} = 3.1$ mm.

FIG A 14

Actual Size of a Plateau Border

Magnified 61 Times

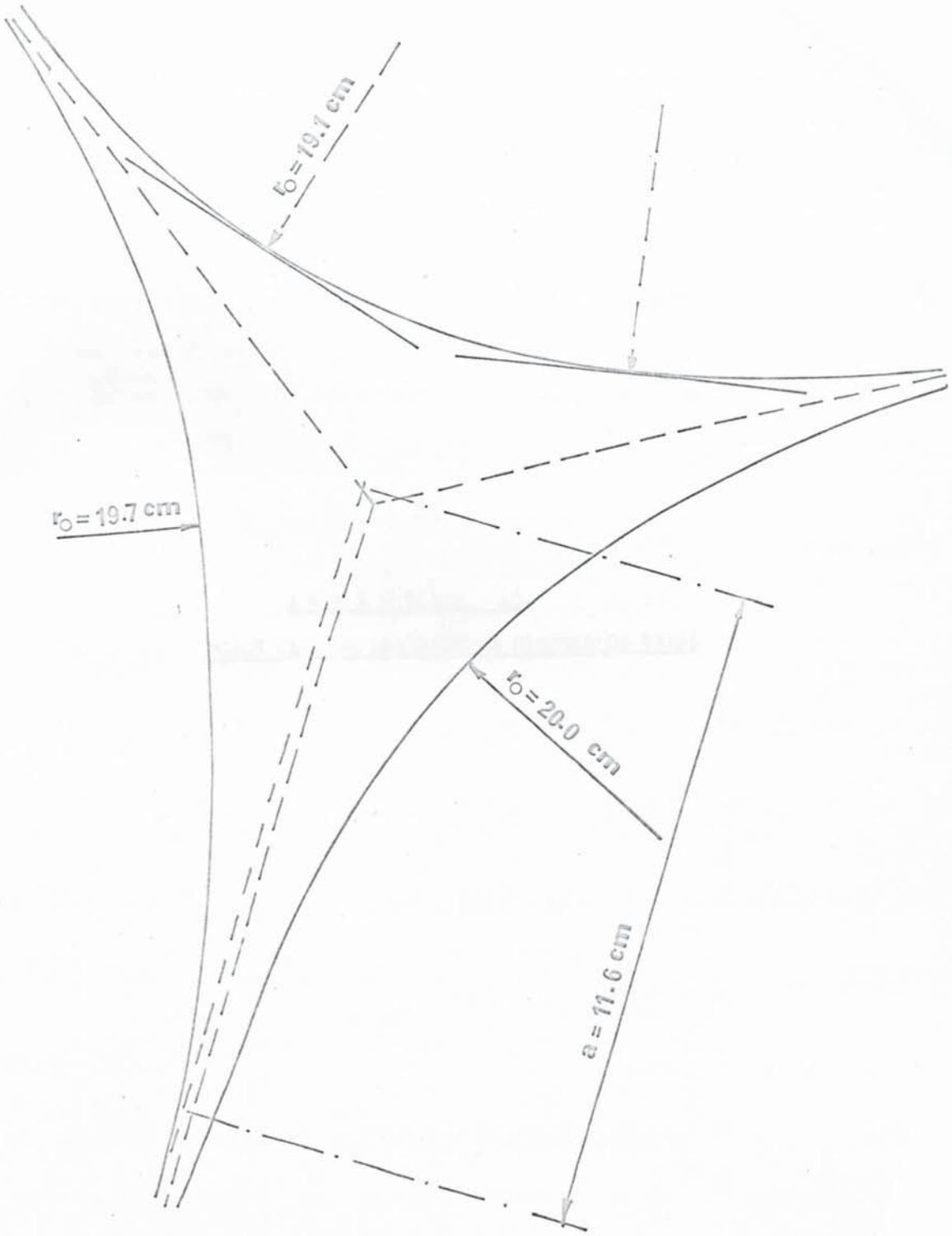

APPENDIX 15.

FORCE CAUSING DRAINAGE IN DISPERSION BANDS

In the model it was considered that the continuous phase flows from the films to the plateau borders and then down through the borders by gravity. To examine the former, the plateau border and three films associated with it will be examined. From paragraph (4.4) it has been established that the excess pressure in the drop over that in the border is given by

$$\Delta P = \frac{\gamma}{r_o}$$

This pressure difference is much greater than that of gravity; orders of magnitude can be shown by a numerical example. Consider system IV and a drop of a diameter of d = 0.5 cm. The area of one face of the dodecahedra = 0.29d. (Appendix 1).

The force due to gravity causing drainage from the film to the plateau border is represented by the weight of the film

$$\therefore F_{gravity} = 0.29d^2 \, h\rho_c g \cos\theta$$

Taking an average value for θ to be 45° and an average of the film thickness from its initial value to its critical value i.e. h = 0.05 cm.

$$F_{gravity} = 0.29 \times 0.25 \times 0.05 \times 1.22 \times 981 \times 0.7$$
$$= 2.76 \text{ dynes.}$$

At rupture of the film i.e. h = 2 microns the force decreases to

$$F_{gravity} = 0.29 \times 0.25 \times 0.0002 \times 1.122 \times 981 \times 0.7$$
$$= 0.11 \text{ dynes}$$

The interfacial forces causing drainage on the other hand is

$$F_{interfacial} = \gamma \times 0.41d \times (\text{No. of edges})$$
$$= 35.6 \times 0.41 \times 0.5 \times 5$$
$$= 36.8 \text{ dynes}$$

Thus the ratio of the interfacial forces to the gravity forces increases from

$$\frac{36.8}{2.76} = 13.3 \text{ to } \frac{36.8}{0.1} = 368$$

It was shown previously that the initial drainage of the film is rapid, therefore the increase in the ratio of the interfacial to gravity forces will also be rapid. It seems reasonable then to assume that gravity forces have a negligible effect on the drainage of the continuous phase from the film to the plateau border in comparison with the interfacial forces.

APPENDIX 16

COMPUTER PROGRAMME

COMPUTER PROGRAMME FOR THE MATHEMATICAL MODEL

```
10  READ B,F,G,C,N,L
14  DIM M(50),U(50)
15  DIM D(50),V(50),R(50),Q(50),H(50),T(50),E(50),K(50)
20  READ E(0),D(0)
25  FOR J=1,10
30  READ U(J)
35  V(0)=U(J)/19.6
40  Q(0)=((1-E(0))*V(0))/E(0)
50  T(0)=.58E-01*((V(0)*B↑5*D(0)↑9)/(F*G*L↑4*E(0)↑2*C↑7))↑.25
60  H(0)=T(0)*V(0)
63  PRINT "Q(0)              T(0)              V(0)              H(0)"
65  PRINT Q(0),T(0),V(0),H(0)
66  PRINT ""
67  PRINT ""
70  S1=0
80  S2=H(0)
85  PRINT "      Q(I)              T(I)              E(I)              H(I)  M(I
90  FOR I=1,20
92  V(I)=(1-N)*V(I-1)
95  M(I)=1-.5594*((L/(B*V(I-1)))↑.536E-01)*((D(I-1)/S2)↑.1903)
97  IF M(I)>=0 GOTO 100
98  M(I)=0
100  D(I)=((1-N)*D(I-1))/(1-N-.21*M(I))
120  K(I)=((1000*V(I)*B)/(F*G*D(I)↑4))↑.5
130  R(I)=(1-(1-(5.04*K(I)↑2*D(I)↑2))↑.5)/(2.52*K(I))
140  E(I)=(D(I)↑2)/(D(I)↑2+1.26*R(I)↑2)
150  T(I)=.58E-01*((V(I)*B↑=*D(I)↑9)/(F*G*L↑4*E(0)↑2*C↑7))↑.25
160  Q(I)=(.41E-02*R(I)↑4*F*G*E(I)↑2)/(3*B*D(I)↑2)
170  H(I)=V(I)*T(I)
180  S2=S2+H(I)
190  S1=S1+Q(I)
200  IF E(I)>.98 GOTO 220
210  NEXT I
220  FOR X=1,I
230  PRINT Q(X),T(X),E(X),H(X),M(X)
231  NEXT X
232  PRINT "        S2              U(J)"
234  PRINT S2,U(J)
235  NEXT J
237  END
```

COMPUTER PROGRAMME FOR THE SUMMATION MATRIX SHOWN IN APPENDIX 10.

```
10   DIM U(90),V(90),D(90),H(90),Z(90),F(90)
20   S1=0,S2=0
30   S3=0,S4=0
40   S5=0,S6=0
50   S7=0,S8=0,S9=0
60   FOR J=1,3
65   READ N(J),Y(J),C(J)
70   FOR I=1,N(J)
75   READ V(I),F(I),H(I),D(I)
80   U(I)=V(I)/19.6
90   Z(I)=LOG(1-F(I))
95   T(I)=LOG((Y(J))/(C(J)*U(I)))
100   W(I)=LOG(H(I)/D(I)(
105   S1=S1+T(I)
110   S2=S2+W(I)
115   S3=S3+Z(I)
120   S4=S4+(T(I)↑2)
125   S5=S5+(T(I)*W(I)
130   S6=S6+(T(I)*Z(I))
135   S7=S7+(Z(I)*W(I))
140   S8=S8+(W(I)↑2)
145   NEXT I
150   S9=S9+N(J)
155   NEXT J
160   PRINT "          S9          S1          S2          S3"
170   PRINT S9,S1,S2,S3
175   PRINT "          S1          S4          S5          S6"
180   PRINT S1,S4,S5,S6
185   PRINT "          S2          S5          S8          S7"
190   PRINT S2,S5,S8,S7
200   END
```

COMPUTER PROGRAMME FOR SOLVING THE SUMMATION MATRIX SHOWN IN APPENDIX 10.

```
10   DIM A(9,9),X(9),Y(9)
20   FOR I=0,2
30   FOR J=0,2
35   READ A(I,J)
40   NEXT J
45   READ X(I)
50   NEXT I
55   R=-1
60   CALL (1,A(0,0),A(0,0),3,R)
70   IF R>0 GOTO 120
80   CALL (4,A(0,3),X(0),Y(0),3,3,1)
90   FOR I=0,2
100   PRINT Y(I)
110   NEXT I
120   END
```

NOTE:- A special basic compiler was required.

NOMENCLATURE.

a = Jet radius (cm) $\quad \bar{a} = \frac{2a}{DN}$

a_N = Jet radius at nozzle exit (cm)

A_{pb} = Area of the plateau border (cm^2)

d = Drop diameter (cm)

D_H = Hydraulic diameter (cm)

D_N = Nozzle diameter (cm)

F = Harkinsand Brown correction factor

g = gravitational acceleration ($cm\ sec^{-2}$)

h = Continuous phase film thickness (cm)

h_k = Critical film thickness (cm)

H = Bed height (cm)

K = A constant for any particular system

$$= \frac{920\ \mu_c\ V_{d_1}}{\rho_c g\ d_1^4}$$

ℓ_{pb} = length of the plateau border (cm)

M = Mass input of dispersed phase through nozzle ($gm\ sec^{-1}$)

N = Rate of drops entering the bed per unit area ($sec^{-1}\ cm^{-2}$)

N_I = Rate of interdrop coalescence per unit area ($sec^{-1}\ cm^{-2}$)

N_W = Rate of drop wall coalescence per unit area ($sec^{-1}\ cm^{-2}$)

ΔP = Pressure drop between the film and the plateau border ($gm\ cm^{-2}$)

Q = Volumetric flow rate of the continuous phase per unit area ($cm\ sec^{-1}$)

q = Volumetric flow rate in the plateau border ($cm^3\ sec^{-1}$)

R = Radius of a disc equivalent to the area of one face of the dodecahedra (cm)

r_o = Radius of curvature of the plateau border (cm)

t = time taken for the continuous film to drain to h_k (sec)

u = velocity of the continucus phase in the film and the plateau border ($cm\ sec^{-1}$)

NOMENCLATURE (contd)

U_I = Interfacial velocity of jet (cm sec^{-1})

U_J = Jetting velocity (cm sec^{-1})

U_N = Average velocity through nozzle (cm sec^{-1})

U_T = Drop terminal velocity (cm sec^{-1})

v = velocity of approach of the faces (cm sec^{-1})

V_d = Volumetric flow rate of dispersed phase per unit area (cm sec^{-1})

V_F = Volume of the released drop (cm^3)

V_{eg} = Drop volume at equilibrium (cm^3)

V_i = Volume of forming drop about horizontal section at increament (cm^3)

$V_{r\ell}$ = Volume added during release (cm^3)

z = axial distance (cm) $\bar{z} = \frac{2z}{D_N}$

GREEK LETTERS

β = Probability of drop wall coalescences

λ = Probability of interdrop coalescence

γ = Interfacial tension (dynes cm^{-1})

ρ = Density (gm cm^{-1})

μ = Viscosity (poise)

ε = Fractional hold up

ξ_o = Initial amplitude of disturbance (cm)

SUBSCRIPTS

0 = Denotes the conditions at the beginning of the bed

1 = Denotes the conditions after the first increment

d = Denotes the dispersed phase

c = Denotes the continuous phase

REFERENCES

1) GUYE P.H.A. and PERROT,F.L. Arch.Sc.Phys.Nat. 11 225,345, (1901)

2) HARKINS,W.D. and BROWN,F.E. J.Am.Chem.Soc. 41 449 (1919)

3) HAUSER,E.A.,EDGERTON,H.E.,HOLT,B.M. and COX,J.T. J.Phys.Chem. 40 973 (1916)

4) DIXON,B.E. and RUSSELL,A.A.W. J.Soc.Chem.Ind.Lond. 47 258 (1955)

5) KEITH,F.W. and HIXSON,A.N. Ind.Eng.Chem. 47 258 (1955)

6) TANWEER,A.K. Imp.Coll.Chem.Eng.Soc. Journal 10 51 (1956)

7) HAYWORTH,C.B. and TREYBAL,R.E. Ind.Eng. Chem. 42 1174 (1950)

8) NULL,R and JOHNSON,H.E., J.A.I.Ch.E. 4 273 (1958)

9) HARKINS,W.D. and F.E.BROWN, Am.Chem.Soc.Journal 41 499 (1919)

10) RYAN,J.T. Thesis Missouri (1966)

11) RAO E.V.L.N.,KUMAR,R., and KULOOR N,R., Chem.Eng.Sci. 21 867 (1966)

12) HEERTJES ,P.M.,DE NIE,L.H., and DE VRIES H.J.,Chem. Eng.Sci. 26 441 (1971)

13) IZARD,J.A., J.A.I.Ch.E. 18 634 (1972)

14) SCHEELE G.F. and MEISTER,B.J. J.A.I.Ch.E. 14 9 (1968)

15) ALLAK A.,JEFFREYS, G.V., and DAVIES,G.A. Paper presented at the 4th CHISA Congress, Czechoslovakia (1972)

16) SCHEELE,G.F. and MEISTER,B.J., J.A.I.Ch.E. 14 5 (1968)

17) Ibid. J.A.I.Ch.E. 13 682 (1967)

18) Ibid. J.A.I.Ch.E. 15 689 (1969)

19) Ibid. J.A.I.Ch.E. 15 700 (1969)

20) KINTNER,R.C. and HU S., J.A.I.Ch.E. 1 42, (1955)

21) HEERTJES,P.M., DE NIE,L.H., and DE VRIES H.J., Chem.Eng. Sci.26 451 (1971)

22) PERRUT,M. and LOUTATY, R., Chem.Eng.J. 3 286 (1972)

23) REYNOLDS, O., Chem.News. 44 211 (1881)

24) GILLESPIE T., and RIDEAL E.K., Trans.Faraday Soc. 52 173 (1956)

25) JEFFREYS,G.V. and HAWKESLEY,J.L., J.Appl.Chem.12 329 (1962)

26) WARK,J.W., and COX,A.B., Nature 136 182 (1935)

27) MAHAGAN,L.D., KOLLDID, Z., 69 16 (1934)

28) LAWSON,G.B., Ph.D.thesis, Univ. of Manchester (1967)

29) COCKBAIN,E.G., and McROBERTS,T.S., J. of Colloid Sci. 8 440 (1953)

30) WATANABE T., and KUSUI M., Bull.Chem.Eng.Soc.Japan 31 30 429 (1969)

31) NEILSEN,L.E.,WALL,R., and ADAMS,G., J.of Colloid Sci. 13 441 (1958)

32) ELTON,G.A. and PICKNETT,R.G.,Proceedings of the 2nd Int.Congress on Surface Activity 1 288, 307, Butterworths, London (1957)

33) JEFFREYS,G.V. and HAWKESLEY,J.L., A.I.Ch.E.J. 11 413 (1965)

34) KONNEKE,H.G., Z.Physik Chem.(Leipzig) 221 208 (1959)

35) SAWITOWSKI,H., and JAMES,B.R., Chem.Eng.Tech. 35 175 (1963)

36) LANG,S.B., Ph.D. thesis.Univ. of California (1962)

37) Recent Advances in Liquid-Liquid Extraction. Edited by HANSON, B., Pergamon (1971)
(JEFFREYS,G.V., and DAVIES,G.A. Chp.14)

38) HITTIT,H.A.,Ph.D. Thesis. Univ. of Aston (1972)

39) JEFFREYS,G.V. and LAWSON,G.B.,Trans.Inst.Chem.Engis.,43 T.294 (1965)

40) SMITH,D.V., and DAVIES,G.A., Canad.I.Chem.Eng. 48 628 (1970)

41) ALI,F.A.,Ph.D. Thesis Univ. of Manchester (1971)

42) HAWKESLEY,J.L., Ph.D.Thesis., Univ. of Birmingham (1963)

43) HARTLAND,S.J., Colloid Sci., 26 383 (1968)

44) LANG,S.B., and WILKE,C.R.,Ind.Eng.Chem.Fundam.10 No.3 329 (1971)

45) CHARLES,G.E. and MASON,S.G., I.Colloid Sci. 15 236 (1960)

46) DAVIES,G.A.,JEFFREYS,G.V., and SMITH,D.V.,I.S.E.C. Hague (1971)

47) ROBINSON.J.D., and HARTLAND,S.,I.S.E.C.Hague (1971)

48) BROWN,A.H., and HANSON C., Trans.Farad.Soc.,61 1754 (1965)

49) SMITH,D.V.,Ph.D. Thesis.Univ. of Manchester (1971)

50) JOHNSON,H.F., and BLISS,H.,Trans.Am.Inst.Chem.Eng. 42 331 (1946)

51) GROOTHIUS, H., and ZUIDERWEG,F.J., Chem.Eng.Sci.12 288 (1960)

52) AL-HEMIRI,A.A.A.,Private Communication (1973)

53) SAWITOWSKI,H.,"Recent Advances in Liquid-Liquid Extraction" edited by HANSON,C.,Pergamon Press, Oxford (1971)

54) MACKAY,G.D.M., and MASON,S.G., J.Colloid Sci.18 674 (1963)

55) HEERTJES,P.M., and DE NIE,L.H., Paper (128) I.S.E.C.Hague (1971)

56) DAVIES,J.T., and RIDEAL, E.K., Interfacial Phenomena. Academic Press, New York (1963)

57) HARTLAND,S., Trans.Inst.Chem.Engrs.46 T275 (1968)

58) DAVIES,J.T.,Advances in Chemical Engineering, Academic Press., 4 (1963)

59) ALLEN,R.S.,CHARLES,G.E., and MASON,S.G.,J.Coll.Sci.16 150 (1961)

60) ALLEN,R.S., MASON,S.G., Trans.Farad.Soc.57 2027 (1961)

61) BROWN,A.H., and HANSON,C.,Chem.Eng.Sci., 23 84 (1968)

62) CHAPPELEAR,D.C.,J.Colloid.Sci. 16 181 (1961)

63) PRINCEN,H.M.,J.Colloid Sci., 18 178 (1963)

64) FRANKEL,S.P., and MYSELS,K.S.,J.Phys.Chem. 66 190 (1962)

65) McAVOY,R.M., and KINTNER,R.C.,J.Colloid Sci., 20 188 (1965)

66) SCHEELE,G.F.,LENG,D.E., Chem.Eng.Sci., 26 1867(1971)

67) ROBINSON,J., and HARTLAND,S., I.S.E.C.Paper No.56 (1971)

68) MALEJICEK,A.,SIVOKOVA, M., and EICHLER,J., Collection Czech Chem.Commun. 36 35 (1971)

69) KINTNER,R.C., Advances in Chem.Eng. 4 87 (1968) Academic Press, New York and London.

70) GUNN,R., Science, 150 695 (1965)

71) PARK,R.W., and CROSBY,E.J., Chem.Eng.Sci. 20 39 (1965)

72) DAMON, K.G., ANGELO,J.B., and PARK,R.W., Chem.Eng.Sci. 21 813 (1966)

73) MacKAY,G.D.H., and MASON,S.G., Cand.J.Chem.Eng. 41 203 (1963)

74) SCHROEDER,R.R., and KINTNER,R.C., A.J.Ch.E.J. 11 5 (1965)

75) MURDOCH,P.G. and LENG,D.E.,Chem.Eng.Sci. 24 1881 (1971)

76) DAVIES,G.A. JEFFREYS,G.V., and ALI,F.A., Can.Journal of Chem.Eng. 48 328 (1970)

77) ISAO KOMASAWA and TSUTAO OTAKE, J.Chem.Eng. Japan 3 234 (1971)

78) TOPLISS,J.A., 1st Chem.Eng.Dept. Research Symposium, Univ. of Aston, May (1970)

79) LEE,J.C., and LEWIS,G., I.Chem.Eng.Symposium Series No.26 Newcastle-upon-Tyne (1967)

80) JEFFREYS,G.V.,SMITH,D.V., and PITT,K., I.Chem.Eng.Symposium Series No.26. Newcastle-upon-Tyne (1967)

81) JEFFREYS,G.V., DAVIES,G.A., and PITT,K.,A.I.Ch.E.J. 16 823 (1970)

82) MARASCHINO,M.J., and TREYBAL,R.E.,A.I.Ch.E. 17 1174 (1971)

83) VAN MEURS,P., I.Petrol Technol, 210 295 (1957)

84) HELLER,J.P., Rev.Sci. Instrum. 30 1056 (1959)

85) RAMAN,C.V.,Proc.Indian Acad.Sci. A29 381 (1949)

86) DE JOSSELIN DE JONG, G., Trans Am.Geog Physical Union 39 1160 (1958)

87) CLOUPEAU,M., and KLARSFELD ,S., Applied Optics 12 No.2 198, (1973)

88) FRANTISAK,F.,PALADE DE IRIBARNE A., SMITH J.W., and HUMMEL,R.L., Ind.Eng.Chem.Fund. 8 1 160 (1969)

89) EXELBY,R., and GRINTER,R., Chem.Rev. 65 2 247 (1965) Eng.

90) ARUNACHALAM Vr, HUMMEL,R.L., and SMITH,J.W., Canad.I.of Chem.Eng. 50 337-343 (June 1972)

91) KEL MIYANAMI, SHIGEMI OHSAKA and TAKEO YANO., I.Chem.Eng. Japan, 5 No.3., 313-315 (1972)

92) GOLDISH,L.H., KOUTSKY,J.A., and ADLER,R.J.,Chem.Eng.Sci. 26 1011-1014 (1965)

93) ROGERS,G.L., J.Sci.Instrum. 43 677 (1966)

94) SCHAWLOW,A.L.,"Lasers and Light". W.H.Freeman & Co., (1970)

95) KLEIN,H.A.,"Holography" J.B.Lippincott Co.,N.Y. (1970)

96) THOMPSON,B.J. WARD,J.H., ZINKY,W.R.,"Applied Optics" 6 No.3 519 (1967)

97) FLETCHER,G.E.,Chem.Eng.J. 4 34 (1968)

98) THOMPSON,B.J., "Particle Size Examination"(Symposium on Engineering Use of Holography) Univ.Strathclye. p.249 (Sept 1968)

99) BERMAN,E.,FOX,R.E.THOMPSON,F.E.,I.Am.Chem.Soc. 81 5605 (1959)

100) TAYLER,L.D.,NICHOLSON,J.,DAVIES,R.B.,"Tetrahedron Letters" No.17, 1585 (1967)

101) CHRISTIANSEN,C., Ann.Phys. 23 294 (1884)

102) RAMAN,C.V.,Proc.Indian Acad.Sci. A29 381 (1949)

103) HO G.E.,MULLER,R.L., and PRINCE,R.G.H., I.Chem.Eng.Symposium, Series No.32, London (1969)

104) LEONARD,R.A., and LEMLICH, R., A.I,Ch.E.I.,11 No.1 18 (1965)

105) Ibid Chem.Eng.Sci. 20 790 (1965)

106) ZOLOTROFE,D.L. and SCHEELE,G.E., Ind.Eng.Chem.9 No.2 293 (1970)

107) RICHARDSON,J.F. and ZAKI,W.N., Trans.Inst.Chem.Engrs. 32 35(1954)

108) CHRISTIANSEN,R.M., and HIXSON,A.N., Ind.Eng.Chem. 49 1017 (1957)

SUPPORTING PUBLICATION

A paper presented at the Fourth Congress of "CHISA" 72, Czechoslovakia.